THRUST SHEET EVOLUTION IN THE KINLOCHEWE REGION OF THE MOINE THRUST ZONE, N. W. SCOTLAND AND THE PELVOUX-BRIANÇONNAIS, FRENCH ALPS

STEPHEN JOHN MATTHEWS

Submitted in accordance with the requirements

for the degree of

DOCTOR OF PHILOSOPHY

The University of Leeds

Department of Earth Sciences. November 1984.

CONTAINS PULLOUTS

ABSTRACT

Balanced and restored cross sections demonstrate a minimum 16 km shortening below the Moine Thrust and minimum restored widths of 17 km between the La Meije and Combeynot Thrusts (external Alps), and 54 km between the frontal Subbriançonnais Thrust and the western Briançonnais Zone (internal Alps). Imbricate thrusts within the Moine Thrust Zone branch off a floor thrust which cuts up stratigraphic section from basement (Lewisian gneiss) to Cambrian shelf sediments parallel to the ESE-WNW movement direction. Cut-off relationships and fold geometries within the Pelvoux-Briançonnais suggest a change in movement direction of thrust sheets during the evolution of the French Alps from ENE-WSW for the Briançonnais and Subbriançonnais Zones to ESE-WNW for the External Zones.

Higher thrust sheets are frequently flexured as a result of slip on lower thrust surfaces (in-sequence thrusting). Important examples occur of lower thrust assemblages which are truncated by higher thrust surfaces (out-of-sequence thrusting). Strains within thrust sheets from the Kinlochewe region suggest 0% - 20% layer parallel shortening may develop in the footwall to an abandoned thrust as a tip strain to a newly developing thrust. Variations in strain may reflect variable propagation rates; differential displacement has resulted in differential movement within thrust sheets.

Fault-bend folds (structurally necessary folds) have developed following slip of thrust sheets across irregular thrust surfaces and buckle folds have grown during shortening within the sheet. Extensional fault sheets (surge zones) can be mapped out in the Briançon region which both truncate and are flexured by thrust structures; important extensional structures have developed during evolution of the thrust belt.

CONTENTS

Page

LIST OF TABLES AND ILLUSTRATIONS

Page

INTRODUCTION

(i) Field of research and aims of project

Field mapping has been carried out in the Pelvoux - Briançonnais region of the French Alps at a scale of 1:25000 over a period of 24 weeks during the summer months of 1981, 1982 and 1983. Approximately 12 weeks have been spent in the Kinlochewe region of the Moine Thrust Zone, N.W. Scotland, where field mapping was carried out at 1:10000 during the spring months of 1981, 1982 and 1983. This mapping was aimed at establishing the 3 dimensional fold and thrust geometry in order to refine ideas on the structural evolution of both regions, and in particular to establish the sequence of development of folds and thrusts and the sequence of emplacement of thrust sheets. Techniques that have been used are based on the approach used by Elliott & Johnson (1980) and Boyer & Elliott (1982) to analyse the geometry of thrust belts. The distribution of strain within thrust sheets has been assessed in terms of strains developed prior to, during and after development of detachment levels. The results that have arisen from this approach are integrated with existing ideas on the structural evolution of both thrust belts.

The field description of thrust sheets, their illustration on carefully drawn cross sections and discussion on the evolutionary sequence of thrusting was incorporated into the classic memoir on the Geological Structure of the N.W. Highlands of Scotland by Peach et al. (1907). Field observation of textures within rocks close to thrust surfaces was standard procedure for the structural aspect of this complete geological review of N.W. Scotland. Early studies in the Western Alps, e.g. Argand (1916,1922) and Collet (1943) further emphasised the use of cross sections in illustration of the geometry of folds within thrust sheets and in the extrapolation of outcrop geology to provide possible alternatives for the cross-sectional structure of the Alps. Rich (1934) observed that in the Appalachians

of N. America thrusts follow ramp and flat trajectories which results in the moving thrust block assuming a modified geometry as it slips. Work carried out in the Canadian Rockies in the early 1960's, e.g. Bally et al. (1966) utilised geophysical data to constrain cross sections based on field mapping and drew conclusions concerning the evolutionary sequence of thrusts. The study of the geometry of thrust belts and the evolutionary sequence of thrust development is therefore a long established field of research.

Current research in the field of thrust tectonics is largely based on the results of oil company exploration in the Rocky Mountains during the early 1960's, e.g. Bally et al. (1966). The idea of constructing balanced cross sections where the geology can be restored to its pre-deformational configuration was formally introduced by Dahlstrom (1969). Theories concerning the driving mechanisms of thrust sheets and hence the relative importance of stress systems resulting from gravitational and compressive crustal forces have been examined by Elliott (1976a) and Chapple (1978). Balanced cross sections through the Rocky Mountains revealed characteristic geometrical features within thrust sheets and subsequent modelling of the strain history of a thrust slab as it slips across an undulating thrust surface has been examined by several workers, e.g. Elliott (1976b), Wiltschko (1979), Berger & Johnson (1980) and Fischer & Coward (1982).

A framework now exists for integration of finite strain markers within thrust belts with the 3 dimensional structural geometry in order carefully to depict the evolutionary sequence of thrust systems.

This thesis is divided into 2 parts, Part One deals with the Moine Thrust Zone and Part Two deals with the French Alps; previous work within each area is discussed in the relevant regional geology chapter. The locations of the two study areas are illustrated in Figs. A and B.

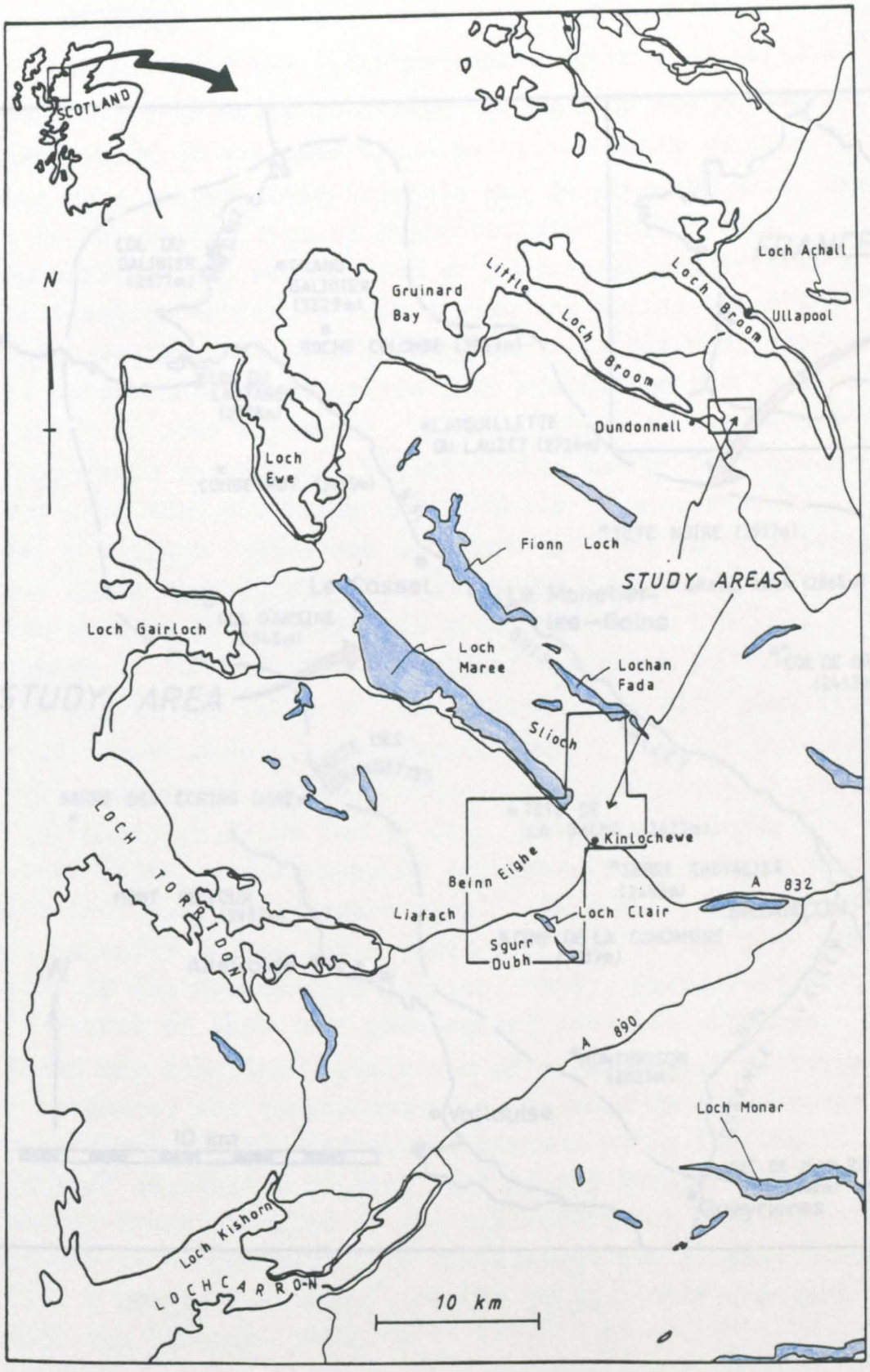

FIG. A Location map of the study area in N.W. Scotland.

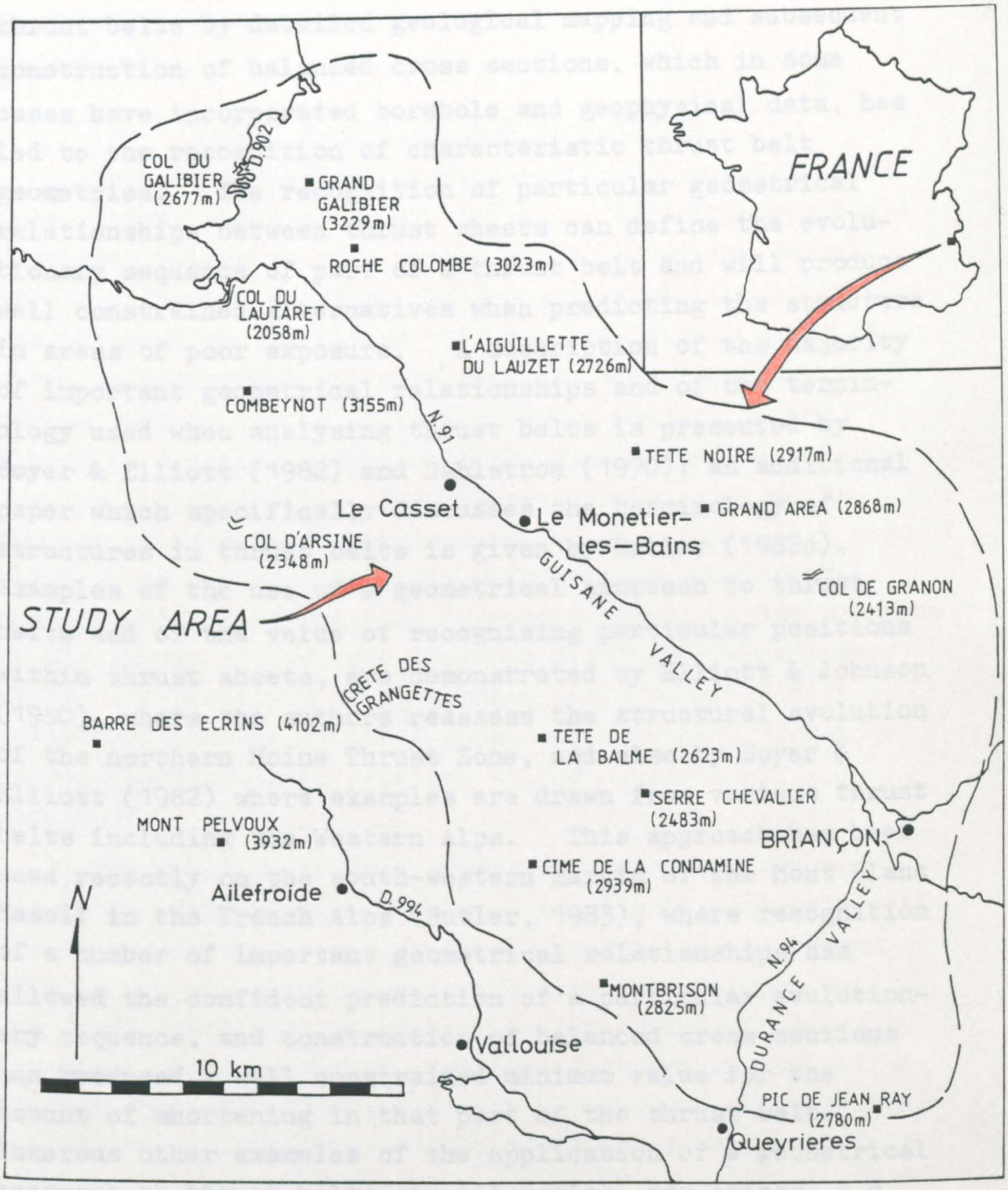

FIG. B Location map of the Pelvoux-Briançonnais region, French Alps.

(ii) Introduction to thrust systems and balanced cross sections

Analysis of the 3 dimensional structure of various thrust belts by detailed geological mapping and subsequent construction of balanced cross sections, which in some cases have incorporated borehole and geophysical data, has led to the recognition of characteristic thrust belt geometries. The recognition of particular geometrical relationships between thrust sheets can define the evolutionary sequence of part of a thrust belt and will produce well constrained alternatives when predicting the structure in areas of poor exposure. A description of the majority of important geometrical relationships and of the terminology used when analysing thrust belts is presented by Boyer & Elliott (1982) and Dahlstrom (1970); an additional paper which specifically discusses the terminology of structures in thrust belts is given by Butler (1982c). Examples of the use of a geometrical approach to thrust belts and of the value of recognising particular positions within thrust sheets, are demonstrated by Elliott & Johnson (1980), where the authors reassess the structural evolution of the northern Moine Thrust Zone, and also by Boyer & Elliott (1982) where examples are drawn from various thrust belts including the Western Alps. This approach has been used recently on the south-western margin of the Mont Blanc Massif in the French Alps (Butler, 1983), where recognition of a number of important geometrical relationships has allowed the confident prediction of a particular evolutionary sequence, and construction of balanced cross sections has produced a well constrained minimum value for the amount of shortening in that part of the thrust belt. Numerous other examples of the application of a geometrical approach to thrust belts, on all scales, now exists, e.g. Butler & Coward (in press), Cooper et al. (1983), Coward (1983) and Hossack (1983).

A complete review of the geometry and terminology of thrust belts is unnecessary at this point, a short

introduction to some simple definitions is given. Specific geometrical variations from the study areas are described in the relevant sections and any terminology or geometrical discussion and comparison are dealt with as necessary.

(a) Thrust sheets and thrust surfaces

Thrusting involves displacement of a volume of rock over another above a thrust surface. Strictly speaking a displaced volume of rock having moved in reverse sense should be termed a thrust sheet once a small amount of slip has occurred on the thrust surface, but usually a thrust sheet is understood to exist when the thrust surface cuts across bedding planes up stratigraphic section in the direction of displacement, thereby duplicating and thickening the sequence . Thrusts are usually assumed to develop as detachment levels parallel to a horizontal datum plane or as detachment levels which cut up towards the erosion surface at the time of displacement; these segments of the thrust surface are known as flats and ramps respectively. Typically a thrust surface has a ramp and flat trajectory through a lithological sequence when viewed on a cross section drawn parallel to the displacement direction.

The zone immediately above the thrust surface is termed the hangingwall and that below the thrust surface is termed the footwall. Clearly, on a cross section drawn parallel to the displacement direction the footwall and hangingwall will get stratigraphically younger in the direction of displacement, provided that the thrust surface is developed through a previously undeformed, subhorizontal succession. On a longitudinal section, drawn parallel to strike, it is often observed that the thrust surface cuts up and down stratigraphic sequence perpendicular to the displacement direction. This is a result of ramp segments of the thrust surface changing orientation from perfectly frontal ramps (90° to movement direction) to perfectly lateral ramps (parallel with movement direction), through

an intermediate stage of oblique ramps. The stratigraphic level of the thrust surface on a longitudinal section, or on a cross section drawn parallel to the movement direction will change as the section crosses a ramp of any orientation. Therefore, on a cross section a ramp may appear to be a perfectly frontal or a perfectly lateral part of the thrust surface; however, it may possibly be oblique. Detachment levels are often observed to die out at tip lines which separate slipped from unslipped rock (Hossack, 1983). Tip lines occur as frontal, oblique and lateral features relative to local movement direction. The structures which have been described in this section are illustrated in Fig. C.

(b) Thrust sequences, duplexes and imbricate fans

The problem of establishing the evolutionary sequence of structures within a thrust belt can be approached on the scale of the belt by carefully studying the age of synorogenic sediments and their structural relationship with overlying and underlying thrust sheets. This geological situation is usually confined to the external parts of the Mesozoic to Recent mountain belts, as a result of erosion of the higher levels of older belts. In order to establish the evolutionary sequence of thrust surfaces that developed a number of kilometres below the synorogenic erosion surface, geometrical criteria can be used.

Boyer & Elliott (1982) illustrate how several thrust sheets may be stacked on top of each other to form duplexes and imbricate fans. A duplex is a stack of thrust sheets, each thrust sheet being termed a horse, when enclosed by an overlying roof thrust and an underlying floor thrust. An imbricate fan is a stack of thrust sheets in which each imbricate thrust cuts the present day erosion surface, this being due to removal of structurally higher thrust sheets by erosion or by the imbricate thrusts having cut up to the synorogenic erosion surface, in which case the structure is termed an emergent imbricate fan.

Typically the roof thrust to a duplex is a regionally significant or major thrust surface overlain by a major thrust sheet. The 'roof' thrust may cut across the underlying stack of horses as a planar feature, thereby removing the upper portion of the duplex as a segment in the hangingwall. In this case it is clear that development of the structurally highest thrust postdates formation of the stack of horses. At the present time the observation of a structurally higher thrust surface having formed later than an underlying thrust surface, irrespective of any contrast in scale between the two thrust sheets is termed out of sequence thrusting. Previously this has been known as the overstep model in which structurally higher thrusts were thought to cut across, and therefore postdate, lower structures.

The currently popular model for the sequence of development of thrust surfaces is that structurally lower thrusts are youngest, and that thrust belts develop from the internal zones (hinterland) towards the external zones (foreland) by accreting slabs of the foreland as thrust sheets. This is termed in sequence thrusting or piggy-back thrusting. One of the geometrical results of thrusts developing in sequence is gentle folding of an overlying thrust as a result of movement on imbricate thrusts within the duplex, see Fig. D. Displacement on imbricate thrusts results in warping of a structurally higher thrust sheet as each horse slips along the higher thrust surface. These bulges, which occur in the hangingwall to the roof thrust are termed culminations. A model which proposes that each horse within a duplex moves up an approximately frontal ramp and then along the upper footwall flat (the roof thrust surface) in sequence, involves a systematic folding and unfolding of the horses as the duplex develops.

Butler & Coward (in press) describe the results of recent remapping of the Moine Thrust Belt, and suggest that it is more common for imbricate thrusts to cut up through a structurally higher major thrust rather than to join with it. Butler (1983) postulated imbricate thrusts

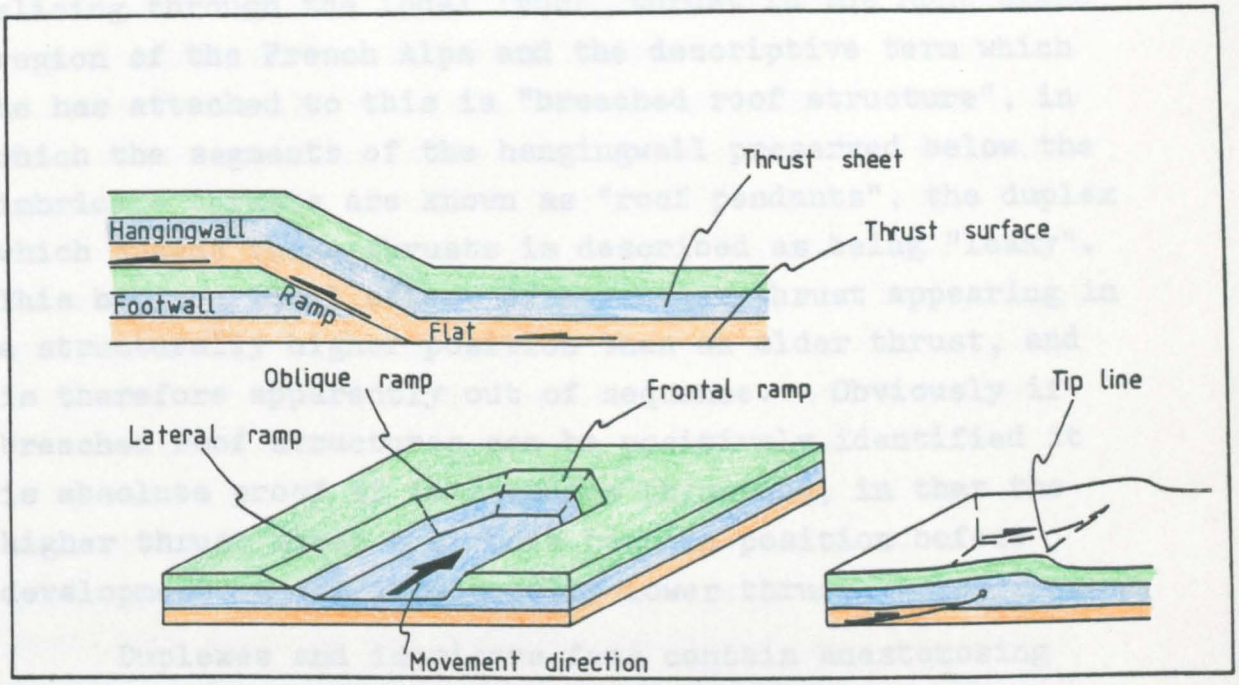

FIG. C. Thrust sheets and thrust surfaces.

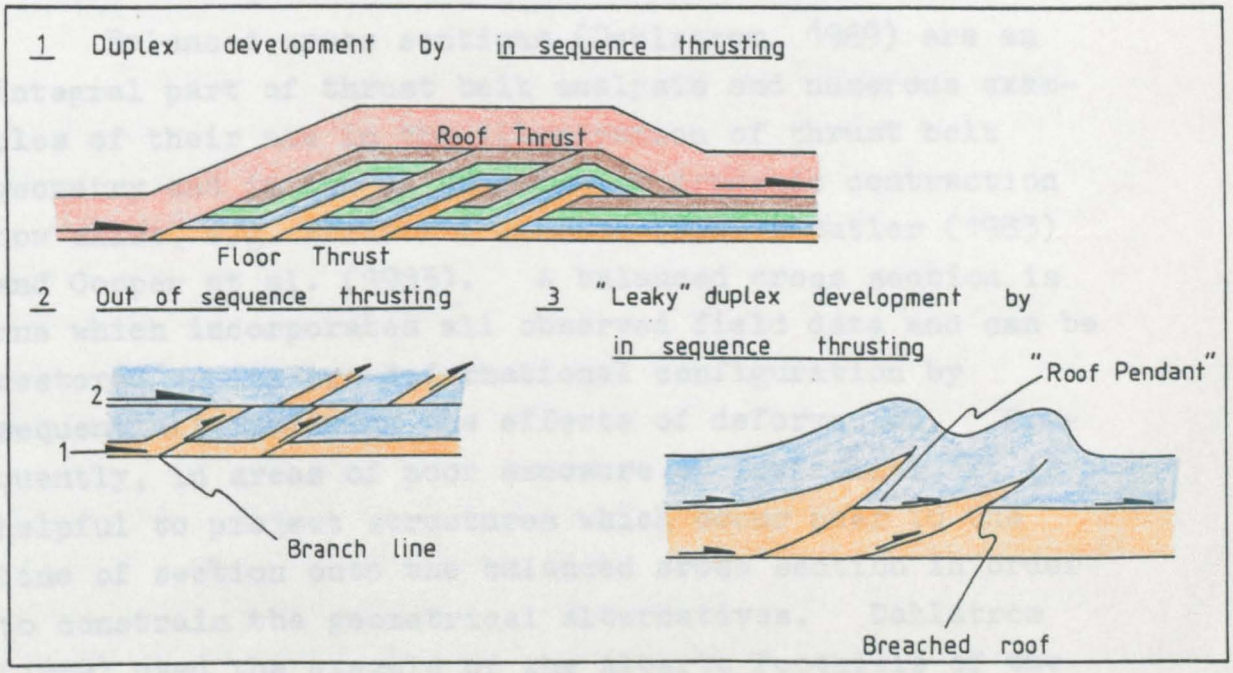

FIG. D. Thrust sequences and resulting geometry.

slicing through the local 'roof' thrust in the Mont Blanc region of the French Alps and the descriptive term which he has attached to this is "breached roof structure", in which the segments of the hangingwall preserved below the imbricate thrusts are known as "roof pendants", the duplex which spawns these thrusts is described as being "leaky". This has the local effect of a younger thrust appearing in a structurally higher position than an older thrust, and is therefore apparently out of sequence. Obviously if breached roof structures can be positively identified it is absolute proof of in sequence thrusting, in that the higher thrust sheet must have been in position before development of the structurally lower thrust.

Duplexes and imbricate fans contain anastomosing thrust surfaces, thrusts are frequently observed to branch off each other and they may rejoin at some position within the duplex. The line along which the lower thrust splays off the higher thrust is termed a trailing branch line, and the line along which the splay rejoins the higher thrust is termed a leading branch line.

(c) Balanced cross sections

Balanced cross sections (Dahlstrom, 1969) are an integral part of thrust belt analysis and numerous examples of their use in the illustration of thrust belt geometry and in the calculation of orogenic contraction now exist, e.g. Elliott & Johnson (1980), Butler (1983) and Cooper et al. (1983). A balanced cross section is one which incorporates all observed field data and can be restored to its pre-deformational configuration by sequentially removing the effects of deformation. Frequently, in areas of poor exposure or low relief, it is helpful to project structures which occur near to the line of section onto the balanced cross section in order to constrain the geometrical alternatives. Dahlstrom (1969) used the example of the Alberta Foothills of the Rocky Mountains to demonstrate how balanced cross sections can be applied to the external, or marginal, thrust zones

of orogenic belts. Sections must be constructed parallel to the movement direction of thrust sheets. In the Alberta Foothills the fold axes trend perpendicular to this direction, the folds are concentric and the thrust surface strike is parallel to the fold axes. As a result of this simple structural geometry, Dahlstrom was able to assume plane strain deformation as along-strike shortening or extension was insignificant. Therefore during the evolution of the Alberta Foothills the cross-sectional area of beds remained constant, allowing the restored cross sections to be checked with the balanced cross section. In order for the balanced section to be admissible the cross-sectional area must equal the cross sectional area on the restored section. In concentric folding situations a further simplification in checking the admissibility of a cross section is possible. The cross-sectional area is a function of the bed length and bed thickness; the bed thickness remains constant during formation of concentric folds, therefore the cross-sectional bed length will also remain constant during deformation. So the most rapid check for cross section admissibility is a verification that the bed lengths on the balanced and restored sections are equal.

Hossack (1979) reviewed the use of balanced cross sections in the calculation of orogenic contraction and demonstrated how balanced cross sections will differ from their restored versions in terms of cross sectional area where the deformation cannot be simplified as due to plane strain. A specific stratigraphic interval within the Etnedal nappes of the Norwegian Caledonides (Hossack, 1979) has undergone an average 20-25% ductile flattening during cleavage formation which has resulted in an equivalent reduction in formation thickness. If the present day cross sectional area is divided by the original stratigraphic thickness of the nappes, then the original length of the section can be estimated. Clearly, the geometrical changes which occur during internal deformation of thrust sheets have to be incorporated on balanced

cross sections. By introducing a simplifying assumption of no volume change during thrust belt evolution, then any along strike elongation can be calculated from consideration of the area reduction in the plane of the balanced cross section, constructed parallel to the displacement direction. Finite strain data must therefore be obtained, if possible, from thrust sheets where there is significant internal deformation in order to produce a final realistic restored section; without this orogenic contraction cannot be calculated.

In practice, construction of restored sections which accurately reflect the pre-deformational configuration of stratigraphic units is problematic unless field mapping can be backed up with borehole or other subsurface data. For this reason, sections constructed in areas of complex thrust patterns often require preliminary assumptions of consistent thickness of stratigraphic units in order to arrive at a 'constrained' value for the amount of local orogenic shortening.

Problems and assumptions involved with construction of balanced cross sections in the two study areas are discussed in the relevant sections.

PART ONE

THE KINLOCHEWE REGION OF THE MOINE THRUST ZONE, N. W. SCOTLAND

Frontispiece : Beinn Eighe

CHAPTER 1

REGIONAL GEOLOGY OF THE KINLOCHEWE REGION

1.1 REGIONAL STRATIGRAPHY

(i) Precambrian

The Precambrian stratigraphy of the southern Moine Thrust Zone consists of a basement of Lewisian gneiss overlain by a thick succession of Proterozoic sandstone (the Torridonian sandstone). This sequence comprises conglomeratic units, sandstones and shales and is subdivided into two groups, the older Stoer group and the younger Torridon group (Stewart, 1969). The Stoer group attains a maximum thickness of approximately 2 km and a Rb/Sr whole rock isochron has yielded an age of 995 ± 24 m.y. (Moorbath, 1969). The Torridon group consists of up to 7 km of sandstone and shale which unconformably overlies the Stoer group. It is subdivided into 4 lithological units, a lower grey shale termed the Diabaig formation, which is overlain by the Applecross, Aultbea and Callaigh Head formations. The Applecross formation has yielded an Rb/Sr age of 810 ± 17 m.y. (Moorbath, 1969). In the south of the Moine Thrust Zone on Skye and on the adjacent mainland the Torridon group conformably overlies the Sleat group which consists of approximately 3500 m of grey sandstone and shale.

In the Kinlochewe area, only a thin (approximately 150 m) equivalent of the Diabaig formation is observed within the thrust zone. In the foreland, the Applecross formation (300-1200 m of sandstone and conglomerate) directly overlies the Lewisian gneiss and no equivalent of the Diabaig formation is observed. A fine grained sandstone and shale sequence which occurs below the Applecross formation within the Kinlochewe Thrust Sheet was mapped by the Geological Survey as an equivalent of the Diabaig formation. Restoration of the Kinlochewe Thrust Sheet to its pre-deformational position (see Section 2.3), illustrates

that there must have been a minimum separation of approximately 25 km between the exposed Diabaig formation in the foreland and the equivalent facies now exposed within the thrust belt. Therefore, although it is clear that local deposition of a shale dominated facies was a feature of lower Torridon group sedimentation, it is unnecessary to label all shale sequences which occur in this position within the thrust zone as "Diabaig". The obvious feature of lower Torridon group sedimentation is the immense variation in thickness of the shale/fine grained sandstone facies. The problems of correlation of the Sleat group with the Diabaig formation are discussed by Potts (1983).

(ii) Cambrian

The Cambrian succession of the Moine Thrust Zone comprises five major lithological units which are illustrated in Fig. 1.1. The Eriboll Sandstone consists of a sequence of quartzites which vary in thickness along the length of the zone, as was noted by Peach et al. (1907) during detailed mapping of the N.W. Highlands. Recent mapping of the Kinlochewe region by S.J. Matthews has revealed a very gradual increase in thickness of the Eriboll sandstone along a present day WNW to ESE direction, from a local thickness of 250 m in the foreland on Beinn Eighe (see Fig. 1.1) to approximately 300 m near to Loch Clair (see Fig. A). This 'down-dip' thickness increase, which is not due to tectonic thickening, is incorporated onto the restored cross section illustrated in Fig. 2.5. This thickness variation is not as marked as the increase observed on the foreland from approximately 130 m near to Lochan Fada in the N to approximately 250 m on Beinn Eighe in the S, an along strike distance of approximately 10 km. Peach et al. (1907) established that the Eriboll Sandstone is often thicker in the south of the Moine Thrust Zone than it is in the north, but no published work has referred to stratigraphic thicknesses in the Kinlochewe area and the figure of 300 m quoted above suggests that the maximum development of Eriboll Sandstone may be observed within

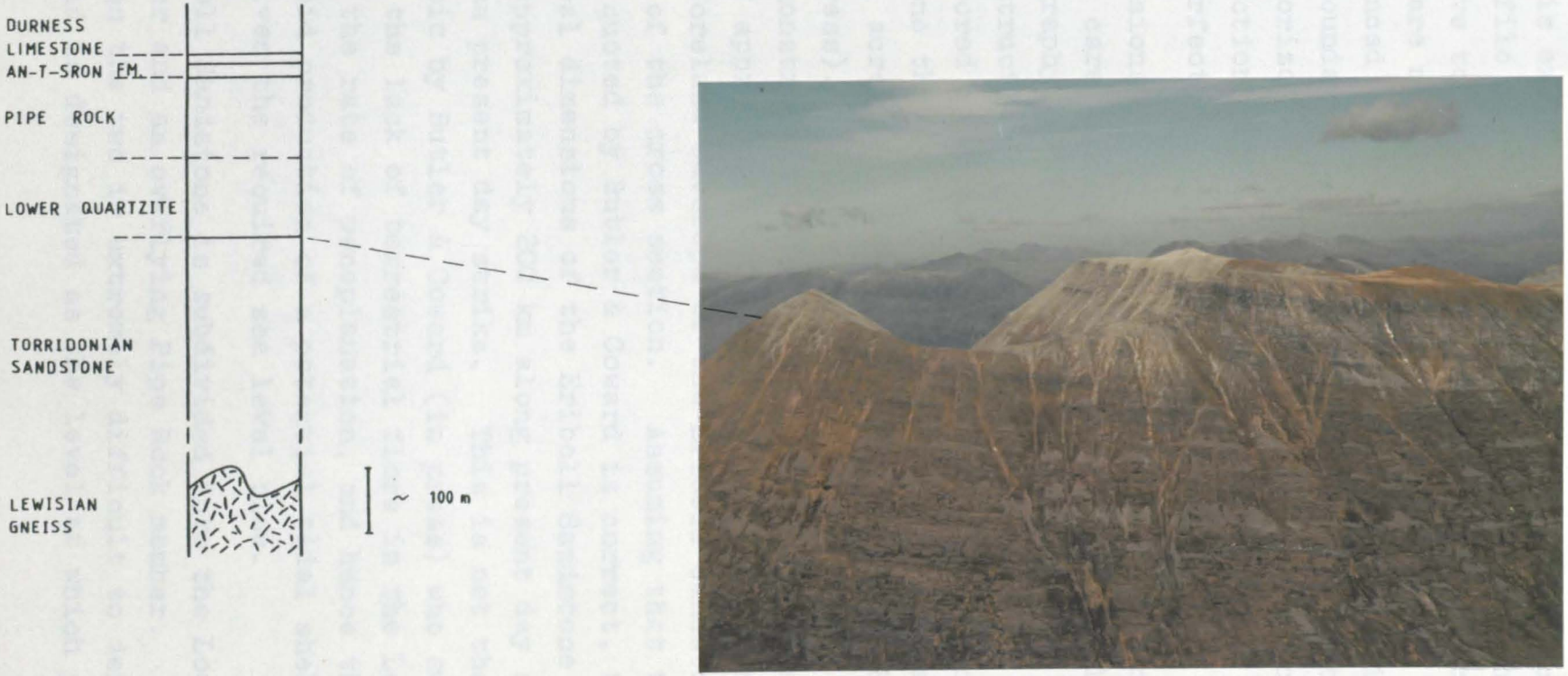

FIG. 1.1 Stratigraphy of the Kinlochewe region of the Moine Thrust Zone.

the thrust zone near to Kinlochewe.

From the point of view of a study of thrust evolution, the original 3 dimensional geometry of the Eriboll Sandstone slab is extremely important. Assumptions concerning the profile of thrust surfaces on restored cross sections relative to a horizontal datum plane at the time of deformation are necessary in order to build up an admissible balanced cross section. However, if bedding planes and/or boundaries between lithologies are substituted for the horizontal datum plane during balanced cross section construction, then the restored sections will illustrate a perfectly layer cake stratigraphy.

The dimensions of the Eriboll Sandstone slab can best be estimated by careful removal of the effects of duplication of stratigraphy as a result of thrusting. This process of constructing restored sections and hence eventually restored maps, reveals that in the northern Moine Thrust Zone the Eriboll Sandstone had an original minimum extent, across present day strike, of 54 km (Butler & Coward, in press). In the Kinlochewe region it is possible to demonstrate a corresponding minimum across strike width of approximately 20 km, a figure which involves projection of foreland outcrops of the Eriboll Sandstone into the plane of the cross section. Assuming that the minimum figure quoted by Butler & Coward is correct, then the minimum areal dimensions of the Eriboll Sandstone slab may have been approximately 200 km along present day strike and 54 km across present day strike. This is not thought to be problematic by Butler & Coward (in press) who suggest a link between the lack of terrestrial flora in the Lower Palaeozoic and the rate of peneplanation, and hence the facility of rapid production of a potential tidal shelf environment, given the required sea level rise.

The Eriboll Sandstone is subdivided into the Lower Quartzite member and an overlying Pipe Rock member. The boundary between the two is extremely difficult to define and in the field is designated as the level at which pipes

(fossil worm burrows) first become abundant. The Lower Quartzite is characterised by a basal conglomerate which represents a marine transgression across the underlying Lewisian Gneiss and Torridonian sandstone. The boundary between the Torridonian sandstone and the Lower Quartzite is a planar unconformity and in several localities within the Moine Thrust Zone the Lower Quartzite is unconformable across Torridonian sandstone onto Lewisian gneiss, revealing a "double-unconformity". The Lower Quartzite typically comprises approximately half of the Eriboll Sandstone formation. The exact age of the basal unit of the Lower Quartzite is problematic, and it is usual to label the whole of the Eriboll Sandstone as Early Cambrian.

The Pipe Rock member was subdivided into 5 zones by Peach et al. (1907) on the basis of characteristic types of pipe, based largely on the diameter of the fossil worm burrow on bedding planes. The validity of this approach was challenged by Swett (1969), who expressed doubt as to the lateral continuity and correlatable value of the Pipe Rock zones. However, Pipe Rock zones are very useful in identification of thrust units in the northern Moine Thrust Zone (Parish, pers. comm.). Two types of pipe have been identified; these are the genus Skolithus and Monocraterion. Skolithus typically occurs as a straight burrow, subperpendicular to bedding, varying in diameter from 3-15 mm and may be up to 1 m long. Monocraterion is similar to Skolithus but differs in that it has a funnel or 'trumpet' appearance on a section normal to bedding. Swett (1969) considers that both types of burrow may have been formed by the same animal and that trumpet pipes are due to rapid upward movement of the animal after an influx of sediment into the burrow. Confident prediction of the position of an exposure of Pipe Rock within the succession, based on the diameter of pipes, is difficult within the thrust zone of the Kinlochewe region. However, the trumpet pipe level appears to be quite consistent within the area, and this is used to locate the position of the Lower Quartzite at depth and the top of the Pipe Rock above.

The Eriboll Sandstone is conformably overlain by the An t-Sron formation which consists of a lower unit of calcareous shale, the Fucoid Beds, typically attaining a thickness of approximately 25 m and an upper unit of quartzite, the Salterella Grit (usually termed the Serpulite Grit), which has a development of approximately 15 m. The Fucoid Beds yield the trilobite Olenellus in the Kinlochewe region (Peach et al., 1907), and the Serpulite Grit yields a small conical fossil now known as Salterella, originally termed Serpulites, hence the popular name for this formation. These fossils date the An t-Sron formation as late Early Cambrian (Bonnia - Olenellus zone).

The An t-Sron formation is overlain by the Durness Limestone, which reaches a maximum development in the Kinlochewe region of approximately 130 m near to Lochan Fada; the lowest unit of the Durness Limestone is the Ghrudaidh formation which also yields Salterella. No younger stratigraphy is exposed in the area, although in the north of the zone a thicker development of Durness Limestone reveals an Ordovician age for the uppermost part of the formation.

1.2 REGIONAL STRUCTURE

The structural units of the Kinlochewe region are illustrated in Fig. 1.2. Four distinct units can be identified; from W to E these are:

1. Foreland (structurally lowest)
2. Beinn Eighe Imbricate Fan
3. Kinlochewe Thrust Sheet
4. Moine Thrust Sheet (structurally highest)

The structure of the area is described by Peach et al. (1907); this description is based on the original mapping of the Moine Thrust Zone by the Geological Survey which was carried out between 1885 and 1895. Since then, no description directly concerned with the structure of the Kinlochewe region has been published. McClay & Coward (1981) provide a brief résumé of the geometric relationships

between the Kinlochewe Thrust Sheet and the underlying imbricates, and Coward & Kim (1981) explain the orientation of fold axes within a part of the Kinlochewe Thrust Sheet in terms of a differential movement model. Coward (1982) uses the fault geometry observed to the N of Kinlochewe to suggest that the "Kinlochewe Fault" is an extensional feature and that the "Kinlochewe Sheet" may be part of an extremely large "surge zone", similar to smaller examples from the Assynt area of the Moine Thrust Zone. These points are examined in detail in Section 2.3.

Previous structural work carried out in the Moine Thrust Zone to the south of the study area since the original Geological Survey mapping includes the unpublished Ph.D. theses of Johnson (1955), Kanungo (1956), Barber (1969) and Potts (1983).

A brief description of the structure of the foreland is now given, the geometry and structural evolution of the Beinn Eighe Imbricate Fan and the Kinlochewe Thrust Sheet is the subject of Chapters 2 and 3.

The geometry of the constituent units of the foreland immediately prior to Caledonian deformation can be gauged from the remaining exposed foreland in the Kinlochewe region. The undulating unconformity between the Lewisian gneiss and overlying Torridonian sandstone is well illustrated in the north of the study area on Slioch (see Fig. A) where the Lewisian topographic surface was moulded to a local relief of at least 700 m. Ten kilometres to the SSE, on Liatach (see Fig. A) the thickness of Torridonian sandstone is between 1000 and 1200 m in a region where the Lewisian topography is less undulating and of lower relief. The dominant control on local thickness variation within the Torridonian sandstone is therefore the 3 dimensional geometry of the Lewisian topography.

Late Precambrian folds are well developed throughout the region and have been recognised along the length of the foreland immediately beneath the Moine Thrust Zone (Peach et al.,1907; Soper & Barber, 1979). Typically these are

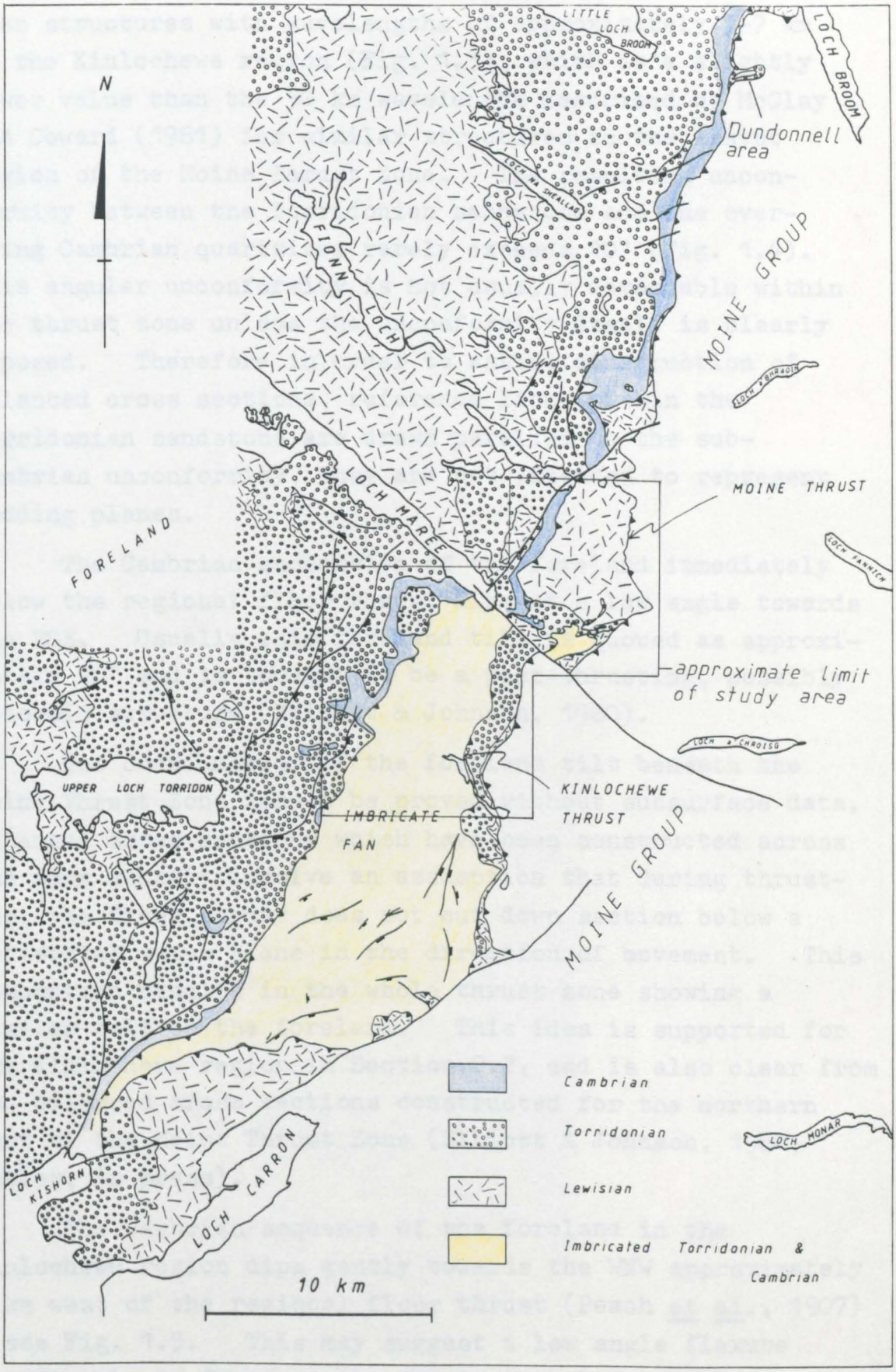

FIG. 1.2 Structure of the Moine Thrust Zone between Loch Broom and Lochcarron.

open structures with wavelengths of approximately 5-7 km in the Kinlochewe region (Fig. 1.3), which is a slightly lower value than the 50 km wavelength described by McClay and Coward (1981) for similar structures in the Assynt region of the Moine Thrust Zone. The resulting unconformity between the Torridonian sandstone and the overlying Cambrian quartzites rarely exceeds 10° (Fig. 1.4). This angular unconformity is not usually detectable within the thrust zone unless the unconformity itself is clearly exposed. Therefore in order to assist construction of balanced cross sections, reference lines within the Torridonian sandstone are drawn parallel to the sub-Cambrian unconformity, they are not intended to represent bedding planes.

The Cambrian succession of the foreland immediately below the regional floor thrust dips at a low angle towards the ESE. Usually this foreland tilt is quoted as approximately 10° and is thought to be a post-thrusting, possibly Mesozoic structure (Elliott & Johnson, 1980).

The continuation of the foreland tilt beneath the Moine Thrust Zone cannot be proved without subsurface data. Balanced cross sections which have been constructed across the zone usually involve an assumption that during thrusting, the floor thrust does not cut down section below a horizontal datum plane in the direction of movement. This assumption results in the whole thrust zone showing a similar tilt to the foreland. This idea is supported for the Kinlochewe region in Section 2.2, and is also clear from the balanced cross sections constructed for the northern part of the Moine Thrust Zone (Elliott & Johnson, 1980; Butler, in press).

The Cambrian sequence of the foreland in the Kinlochewe region dips gently towards the WNW approximately 6 km west of the regional floor thrust (Peach et al., 1907) - see Fig. 1.5. This may suggest a low angle flexure immediately in front of the developing thrust belt. However, in this area several regionally significant high

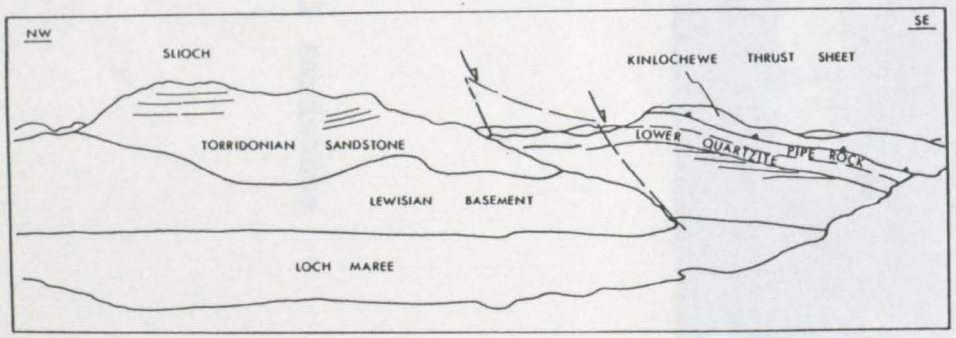

FIG. 1.3 Foreland structure N of Loch Maree, illustrating Lewisian topography, and the unconformity between the Eriboll Sandstone and the Torridonian Sandstone.

FIG. 1.4 Torridonian sandstone - Eriboll sandstone unconformity N of Loch Maree

angle normal faults offset the foreland stratigraphy, and these may be associated with regional post-thrusting extension and hence warping and tilting of the foreland and thrust zone. The major normal faults recognised by the Geological Survey are illustrated in Fig. 1.2.

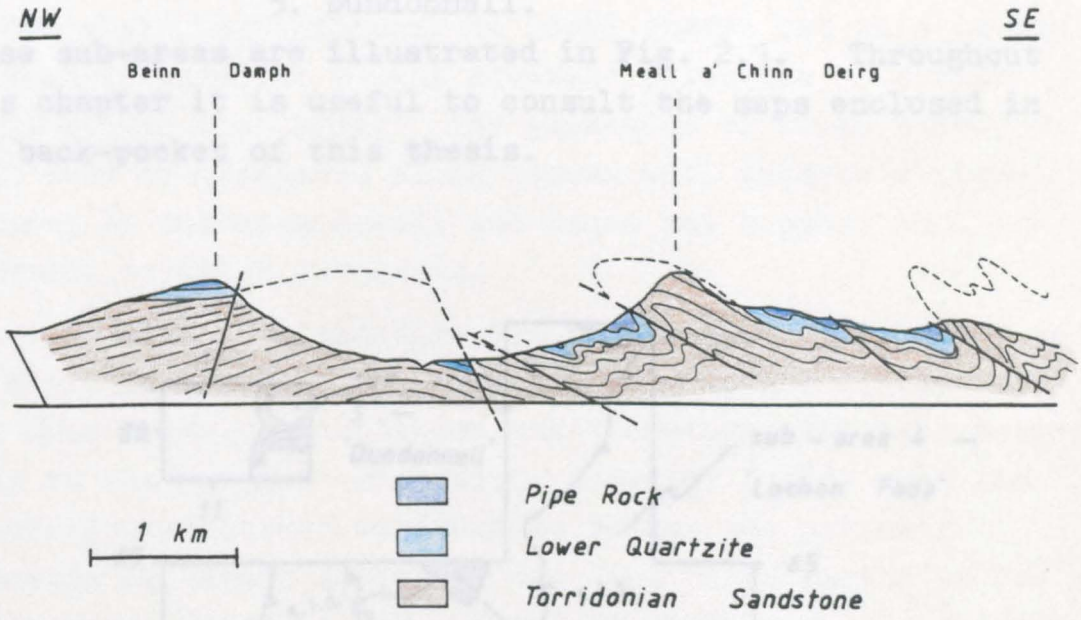

FIG. 1.5 Part of a Geological Survey cross section (Peach et al., 1907), illustrating the Eriboll Sandstone dipping to the WNW.

C H A P T E R 2

THRUST SHEET GEOMETRY IN THE KINLOCHEWE REGION

This chapter describes the 3 dimensional structure of the Beinn Eighe Imbricate Fan and the overlying Kinlochewe Thrust Sheet. For ease of description the study area has been subdivided into 5 sub-areas. These are;

1. Sgurr Dubh
2. Beinn Eighe
3. Meall a'Ghiubias
4. Lochan Fada - Kinlochewe
5. Dundonnell.

These sub-areas are illustrated in Fig. 2.1. Throughout this chapter it is useful to consult the maps enclosed in the back-pocket of this thesis.

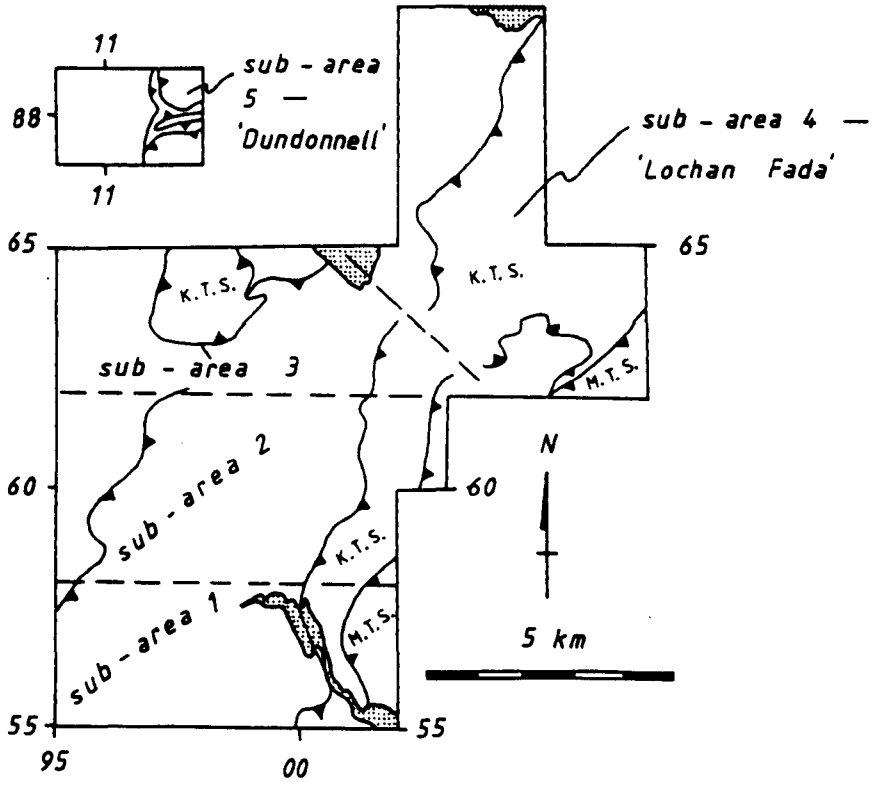

FIG. 2.1 Location map of sub-areas within the study region, K.T.S. (Kinlochewe Thrust Sheet), M.T.S. (Moine Thrust Sheet).

2.1 GEOMETRY OF THE BEINN EIGHE IMBRICATE FAN

(i) Movement direction of thrust sheets

The most useful direction of cross section construction is parallel to the movement direction of the thrust sheets as this allows the amount of shortening to be measured directly from the cross section. Elliott and Johnson (1980) suggest use of the procedure of finding the mean great circle through bedding normals on a stereogram and constructing the plane of cross section parallel to this mean great circle. This will inevitably produce a section approximately perpendicular to local strike but this is not necessarily parallel to the movement direction of thrust sheets within that area. The accretion of large horses which vary in thickness along strike will produce oblique flexures in the hangingwall and hence may suggest an incorrect movement direction.

Assuming foreland-directed thrusting is applicable to the Moine Thrust Zone, the structurally lowest imbricates will show least reorientation and therefore will be a better guide to the movement direction. Butler (1983) uses the orientation of thrust surfaces to deduce the movement direction of thrust sheets in the Mont Blanc region of the French Alps, where he has identified perfectly lateral ramps which strike parallel to the movement direction.

In the Kinlochewe region the most southerly imbricates show the effect of reorientation of strike as a result of the accretion of thicker imbricate slices, but the lowest imbricate slices within this part of the study area suggest a movement direction towards the WNW (290°). This is in agreement with the WNW movement direction deduced by Butler (1982a) for the region to the south of Loch Eriboll. Balanced cross sections have therefore been constructed in a WNW to ESE direction. The poles to bedding from the foreland and imbricates within each of the 5 sub-areas are illustrated on contoured stereograms in Fig. 2.2. This illustrates quite clearly the danger of invoking a movement direction perpendicular to local strike.

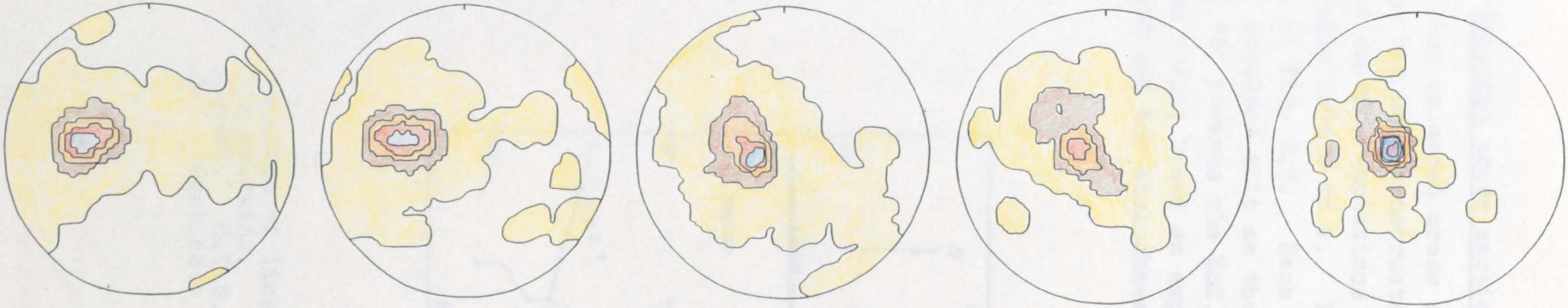

1 Sgurr Dubh n = 557

2 Beinn Eighe n = 387

3 Meall a'Ghiubias n = 337

4 Lochan Fada n = 289

5 Dundonnell n = 53

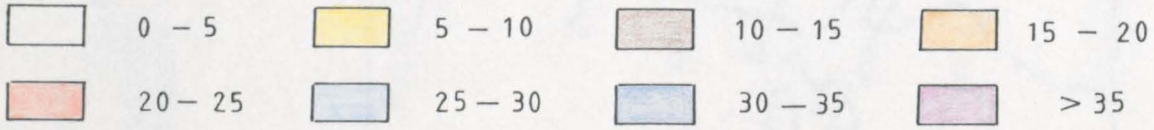

FIG. 2.2 Contoured stereograms of poles to bedding for each sub-area. Contours drawn at 5% of data intervals.

(ii) Balanced cross sections and tectonic shortening

Four balanced cross sections are presented. One section has been constructed across each sub-area to examine variations in cross sectional geometry and shortening from S to N. The lines of section are illustrated in Fig. 2.3. Each cross section shows the effect of the foreland tilt as the floor thrust dips at between 8° and 15° towards the ESE. Shortening estimates are minimum values based on exposed imbricates between the foreland and the Kinlochewe Thrust.

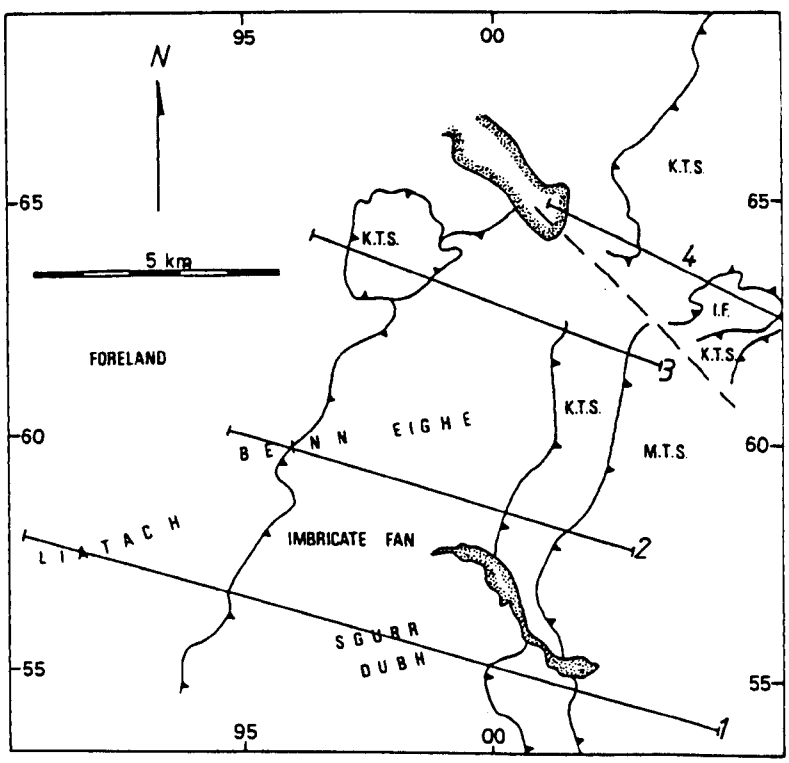

FIG. 2.3 Location of lines of balanced cross section construction. K.T.S. (Kinlochewe Thrust Sheet). M.T.S. (Moine Thrust Sheet), I.F. (Imbricate Fan).

Balanced cross section 1

Liatach (NG 91305765) to Loch Coulin (NH 01505520)

This balanced cross section is illustrated in Fig. 2.4. In the E of this section the immediate footwall to the Kinlochewe Thrust is in Fucoid Beds. The Kinlochewe Thrust Sheet and the upper part of the underlying duplex have been removed by erosion to expose the Sgurr Dubh imbricates. From outcrop data along this section line it is not possible to predict the stratigraphic level of the footwall to the Kinlochewe Thrust above present day ground level. This is the case for most of the study area except in the region of Meall a'Ghiubias where the footwall to the Kinlochewe Thrust in the foreland is in Fucoid Beds. The implications of subtle changes in the footwall level are examined in Section 2.3, but for the purpose of determining shortening within the imbricates it is assumed on the balanced cross sections that the "glide horizon" or footwall to the Kinlochewe Thrust is consistently in Fucoid Beds.

The maximum stratigraphic range observed within any imbricate slice is approximately 900 m of Torridonian and Eriboll Sandstone. It has been assumed that the stratigraphy above the sub-Cambrian unconformity was subhorizontal prior to deformation and that the floor thrust to the imbricates does not cut down stratigraphic section on the restored cross section. Therefore as approximately 600 m of Torridonian sandstone is exposed within one horse, this is the minimum depth of the floor thrust below the sub-Cambrian unconformity. Careful balancing of the section suggests a floor thrust level that cuts gradually up section from a depth of 850 m to 700 m below the sub-Cambrian unconformity over a horizontal distance of 10.5 km, an average floor thrust climb of less than 1°. The exposed imbricate fan restores to an across strike width of 12.8 km from the "pin-line" denoted by X on the cross sections. The present distance between points A' and B' on the balanced cross section is 5.47 km which indicates a shortening of approximately 7.33 km or 57.3%. The internal deformation within the imbricate fan is small (see Chapter 3) and the duplex areas on the balanced and restored cross sections are equal.

Fig. 2.4

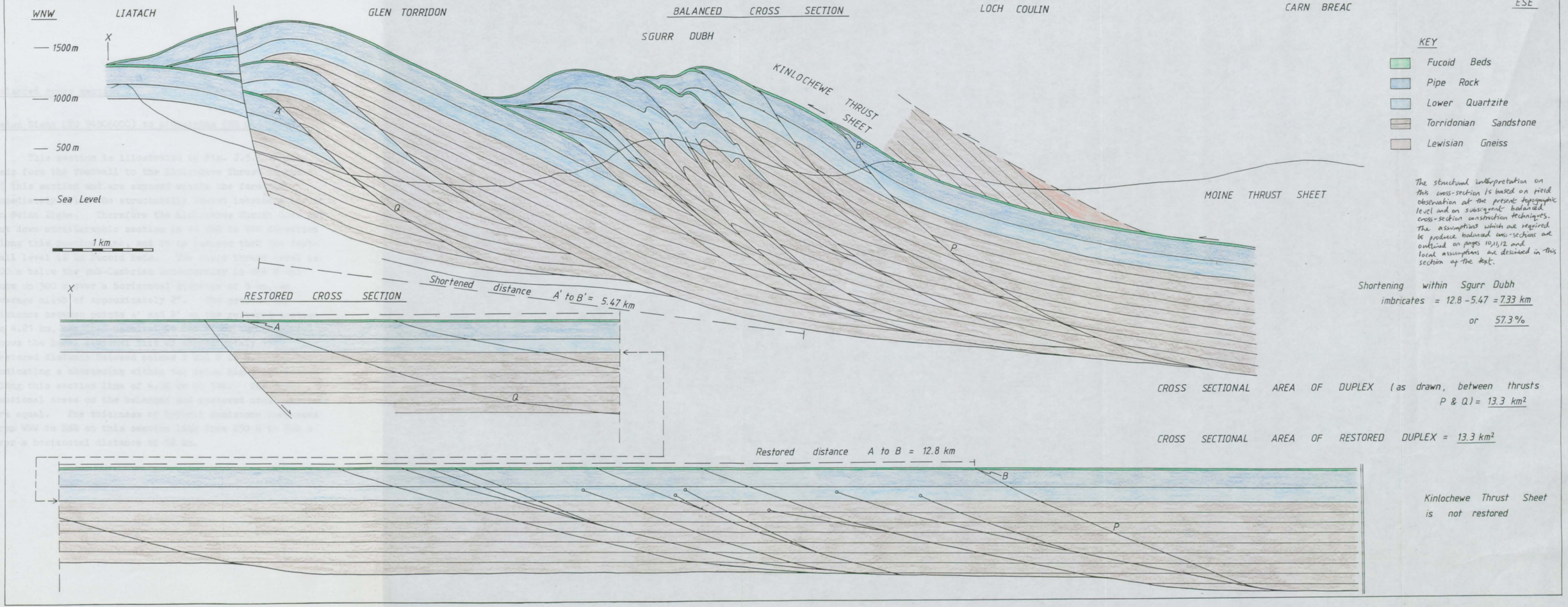

The structural interpretation on this cross-section is based on field observation at the present topographic level and on subsequent balanced cross-section construction techniques. The assumptions which are required to produce balanced cross-sections are outlined on pages 10,11,12 and local assumptions are described in this section of the text.

Shortening within Sgurr Dubh imbricates = 12.8 - 5.47 = 7.33 km

or 57.3%

CROSS SECTIONAL AREA OF DUPLEX (as drawn, between thrusts P & Q) = 13.3 km²

CROSS SECTIONAL AREA OF RESTORED DUPLEX = 13.3 km²

Kinlochewe Thrust Sheet is not restored

Balanced cross section 2

Beinn Eighe (NG 94806000) to A'Ghairbhe (NH 00505800)

This section is illustrated in Fig. 2.5. Fucoid Beds form the footwall to the Kinlochewe Thrust in the E of this section and are exposed within the foreland immediately below the structurally lowest imbricate thrust on Beinn Eighe. Therefore the Kinlochewe Thrust does not cut down stratigraphic section in an ESE to WNW direction along this section line, and it is assumed that the footwall level is in Fucoid Beds. The floor thrust level is 900 m below the sub-Cambrian unconformity in the E and cuts up 300 m over a horizontal distance of 9 km, an average climb of approximately 2°. The present day distance between points A' and B' on the restored section is 4.21 km, measured parallel to the floor thrust, which shows the local regional tilt of approximately 12°. The restored distance between points A and B is 9.17 km, indicating a shortening within the Beinn Eighe imbricates along this section line of 4.96 km or 54%. The cross sectional areas on the balanced and restored cross sections are equal. The thickness of Eriboll Sandstone increases from WNW to ESE on this section line from 250 m to 300 m over a horizontal distance of 12 km.

Fig. 2.5

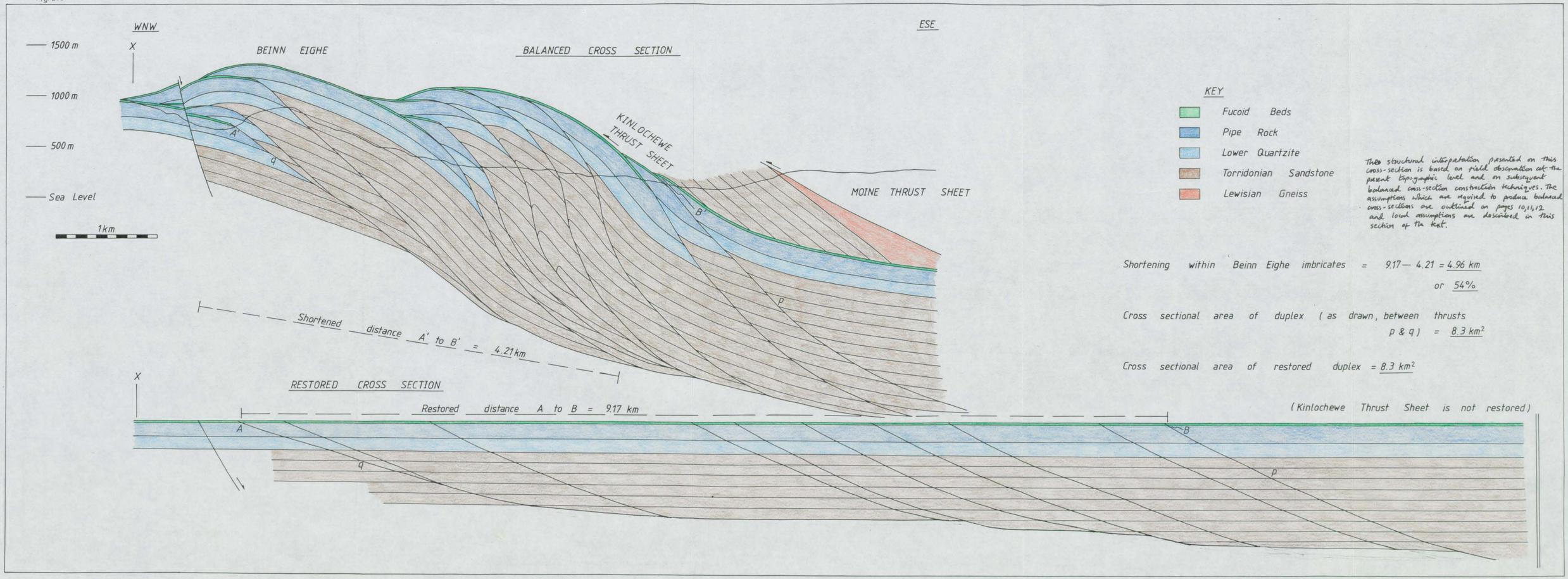
WNW
ESE
1500 m
1000 m
500 m
Sea Level
1km
X
BEINN EIGHE
BALANCED CROSS SECTION
KINLOCHEWE THRUST SHEET
MOINE THRUST SHEET
A'
B'
q
p
Shortened distance A' to B' = 4.21km
RESTORED CROSS SECTION
Restored distance A to B = 9.17 km
A
B
KEY
Fucoid Beds
Pipe Rock
Lower Quartzite
Torridonian Sandstone
Lewisian Gneiss
This structural interpretation presented on this cross-section is based on field observation at the present topographic level and on subsequent balanced cross-section construction techniques. The assumptions which are required to produce balanced cross-sections are outlined on pages 10,11,12 and local assumptions are described in this section of the text.
Shortening within Beinn Eighe imbricates = 9.17 — 4.21 = 4.96 km
or 54%
Cross sectional area of duplex (as drawn, between thrusts p & q) = 8.3 km²
Cross sectional area of restored duplex = 8.3 km²
(Kinlochewe Thrust Sheet is not restored)

Balanced cross section 3

Meall a'Ghiubias (NG 96506350) to Cathair Ruadh (NH 01806260)

This section is illustrated in Fig. 2.6. The footwall to the Kinlochewe Thrust in the E of this section is in Pipe Rock and in the foreland it is in Fucoid Beds. The Kinlochewe Thrust therefore cuts up stratigraphic section in the direction of movement. The floor thrust to the imbricates is 300 m below the sub-Cambrian unconformity in the E of the section and climbs to 150 m below the sub-Cambrian unconformity over a horizontal distance of 5.3 km, an averege climb of approximately 1.5°. The present distance between points A' and B' on the balanced cross section is 3.28 km and the restored distance between A and B is 6.03 km, a shortening of 2.75 km or 45.6%. The exposure along this section line between (NH 00806320) and (NH 00206330) is extremely poor and the predicted thrust geometry is illustrated on the balanced cross section.

Fig. 2.6

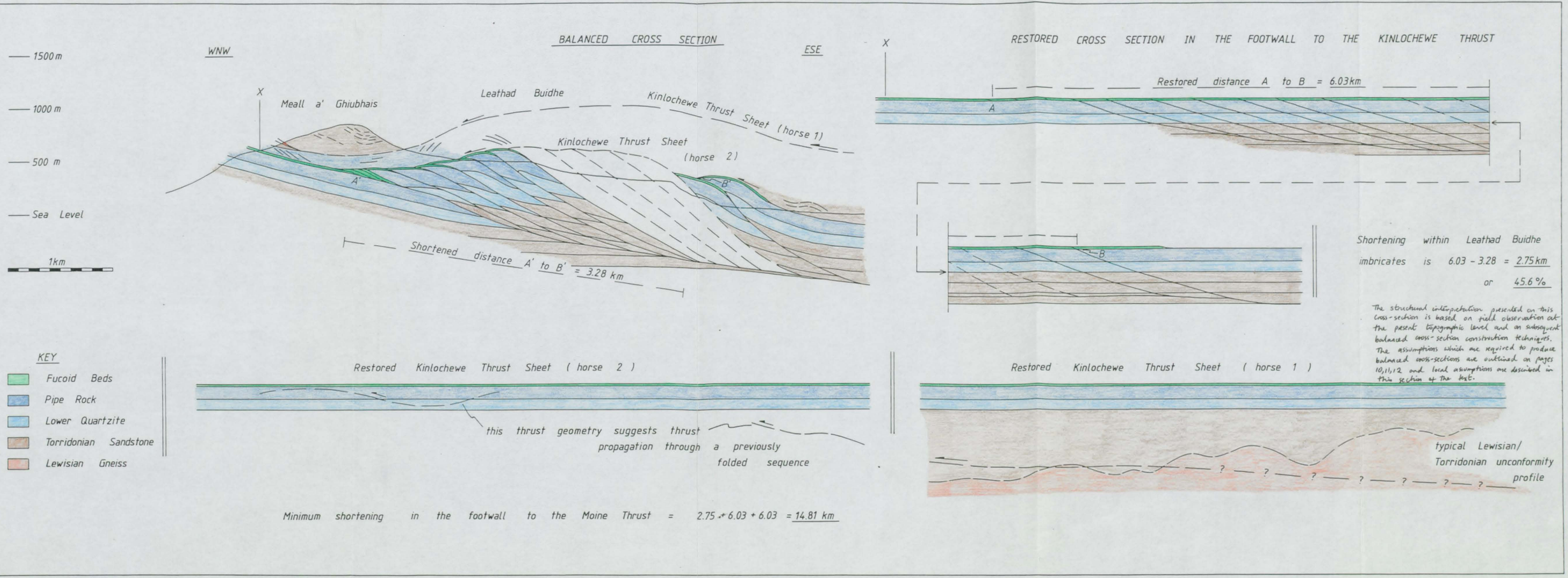
1500 m
1000 m
500 m
Sea Level
1km
BALANCED CROSS SECTION
WNW
ESE
X
Meall a' Ghiubhais
Leathad Buidhe
Kinlochewe Thrust Sheet (horse 1)
Kinlochewe Thrust Sheet (horse 2)
A'
B'
Shortened distance A' to B' = 3.28 km
RESTORED CROSS SECTION IN THE FOOTWALL TO THE KINLOCHEWE THRUST
X
Restored distance A to B = 6.03km
A
B
Shortening within Leathad Buidhe imbricates is 6.03 - 3.28 = 2.75km or 45.6%
The structural interpretation presented on this cross-section is based on field observation at the present topographic level and on subsequent balanced cross-section construction techniques. The assumptions which are required to produce balanced cross-sections are outlined on pages 10,11,12 and local assumptions are described in this section of the text.
KEY
Fucoid Beds
Pipe Rock
Lower Quartzite
Torridonian Sandstone
Lewisian Gneiss
Restored Kinlochewe Thrust Sheet (horse 2)
this thrust geometry suggests thrust propagation through a previously folded sequence
Restored Kinlochewe Thrust Sheet (horse 1)
typical Lewisian/ Torridonian unconformity profile
Minimum shortening in the footwall to the Moine Thrust = 2.75 + 6.03 + 6.03 = 14.81 km

Balanced cross section 4

Loch Maree (NH 01006450) to Heights of Kinlochewe (NH 05806280)

This section is illustrated in Fig. 2.7. The footwall to the Kinlochewe Thrust along this section line becomes progressively older from ESE to WNW, from Durness Limestone to the top of the Pipe Rock formation. The Kinlochewe Thrust therefore cuts down stratigraphic sequence along this section line. The implications of this geometry are discussed in Section 2.3. Two floor thrust levels are apparent from the balanced cross section, the lowest floor thrust cuts up stratigraphic section from 250 m to 100 m below the sub-Cambrian unconformity over a distance of 3.7 km, an average climb of 2.3°. The upper floor thrust level has developed near to the top of the Pipe Rock formation and encloses a separate, smaller imbricate system of Pipe Rock, Fucoid Beds, Serpulite Grit and Durness Limestone. The present distance between A' and B' on the balanced cross section is 2.1 km; removal of the shortening within both imbricate systems provides a restored distance between A and B of 6.2 km, a shortening of 4.1 km or 66%.

Cross sections constructed along similar section lines to those used here were presented by Peach et al. (1907), and these are illustrated in Figs. 2.8, 2.9, 2.10 and 2.11. Restored versions have been drawn based on projection of the Cambrian quartzites, to provide an estimate of the shortening implied by these original cross sections.

Fig. 2.7

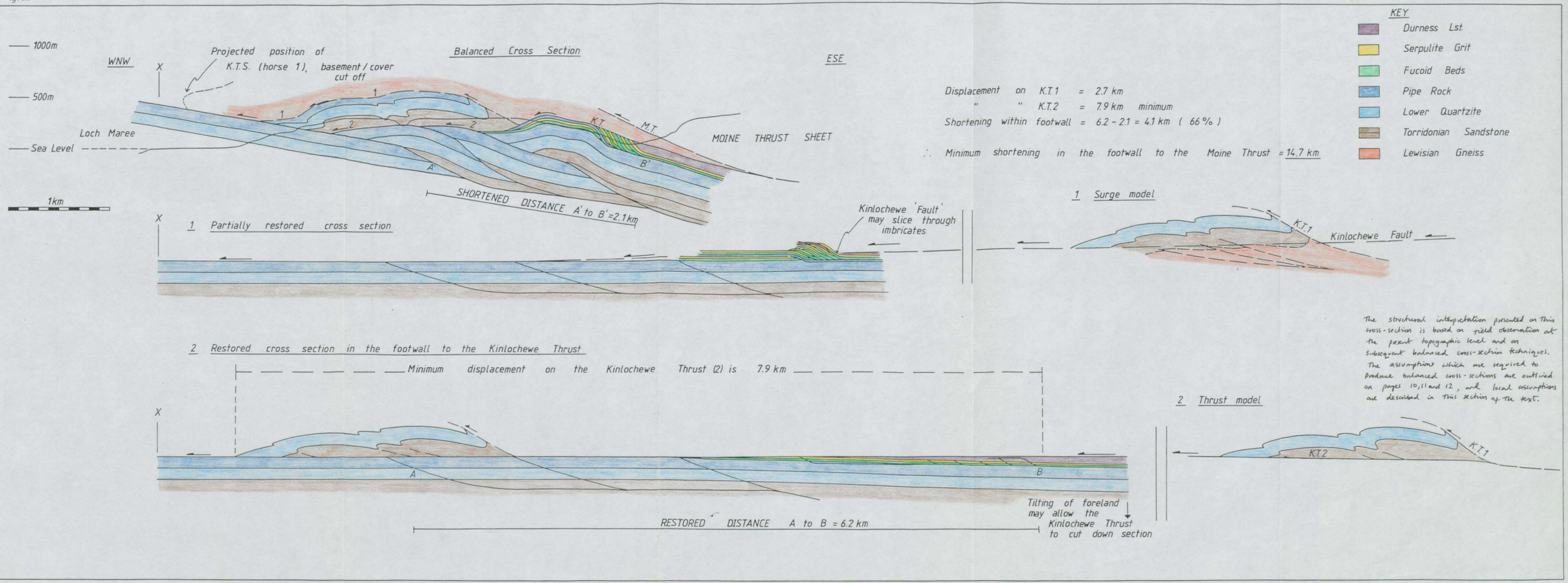

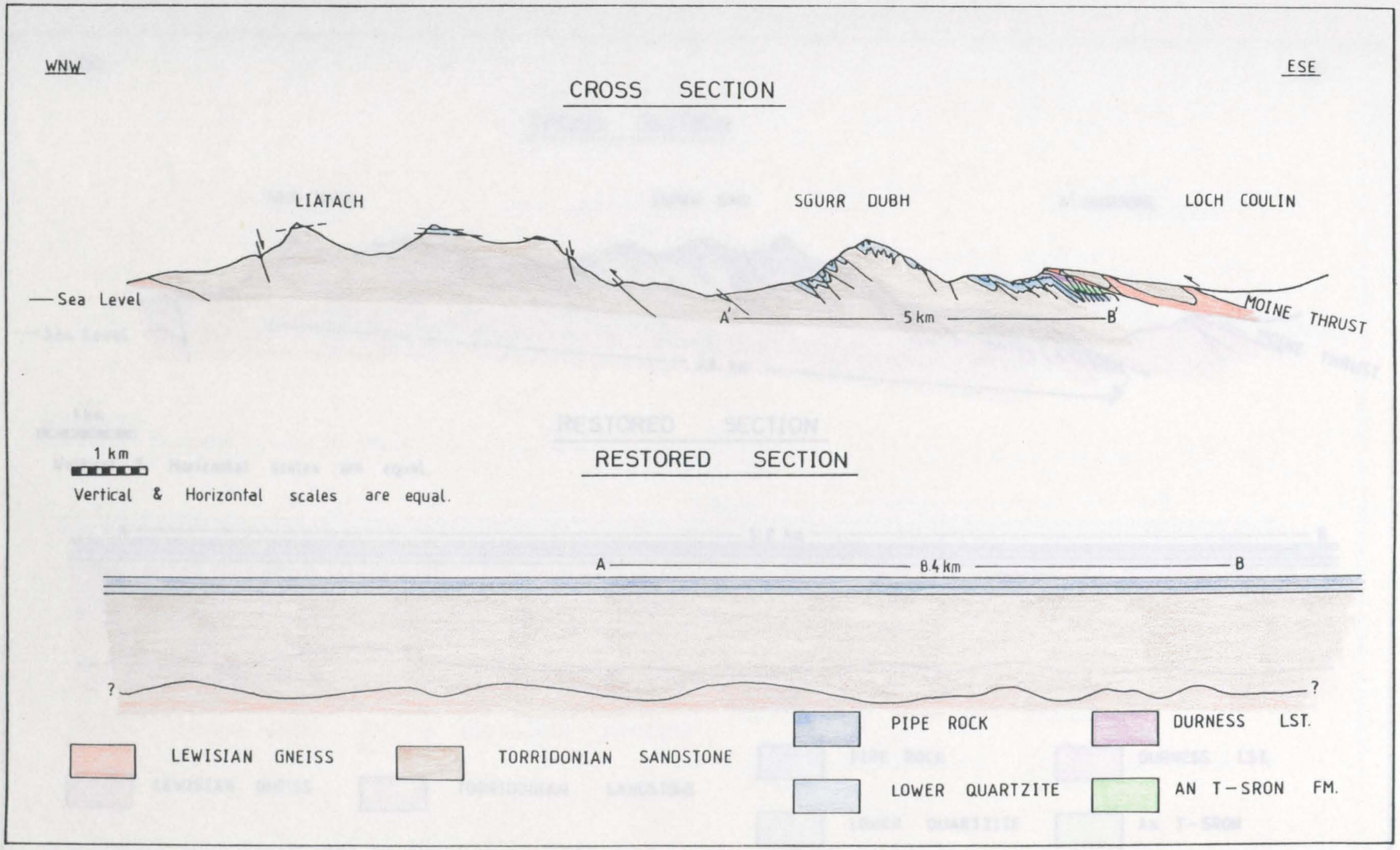

FIG. 2.8 Geological Survey cross section from Liatach to Loch Coulin. Restored version drawn by this author.

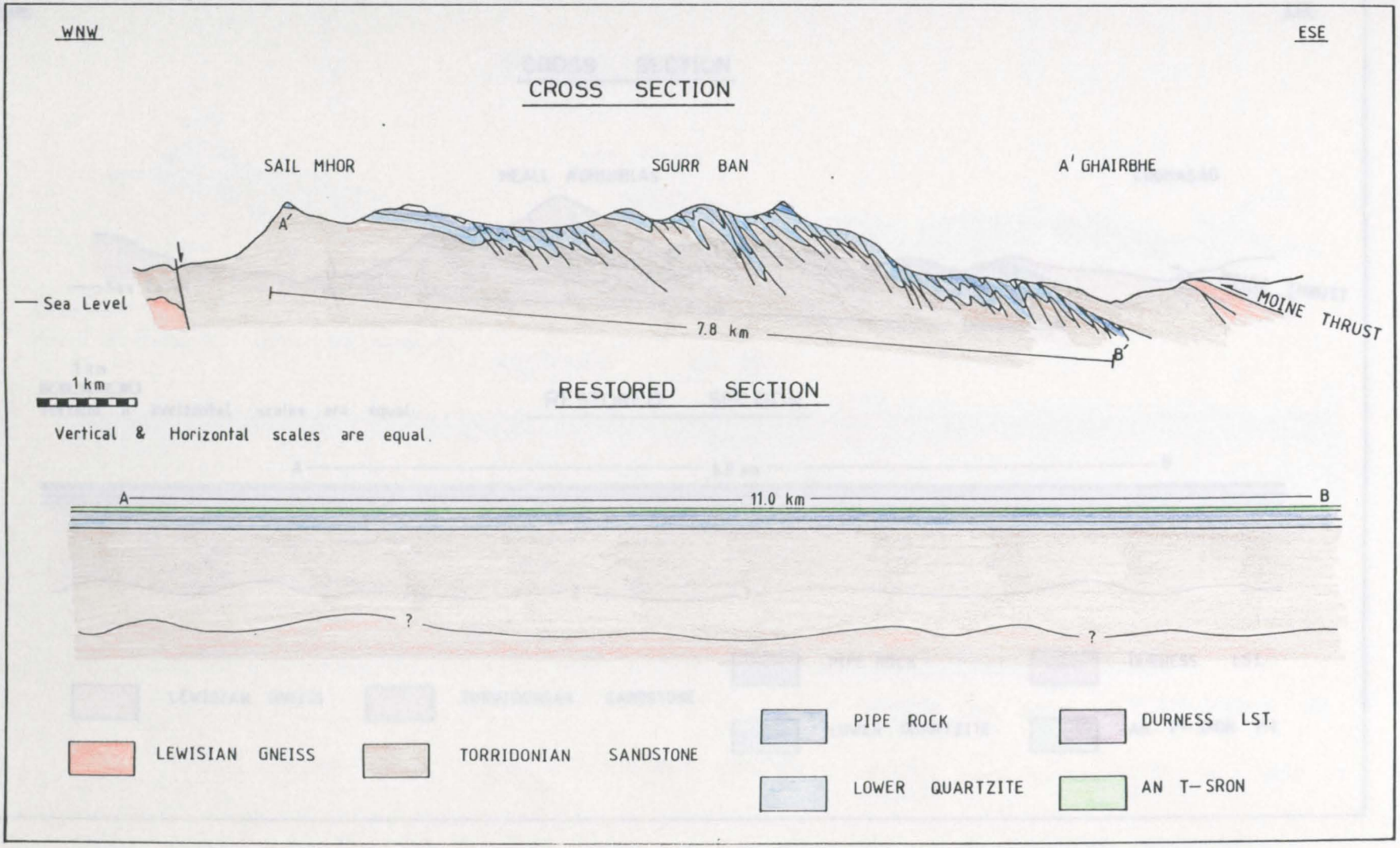

FIG. 2.9 Geological Survey cross section from Sail Mhor to A'Ghairbhe. Restored version drawn by this author.

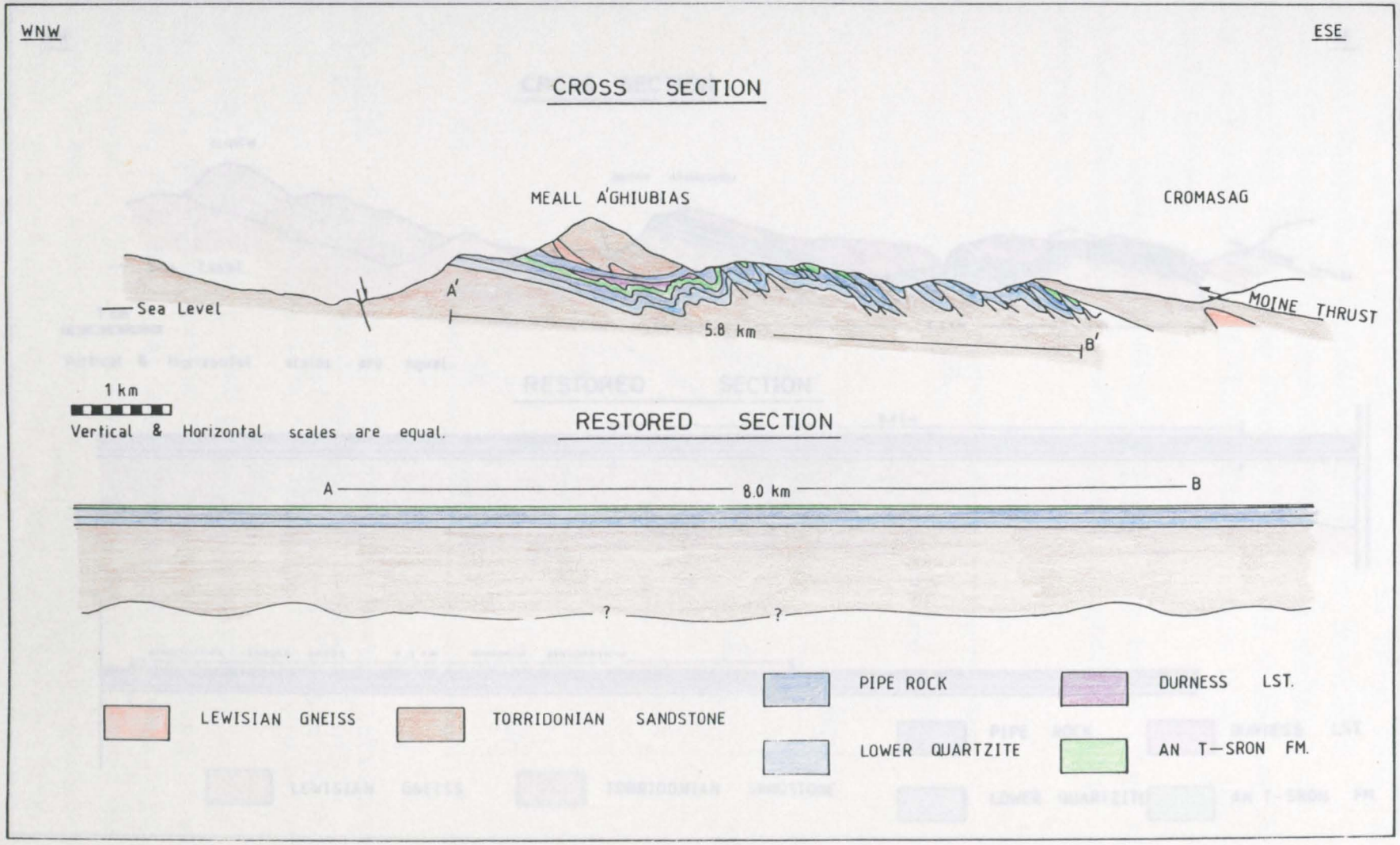

FIG. 2.10 Geological Survey cross section from Meall a'Ghiubias to Cromasag. Restored version drawn by this author.

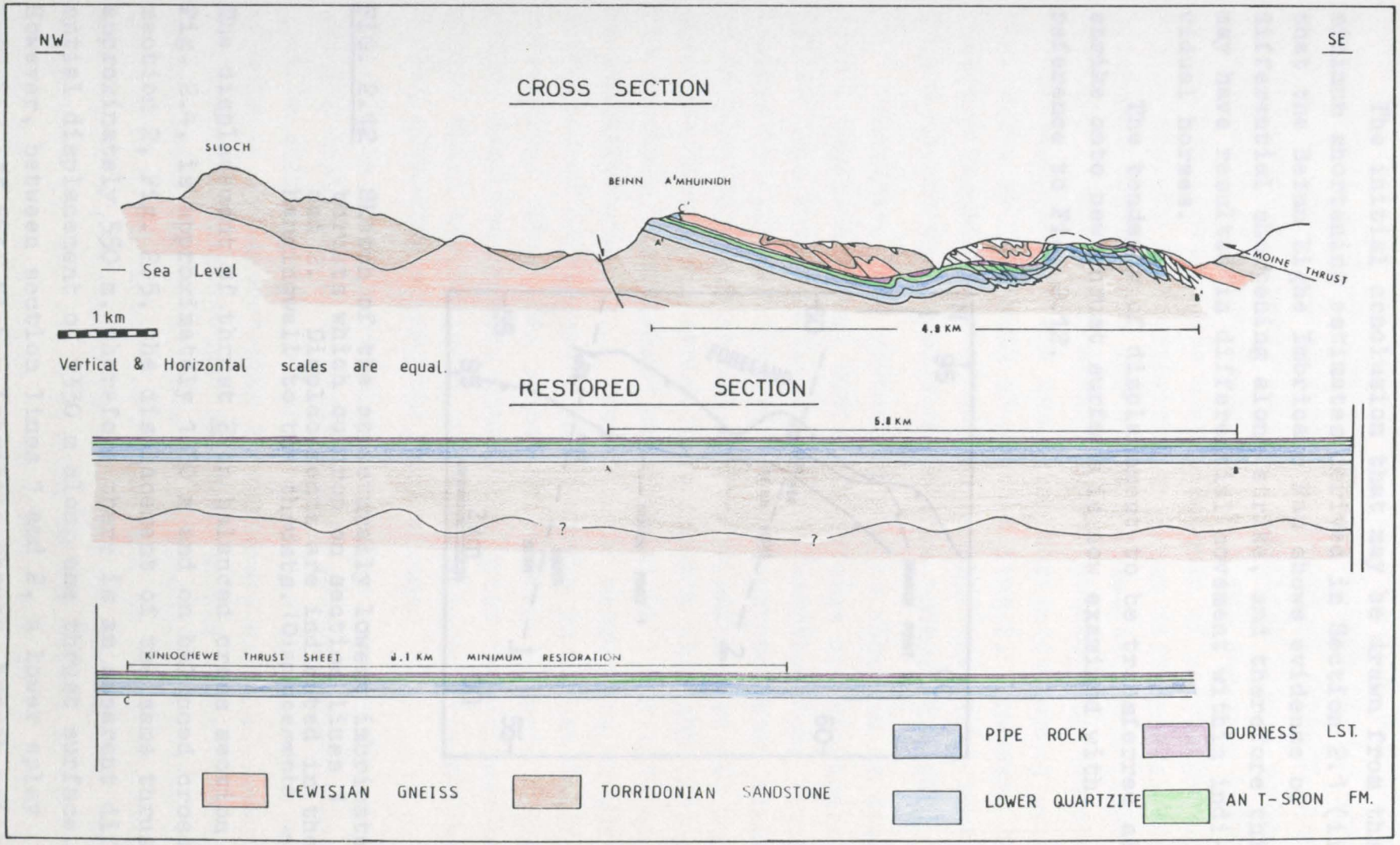

FIG. 2.11 Geological Survey cross section from Slioch to Abhuinn Bruachaig. Restored version drawn by this author.

(iii) Implications of shortening estimates

The initial conclusion that may be drawn from the minimum shortening estimates derived in Section 2.1 (ii) is that the Beinn Eighe Imbricate Fan shows evidence of differential shortening along strike, and therefore this may have resulted in differential movement within individual horses.

The tendency of displacement to be transferred along strike onto new thrust surfaces is now examined with reference to Fig. 2.12.

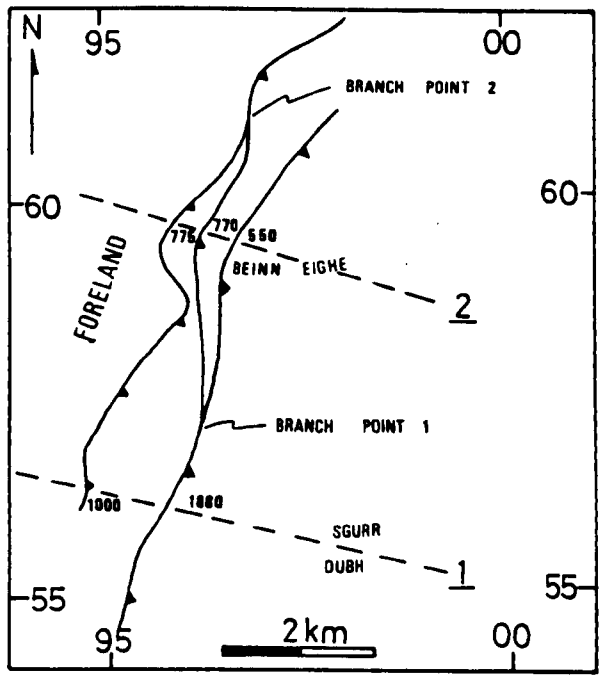

FIG. 2.12 Sketch of the structurally lowest imbricate thrusts which outcrop on section lines 1 and 2. Displacements are indicated in the hangingwall to the thrusts. (Displacements in metres).

The displacement of thrust 2 on balanced cross section 1, Fig. 2.4, is approximately 1880 m and on balanced cross section 2, Fig. 2.5, the displacement of the same thrust is approximately 550 m, therefore there is an apparent differential displacement of 1330 m along one thrust surface. However, between section lines 1 and 2, a lower splay branches off this higher imbricate thrust, branch point 1,

Fig. 2.12. The displacement of this lower splay on section line 2 is approximately 770 m, giving a combined displacement of 1320 m on a part of section line 2 as opposed to 1880 m on an equivalent part of section line 1. The structurally lowest thrust on section line 1 shows a displacement of approximately 1000 m and the same thrust on section line 2 shows a displacement of approximately 775 m, thereby increasing the apparent differential displacement between the two section lines to 785 m (2880 m - 2095 m). This structurally lowest outcropping imbricate thrust branches off the overlying thrust at branch point 2, Fig. 2.12, to the north of section line 2; however, the observed displacement of 1000 m on this thrust on section line 1 is not conserved along strike towards the NNE.

Therefore if a thrust surface is observed to branch into 2 separate thrust surfaces, it does not necessarily follow that total displacement is conserved along strike. A simplification of the real example quoted above might state that if a thrust (A) showing displacement (X) branches some distance along strike into thrusts (A') and (A") then the combined displacement on surfaces (A') and (A") need not be equivalent to (X). Therefore an assumption of conservation of displacement along strike in thrust belts is not valid. This idea is not at all new; Coward & Kim (1981) describe strains within the Moine Thrust Zone at Assynt which are believed to have developed from differential movements within the thrust zone.

It is clear that thrust surfaces splay off each other and the implication of differential shortening is that there must be differential movement of horses within imbricate systems. As demonstrated in the above example, some of the differential displacement observed on one thrust surface can be accounted for by a lower splay branching off that thrust surface along strike. Assuming that an imbricate system evolves as a foreland directed sequence then it can be suggested that any extra displacement observed along strike within the imbricate fan is accounted for by an equivalent amount of compensating displacement on the higher thrust

surface, in this case the Kinlochewe Thrust. In an ideal duplex system (Boyer & Elliott, 1982, p.1208) structurally higher horses are carried piggy-back as each developing imbricate thrust moves along the floor thrust surface. The hangingwall to the duplex, in this case the Kinlochewe Thrust Sheet, is also carried piggy-back. Therefore the differential shortening occurring within a developing duplex must be reflected by differential movement strains within the horses and also within the overlying thrust sheet. It has been demonstrated that it is an oversimplification to 'add' displacements and assume that all displacement is transferred along strike within an imbricate system. It is also an oversimplification to assume that the 'missing' displacement necessary for consistent along strike shortening can be transferred from within an imbricate system up onto the roof thrust, which would typically be a regionally significant major thrust.

Evidence of differential movement within the Beinn Eighe Imbricate Fan is dealt with in Chapter 3, and oblique folds within the Kinlochewe Thrust Sheet are discussed in terms of a differential movement model in Section 2.3. Differential movement within a thrust sheet is dependent on variable displacement on thrust surfaces. The influence of the dimensions of horses, and hence the level of the floor thrust, on the displacement is now examined.

(iv) Horse dimensions, displacement and ramp angles

The influence of the size of a horse on displacement on the underlying thrust surface is now examined on balanced cross sections 1, 2 and 3. The thickness of each horse in its central portion (T) has been measured and then multiplied by the ramp length (R) to give an approximate cross sectional area for the horse. This value is then compared with the displacement (D) on the underlying thrust. The values obtained from direct measurement off the balanced cross sections are illustrated in Table 2.1. These values have been plotted graphically and the graphs are illustrated in Fig. 2.13.

SGURR DUBH

Horse	Thickness (T)	Ramp length (R)	R.T.	Displacement (D)
1	0.53	3.67	1.94	1.00
2	1.13	4.89	5.54	1.88
3	0.18	4.78	0.85	0.98
4	0.07	2.00	0.13	0.44
5	0.07	1.67	0.12	0.11
6	0.27	3.78	1.01	0.78
7	0.22	2.89	0.64	0.09
8	0.09	3.11	0.28	0.18
9	0.29	2.22	0.64	0.22
10	0.27	4.89	1.31	1.00
11	0.22	2.89	0.64	0.31
12	0.38	4.00	1.51	0.04

N.B. The thrusts which underly horses 7 and 9 are blind thrusts, see Sgurr Dubh balanced cross section, Fig. 2.7.

BEINN EIGHE

Horse	Thickness (T)	Ramp length (R)	R.T.	Displacement (D)
1	0.09	2.11	0.19	0.78
2	0.51	3.89	1.99	0.77
3	0.98	2.67	2.60	0.55
4	0.13	2.67	0.35	0.47
5	0.31	2.67	0.83	0.89
6	0.31	3.56	1.11	0.44
7	0.31	3.44	1.07	0.27
8	0.53	3.33	1.78	0.09
9	0.26	3.22	0.86	0.42

MEALL A'GHIUBIAS

Horse	Thickness (T)	Ramp length (R)	R.T.	Displacement (D)
1	0.08	1.67	0.15	0.67
2	0.11	1.44	0.16	0.07
3	0.11	1.66	0.18	0.18
4	0.11	2.04	0.23	0.38
5	0.09	1.89	0.17	0.20
6	0.13	1.89	0.25	0.20

TABLE 2.1 Horse dimensions and displacement on imbricate thrusts for balanced cross sections 1, 2 and 3. All measurements are km except R.T. which is km^2.

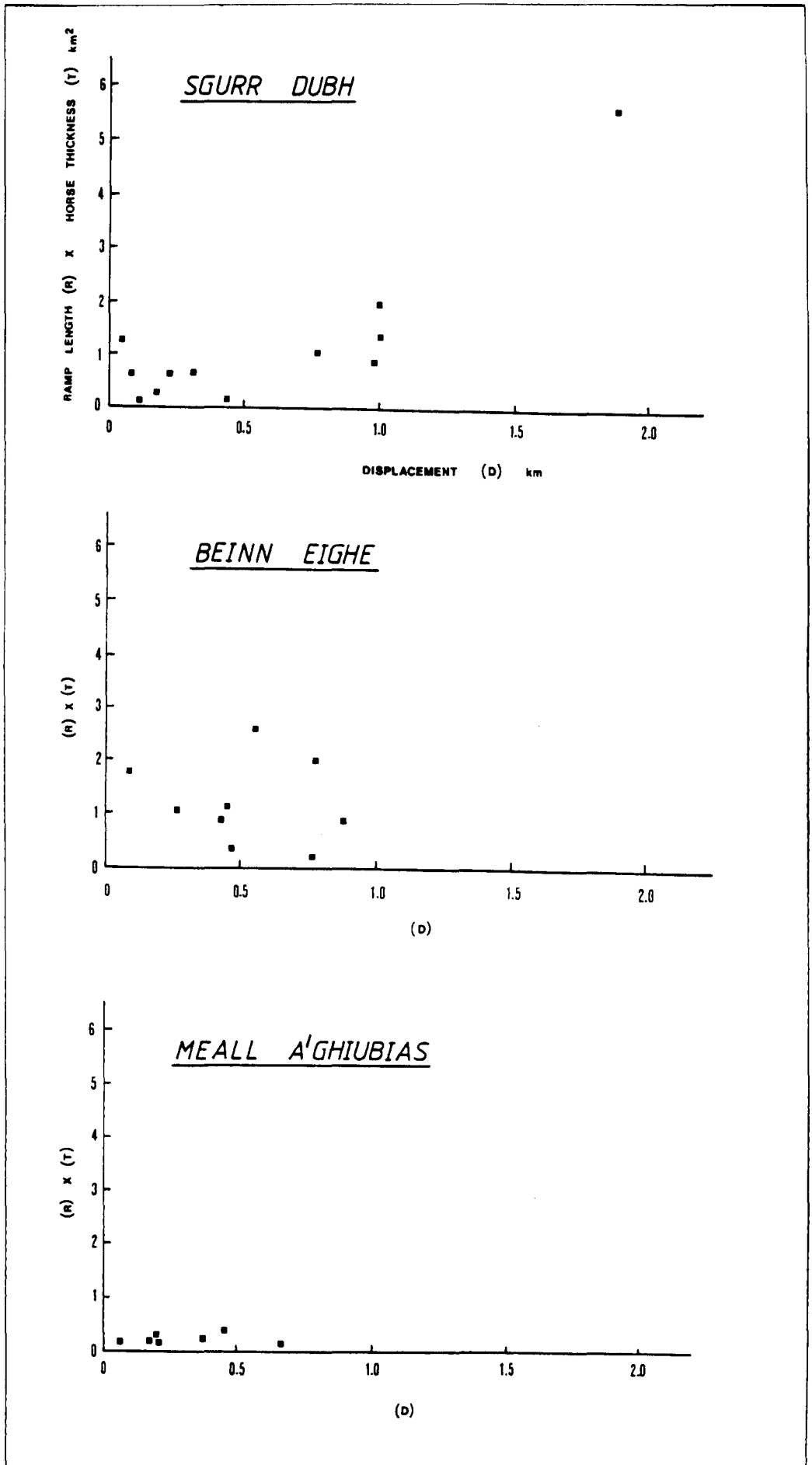

FIG. 2.13 Graphical plots of horse thickness (T) x ramp length (R) against displacement (D).

It is clear from these graphs that there is no simple relationship between the cross sectional area of a horse and displacement on the underlying thrust. Displacements of between 0.75 km and 2 km on the Sgurr Dubh cross section occur on 5 thrust surfaces which carry 5 of the largest 6 horses within this part of the imbricate fan. Therefore there is a tendency for horses with large cross sectional areas also to show the largest displacements. On the Beinn Eighe and Meall a'Ghiubias cross sections the relationship between cross sectional area and displacement is less clear and the graphs of (RT) against (D) do not suggest any direct link between cross sectional area of a horse and displacement. This may be expected as the Beinn Eighe Imbricate Fan represents the frontal imbricate zone to much larger overlying thrust sheets. The variation in size of horses within the imbricate zone relative to the now eroded, overlying thrust sheets is likely to have been insignificant and therefore no simple relationship of thrust displacement to horse size need be expected.

However, the graphs of Fig. 2.13 are useful. They indicate that maximum displacements are greater on the Sgurr Dubh cross section than on the Beinn Eighe cross section, and similarly are greater on the Beinn Eighe cross section than on the Meall a'Ghiubias cross section. Imbricate thrusts which develop from the deeper level floor thrusts show slightly greater displacements than imbricate thrusts which develop off the shallow floor thrusts. The amount of differential movement within an imbricate fan may be partially controlled by the level of the floor thrust.

This approach is simplistic. No attempt has been made to incorporate variable rates of thrust plane propagation as a method of producing differential movement of a horse. The above examples assume the presence of a thrust plane beneath the horse prior to movement. It is regularly observed within thrust belts that folds form above thrust tips when thrust plane development ceases; excellent examples of folds within horses occur in the Kinlochewe region and these are described in Section 2.2.

Boyer and Elliott (1982) draw attention to duplex dimensions and the angle between bedding and imbricate thrusts in the central portion of a horse; this angle is the ramp angle. These authors found that by comparing the contraction ratio, the ratio of current duplex length to its restored length, with the approximate angle of the central portion of a subsidiary thrust to the floor thrust, an inverse relationship was apparent. Table 1 of Boyer & Elliott (1982, p.1202) is modified below in Table 2.2 to include the contraction ratio (L'/L°) and the ramp angles from the 4 balanced cross sections from the Kinlochewe region. Also included in this table is the number of horses within the duplex. Inevitably many minor horses occur within imbricate fans and this table does not take account of these. Boyer and Elliott suggest in this table that the number of horses that significantly contribute to the geometry of the Foinaven duplex in the northern Moine Thrust Zone is approximately 34. Recent remapping of an adjacent area (Butler, pers. comm.) suggests that the number of horses is "probably nearer 200".

DUPLEX	CONTRACTION RATIO	NO. OF HORSES	RAMP ANGLE
1. Foinaven (Moine Thrust Zone)	0.29	34	40°
2. Window's duplex (southern Appalacians)	0.36	21	30°-50°
3. Beinn Eighe (section 4)	0.33	(3)	18°
Beinn Eighe (section 1)	0.42	12	18°
Beinn Eighe (section 2)	0.46	9	23°
Beinn Eighe (section 3)	0.54	11	23°
4. Lewis Thrust (floor of duplex), North American Cordillera			
Chief Mountain	-	2	23°
Mt. Crandell	0.57	6	33°
Cate Creek	0.58	2	31°
Haig Brook	0.6	12	27°
5. Central Appalachian Valley and Ridge	0.54	4	33°
6. Idealised model Duplex constructed with kink folds	0.50	-	30°

TABLE 2.2 Table 1 of Boyer & Elliott (1982, p.1202), modified to include data from the Kinlochewe Region.

The implication of Boyer and Elliott (1982, p.1207) is that duplexes with higher ramp angles may show a lower contraction ratio and hence a higher % shortening. The statistics from the Kinlochewe region do not support this simple relationship. This presents a similar problem to the question of relating horse size to displacement. The scale of duplexes within different thrust belts is obviously highly variable, the driving mechanisms which induce movement of thrust sheets will also differ between thrust belts and therefore any direct comparison using the above approach for imbricate zones from different thrust belts cannot be conclusive.

The cross sectional profile of a ramp is important when considering the deformation in the hangingwall as the overyling thrust sheet slips along the thrust surface. Accurate ramp angle measurements are given below for the Sgurr Dubh balanced cross section. Two measurements have been made from each ramp, one within the Eriboll sandstone and a second within the Torridonian sandstone; the results are given in Table 2.3.

RAMP		ANGLE IN ERIBOLL SANDSTONE (°)	ANGLE IN TORRIDONIAN SANDSTONE (°)
1	(west)	19	16
2		12	12
3		16	15
4		16	16
5		16	16
6		16	16
7		20	20
8		22	16
9		22	17
10		30	17
11		23	18
12		21	19
13		22	18
14	(east)	23	18
	AVERAGE	19.8	16.7

TABLE 2.3 Ramp angles from the Beinn Eighe Imbricate Fan on balanced cross section 1 (Sgurr Dubh).

The ramp angle figures suggest that on the scale of the imbricate fan each thrust develops as a slightly upwards concave fault (listric shaped). Thrust surfaces are usually assumed to follow a staircase trajectory in response to development through different lithologies. The extent to which imbricate thrusts within the Kinlochewe region follow a staircase trajectory has been examined by construction of simple structure contours on thrust surfaces which locally show 900 m relief. One example of this is illustrated below in Fig. 2.14. This diagram demonstrates the smooth thrust profile when examined on the scale of the imbricate fan.

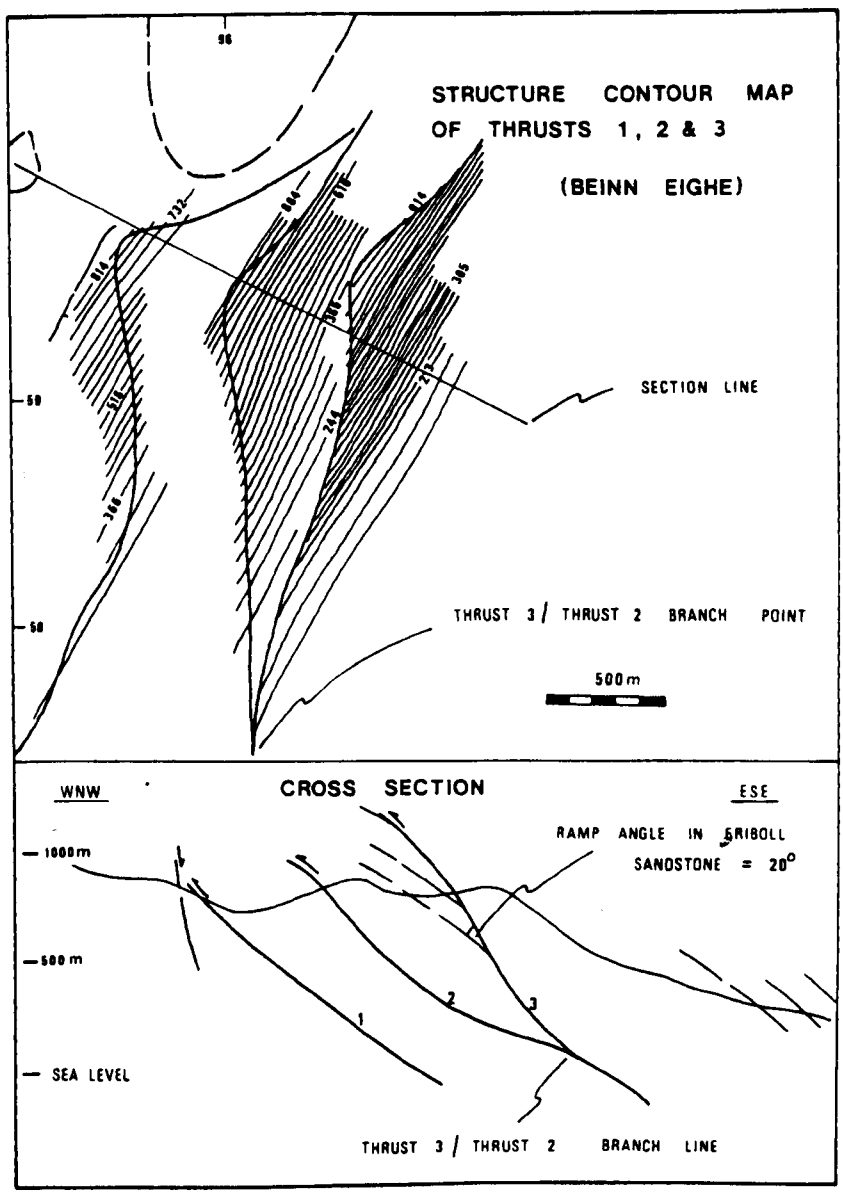

FIG. 2.14 Structure contour map of the 3 structurally lowest imbricate thrusts on Beinn Eighe, illustrating the listric profile. (Heights are in metres).

(v) Lateral continuity of horses

The 2 dimensional geometry of the Beinn Eighe Imbricate Fan is illustrated on the balanced cross sections and the dimensions of horses in the plane of section are described in Section 2.2(iv). The dimensions of horses perpendicular to this direction, along present day strike, are now examined. The lateral continuity of horses is more easily determined than the 'down-dip' continuity, simply by study of the geological map. This description of along strike continuity is augmented by longitudinal sections to illustrate the 2 dimensional geometry perpendicular to the movement direction.

The minimum along strike continuity of individual horses is presented in Table 2.4, which is based on measurement of the lengths of thrusts between branch points, the minimum along strike length of a horse is therefore the length of the footwall thrust. The horses are numbered and illustrated in Fig. 2.15; only the 2 southernmost sub-areas are examined in this section, and only the major horses have been measured.

Horse	Map length of footwall thrust	Probable map length of horse
1	3.75	17.0
2	5.60	6.7
3	4.12	16.1
4	1.83	-
5	2.04	2.1
6	1.74	6.1
7	1.90	-
8	2.33	11.1
9	2.25	-
10	7.30	-
11	1.41	2.0
12	5.12	-
13	5.23	-
14	2.31	-
15	4.85	-
16	2.71	-
17	1.21	-

TABLE 2.4 Minimum map lengths of horses as measured from field maps by this author, and probable map lengths based on Geological Survey maps.

The imbricates exposed in the "half-window" to the N of Kinlochewe have an unsuitable 3 dimensional geometry for accurate measurements to be made. The probable map lengths of horses to the S of the study area are also included in the table, based on examination of Geological Survey maps. All measurements are in kilometres.

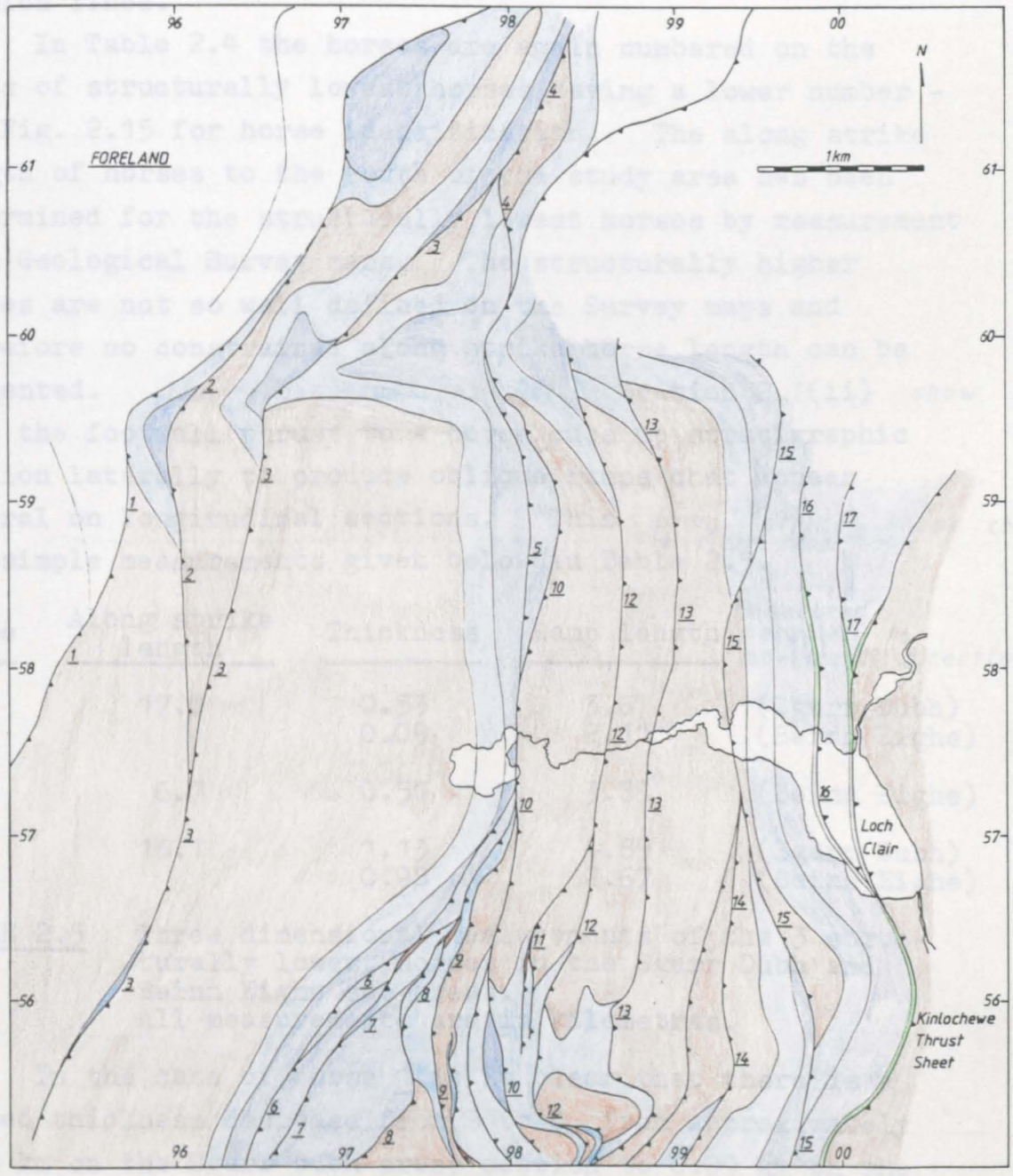

FIG. 2.15 Map of the Beinn Eighe Imbricate Fan in sub-areas 1 and 2. *(See main maps for key)*

It is now possible to determine the 3 dimensional shape of individual horses by combining the data in Table 2.1 with that in Table 2.4. The horses in Table 2.1 are numbered according to their structural position on the relevant balanced cross section, the structurally lowest horse being denoted as horse 1, therefore different horses may be denoted by the same number on different cross section lines.

In Table 2.4 the horses are again numbered on the basis of structurally lowest horses having a lower number - see Fig. 2.15 for horse identification. The along strike length of horses to the south of the study area has been determined for the structurally lowest horses by measurement from Geological Survey maps. The structurally higher horses are not so well defined on the Survey maps and therefore no constrained along strike horse length can be presented. The cross-sections of Section 2.1(ii) show that the footwall thrust to a horse cuts up stratigraphic section laterally to produce oblique ramps that appear lateral on longitudinal sections. This along-strike shape change is clear from the simple measurements given below in Table 2.5.

Horse	Along strike length	Thickness	Ramp length (measured parallel to movement direction)	
1	17.0	0.53	3.67	(Sgurr Dubh)
		0.09	2.11	(Beinn Eighe)
2	6.7	0.51	3.89	(Beinn Eighe)
3	16.1	1.13	4.89	(Sgurr Dubh)
		0.98	2.67	(Beinn Eighe)

TABLE 2.5 Three dimensional measurements of the 3 structurally lowest horses in the Sgurr Dubh and Beinn Eighe sub-areas.
All measurements are in kilometres.

In the case of horse 1 it is clear that there is a marked thickness decrease from S to N, from approximately 0.53 km on the Sgurr Dubh cross section to 0.09 km on the Beinn Eighe cross section; similarly in the case of horse 3 there is a decrease from 1.13 km on the Sgurr Dubh cross section to 0.98 km on the Beinn Eighe cross section. These figures suggest an approximate angle of upward tapering of

the horse from S to N of between 2.5° and 8°. It is important to note that the comparative measurements of horse thickness are not made on a section line perpendicular to the movement direction, therefore the approximate lateral tapering angles cannot be used as approximate lateral ramp angles. However, it is obvious that the lateral/oblique ramp angles are low as the thrust surfaces cut up section from S to N, probably between 2° and 10°.

Using the data presented in Table 2.5, it is now possible to construct a 3 dimensional restoration of the 3 structurally lowest horses which also gives a useful visual impression of the actual 3 dimensional geometry of a horse, Fig. 2.16. It is assumed for simplicity that the level of the floor thrust is approximately constant to the south of the study area. This is a large oversimplification; however, there is little doubt that the floor thrust lies at least 500 m below the sub-Cambrian unconformity over the bulk of this area (P. Nell, pers. comm.).

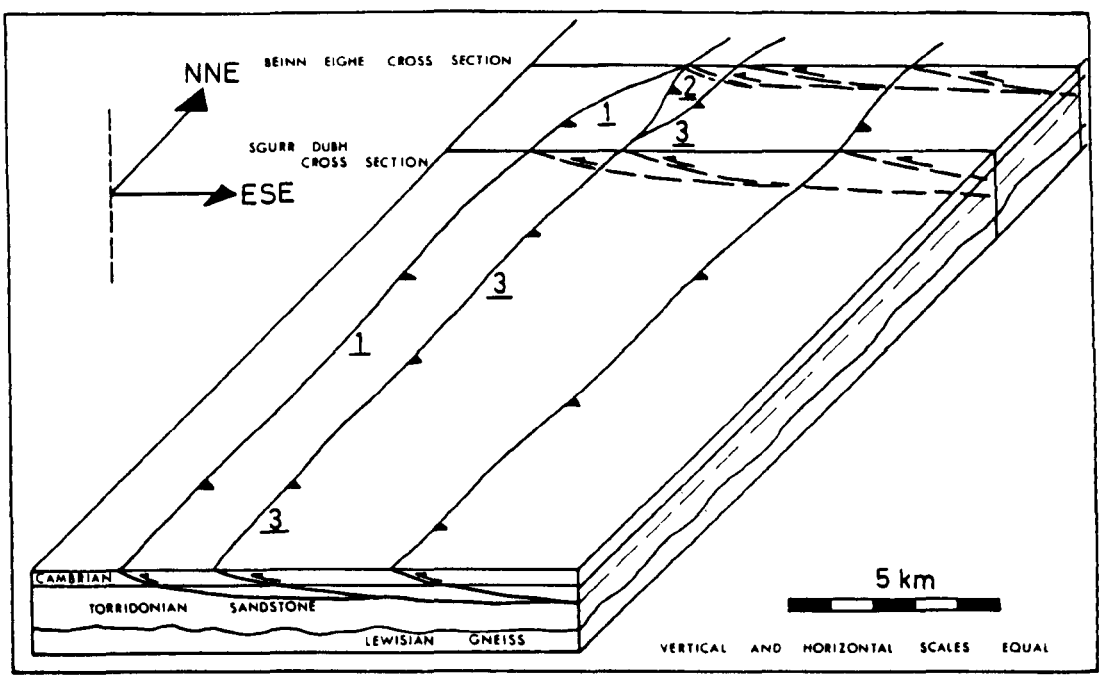

FIG. 2.16 Three dimensional restoration of the 3 structurally lowest horses in the Sgurr Dubh and Beinn Eighe sub-areas.

To the SSW of the area represented on this 3 dimensional illustration, in the Kishorn region, the floor thrust cuts up section towards the S in similar style to the inferred tapering in the Beinn Eighe region. This suggests that the larger frontal horses have approximate length : width : thickness ratios of 19 : 3 : 0.5 and 19 : 4.5 : 1.2, where the width of a horse is the horizontal distance between footwall and hangingwall thrusts on a restored cross section. These ratios suggest that for the horses within the structurally lower imbricates between Loch Carron in the S and Loch Maree in the N, the thickness is approximately 15-25% of the width which is approximately 15-25% of the length.

Only a small portion of the length of the structurally higher horses has been encountered in the study area. It is clear from the balanced cross sections that the dimensions of these structurally higher horses are very similar to those observed for the lower horses in a plane subparallel to the movement direction. It is therefore probable that these higher horses have similar length : width : thickness ratios to the lower horses. Recent fieldwork has been carried out to the south of the study area (P. Nell, pers. comm.); results from this may confirm the above suggestion.

The 2 dimensional geometry on section lines perpendicular to the movement direction are illustrated in Fig. 2.17, Meall a'Ghiubias to Glen Torridon and Fig. 2.18, Heights of Kinlochewe to Kinlochewe. Both of these longitudinal sections illustrate the Kinlochewe Thrust Sheet overlying the Beinn Eighe Imbricate Fan and imply that the Kinlochewe Thrust Sheet is gently bulged by accretion of horses during formation of the imbricate fan. The sequence of thrusting is examined in detail in Section 2.3.

Displacement estimates, and horse dimensions which are used throughout this chapter are derived from construction of balanced and restored cross sections. The errors arising from this approach cannot be assessed due to numerous difficulties, particularly in accurately predicting the depth to the floor thrust, the frequency of blind

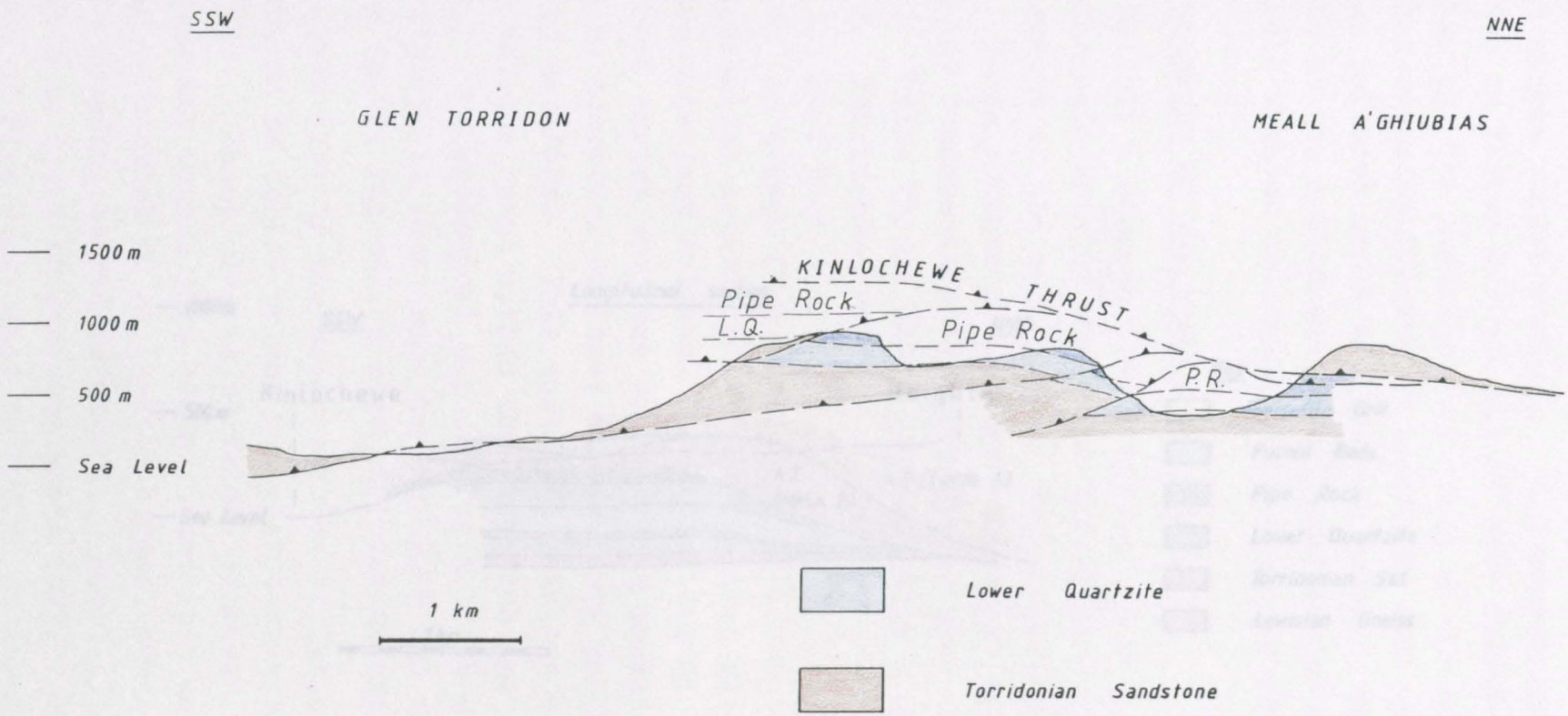

FIG. 2.17 Longitudinal section from Meall a'Ghiubias to Glen Torridon. (Movement direction into page).

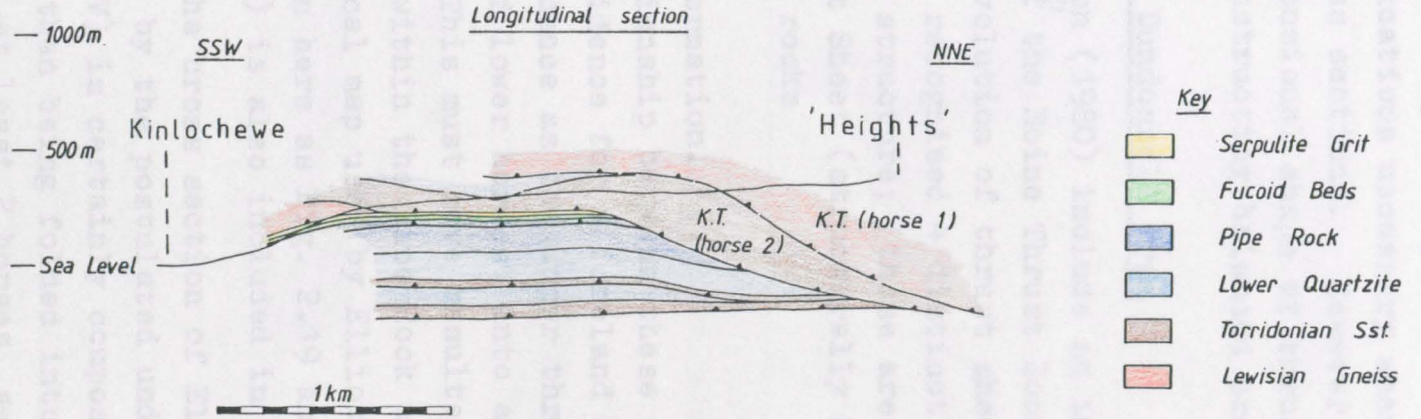

FIG. 2.18 Longitudinal section from Heights of Kinlochewe to Kinlochewe. (Movement direction into page).

thrusts, the geometrical configuration of the now eroded overlying thrust sheets and the consistency of displacement along a single thrust surface. The geometrical data presented in Tables 2.1 and 2.3 of this chapter are a series of estimates, the inaccuracy of which is due to the assumptions and oversimplifications necessary when constructing regional balanced cross sections. However, the regional analysis of the 3 dimensional shape of thrust sheets is impossible without constructing balanced cross sections.

(vi) Geometry of the Dundonnell area

Elliott & Johnson (1980) include an interpretation of the Dundonnell area (Fig.1.2) of the Moine Thrust Zone in their reassessment of the evolution of thrust sheets within the zone. These authors recognised 4 distinct thrust sheets within the Dundonnell structure; these are:

1. Moine Thrust Sheet (structurally highest)
2. Torridonian rocks
3. Pipe Rock
4. An t-Sron formation.

The geometrical relationship between these thrust sheets provides excellent evidence for a foreland directed or piggy-back thrust sequence as the upper thrust sheets are folded by accretion of lower horses, into an ENE-WSW trending antiform. This must have resulted from slip across oblique ramps within the Pipe Rock and An t-Sron formations. The geological map used by Elliott & Johnson (1980, p.91, fig.23) is shown here as Fig. 2.19 and their cross section (p.92, fig.24) is also included in this diagram.

Sheet (IV) of the cross section of Elliott & Johnson is shown to be folded by the postulated underlying horse, sheet (V). Sheet (IV) is certainly composed of An t-Sron formation but rather than being folded into an anticline it appears to consist of at least 2 horses, separated by an ENE-WSW trending imbricate thrust. Sheet (III) of Elliott & Johnson is shown to surround sheet (IV). No outcrops of Pipe Rock exist to the SE of sheet (IV) in the area mapped by this author therefore the geometry of the

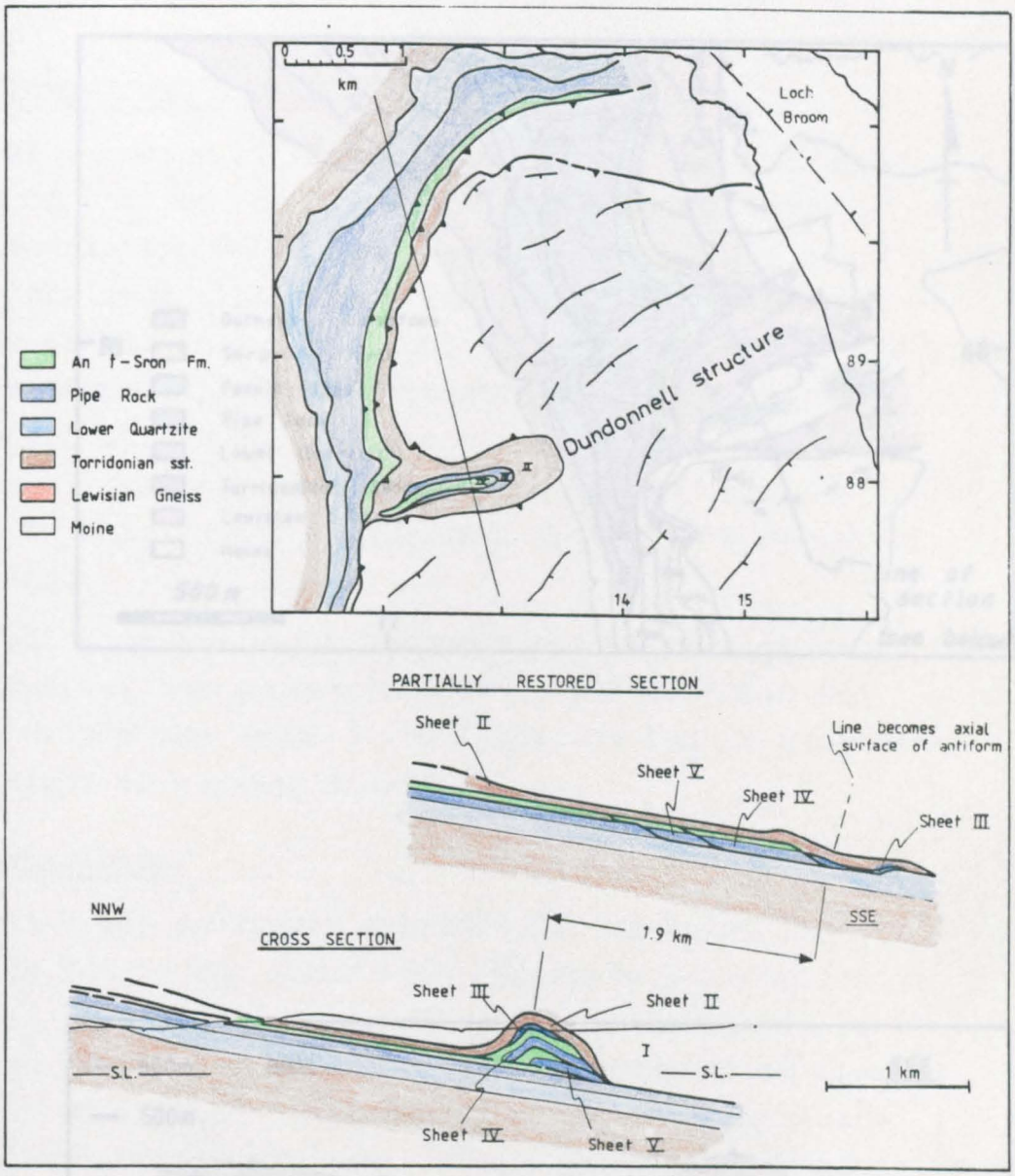

FIG. 2.19 Geological map, cross section and partially restored cross section based on Elliott & Johnson (1980).

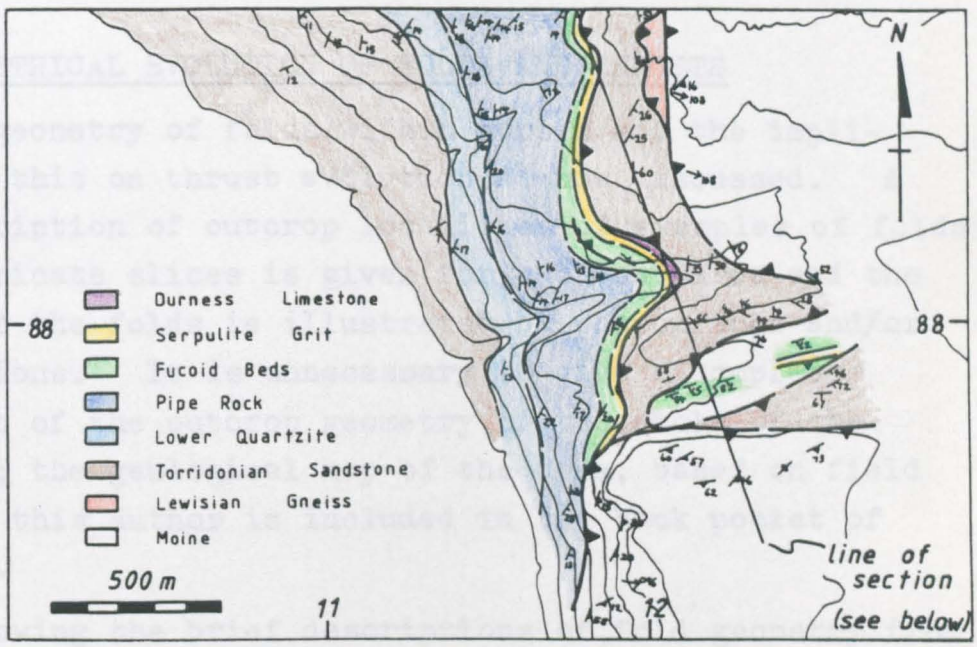

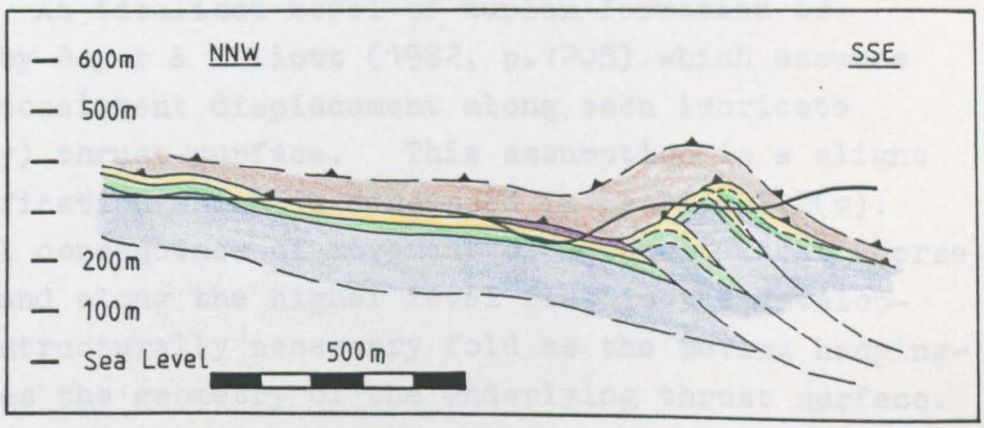

FIG. 2.20 Possible cross section from NNW to SSE across the Dundonnell structure.

Dundonnell structure may not be exactly as suggested by Elliott & Johnson, a fact that was admitted by these authors, who suggest that their solution is not unique. An equally valid cross section, from NNW to SSE (oblique to the movement direction) is shown in Fig. 2.20.

2.2 GEOMETRICAL EVOLUTION OF FOLDS AND THRUSTS

The geometry of folds within horses and the implications of this on thrust evolution are now discussed. A brief description of outcrop localities of examples of folds within imbricate slices is given for each sub-area and the geometry of the folds is illustrated by photographs and/or cross sections. It is unnecessary to give a complete description of the outcrop geometry of the whole of the study area; the geological map of the area, based on field mapping by this author is included in the back pocket of the thesis.

Following the brief descriptions of fold geometry from each sub-area, the geometrical evolution of folds and thrusts within the Beinn Eighe Imbricate Fan is summarised in the light of current models.

(i) Sgurr Dubh

The cross sectional geometry of the Beinn Eighe Imbricate Fan in the Sgurr Dubh region is illustrated in Fig. 2.4. An idealised model of duplex formation is presented by Boyer & Elliott (1982, p.1208) which assumes perfectly consistent displacement along each imbricate (subsidiary) thrust surface. This assumption is a slight oversimplification which is discussed in Section 2.2(v). The natural consequence of movement of a thrust sheet (horse) up a ramp and along the higher level flat is the development of a structurally necessary fold as the moving hanging-wall assumes the geometry of the underlying thrust surface. The applicability of this model to the Sgurr Dubh sub-area is now discussed.

In the area between (NG 96705525) and (NG 97705505) an anticline is developed in Torridonian sandstone in the

hangingwall to a major imbricate thrust. The underlying horse is exposed as subhorizontal to gently dipping Pipe Rock and an illustration of the cross sectional geometry is shown in Fig. 2.21 and Fig. 2.22.

FIG. 2.21 Photograph of hangingwall anticline in Torridonian sandstone in the vicinity of (NG 97455530). *(Looking to 195°)*

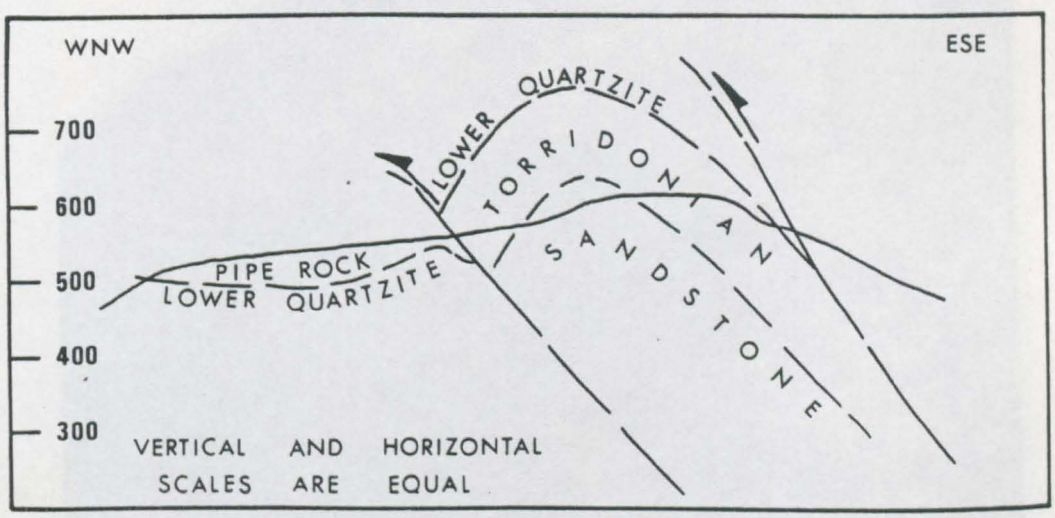

FIG. 2.22 Cross section of hangingwall anticline between (NG 96705525) and (NG 97705505). Heights are in metres, dips in Torridonian are correct.

Hangingwall folds are also exposed in the area between (NG 97805612) and (NG 98705575). The outcrop geometry along this section line is illustrated in Fig. 2.23, and 2 photographs illustrating the outcrops of hangingwall anticlines in Torridonian sandstone near to this section line are presented in Fig. 2.24 and Fig. 2.25.

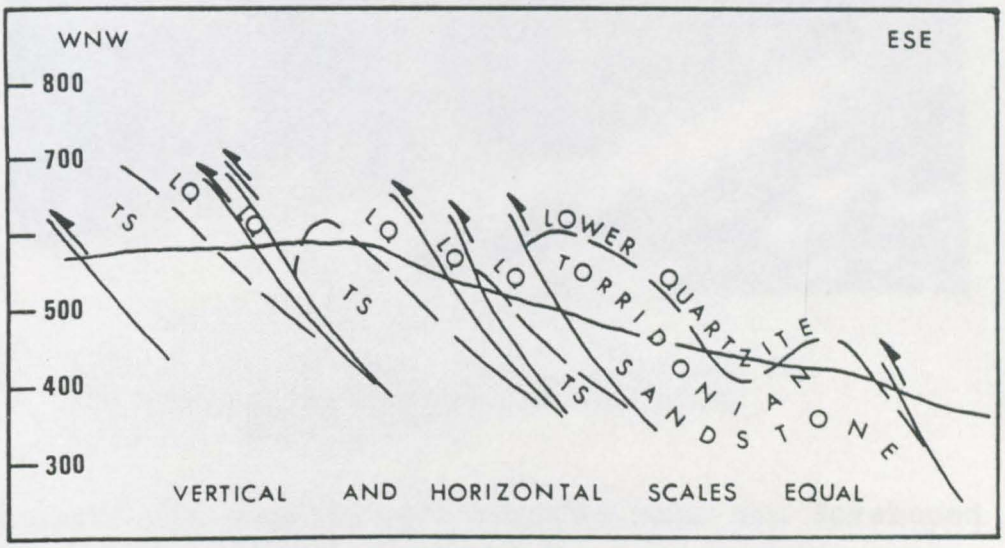

FIG. 2.23 Cross section from (NG 97805612) to (NG 98705575) illustrating hangingwall folds. Heights are in metres.

FIG. 2.24 Photograph of hangingwall anticline in Torridonian sandstone (NG 97955610), looking towards 194°.

FIG. 2.25 Photograph of hangingwall anticline in Torridonian sandstone (NG 98555630), looking towards 172°.

The folds illustrated here clearly have not developed as a direct response to the hangingwall thrust slab moulding itself to the underlying thrust surface as it slips. Fischer & Coward (1982) concluded that folds within imbricate slices of the Heilam area of the northern Moine Thrust Zone had formed as a result of buckling of the hangingwall prior to development of a ramp; this idea is summarised in Fig. 2.26.

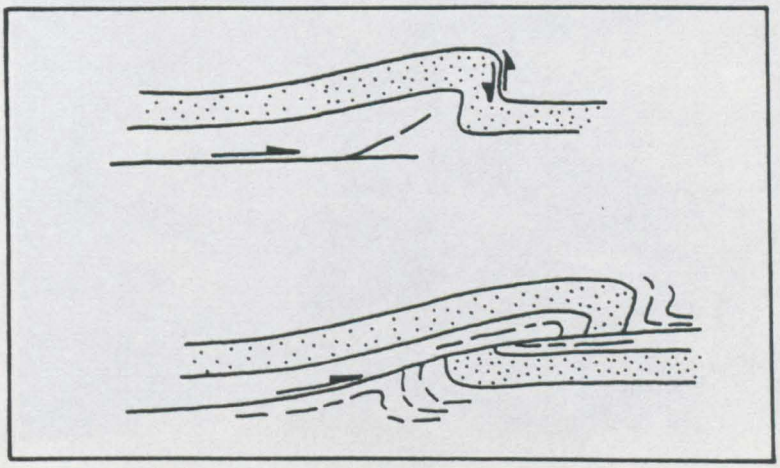

FIG. 2.26 The production of asymmetric folds; a model for the Heilam sheet, after Fischer & Coward (1982), Fig. 19.

FIG. 2.27 Oblique - lateral ramp at (NG 97655520)
(Looking to 083°)

FIG. 2.28 Oblique - lateral ramp at (NG 98605594)
(Looking to 182°)

These authors were able to arrive at this conclusion as the footwall rocks at Heilam are folded and footwall synclines can be identified in outcrop. This model differs from the alternative idea of Berger & Johnson (1980) who suggest that the footwall can remain undeformed while asymmetric folds form in the hangingwall due to stick or drag on a ramp. Clearly an intermediate stage exists in which a ramp surface is developed prior to buckling which dies out within the succession at a tip line. Slip on this thrust surface will decrease towards the tip line and asymmetric folds may develop in the hangingwall due to slip on the flat behind the ramp.

In the Sgurr Dubh area there is no evidence to suggest that footwall synclines exist at depth below the present erosion level. The local relief of 750 m is considerable and it is logical to assume that if significant footwall synclines were present within the imbricate fan, then some evidence of their existence would have been encountered during field mapping. It is clear from the geological map that the lower portions of the imbricate fan are characterised by Torridonian sandstone dipping at between 20° and 45° to the ESE, while the mid-upper portion commonly shows development of folds in the hangingwall to imbricate thrusts.

Outcrops of thrust surfaces are rare but a number of excellent exposures exist on Sgurr Dubh and 2 of these are illustrated in Figs. 2.27 and 2.28. Each of these photographs shows horses involving Torridonian sandstone and Lower Quartzite.

(ii) Beinn Eighe

The Beinn Eighe sub-area shows a similar style of hangingwall folding to that seen on Sgurr Dubh, 2 hangingwall folds are exposed and in both cases there is no evidence for the presence of a footwall syncline; one of these folds is illustrated in Fig. 2.29. The greater relief of Beinn Eighe compared with Sgurr Dubh, 950 m as

(Looking to 230°)

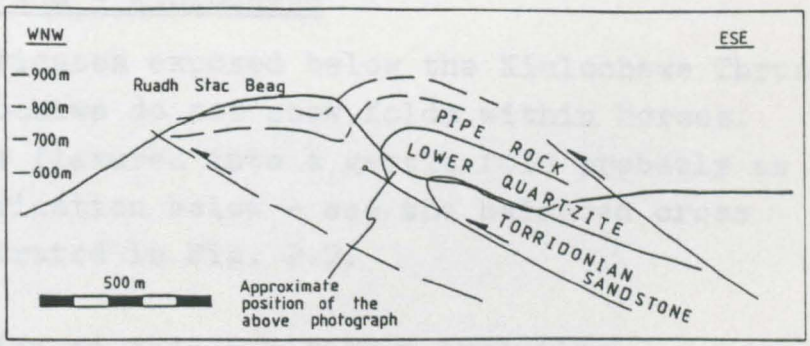

FIG. 2.29 Photograph and cross section illustrating hangingwall fold at (NG 97706170).

opposed to 750 m, allows a confident prediction that in the majority of horses no hangingwall folds developed except for flexures resulting from slip along the curved thrust surface. Subvertical cliff faces which face NW, Fig. 2.30, provide a series of natural longitudinal sections, illustrating the 3 dimensional geometry of the horses. The level of erosion over most of Beinn Eighe is just below the roof thrust to the imbricate fan, assuming that the immediate footwall to the Kinlochewe Thrust is near to the top of the Fucoid Beds. This allows the geometry of the horses to be examined in a potentially interesting position, on the flat in front of the ramp. This is possible to the N of Loch Clair, Fig. 2.31; the internal strain within these horses is discussed in Chapter 3.

(iii) Meall a'Ghiubias

The geological map shows that there are numerous examples of small scale folds within horses. These are dealt with in terms of the evolution of strain within thrust sheets in Chapter 3. One larger example of a hangingwall anticline exists near to (NH 00106480) and has similar geometry to the folds observed in the hangingwall to thrusts on Beinn Eighe and Sgurr Dubh.

(iv) Lochan Fada - Kinlochewe

The imbricates exposed below the Kinlochewe Thrust to the N of Kinlochewe do not show folds within horses. The imbricates are flexured into a gentle fold probably as a result of imbrication below - see the balanced cross section illustrated in Fig. 2.7.

(v) Discussion on fold and thrust evolution

Various models of fold development in thrust belts have been recently proposed, e.g. Berger & Johnson (1980), Boyer & Elliott (1982), Fischer & Coward (1982) and Suppe (1983). It is clear from the balanced cross sections,

FIG. 2.30 Natural longitudinal sections on the NW facing cliff faces of Beinn Eighe. *(Looking to 110°)*

FIG. 2.31 Horses immediately below the Kinlochewe Thrust to the N of Loch Clair. *(Looking to 020°)*

Figs. 2.4 to 2.7, that the flexures observed within the horses which constitute the Beinn Eighe Imbricate Fan can be attributed to slip of a thrust sheet along a flat - ramp - flat thrust surface and therefore broadly conform to the idealised duplex model of Boyer & Elliott (1982, p.1208). However, the evolution of the imbricate fan is not as simple as this model suggests. The presence of hangingwall folds similar to the examples of Fig. 2.23 implies that buckling of the hangingwall resulted from stick on a floor thrust surface or from stick at a ramp tip line. So the development of folds within horses may be a direct consequence of the ability of the thrust plane to propagate forwards.

If a model of stick at a ramp tip line is applicable, then a stage must have been reached where the fold locked and the ramp continued to propagate from the tip line, at which thrust development had temporarily ceased. In the case of one of the anticline - syncline fold pairs on Sgurr Dubh (NG 98505600) it appears that the ramp did not develop from the tip line, but was abandoned at depth as a blind thrust. This interpretation is also preferred for the hangingwall fold on Ruadh Stac Beag (NG 97706170), Fig. 2.29, where it is proposed that following locking of the fold, a new, structurally lower thrust plane propagated from the floor thrust - ramp branch line. This situation does not involve the ramp cutting across the fold, therefore the ramp angles are likely to be low.

The weakness of this idea of stick at a ramp tip line, followed by buckling and then either regeneration of the existing ramp or development of a new ramp, is that it suggests a rigid, exclusive deformation sequence. A slight modification of this would suggest that if the rate of slip on the floor thrust was greater than the rate of propagation of the ramp, the hangingwall may be expected to buckle as the ramp is slowly developing below it.

Differential movement was significant during the evolution of the Beinn Eighe Imbricate Fan, implying

variable rates of thrust plane development along strike. The detailed structural history of hangingwall fold development is perhaps more likely to be dictated by a gradually accelerating and decelerating rate of thrust plane propagation, rather than the simple sequence of stick, fold and thrust. If so then the growth of hangingwall folds is likely to be synchronous with thrust plane development. Differential movement or variable rates of thrust plane propagation along strike will result in hangingwall fold axes varying in trend from perpendicular to the movement direction to more oblique trends. The fold axes on Sgurr Dubh do show very strong evidence for some differential movement on the underlying thrust surface - see the geological map.

The development of folds within horses is therefore believed to be a function of the rate of slip of the thrust sheet along the pre-existing floor thrust and the rate of propagation of the floor thrust or a subsidiary (ramp) thrust. Clearly if the rate of slip on the floor thrust is greater than the rate of thrust plane development, then folding may occur. Alternatively, layer parallel shortening by straining the region above the developing thrust may occur as well as buckling. The amount of internal strain within the imbricate fan is examined in Chapter 3; this leads to a better constrained evolutionary sequence than can be deduced from geometrical observations alone. The majority of the horses that constitute the Beinn Eighe Imbricate Fan do not show internal folding; this implies that it was more usual for the rate of slip on the floor thrust to be very similar to the rate of ramp development. This inevitably leads to the production of passive folds as originally suggested by Rich (1934) and more recently by Boyer & Elliott (1982).

2.3 GEOMETRICAL EVOLUTION OF THE KINLOCHEWE THRUST SHEET

The Kinlochewe Thrust Sheet consists of Lewisian gneiss, Torridonian sandstone and Lower Quartzite. It is exposed in 3 areas:

1. between Lochan Fada and Kinlochewe
2. to the N and E of Loch Clair
3. as a klippe in the region of Meall a'Ghiubias.

Each of these areas is now discussed, and the relationship of the Kinlochewe Thrust to the underlying imbricate thrusts is investigated.

(i) Lochan Fada - Kinlochewe

The Kinlochewe Thrust Sheet in this region can be subdivided into 2 major horses which show more complex internal deformation than the horses within the underlying imbricate fan. The upper horse (horse 1) is exposed as a slab of Lewisian gneiss with small accumulations of Torridonian sandstone and an exposure of inverted Lower Quartzite, which unconformably overlies the Lewisian gneiss. This suggests that the planar sub-Cambrian unconformity cuts an erosion surface across a thick Torridonian subsurface in the present day W and across a much thinner Torridonian and Lewisian subsurface in the E. This is not intended to imply that pre-Caledonian gentle folding combined with the effect of variable Lewisian topography were wholly responsible for regional thinning of the Torridonian sandstone to the E below the sub-Cambrian unconformity. It is more likely to be due to normal faulting during accumulation of Torridonian sediments, *possibly due to movement on the Loch Maree Fault.*

The lower horse (horse 2) shows a 100-200 m development of Torridonian sandstone between the Lewisian gneiss and the Lower Quartzite; the Lower Quartzite crops out in the core regions of synclines within this horse. There is no evidence for the presence of imbricate thrusts immediately above these synclines, the internal geometry of the horse may therefore have evolved in similar fashion to the development of asymmetric folds above blind thrusts in

the Sgurr Dubh region. The internal geometry of horse 2 is therefore a fold train of NW verging folds which may overlie blind thrusts. This geometry is illustrated on the balanced cross section shown in Fig. 2.7.

The hangingwall cut-off of the Lewisian/Cambrian unconformity of horse 1 is projected onto this balanced cross section to provide a minimum displacement estimate for the upper Kinlochewe Thrust of 2.7 km, based on the offset of the sub-Cambrian unconformity on this thrust plane. The displacement on the lower Kinlochewe Thrust is at least 7.9 km; this is deduced by restoring the postulated duplex which underlies this thrust; this restores to 6.2 km. The position of the Kinlochewe Floor Thrust/upper Kinlochewe Thrust branch line must be approximately 1.7 km forwards of the lowest underlying imbricate thrust, therefore the minimum displacement on the lower Kinlochewe Thrust is 7.9 km. The shortening within the underlying duplex is at least 4.1 km and therefore the minimum shortening below the Moine Thrust along a WNW - ESE section line, in this region, is (7.9 + 4.1 + 2.7) = 14.7 km.

The sequence of thrusting can be deduced from this sub-area by reconciling the following field observations.

1. The Kinlochewe Floor Thrust cuts down stratigraphic section in the footwall from ESE to WNW, from Durness limestone to the top of the Pipe Rock.

2. The upper and lower Kinlochewe Thrusts cut up stratigraphic section in the hangingwall from ESE to WNW.

3. The Kinlochewe Thrust Sheet is flexured by movement on underlying major imbricate thrusts.

4. The Kinlochewe Floor Thrust cuts across a previously developed imbricate system of upper Pipe Rock, Fucoid Beds, Serpulite Grit and Durness Limestone - see Fig. 2.7 and the geological map.

In order to reconcile these observations it will initially be assumed that the present day geometry is a result of thrusting.

A high level imbricate system, composed largely of repetitions of the An t-Sron formation, is clearly truncated by the overlying Kinlochewe Thrust in the region near to (NH 05806304). Therefore imbrication of the An t-Sron formation predates propagation of the Kinlochewe Thrust through these high level imbricates, confirming the conclusion of McClay & Coward (1981) that the Kinlochewe Thrust is not a roof thrust to this particular imbricate system. However, the Kinlochewe Thrust is clearly bulged or flexured by development of major imbricates in its footwall, suggesting that the Kinlochewe Thrust is a roof thrust to this lower imbricate system. The upper and lower Kinlochewe Thrusts both cut up stratigraphic section in the hangingwall and it seems likely that this is a result of thrusting. Therefore the most likely sequence of thrusting is:

1. Displacement on the upper Kinlochewe Thrust
2. Development of the An t-Sron imbricates
3. Displacement on the lower Kinlochewe Thrust across the An t-Sron imbricates
4. Development of the lower imbricates.

If this sequence of thrusting is correct, then it is an excellent example of out of sequence thrusting as high level thrusts cut across lower ones. This does not mean that displacement on the Kinlochewe Thrust had ceased while the An t-Sron duplex was developing, it implies that the rate of propagation of the Kinlochewe Thrust was slower than the rate of propagation of a structurally lower thrust which must have spawned the An t-Sron imbricates.

This deformation sequence does not reconcile all of the geometrical observations listed above. The footwall to the Kinlochewe Thrust becomes stratigraphically older to the WNW, therefore the Kinlochewe Thrust cuts down section. The average angle of cutting down section relative to a horizontal datum plane is between 1° and 2°. A remarkably similar situation exists in the northern Moine Thrust Zone in the Loch More region, where the Glencoul Thrust also cuts down section towards the WNW, with an

average angle of cutting down section of between 3° and 5°, (Butler, in press). Butler (op. cit.) invokes a regional dip of the foreland sequence towards the ESE prior to thrusting to allow a future, regionally horizontal thrust plane to cut down carefully through the succession at an angle of between 3° and 5° to bedding.

This alternative is illustrated for the Kinlochewe region in Fig. 2.7 (lower diagram), where the most easterly portion of the foreland sequence is considered to have been tilted to the ESE. This possibility is supported by the presence of Pipe Rock within one of the structurally lower horses within the higher level imbricate system. Therefore the local floor thrust to this imbricate system may also cut down stratigraphic section from the base of the Fucoid Beds into the Pipe Rock. It is therefore possible to reconcile the observed geometrical relationships by invoking a combination of gentle foreland tilting and out of sequence thrusting. The cause of this proposed foreland tilting cannot be deduced from the field geometry. Prior to imbrication the foreland was probably overlain by between 5 and 10 km of overthrust Moine rocks (Soper & Barber, 1979); the possibility that this may have induced tilting in the underlying foreland cannot be discounted.

An alternative model for the evolution of these geometrical relationships has been proposed by Coward (1982) who suggests that the Kinlochewe Thrust is not a thrust, but instead is a low angle extensional fault which has sliced down through the Kinlochewe Thrust Sheet and down onto the foreland, thereby explaining the footwall geometry. This situation is summarised in Fig. 2.7 (upper diagram), which illustrates the "Kinlochewe Fault" slicing down through a previously thrust succession. Coward (1982) suggests that the Kinlochewe Sheet is therefore part of a large "surge zone" which is similar to smaller surge zones in the Assynt region of the Moine Thrust Zone, where "surges" defined by extensional faults, tear faults and thrusts can be mapped out. This is clearly not the case for the Kinlochewe region where there is no unequivocal

evidence for the presence of an extensional fault, and certainly no evidence of tear faults or subvertical shear zones associated with a surge zone.

Coward & Kim (1981, p.289, Fig.18) draw attention to oblique folds within the Kinlochewe Thrust Sheet to the N of Kinlochewe. These authors suggest that the structure within the Kinlochewe Thrust Sheet is a sheath-like fold resulting from differential movement of the Kinlochewe Thrust Sheet. Mapping by this author suggests that the fold axes within the lower horse are oblique to the movement direction. This obliquity varies from 45° to 90° to the movement direction; however, these folds are W to NW facing, and not SW facing with SE plunging hinges as suggested by Coward & Kim.

(ii) Loch Clair - Meall a'Ghiubias

The geometry of the Kinlochewe Sheet as illustrated by Coward (1982, p.253, Fig.14) - see Fig. 2.32 - suggests that the Kinlochewe Fault cuts through a major recumbent syncline, thought to be equivalent to the Lochalsh syncline which occurs to the S of Lochcarron. Re-mapping of this area by the present author may cast doubt on this interpretation. A close examination of Fig. 2.32 illustrates that if this geometry is correct, then the Torridonian sandstone must be approximately 2.5 km thick.

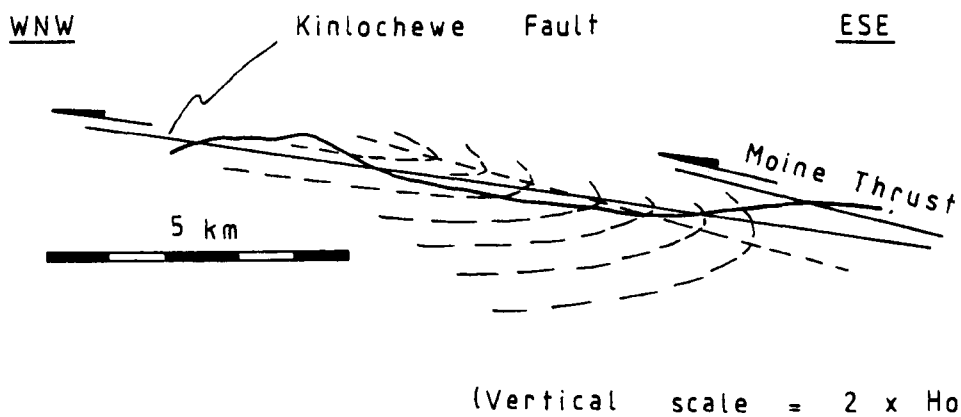

FIG. 2.32 Cross section illustrating the geometry of the Kinlochewe Fault; this diagram is slightly modified from Fig. 14 of Coward (1982).

This would imply a decrease in thickness of the Torridonian sandstone within the Kinlochewe Thrust Sheet from 2.5 km to the SW of Kinlochewe to a maximum of 200 m to the N of Kinlochewe, a decrease in thickness from S to N of approximately 2.3 km over a horizontal distance of 3 km. This seems rather rapid. The maximum thickness of Torridonian sandstone in the foreland of the Beinn Eighe region is approximately 1200 m. An alternative model is proposed on the balanced cross section shown in Fig. 2.6; 2 horses can be identified within the Kinlochewe Thrust Sheet in the region of Meall a'Ghiubias, Figs. 2.33 and 2.34. The upper horse on Meall a'Ghiubias is composed of Torridonian sandstone which is the correct way up based on cross bedding and on "Diabaig" sediments being overlain by "Applecross" lithologies. The lower horse is composed of Lower Quartzite and Pipe Rock.

FIG. 2.33 Meall a'Ghiubias, illustrating the two horses within the Kinlochewe Thrust Sheet.
(Looking north)

FIG. 2.34 Meall a'Ghiubias looking towards 080°, illustrating flexuring of the upper horse due to oblique footwall ramps.

To the ESE, in the region of Loch Clair, Torridonian Sandstone is exposed in the hangingwall to the Kinlochewe Thrust and this may be part of either of the horses on Meall a'Ghiubias. In Fig. 2.35 it is considered to be part of the lower horse, suggesting that the thrust cuts up section in the hangingwall from Torridonian sandstone to Pipe Rock over a horizontal distance of approximately 3 km. Fig. 2.35 illustrates the possible geometry on a section line drawn through Meall a'Ghiubias from WNW to ESE and illustrates quite clearly that the Kinlochewe Thrust may cut up section in the footwall from ESE to WNW and therefore does not show extensional geometry in the hangingwall or in the footwall.

To the E of Loch Clair - see geological map - the hangingwall to the Kinlochewe Thrust consists of inverted Torridonian sandstone and Lewisian gneiss - see Figs. 2.4 and 2.5. The Kinlochewe Thrust therefore slices through a fold, and if this is part of the lower horse exposed on Meall a'Ghiubias then correct way up strata overlie the thrust to the WNW. This geometry can develop from out of sequence thrusting and there is no need to invoke any major extensional faulting in the Kinlochewe region.

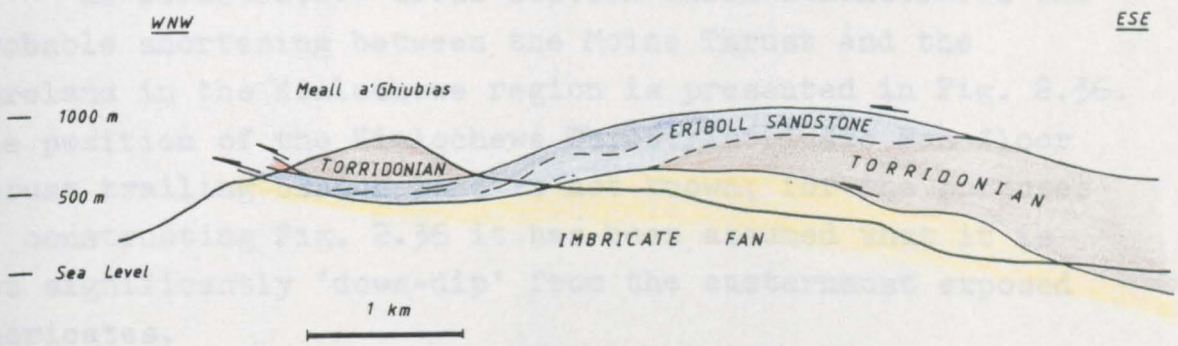

FIG. 2.35 WNW-ESE cross section through Meall a'Ghiubias.

It is not possible to prove or disprove an out of sequence thrust model or a surge model for the geometrical evolution of the Kinlochewe Thrust Sheet. However, the geological evidence for a surge model is slight, relying on an inbuilt preference for the foreland to be subhorizontal prior to deformation and for thrusts not to form out of sequence. It is argued here that the geology of the Kinlochewe Thrust Sheet is good evidence for thrusts developing out of sequence.

The 3 dimensional geometry of the Beinn Eighe Imbricate Fan and the Kinlochewe Thrust Sheet demonstrates that the evolution of thrust surfaces was broadly from ESE to WNW, a foreland directed thrust sequence. The detailed evolution of individual thrust systems may not have been rigidly in sequence and there is strong evidence for out of sequence thrusting from the geometrical relationships between the Kinlochewe Thrust Sheet and the underlying imbricates.

Differential movement along thrust surfaces and the rate of slip on the pre-existing floor thrust compared to the rate of thrust plane propagation may have led to the growth of folds within the thrust sheets. The obliquity of fold axes to the movement direction and the occurrence of folds is greater within the Kinlochewe Thrust Sheet than in the underlying imbricate fan.

An illustrative cross section which demonstrates the probable shortening between the Moine Thrust and the foreland in the Kinlochewe region is presented in Fig. 2.36. The position of the Kinlochewe Thrust/Imbricate Fan floor thrust trailing branch line is not known; for the purposes of constructing Fig. 2.36 it has been assumed that it is not significantly 'down-dip' from the easternmost exposed imbricates.

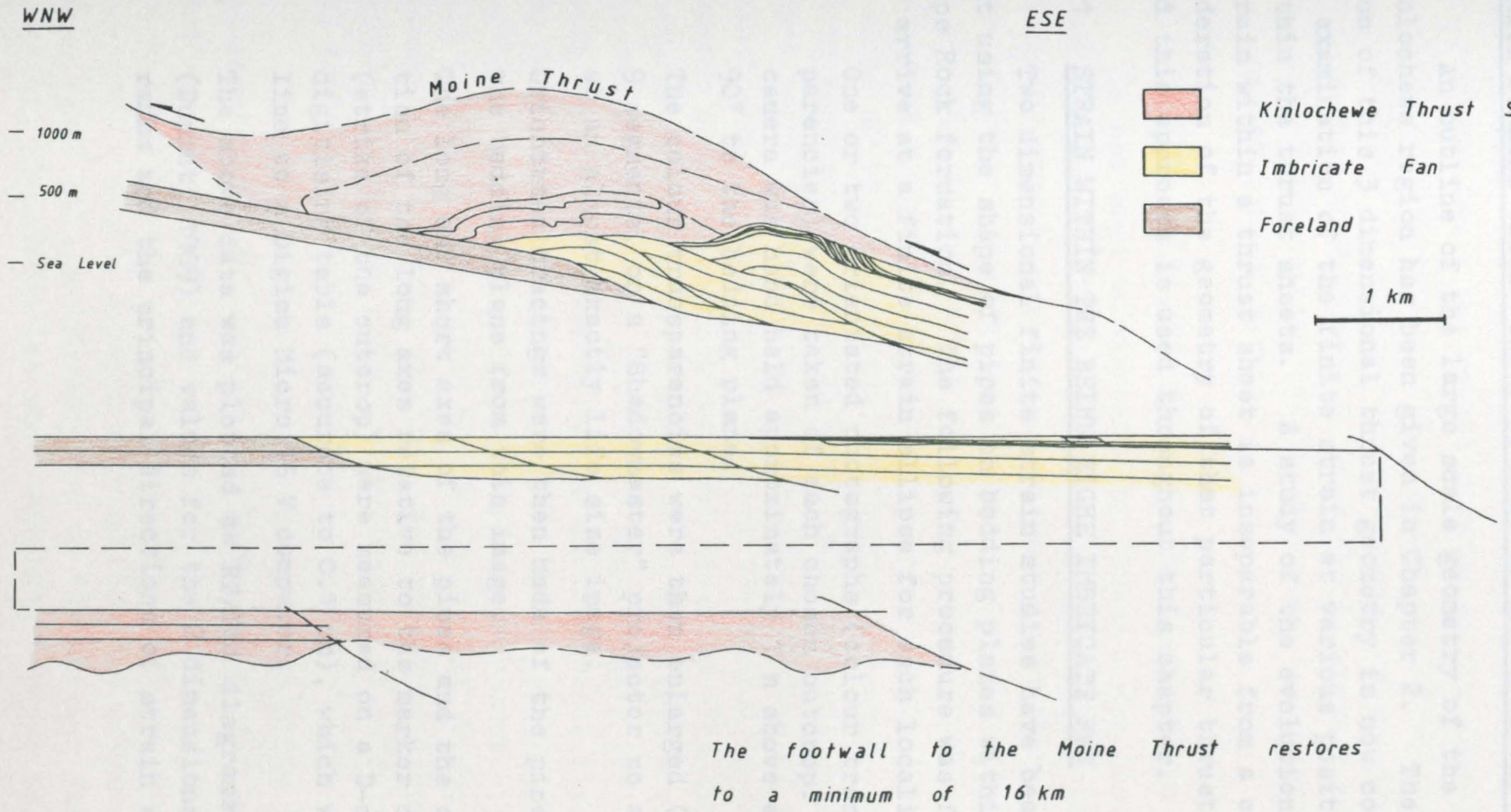

FIG. 2.36 Cross section between the Moine Thrust and the foreland in the Kinlochewe region.

C H A P T E R 3

FINITE STRAINS WITHIN THRUST SHEETS IN THE KINLOCHEWE REGION

An outline of the large scale geometry of the Kinlochewe region has been given in Chapter 2. The evolution of this 3 dimensional thrust geometry is now constrained by examination of the finite strain at various positions within the thrust sheets. A study of the evolution of strain within a thrust sheet is inseparable from a consideration of the geometry of that particular thrust sheet and this approach is used throughout this chapter.

3.1 STRAIN WITHIN THE BEINN EIGHE IMBRICATE FAN

Two dimensional finite strain studies have been carried out using the shape of pipes on bedding planes within the Pipe Rock formation. The following procedure was followed to arrive at a finite strain ellipse for each locality:

1. One or two orientated photographs (colour transparencies) were taken of each chosen outcrop. The camera was hand held approximately 1 m above and at 90° to the bedding plane.

2. The colour transparencies were then enlarged (x25), in 9 segments, on a "Shadowmaster" projector to arrive at an almost exactly life size image.

3. Orientated tracings were then made of the pipes on the bedding plane from this image.

4. The long and short axes of the pipes and the orientation of the long axes relative to the marker direction (strike of the outcrop) were measured on a D-mac digitising table (accurate to 0.1 mm), which was on line to a Digico Micro 16 V computer.

5. The above data was plotted as RF/Phi diagrams (Dunnet, 1969) and values for the 2 dimensional strain ratios and the principal directions of strain were

obtained using the 'Theta-Curve' method of Lisle (1977).

6. As a comparison and as a check on the 'Theta-Curve' results, the above data was also plotted on a polar graph, using the method of Wheeler (in press), which is a modification of the method introduced by Elliott (1970). A computer program based on the numerical method of Shimamoto & Ikeda (1976) gives a value for the 2 dimensional strain ratio and the principal directions of strain.

(i) Strains below the imbricate fan floor thrust

It has been demonstrated by Coward & Kim (1981), Fischer & Coward (1982) and Cooper et al. (1983) that imbricate thrusts may develop through a "ductile bead" or zone of layer parallel shortening which travels immediately at the head of the thrust tip line. This ductile bead may represent a significant amount of layer parallel shortening, a value of 33% is suggested by Fischer & Coward (1982), based on measurement of deformed pipes, for the maximum amount of layer parallel shortening in the Heilam region of the Moine Thrust Zone. This layer parallel shortening is thought to develop prior to bedding parallel shear strains due to flexural shear and development of an imbricate thrust across the beds. Cooper et al. (1983) suggest that 27% of the total shortening observed within Carboniferous Limestone of the Basse Normandie duplex of N.E. France was due to layer parallel shortening prior to thrust development. This is a bulk figure for the whole of the duplex and is not based on measurement of strain markers; the amount of localised layer parallel shortening prior to development of individual thrusts may therefore have been greater or less than 27%.

It is clear from a description of the large scale geometry of the Beinn Eighe Imbricate Fan that a significant stage in the evolution of some of the horses is the growth of folds associated with differential movement on thrust surfaces. Finite strains arising from the development of these folds will be superimposed on any earlier ductile bead strains. Therefore the most suitable position to study any

internal deformation which has developed ahead of the thrust tip is in the footwall to imbricate thrusts.

This section examines the results from 12 localities within the foreland, 100 m to 800 m to the WNW of the floor thrust. These localities are illustrated in Fig. 3.1. The results from the 'Theta-curve' and Shimamoto & Ikeda methods are presented in Table 3.1 and the data is plotted as Rf/Phi diagrams and as plots based on the Wheeler method in Figs. 3.3, 3.4, 3.5, 3.6 and 3.7.

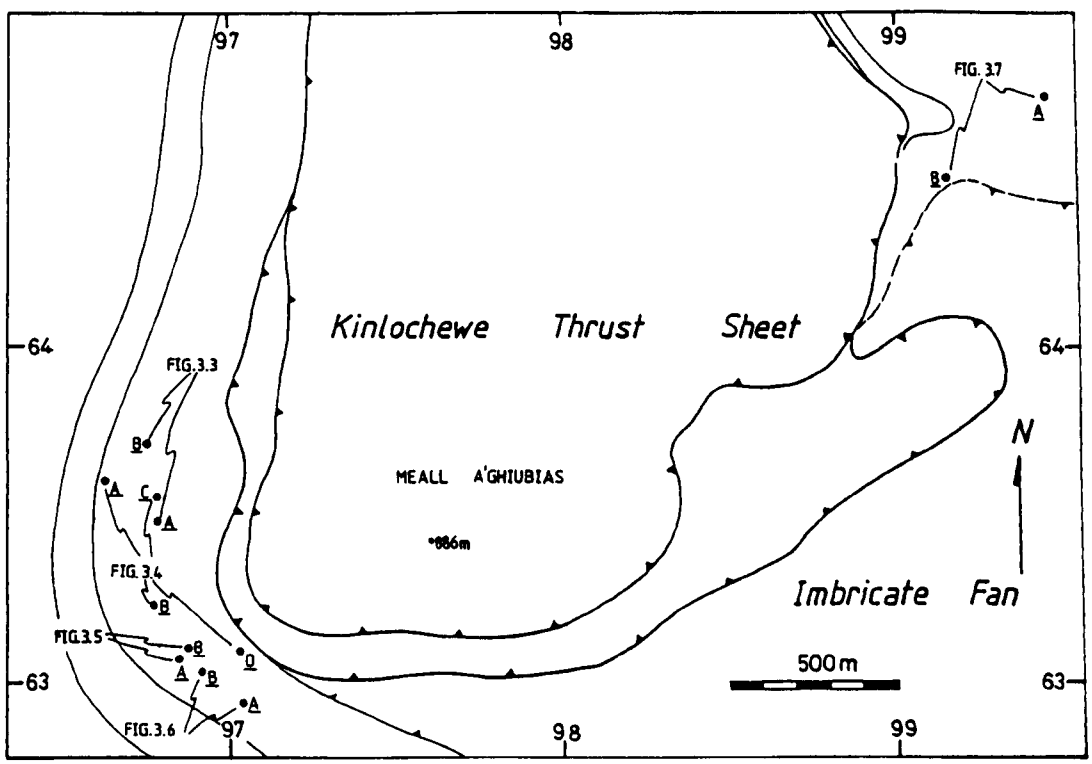

FIG. 3.1 Foreland localities used for finite strain estimates within the Pipe Rock.

Locality	Fig.	No. of Pipes	'Theta-Curve' Rs	'Theta-Curve' Direction	'Shimamoto & Ikeda' Rs	'Shimamoto & Ikeda' Direction
96816348	3.3	202	1.04	070	1.05	078
96776371	3.3	178	1.03	050	1.03	061
96646360	3.4	41	1.13	050	1.07	063
96806323	3.4	53	1.01	004	1.00	-
96806355	3.4	81	1.07	049	1.07	049
97036309	3.4	41	1.07	040	1.07	053
96866307	3.5	170	1.03	000	1.06	080
96896310	3.5	301	1.09	069	1.06	073
97026294	3.6	63	1.10	058	1.12	062
96946303	3.6	177	1.05	042	1.03	054
99456475	3.7	155	1.11	076	1.11	075
99156450	3.7	37	1.02	000	1.02	028

TABLE 3.1 Two dimensional strain ratios and orientations of the long axes of the strain ellipse on the bedding surface. The effect of the tilt of the beds has been removed and each orientation is a bearing relative to present day grid north.

The results presented in Table 3.1 suggest that the strain ratios in a plane parallel to bedding vary from 1.00 to 1.12 for the 12 localities. These strain ratios and long axis orientations, based on the results from the Shimamoto & Ikeda method are illustrated in Fig. 3.2.

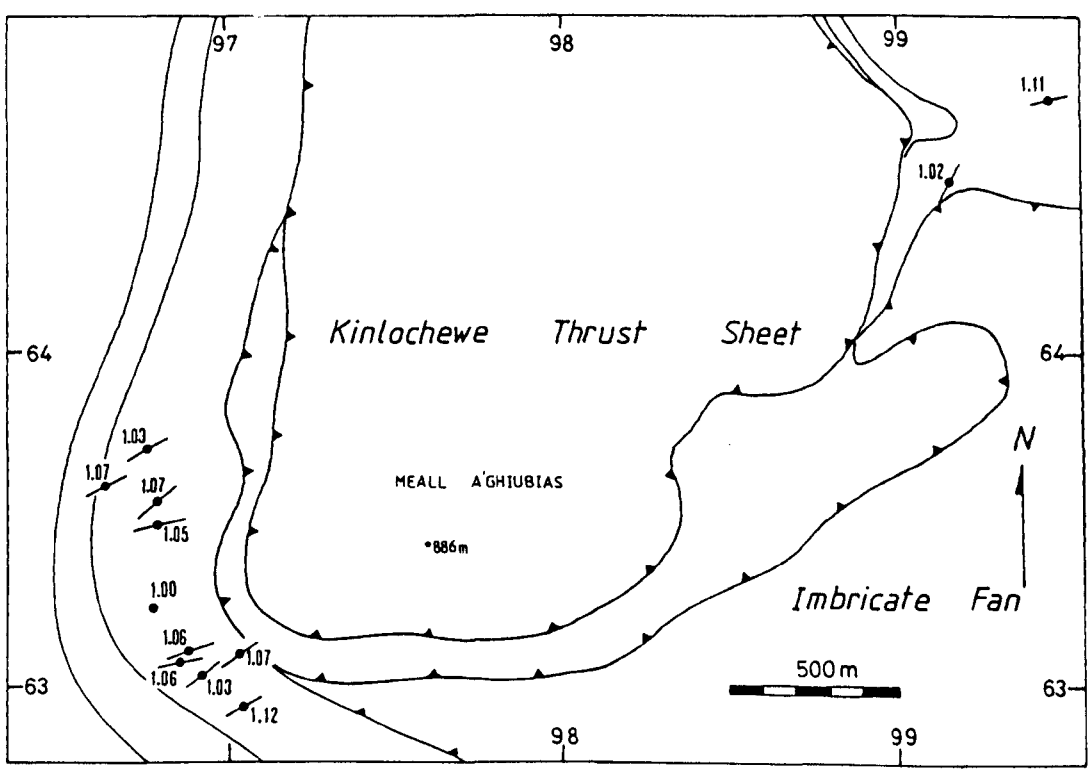

FIG. 3.2 Strain ratios and long axis orientations based on the results given in Table 3.1.

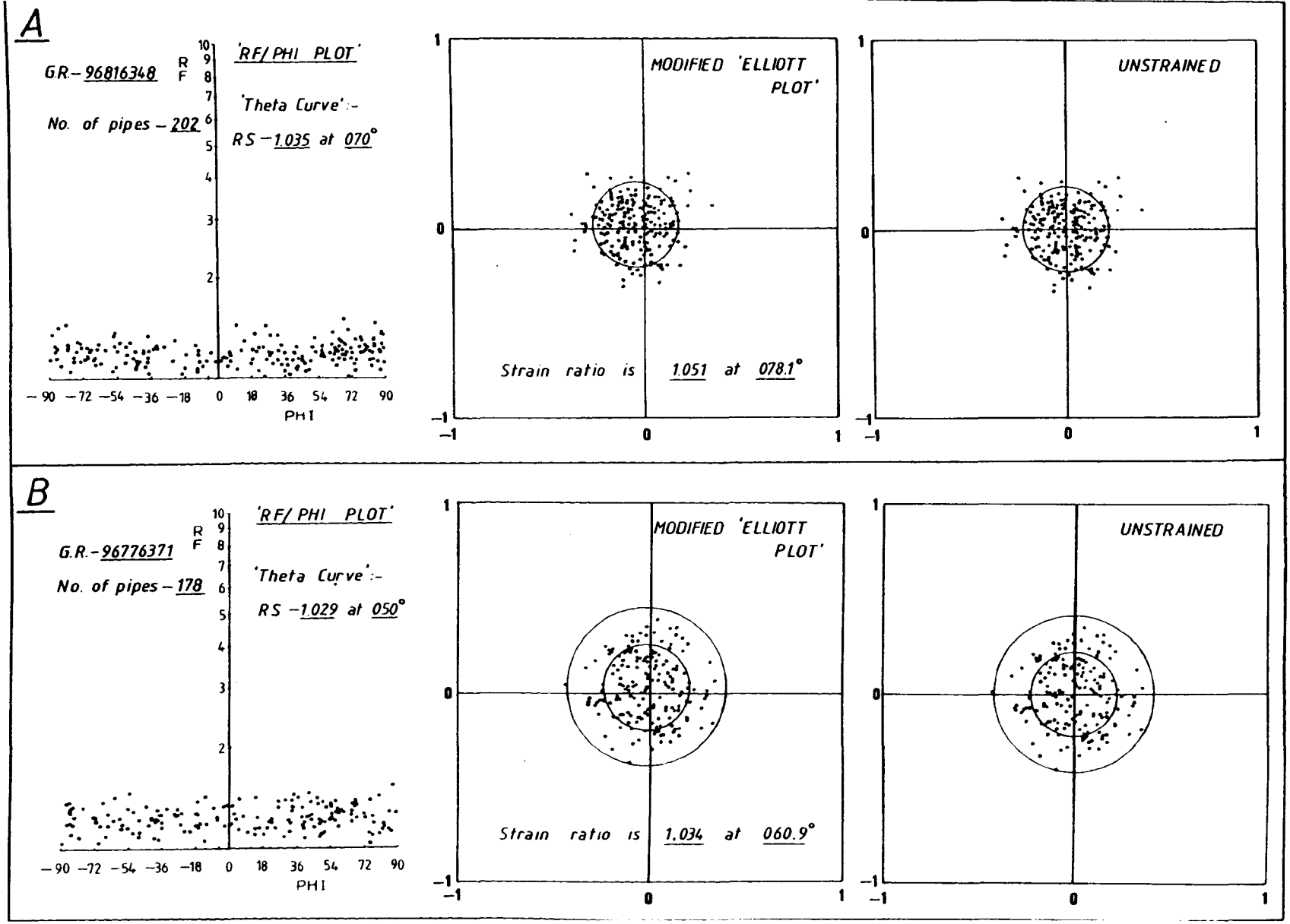

FIG. 3.3 'Rf/Phi' and 'Wheeler' plots for localities (96816348) and (96776371).

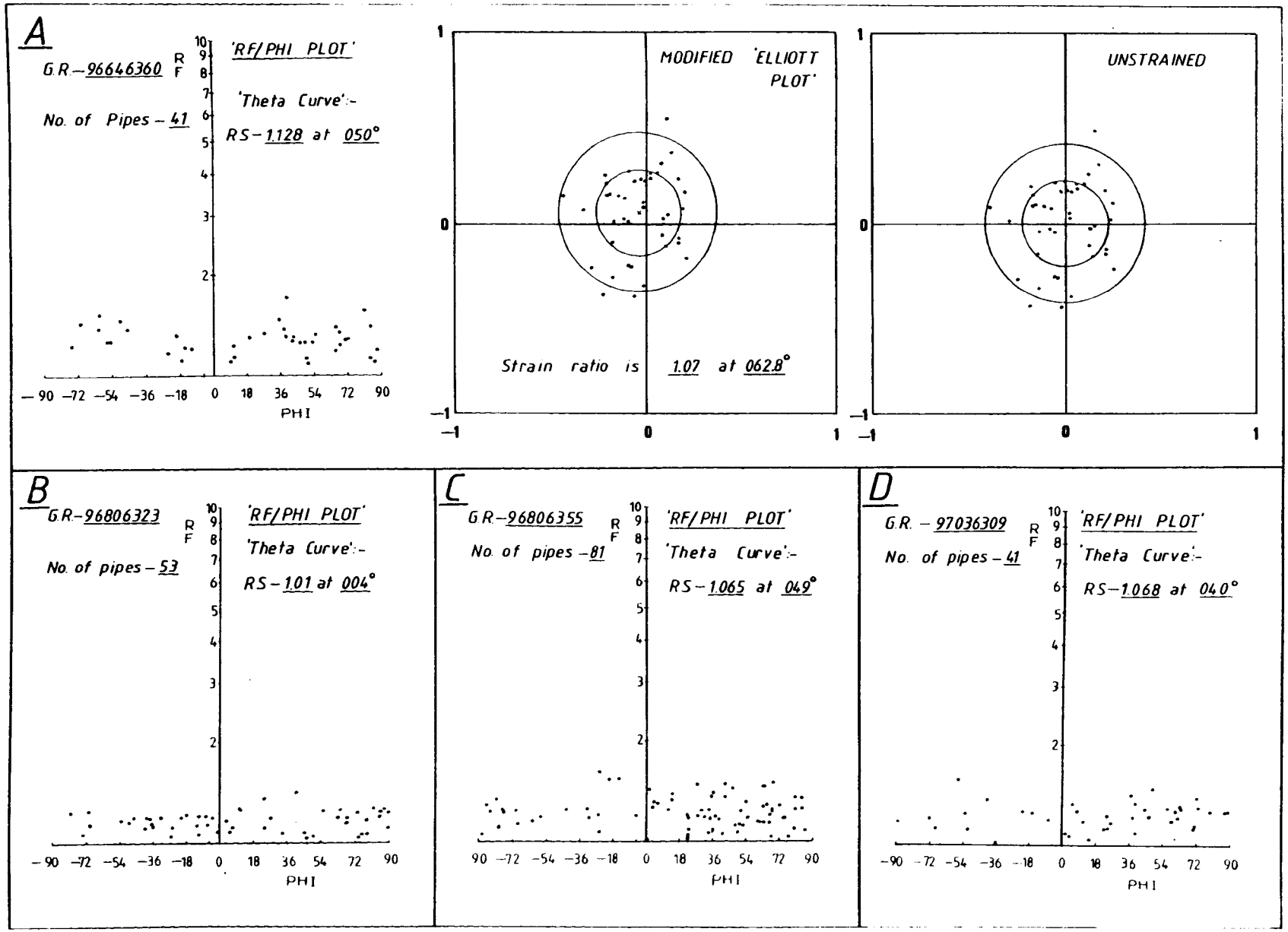

FIG. 3.4 'Rf/Phi' and 'Wheeler' plots for localities (96646360) and (96806323). 'Rf/Phi' plots for localities (96806355) and (97036309).

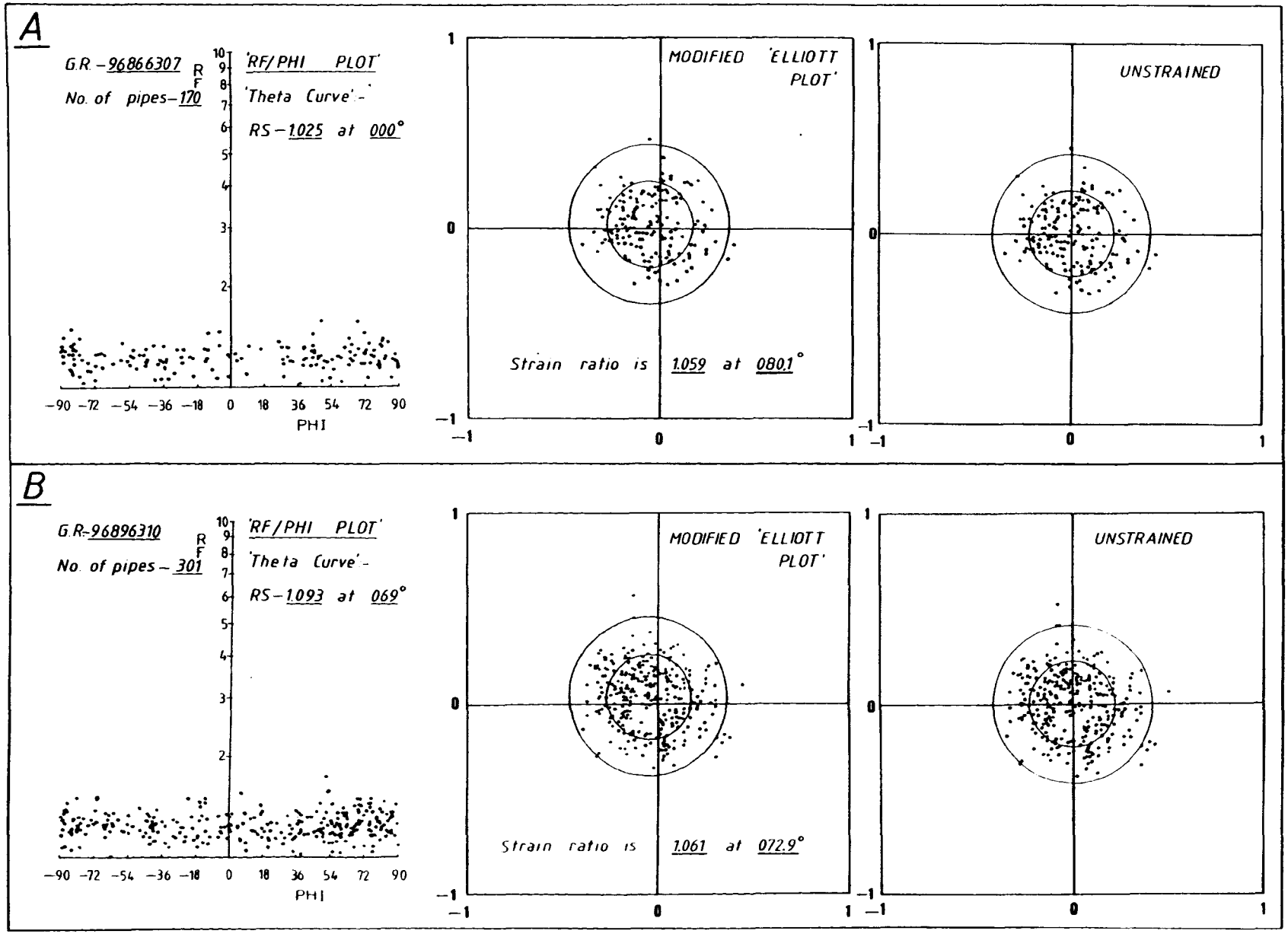

FIG. 3.5 'Rf/Phi' and 'Wheeler' plots for localities (96866307) and (96896310).

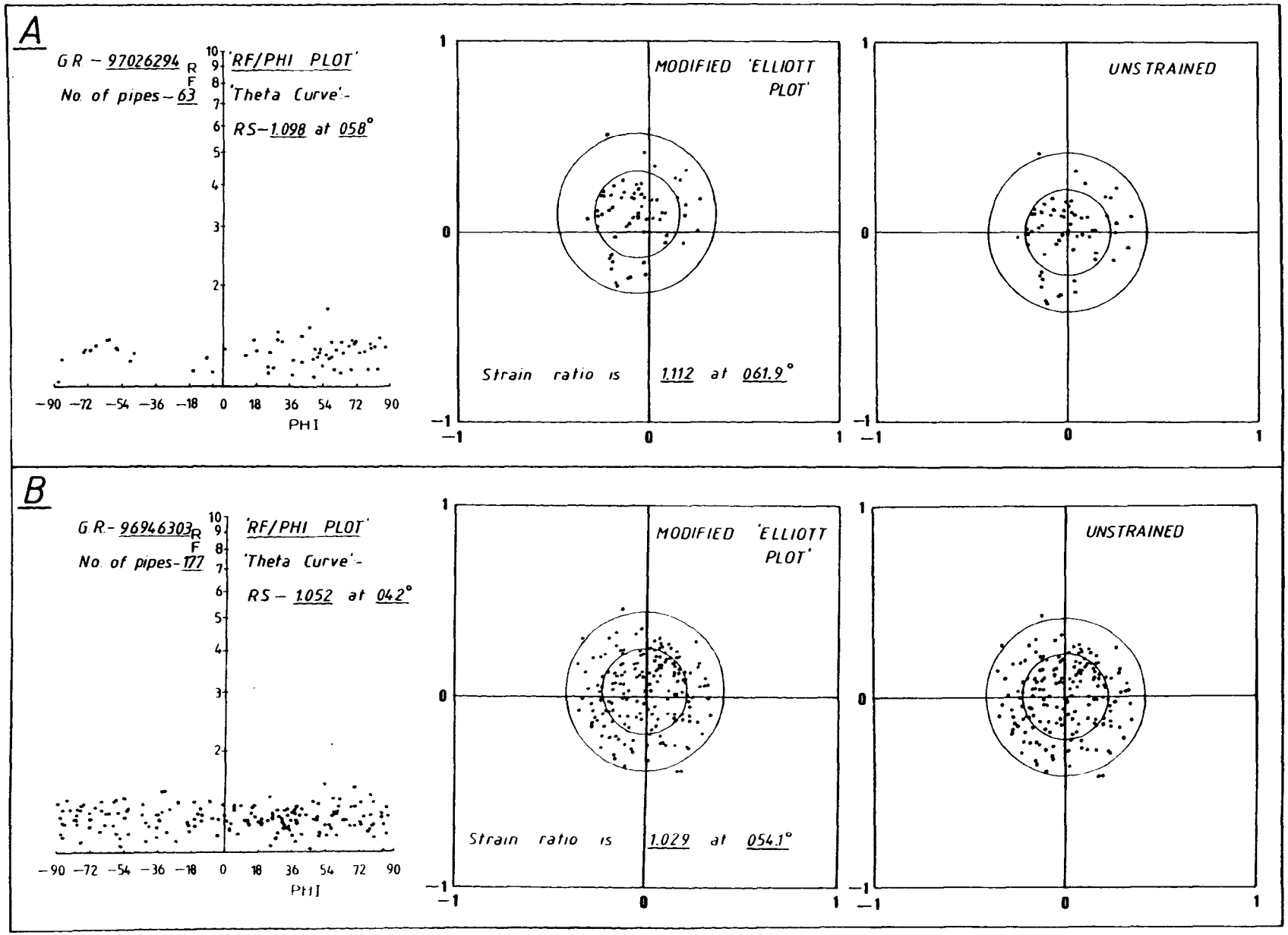

FIG. 3.6 'Rf/Phi' and 'Wheeler' plots for localities (97026294) and (96946303).

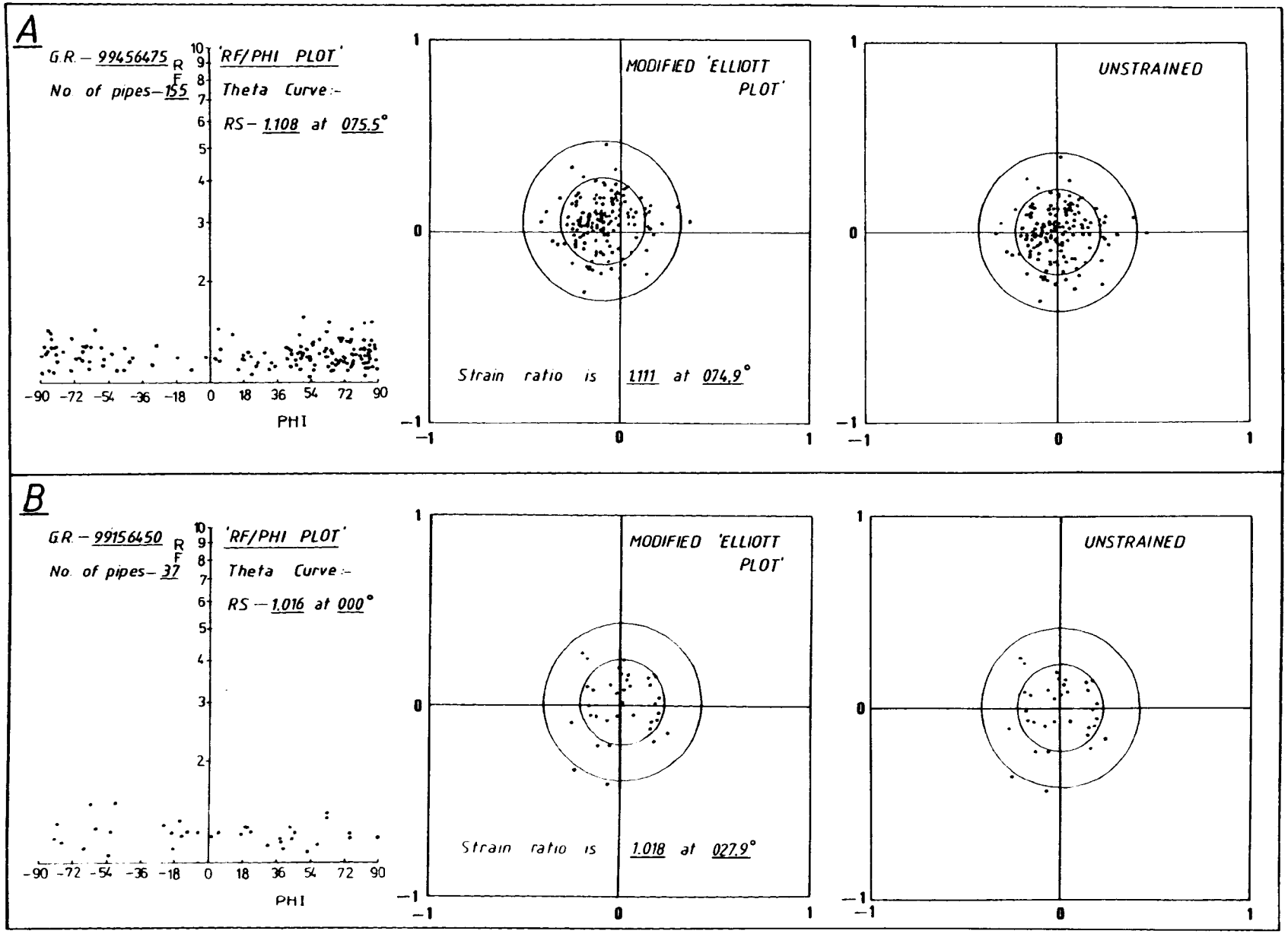

FIG. 3.7 'Rf/Phi' and 'Wheeler' plots for localities (99456475) and (99156450).

The strain ratio and orientation of the pipes on a plane parallel to bedding can be used to evaluate the amount of differential movement (the layer normal shear component) and the amount of layer parallel shortening. This method of factorising strain ratios into components of layer parallel shortening and layer normal shear was introduced by Coward & Kim (1981). Their model for factorisation of displacements is illustrated in Fig. 3.8, based on a subdivision of strains into longitudinal strains (layer parallel shortening or extension), layer parallel shear and layer normal shear. In this diagram the XY coordinate plane is parallel to bedding. Note that Coward & Kim (1981) do not follow this procedure; instead these authors illustrate the YZ coordinate plane as parallel to bedding.

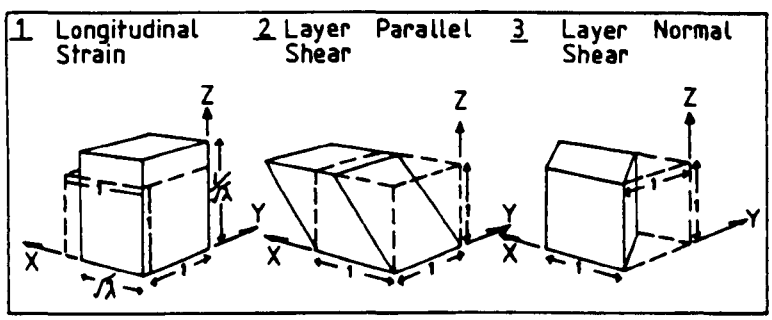

FIG. 3.8 Displacement components for the factorisation model of Coward & Kim (1981).

To factorise the observed strain into components of layer parallel shortening and layer normal shear, it is necessary to assume one of the strain sequences listed below.

1. Longitudinal strain followed by layer normal shear.
2. Layer normal shear followed by longitudinal strain.
3. Simultaneous development of layer normal shear and longitudinal strain.

Coward & Kim (1981) and Fischer & Coward (1982) were

able to assume that longitudinal strain predates shear in the evolution of the Assynt and Heilam regions of the northern Moine Thrust Zone. This will be assumed to be a valid approach here and reassessed at a later stage. The orientation of the long axes of the strain ellipse relative to the shear direction is plotted against the strain ratio, see Fig. 3.9. The contours on this diagram refer to lines of equal values of layer parallel shortening ($\sqrt{\lambda}$) and lines of equal shear strain (γ_2). This diagram is valid for a deformation sequence of longitudinal strain followed by simple shear. *The strain ellipse lies in the bedding plane.*

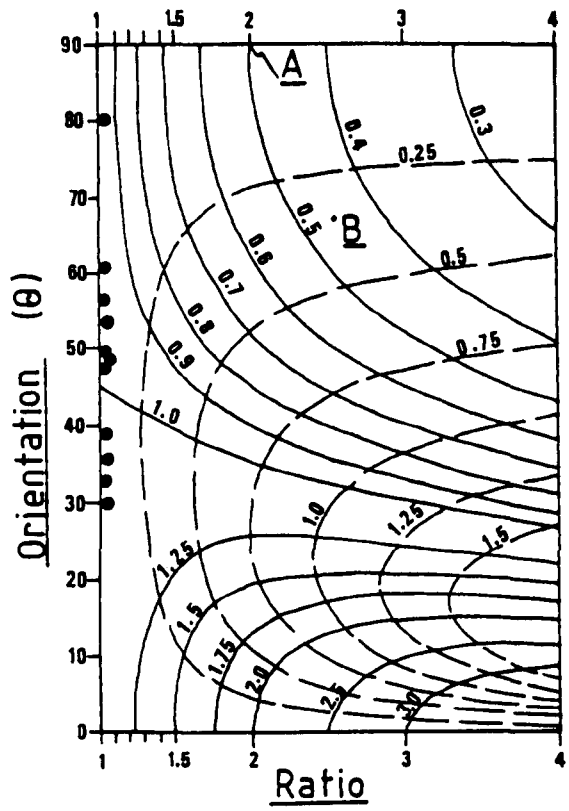

FIG. 3.9 Strain ratio plotted against the orientation of the long axis of the strain ellipse relative to the movement direction.

If a strain locality indicated a finite strain ratio (Rs) of 2:1 with the long axis of the strain ellipse orientated at 90° to the movement direction (θ = 90), then that locality would plot on Fig. 3.9 at position A. This would indicate deformation involving layer parallel shortening

only, where $\sqrt{\lambda}$ = 0.5 and the local shortening would therefore be 50%. If, however, a different strain locality indicated a finite strain ratio (Rs) of 2.5 : 1 with the long axis orientated at 65° to the movement direction, B on Fig. 3.9, then a deformation sequence of layer parallel shortening followed by layer normal shear is inferred. The component of layer parallel shortening $\sqrt{\lambda}$ can be estimated by tracing the plotted position of the strain locality parallel to the $\sqrt{\lambda}$ contours to the upper boundary of the diagram, a value for the strain ratio prior to shearing would be 2.25 and the value of $\sqrt{\lambda}$ is therefore 0.44. The value of the layer normal shear component can be estimated by gauging the approximate γ_2 contour which passes through the plotted position of the strain locality and in this case γ_2 is approximately 0.35.

The foreland pipe localities illustrated in Fig. 3.9 clearly do not show high strain ratios. This may be expected, as by definition the foreland is immediately below the structurally lowest thrust and therefore represents the position at which deformation ceased in that part of the thrust belt. However, it is important to sample the region near to the floor thrust of the imbricate fan, in order to search for a subdued version of ductile bead strains for this part of the thrust zone.

The maximum strain ratios resulting from the Shimamoto & Ikeda method indicate an Rs value of 1.11 and 1.12 orientated at 35° and 48° to the shear direction respectively; the shear direction is assumed to be parallel to the movement direction of structurally higher thrusts as suggested by thrust geometries. In the case of the locality which shows a θ value of 48° and an Rs value of 1.12, a $\sqrt{\lambda}$ value of approximately 0.98 is suggested from the graph, an early layer parallel shortening component of approximately 2%. This locality (97026294) represents the maximum layer parallel shortening component from any of the foreland localities. A very small amount of early layer parallel extension is suggested by locality (99456475), the Rs and θ values of 1.11 and 35° respectively, suggest a $\sqrt{\lambda}$ component of less than 1.03, which indicates a layer parallel extension

component of less than 3%. The most obvious feature of the strain map in Fig. 3.2 is that all of these foreland localities show principal extension directions which are oblique to the movement direction and therefore suggest a small component of layer normal shear in the northern part of the study area. This is consistent with the greater displacement observed within the imbricate fan in the south of the study area. The amount of early layer parallel shortening or extension is therefore extremely small, and certainly less than 3% in the zone immediately below the imbricate fan floor thrust. However, the most important feature of these foreland results is that a small layer normal shear is suggested from the orientations of the principal extension directions.

Before proceeding it is essential to question the validity of these results; the Rs values are small and if they are a product of the analytical method providing a finite strain ratio which may not exist in reality, then the principal extension directions presented in Table 3.1 may be meaningless. In order to examine this point, a short discussion on the Theta-Curve and Wheeler methods is required.

The Theta-Curve method of Lisle (1977) is intended to be used in conjunction with the Rf/Phi plot of Ramsay (1967, p.201-211) and Dunnet (1969). Simply, the Rf/Phi plot consists of the axial ratio of the strain marker (Rf) plotted against the orientation of the long axis relative to a reference direction (Phi). Assuming homogeneous strain, the finite strain ratio (Rs) can be estimated by a process of visual 'best-fit' using 'onion-curves' (Dunnet, 1969). This is the most rapid method of providing an estimate of the actual Rs value. However, it is not possible to be confident of an Rs value determined by this method unless the strain markers were originally all of similar shape, the initial ratios (Ri) must therefore be quite consistent. The bedding plane section of a set of pipes certainly falls into this category, see Fig. 3.10, and for high values of shortening, the visual 'best-fit' method using 'onion-curves' is rapid and accurate. The pipe data from the Beinn Eighe region

suggests that there is a very small amount of internal deformation within the study area and it is not possible to use a visual 'best-fit' method on these Rf/Phi plots.

FIG. 3.10 View of one of the bedding plane exposures of Pipe Rock used in this foreland study (96896310); 310 pipes were measured at this locality.

The Theta-Curve method provides an alternative approach and is described here. Any set of strain markers which are initially elliptical and randomly orientated will obviously show a statistically random set of long axis orientations prior to deformation. Therefore an Ri/Theta diagram, illustrating the initial ratio and long axis orientation prior to deformation, can be subdivided into intervals representing equal segments along the Theta axis; each of these intervals should contain an equal number of markers, see Fig. 3.11. If, for example, 9° intervals are used, then each interval should contain 5% of the total number of markers.

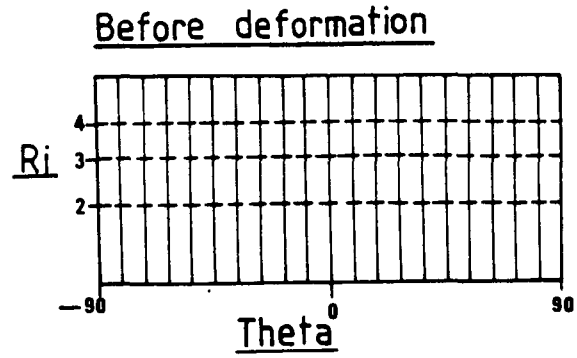

FIG. 3.11 Ri/Theta diagram. If there is a perfectly random orientation distribution of markers before deformation, then each sub-area of 9° width will contain 5% of the total number of markers (Lisle, 1977, p.384, Fig. 1).

After deformation, the theta-curves will adopt a shape similar to that shown in Fig. 3.12, which illustrates the case for an Rs value of 2.2, each interval between the theta curves should therefore contain 5% of the total number of strain markers, assuming an initially random orientation.

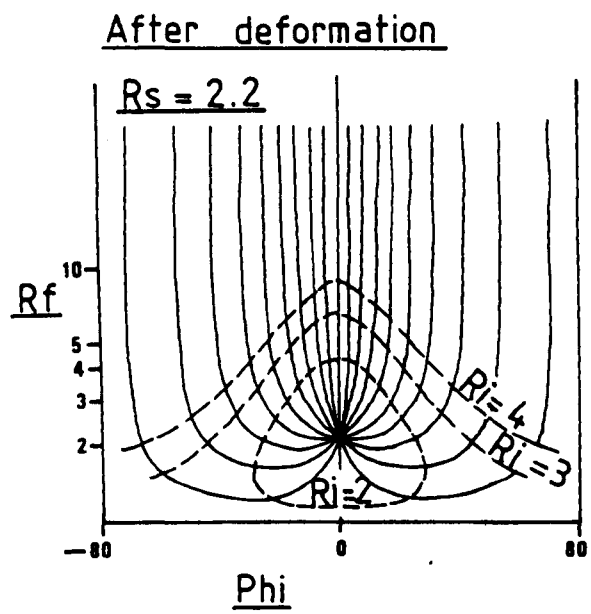

FIG. 3.12 Rf/Phi diagram for Rs = 2.2, showing shapes of curves of constant Ri ("onion-curves") and constant theta ("theta-curves") (Lisle, 1977, p.384, Fig. 1).

Therefore it is now possible to provide an Rs value by choosing the 'best-fit' of theta-curves using a chi-squared test; the lowest value of chi-squared is selected and indicates the Rs value. This method has been carried out using the computer program for the Theta-Curve method, devised by Peach & Lisle (1979), which sequentially tests the data for various Rs values in increments of 0.05. The Rs value which gives the lowest value of chi-squared, and hence the most even distribution of strain markers within the theta-curve intervals, is taken as the axial ratio of the finite strain ellipse. The Rs value is given to a precision of 0.001 by the Theta-Curve program.

The dispersal of data points in the Rf/Phi plots of Figs. 3.3 to 3.7 suggests that the strain markers were randomly orientated prior to deformation. This observation is possible as the strain is so low. Obviously it is not advisable to judge the degree of initial randomness of a population by visually assessing the strained distribution. The procedure of pipe measurement has been described and every pipe that was measurable has been included in this study, and therefore the sample population is felt to reflect the actual distribution.

If the sample population did not show a perfectly random orientation distribution prior to deformation, then a false small strain will result from application of the Theta-Curve program; this background 'strain' will be present on every sampled locality which did not have a perfectly random pretectonic orientation distribution. It is interesting that the Theta-Curve program gives Rs values of 1.01, 1.02 and 1.03 for the localities (96806323), (99156450) and (96866307) respectively, and more importantly principal extension directions of 000°, 004° and 000°. Therefore, there may be a small background 'strain' at some of the localities which has not been modified by any real internal deformation, in which case the Theta-Curve program appears to choose the reference direction as the principal extension direction. If the population did not have a random pretectonic orientation distribution then chi-squared for the

chosen Rs value is likely to be high (Peach & Lisle, 1979). It is noticeable that the chi-squared value for locality (96866307) is anomalously high, Table 3.2. However, despite the evidence for an initial random orientation distribution, the Theta-Curve results from the foreland show consistent obliquity of principal extension directions, except for the 3 localities discussed above. It is therefore felt that the information produced by the Theta-Curve method in this foreland region is valuable. In order to substantiate any conclusions that may be drawn from these results, it was decided to replot all of the data using a different strain analysis technique based on the method of Elliott (1970) and modified by Wheeler (in press).

	'Theta-Curve'		
Locality	Rs	Direction	Chi-Squared
96816348	1.04	070	10.2
96776371	1.03	050	8.4
96646360	1.13	050	0.5
96806323	1.01	004	9.5
96806355	1.07	049	5.3
97036309	1.07	040	0.7
96866307	1.03	000	44.5
96896310	1.09	069	9.5
97026294	1.10	058	3.8
96946303	1.05	042	7.9
99456475	1.11	076	14.5
99156450	1.02	000	0.9

TABLE 3.2 Table illustrating the chi-squared values for each of the foreland localities, based on the Rs value provided by Theta-Curve program (Peach & Lisle, 1979).

Wheeler (in press) describes a modification of the 'Shape Factor Grid' of Elliott (1970), to produce a new graphical method for displaying strain data on a polar graph. The 'Shape Factor Grid' is a plot of the double-angle between the long axis of the strain marker and the reference direction, as the angular coordinate, and $\frac{1}{2}\ln$ (axial ratio) as the radial coordinate (ε). The modification proposed by Wheeler involves plotting $\sinh 2\varepsilon = \frac{1}{2}(R - \frac{1}{R})$ instead of $\frac{1}{2}\ln R$, as the radial coordinate, Fig. 3.13. This modification results in all points moving along straight parallel

lines when a strain is imposed. The hyperbolae on the grid are separated by constant ln R increments of 0.2.

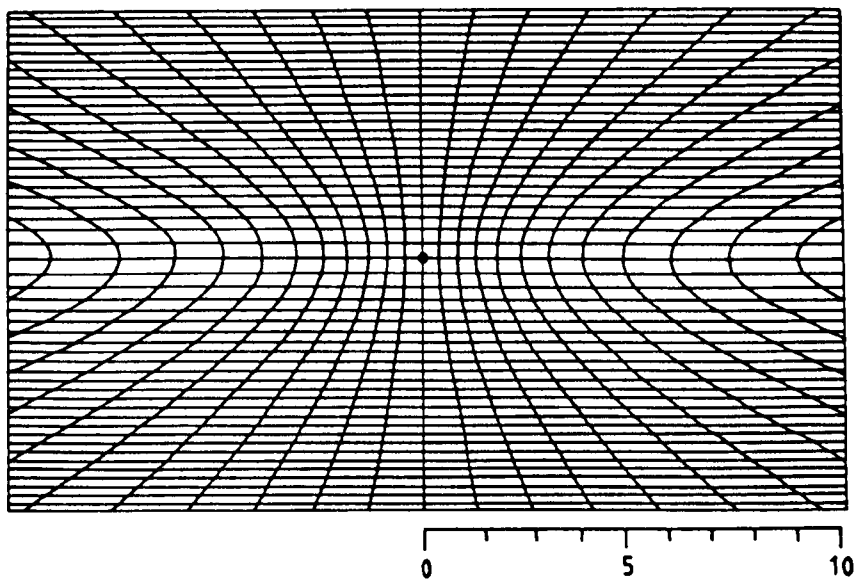

FIG. 3.13 The modified 'Elliott Grid'. The scale shows the radius in terms of R. Increment in R along Y-axis is 0.2; increment in ln R for hyperbolae is 0.2.

To plot a strain marker on the Wheeler grid, the angle between the long axis of the strain marker and the reference direction (θ) is doubled (2θ) and measured anticlockwise from the datum to give the ray on which the point will lie. The radial coordinate is simply calculated as $\frac{1}{2}(R - \frac{1}{R})$. The strained distribution can be unstrained by imposing an additional strain ($^{1}/R_{S_1}\theta_S$) on a distribution which has been deformed by a strain ($R_{S_1}\theta_S$). The strained plots illustrate a 'best-fit' set of ellipses for equal values of Ri, according to the numerical result of Rs from the Shimamoto & Ikeda method. Simply, these ellipses represent strained distributions that prior to deformation lay in a circle around the origin. They are therefore the analogues of the 'onion-curves' of Dunnet (1969). It is important to note that they do not represent the finite strain ellipse for the strained distribution. A measure of the spread of the

axial ratios in the initial distribution, 'the distribution spread invariant' (J), can be calculated from the unstrained distribution and J = $\frac{1}{2}$ av. (Ri + $^{1}/_{Ri}$). Clearly, if the Ri value of all of the strain markers was 1 then the J value will also be 1. The J values for the foreland strain localities are illustrated in Table 3.3.

	'Shimamoto & Ikeda'		
Locality	Rs	Direction	J
96816348	1.05	078	1.02
96776371	1.03	061	1.03
96646360	1.07	063	1.03
96806323	1.00	-	1.01
96806355	1.07	049	1.02
97036309	1.07	054	1.02
96866307	1.06	080	1.02
96896310	1.06	073	1.03
97026294	1.12	062	1.02
96946303	1.03	054	1.03
99456475	1.11	075	1.02
99156450	1.02	028	1.02

TABLE 3.3 Foreland Pipe Rock localities illustrating J values.

The values of Rs and the principal extension directions derived from the Theta-Curve method are certainly supported by the equivalent results from the Shimamoto & Ikeda method, Table 3.1. The major discrepancies occur in the case of the 3 localities which show very low strain and in which the Theta-Curve program appears to choose a principal extension direction close to the reference direction. Therefore the values from the Shimamoto & Ikeda method are used for the strain maps throughout this chapter. It is felt that the close similarity between values derived from both the 'Theta-Curve' and Shimamoto & Ikeda methods suggests that there is a small strain present within the zone immediately below the imbricate fan floor thrust. The amount of layer parallel shortening or extension varies between 0% and 3% and there is strong evidence for a small component of layer normal shear within this part of the foreland.

Having introduced the methods used to assess the finite strain within the Pipe Rock, the strain within the imbricate fan will now be examined.

(ii) Strains within the imbricate fan

The topographic level at which Pipe Rock is exposed within the imbricate fan is determined by the level of the floor thrust. In the S, on Sgurr Dubh, the horses are typically exposed as Torridonian sandstone and Lower Quartzite. In the N, in the region of the Beinn Eighe Nature Reserve, virtually all of the exposure between sea level and 600 m is composed of Pipe Rock. This allows determination of the strain at numerous positions within the Pipe Rock formation and hence in numerous positions within the imbricate geometry framework. The local geometry and strain is described from N to S within this region. The strain localities have been grouped into 4 separate zones for ease of description; the northernmost of these zones is illustrated in Fig. 3.14.

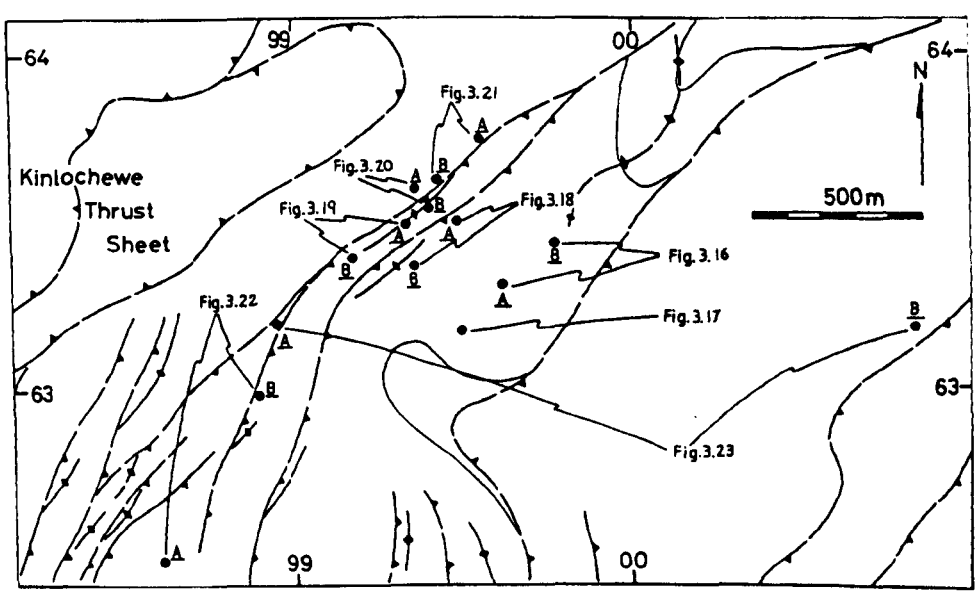

FIG. 3.14 Location of the northernmost strain localities within the imbricate fan.

The internal geometries of horses in the Beinn Eighe Nature Reserve region are characterised by the presence of anticlines in the hangingwall to imbricate thrusts. Interlimb angles of between 80° and 110° are common, suggesting folds resulting from differential movement or differential propagation of thrust surfaces. More open folds with interlimb angles nearer to 150° - 160° also occur in the hangingwall to imbricate thrusts and these may be structurally necessary flexures due to slip of the horse along a flat-ramp-flat footwall. It is now possible to assess the variation in longitudinal strain within a horse.

The finite strain ratios and principal strain directions from these northern localities are presented in Table 3.4. The strain ratios are plotted against the orientation of the long axis of the strain ellipse in Fig. 3.15.

			'Theta-Curve'		'Shimamoto & Ikeda/Wheeler'		
Locality	Fig.	No. of Pipes	Rs	Direction	Rs	Direction	J
99786344	3.16	200	1.13	090	1.09	092	1.03
99646331	3.16	55	1.27	036	1.21	039	1.03
99506317	3.17	205	1.04	112	1.07	112	1.04
99486350	3.18	49	1.11	054	1.07	056	1.03
99356337	3.18	60	1.06	111	1.07	097	1.04
99166339	3.19	116	1.12	062	1.14	062	1.03
99326349	3.19	147	1.12	037	1.13	037	1.03
99356360	3.20	94	1.15	065	1.11	067	1.02
99396354	3.20	197	1.05	041	1.03	042	1.02
99426362	3.21	196	1.13	098	1.12	100	1.02
99556374	3.21	314	1.17	071	1.10	073	1.03
98886298	3.22	58	1.27	040	1.23	039	1.03
98606249	3.22	83	1.12	057	1.09	065	1.03
98956320	3.23	388	1.10	050	1.08	046	1.04
00816317	3.23	187	1.20	083	1.22	084	1.02

TABLE 3.4 Rs values and principal strain directions for the localities illustrated in Fig. 3.14.

Assuming a deformation sequence of longitudinal strain followed by simple shear, Fig. 3.15, the maximum layer parallel shortening component is shown by localities (99646331), (99326349) and (98886298). In each case $\sqrt{\lambda}$ is between 0.8 and 0.9 indicating a layer parallel shortening component of

between 10% and 20%. The finite strain ellipses at these 3 localities show similar orientations, suggesting similar components of layer normal shear (from Fig. 3.15, $\gamma_2 < 0.25$). Localities (99326349) and (98886298) are situated near to the axial trace of hangingwall anticlines situated above imbricate thrusts. This is significant; it suggests that internal deformation may account for between 10% and 20% layer parallel shortening within the Pipe Rock prior to buckling and subsequent development of a thrust through the fold. In the case of locality (99646331), the layer parallel shortening may result from localised differential movement within one horse. There is good evidence for differential movement from the large scale geometry. To the NE of this locality a significant hangingwall anticline in Torridonian sandstone and Lower Quartzite is well exposed but is not a continuous structure to the SW; differential movement within this horse may have led to localised zones of layer parallel shortening. Growth of this hangingwall fold may have led to a small dextral shear within the horse. This idea is supported by the orientation of the strain ellipse at all 3 localities; each shows evidence for a small dextral shear superimposed on between 10% and 20% layer parallel shortening.

High values of layer parallel extension are also suggested by localities (00816317) and (99426362) situated in the footwall to a major imbricate thrust, between 20 m and 50 m below the thrust surface. The $\sqrt{\lambda}$ values suggested by these localities are between 1.1 and 1.2, indicating between 10% and 20% layer parallel extension. The position of these localities relative to the overlying thrust surface may not be significant; however, their position relative to the underlying thrust surface, which determines the geometry of the horse and hence the internal strain, is likely to be important. At this stage it will be noted that there is strong evidence for layer parallel extension developing within a horse above or behind the ramp.

A small component of layer parallel extension within a horse is suggested at localities (99506317) and (99786344) where there is a $\sqrt{\lambda}$ component of between 1.02 and 1.10,

indicating between 2% and 10% layer parallel extension prior to a small layer normal shear. It must be noted that these 2 localities occur within 200 m of locality (99646331), which shows evidence for up to 20% early layer parallel shortening. The deformation within this horse is therefore heterogeneous; this heterogeneity is clear from the strain map, Fig. 3.24, which shows varying components of layer

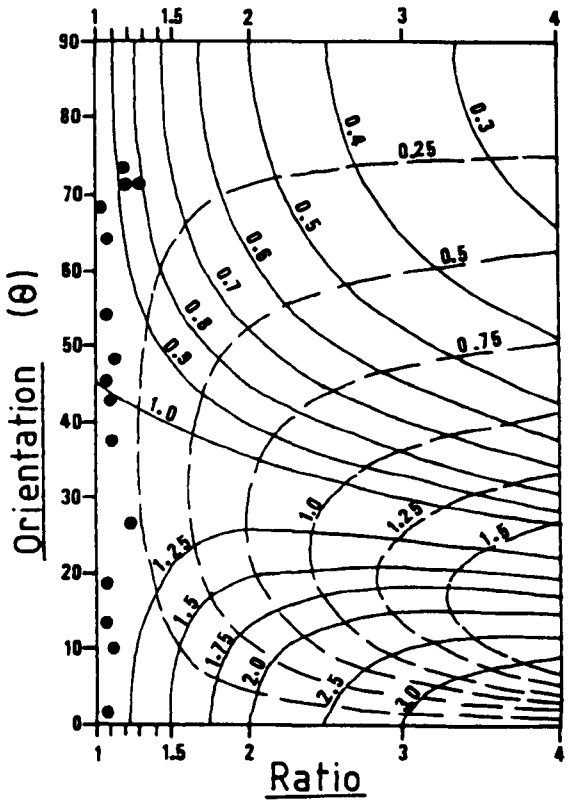

FIG. 3.15 Strain ratio plotted against the orientation of the long axis of the strain ellipse relative to the movement direction for the localities of Fig. 3.14.

normal shear and longitudinal strain for similar structural positions within a horse. It is therefore clear from the most significant strain results from this northern zone that a localised zone of layer parallel shortening may develop and lead to subsequent buckling prior to development of a thrust across this zone. There is evidence for a significant component of layer parallel extension within the horse above

or behind the ramp. Differential movement and hence layer normal shear is developed heterogeneously throughout the area shown in Fig. 3.14, and is also suggested by the sinuous axial trace of the hangingwall anticline in the NE of this area. The data from the 15 localities examined in this northern area of the Beinn Eighe Nature Reserve is illustrated as 'Rf/Phi' and 'Wheeler' plots in Figs. 3.16 to 3.23.

The finite strain on a plane parallel to bedding has been determined at a further 10 localities immediately to the S of the area shown in Fig. 3.24. The localities are illustrated in Fig. 3.25 and the results of application of the 'Theta-Curve' and 'Shimamoto & Ikeda methods are presented in Table 3.5. 'Rf/Phi' and 'Wheeler' plots are illustrated in Figs. 3.26 to 3.30.

The maximum layer parallel shortening component observed within this area is approximately 0.89, at locality (98746146), Fig. 3.28, suggesting approximately 11% layer parallel shortening at this position within this horse. This contrasts with the following 3 localities within the same horse, (98726188), (98756177) and (98726169). These 3 localities show evidence for deformation sequences of layer parallel extension followed by simple shear, simple shear only and layer parallel shortening followed by simple shear. All 4 of the localities discussed here occur within one horse in a position above or behind the underlying ramp.

It is clear that the strain within individual horses at similar structural positions is heterogeneous. The strain map for this area is shown in Fig. 3.32. The early layer parallel shortening component at these localities varies between 2% and 11%, and the early layer parallel extension varies between 0% and 10%. The locality which suggests the maximum layer parallel extension component is (98726188) which is referred to above and suggests extension within the horse in a position above or behind the ramp.

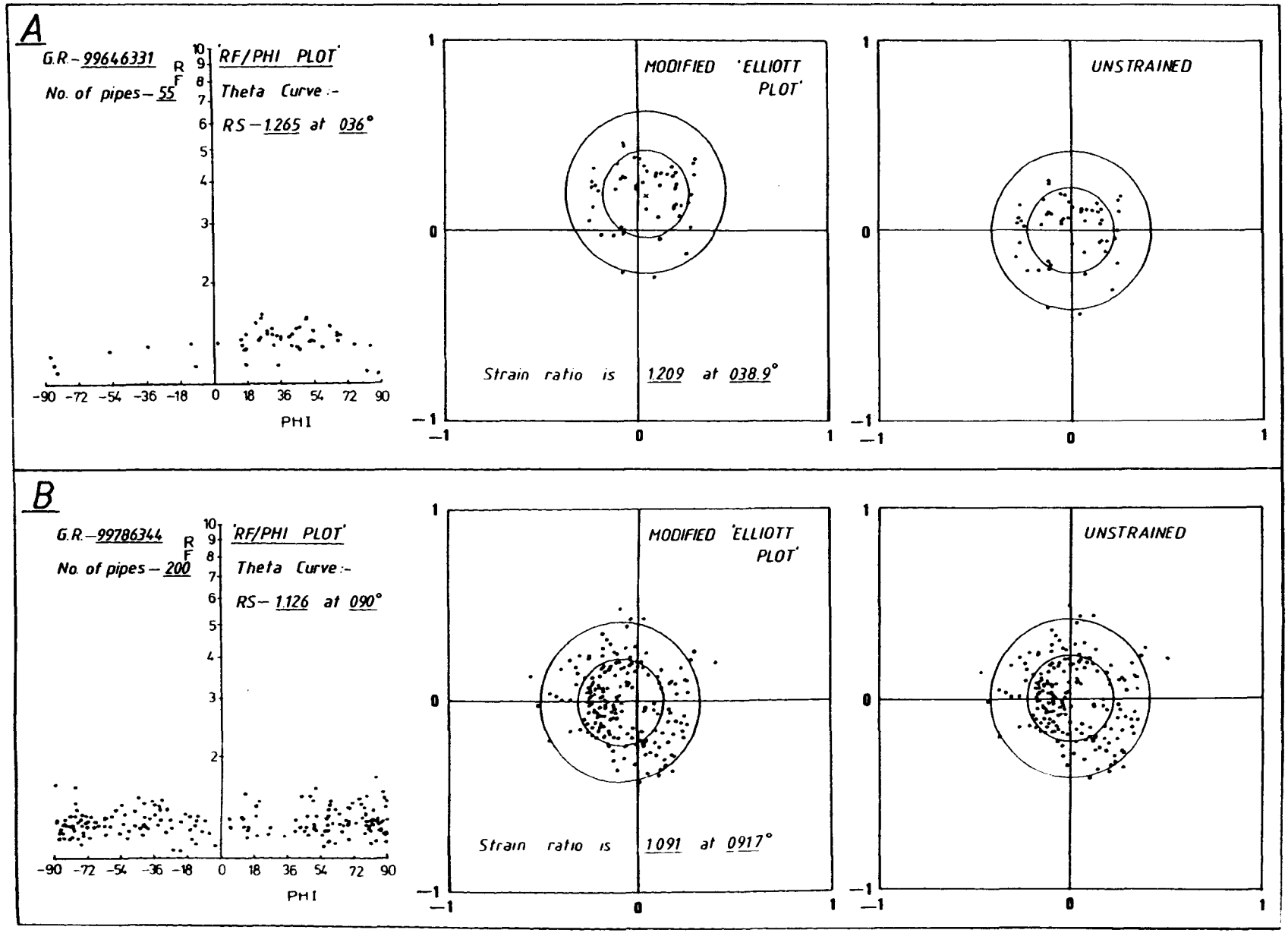

FIG. 3.16 'Rf/Phi' and 'Wheeler' plots for localities (99646331) and (99786344).

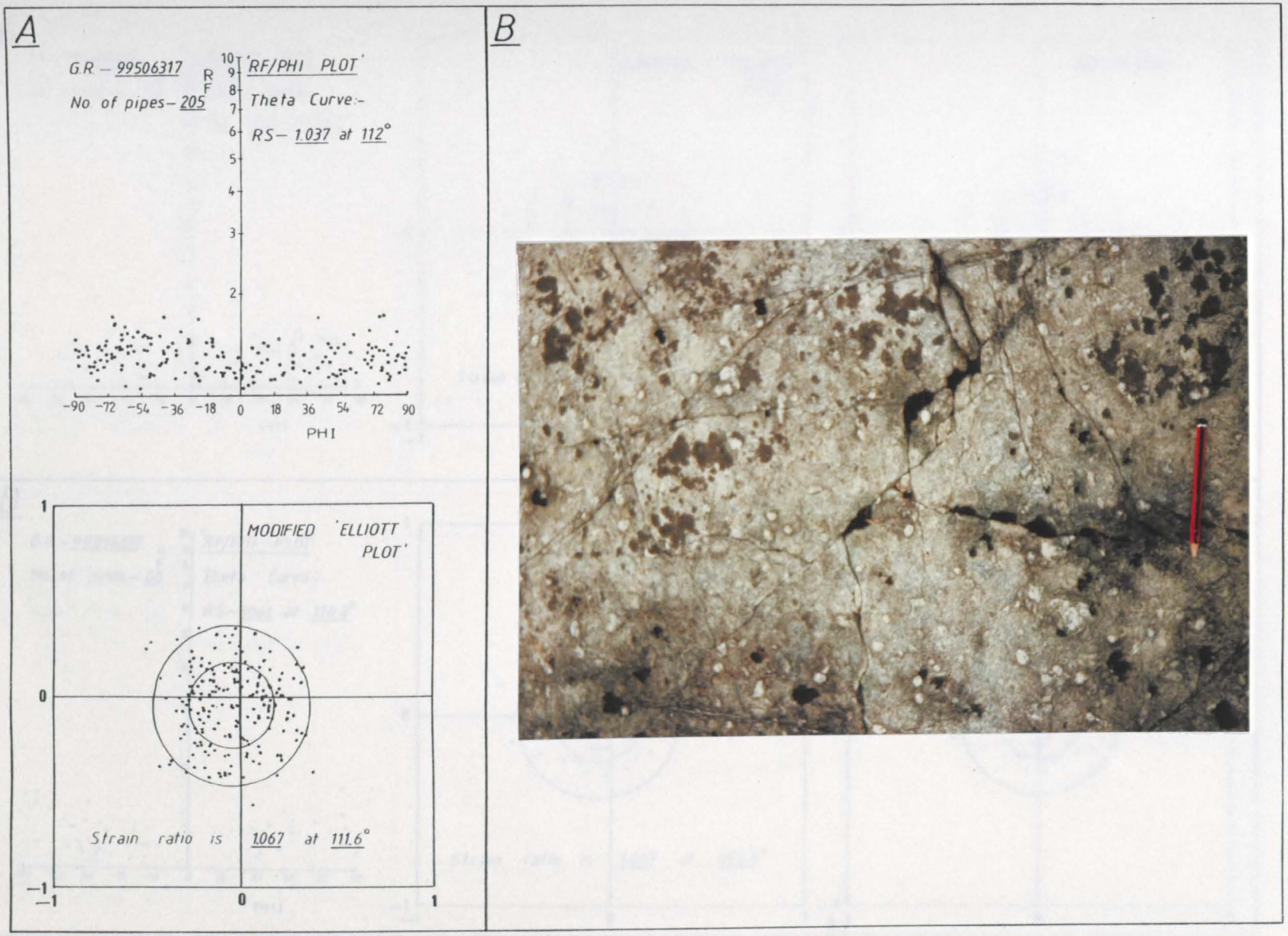

FIG. 3.17 'Rf/Phi' and 'Wheeler' plot for locality (99506317).

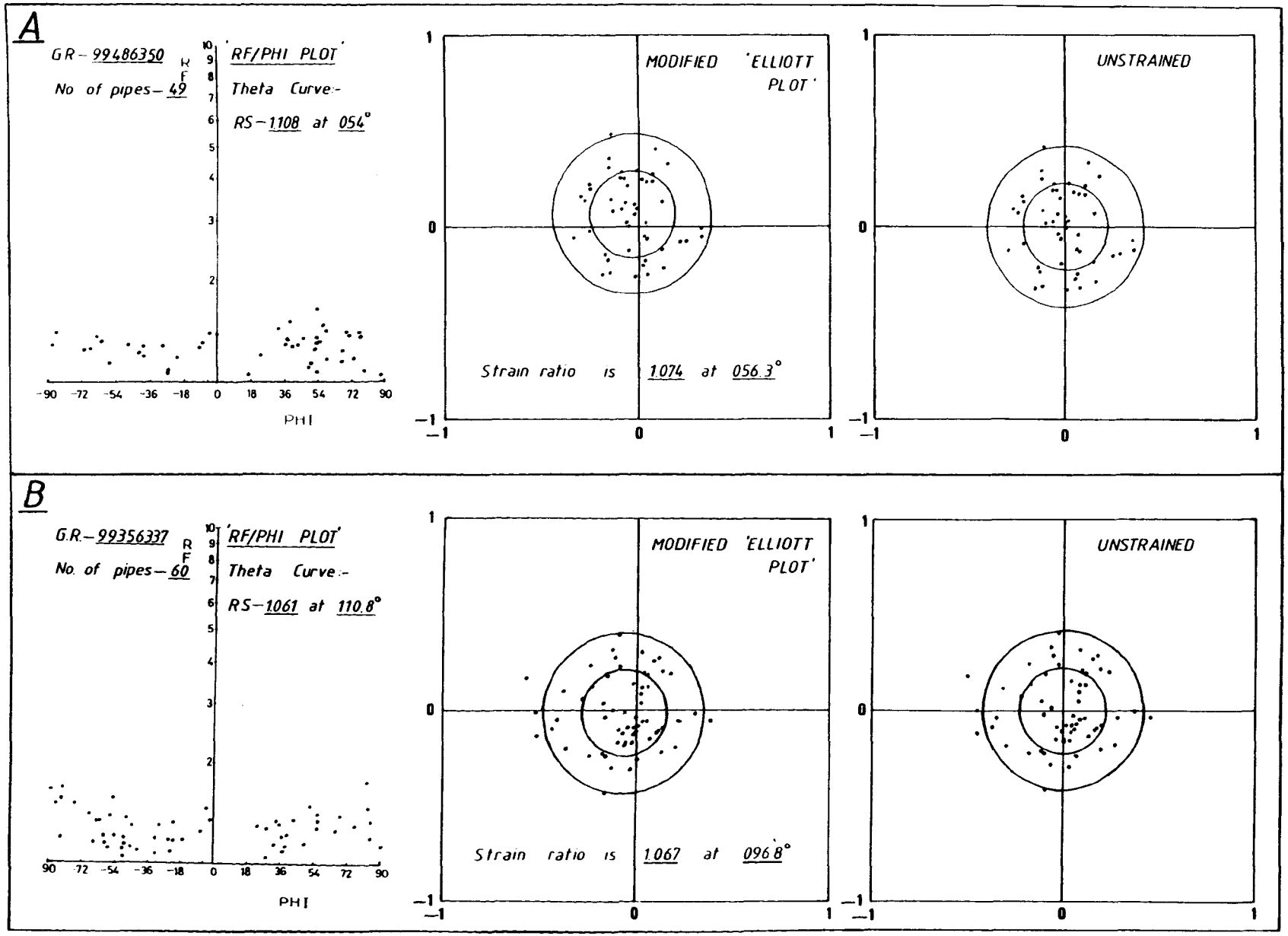

FIG. 3.18 'Rf/Phi' and 'Wheeler' plots for localities (99486350) and (99356337).

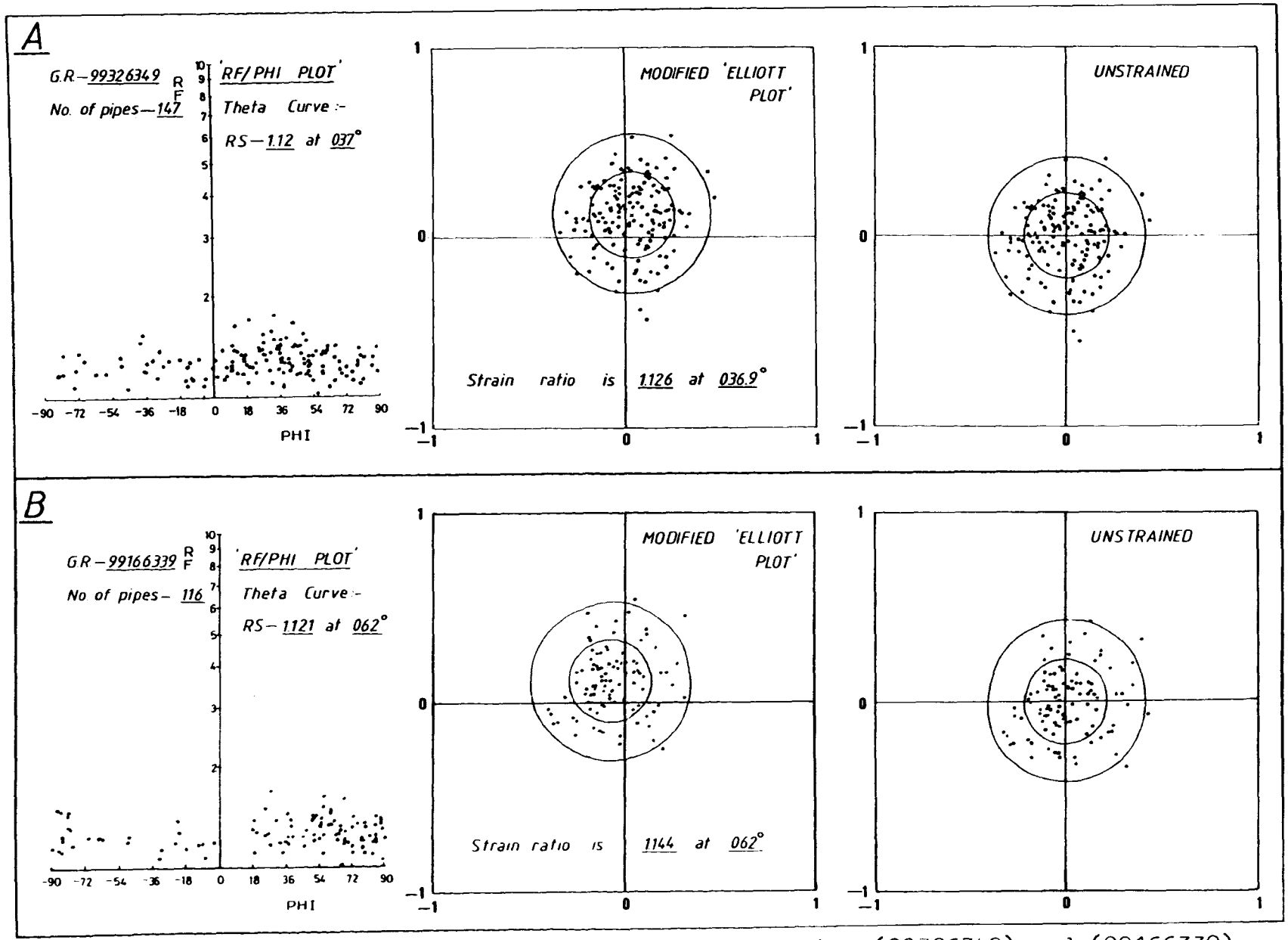

FIG. 3.19 'Rf/Phi' and 'Wheeler' plots for localities (99326349) and (99166339).

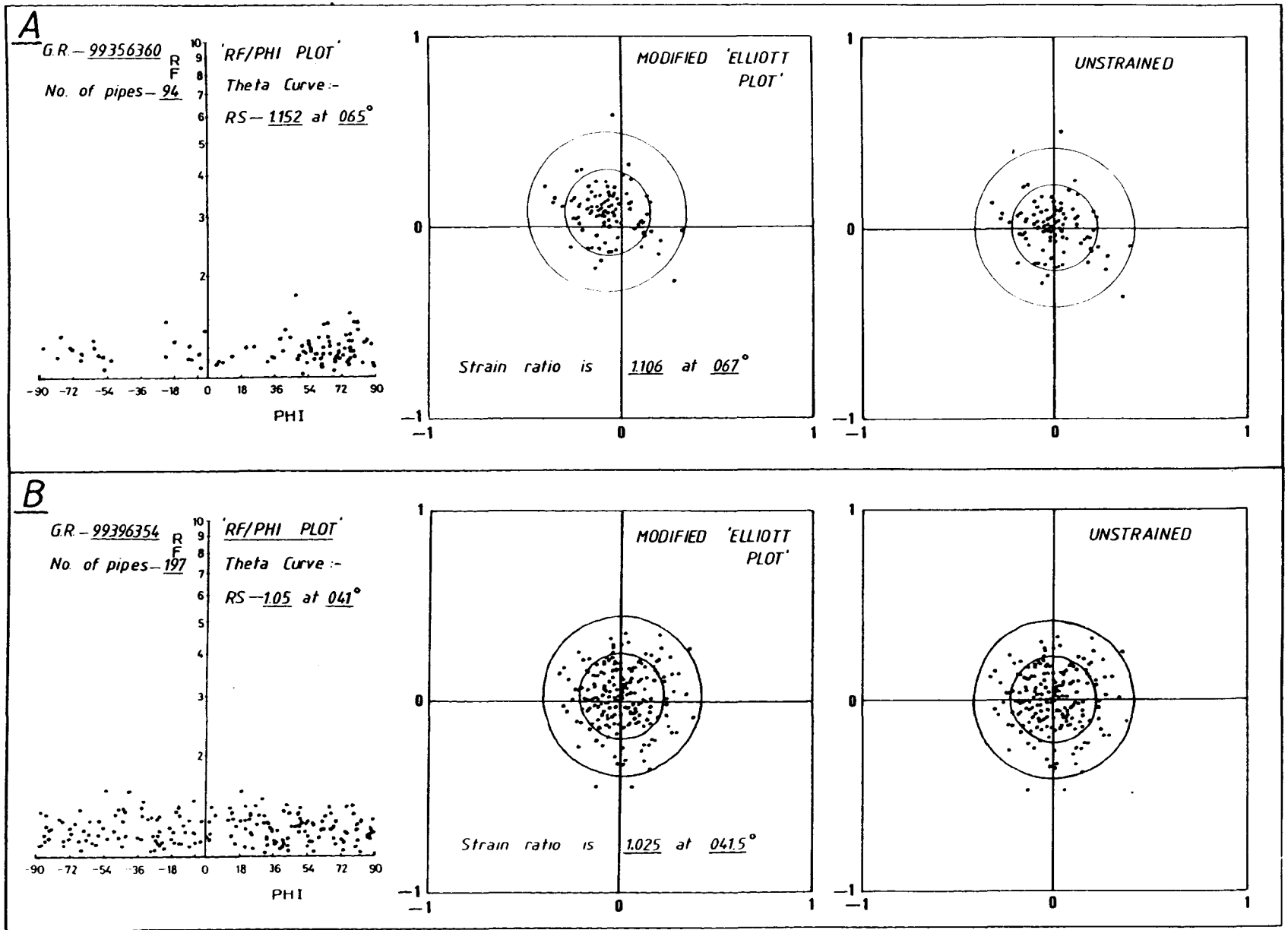

FIG. 3.20 'Rf/Phi' and 'Wheeler' plots for localities (99356360) and (99396354).

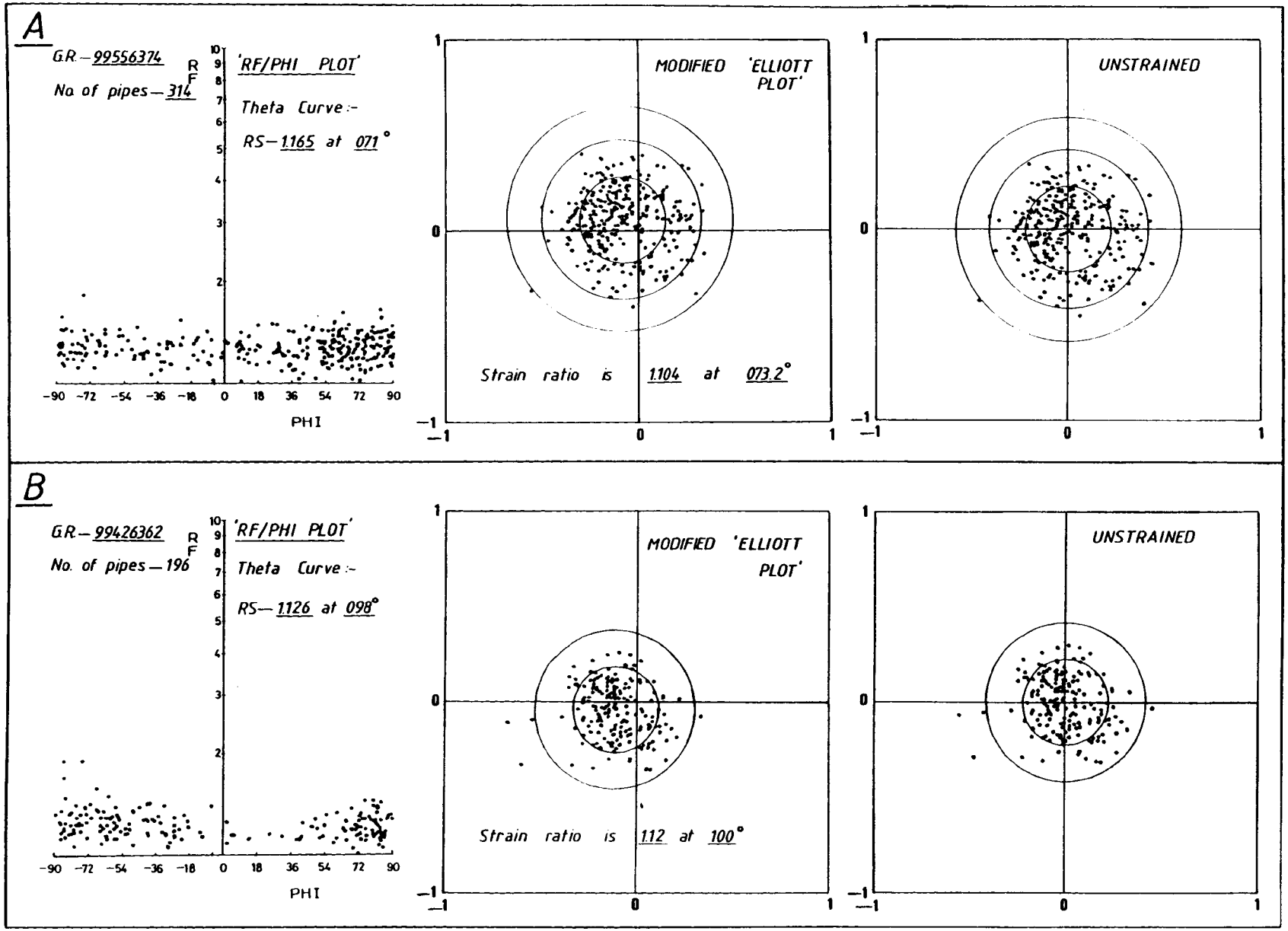

FIG. 3.21 'Rf/Phi' and 'Wheeler' plots for localities (99556374) and (99426362).

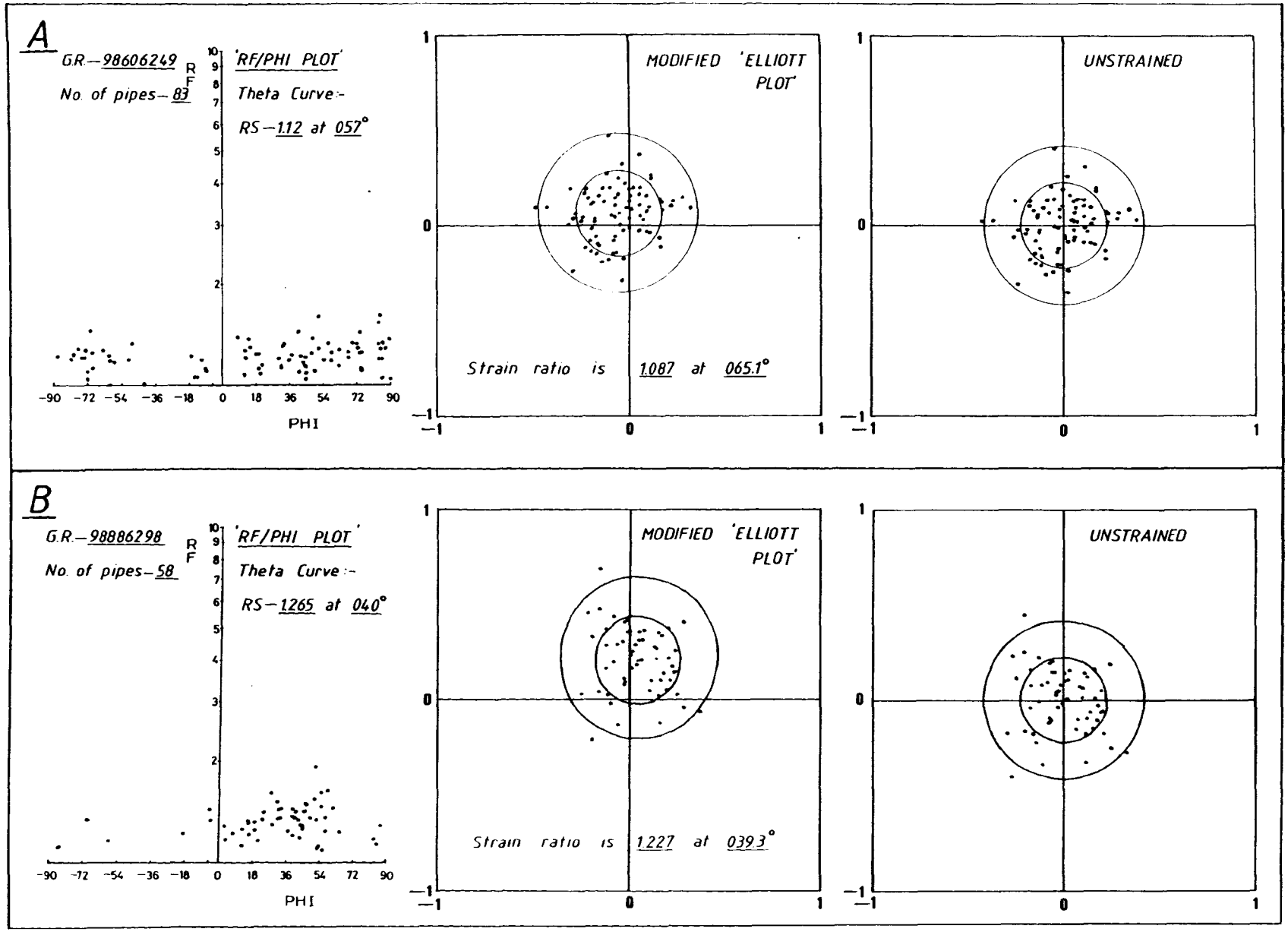

FIG. 3.22 'Rf/Phi' and 'Wheeler' plots for localities (98606249) and (98886298).

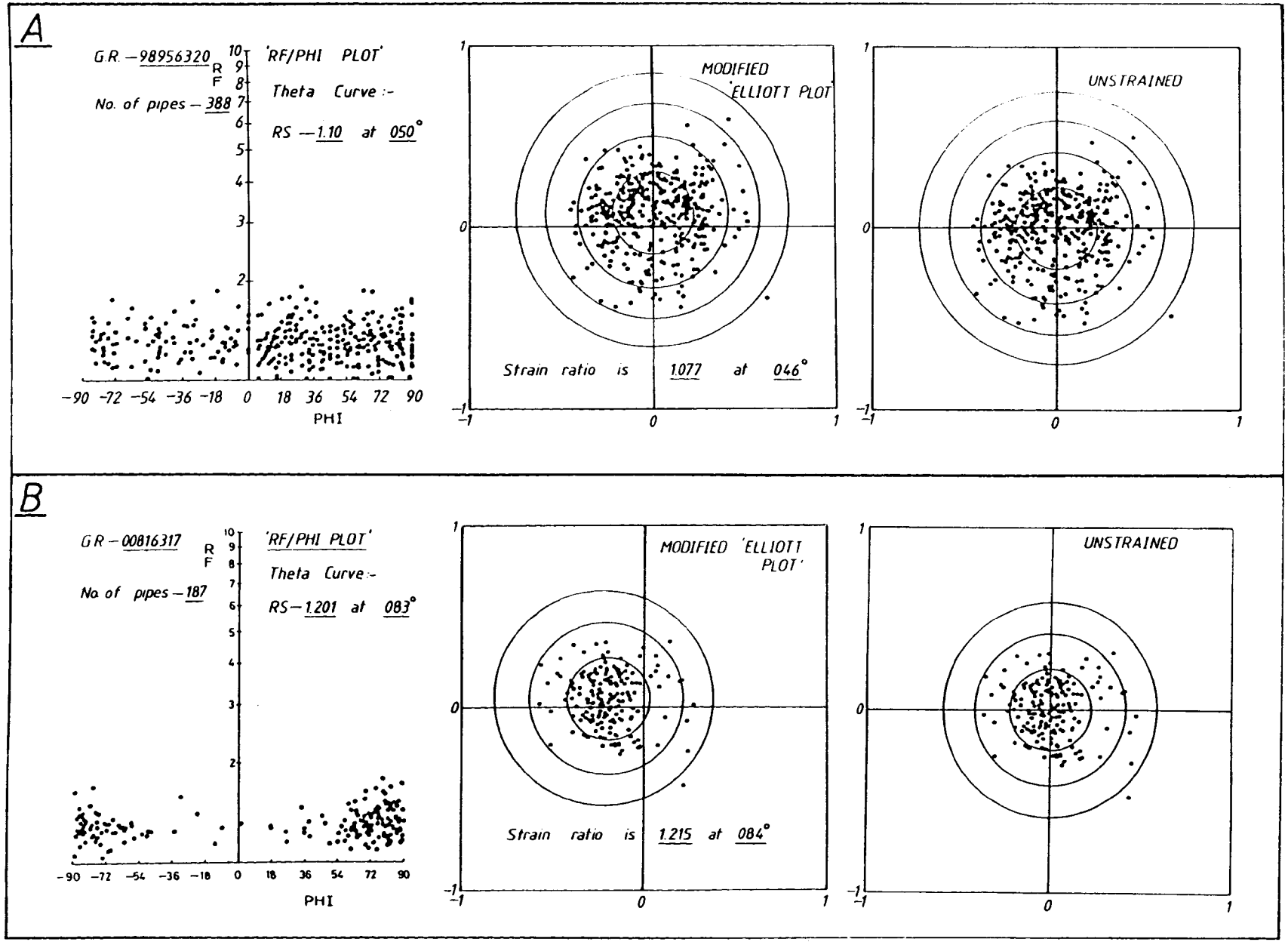

FIG. 3.23 'Rf/Phi' and 'Wheeler' plots for localities (98956320) and (00816317).

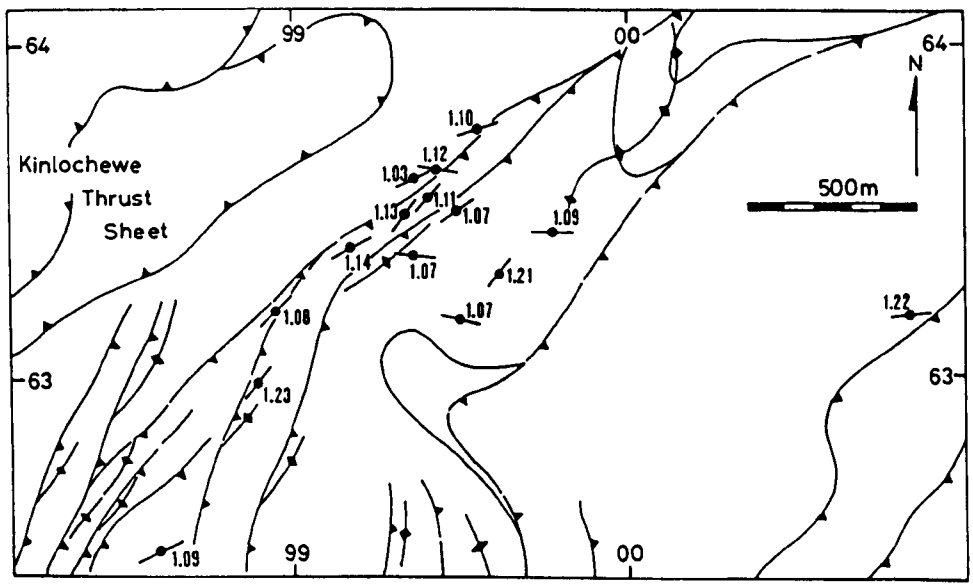

FIG. 3.24 Strain map of the northern part of the Beinn Eighe Imbricate Fan in the region of the Beinn Eighe Nature Reserve.

Although the 2 sets of finite strain results for the Beinn Eighe Nature Reserve area, presented in Tables 3.4 and 3.5, appear to be similar in terms of their heterogeneity, it is noticeable that there is a slight decrease in the component of early longitudinal strain from up to 20% in the N to a maximum value of near to 10% in the S. This occurs over an along strike distance of approximately 2 km. The occurrence of zones of buckling within the horses and hence development of hangingwall folds is greater in the northern sector than it is in the S. This perceptible gradation in the decrease in early ductile thickening to the S is coincident with an increase in the depth of the floor thrust to the imbricate fan from N to S. These observations suggest that variable components of longitudinal strain and layer normal shear are closely linked to the level of the imbricate fan floor thrust.

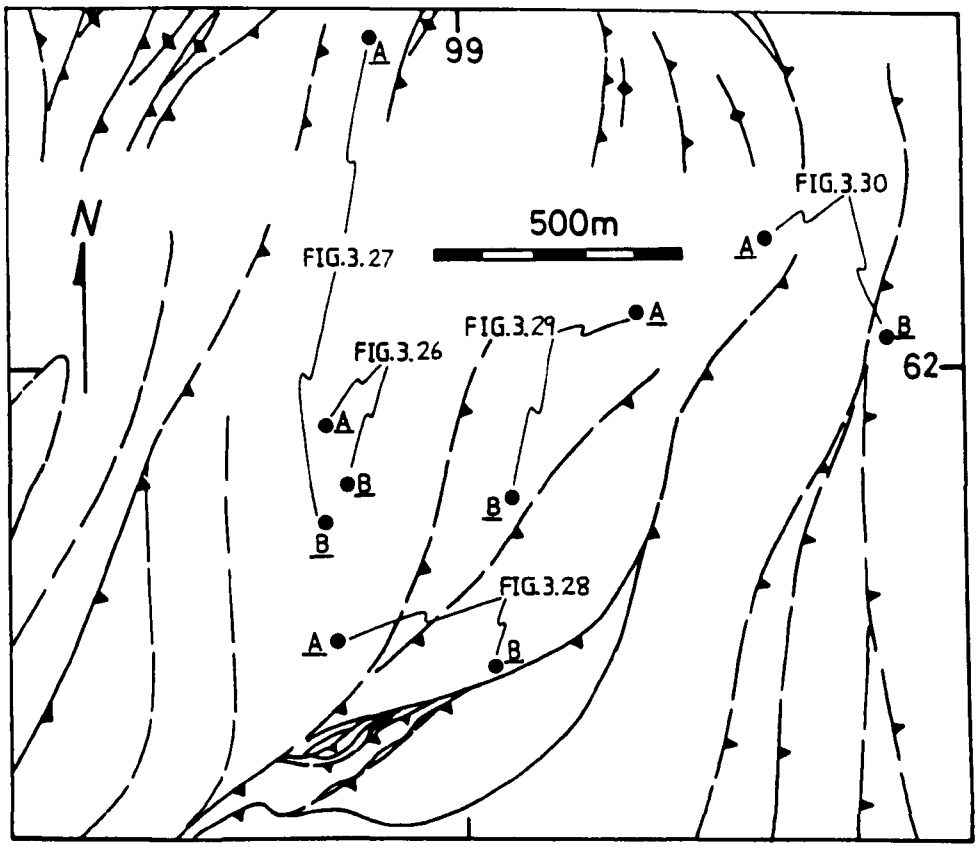

FIG. 3.25 Location map of the strain localities presented in Table 3.5.

Locality	Fig.	No. of Pipes	'Theta-Curve' Rs	'Theta-Curve' Direction	'Shimamoto & Ikeda/Wheeler' Rs	'Shimamoto & Ikeda/Wheeler' Direction	'Shimamoto & Ikeda/Wheeler' J
98726188	3.26	61	1.15	089	1.13	092	1.02
98756177	3.26	101	1.14	062	1.14	066	1.03
98806265	3.27	64	1.10	076	1.08	082	1.02
98726169	3.27	101	1.15	051	1.11	054	1.02
98746146	3.28	99	1.17	029	1.14	031	1.02
99056141	3.28	63	1.06	024	1.06	027	1.03
99346211	3.29	145	1.12	068	1.11	067	1.02
99096174	3.29	100	1.18	060	1.12	061	1.03
99596226	3.30	64	1.02	018	1.04	047	1.02
99846206	3.30	102	1.03	123	1.06	130	1.03

TABLE 3.5 Rs values and principal strain directions for the localities illustrated in Fig. 3.25.

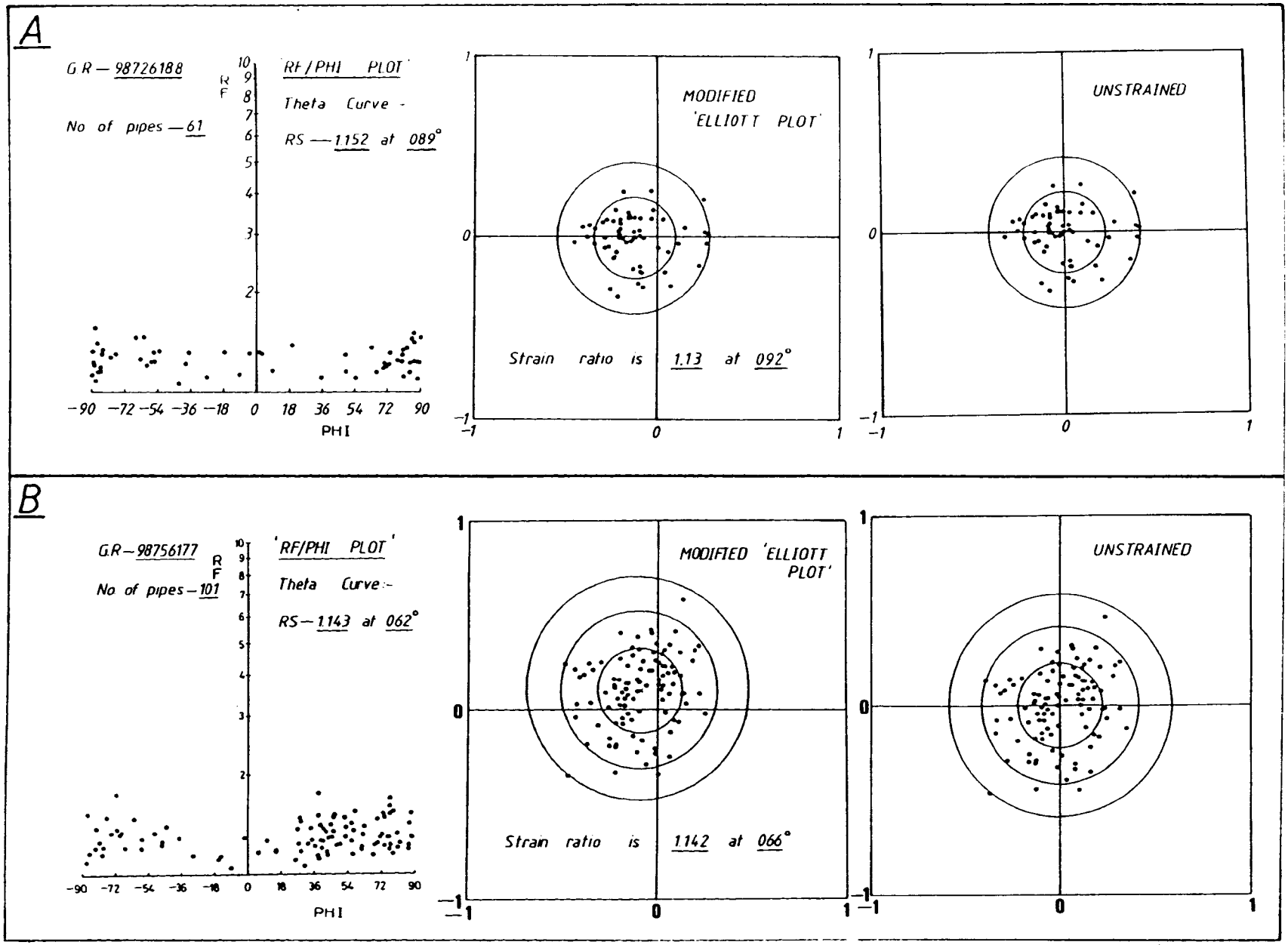

FIG. 3.26 'Rf/Phi' and 'Wheeler' plots for localities (98726188) and (98756177).

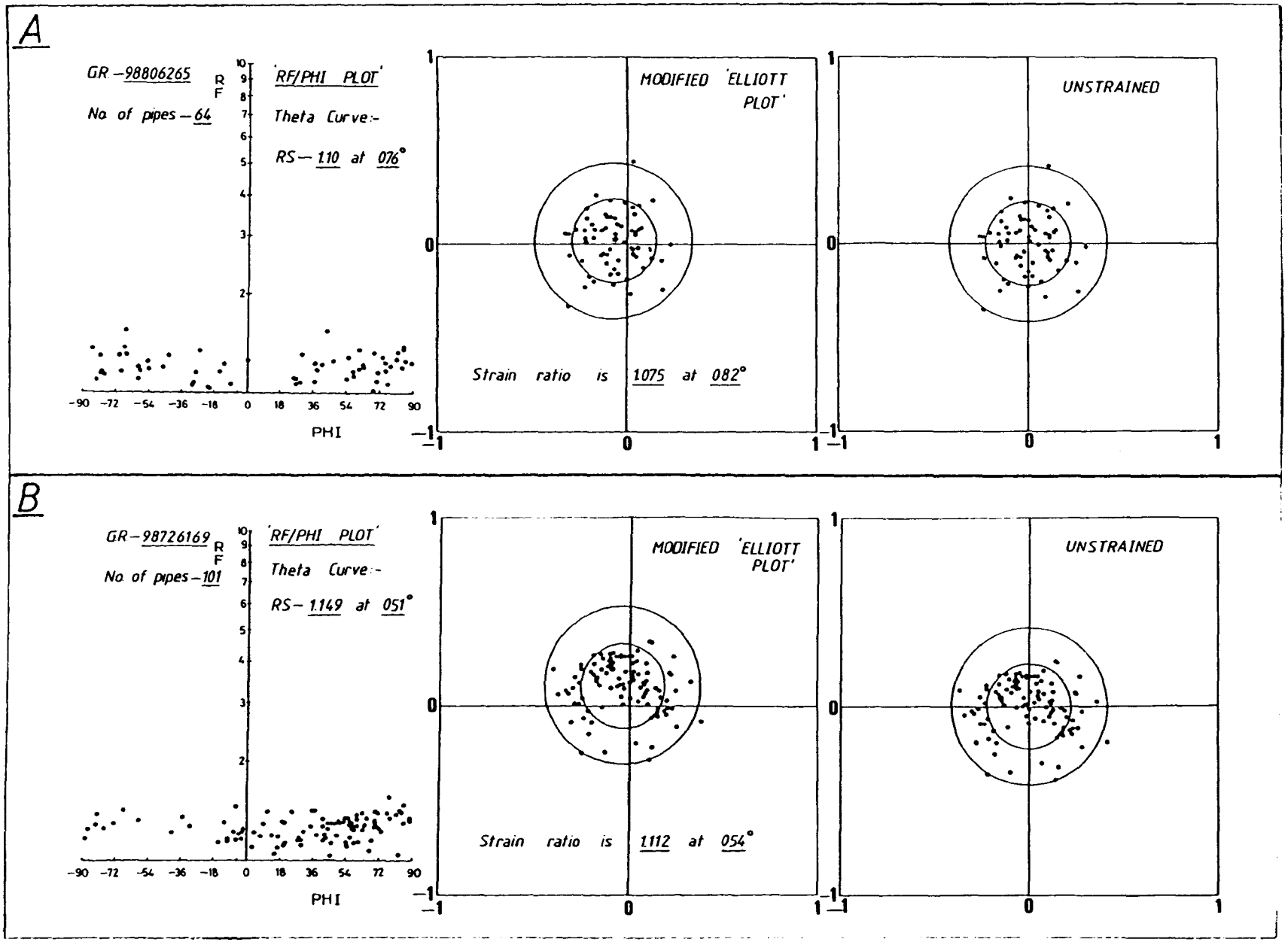

FIG. 3.27 'Rf/Phi' and 'Wheeler' plots for localities (98806265) and (98726169).

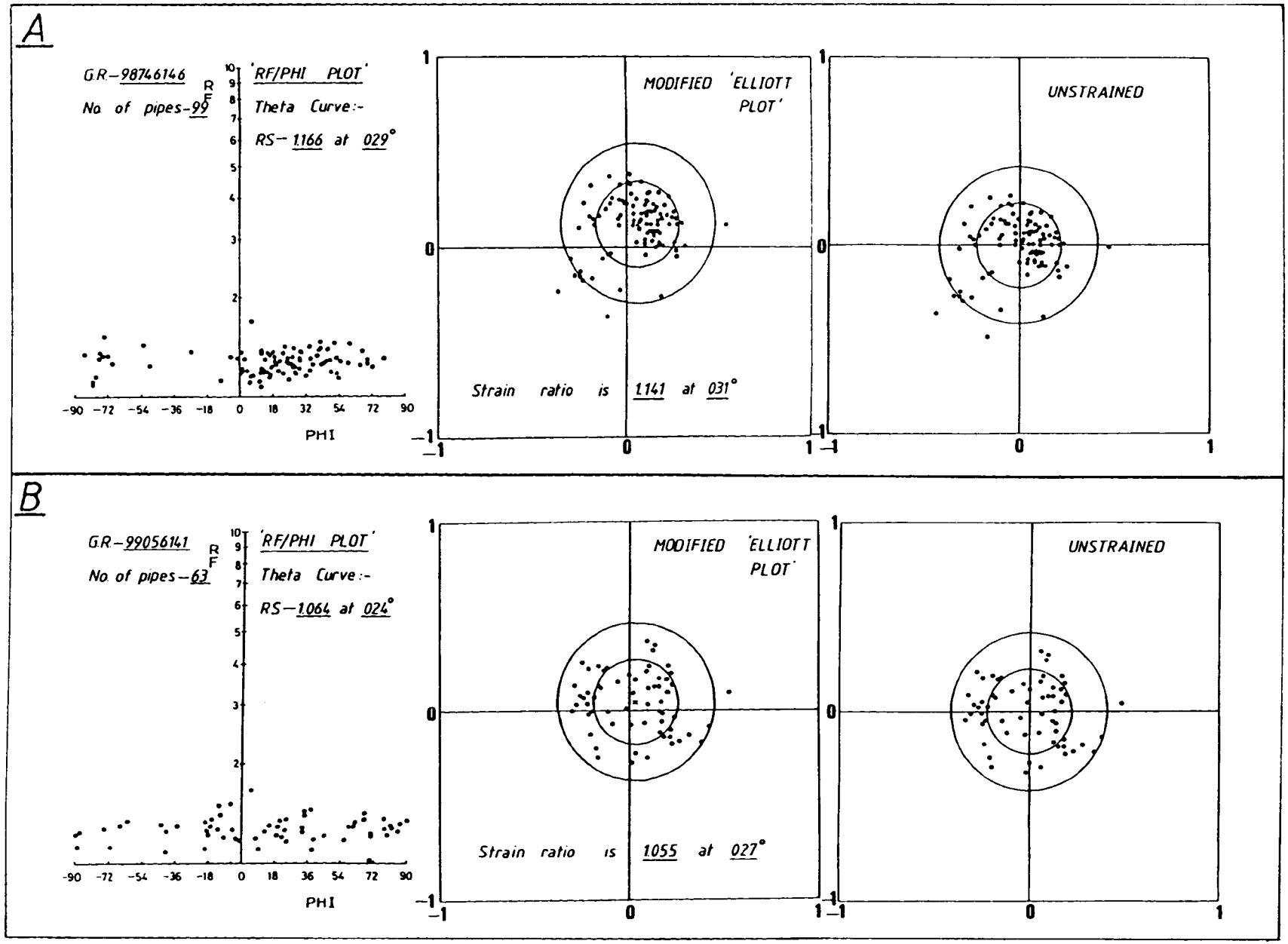

FIG. 3.28 'Rf/Phi' and 'Wheeler' plots for localities (98746146) and (99056141).

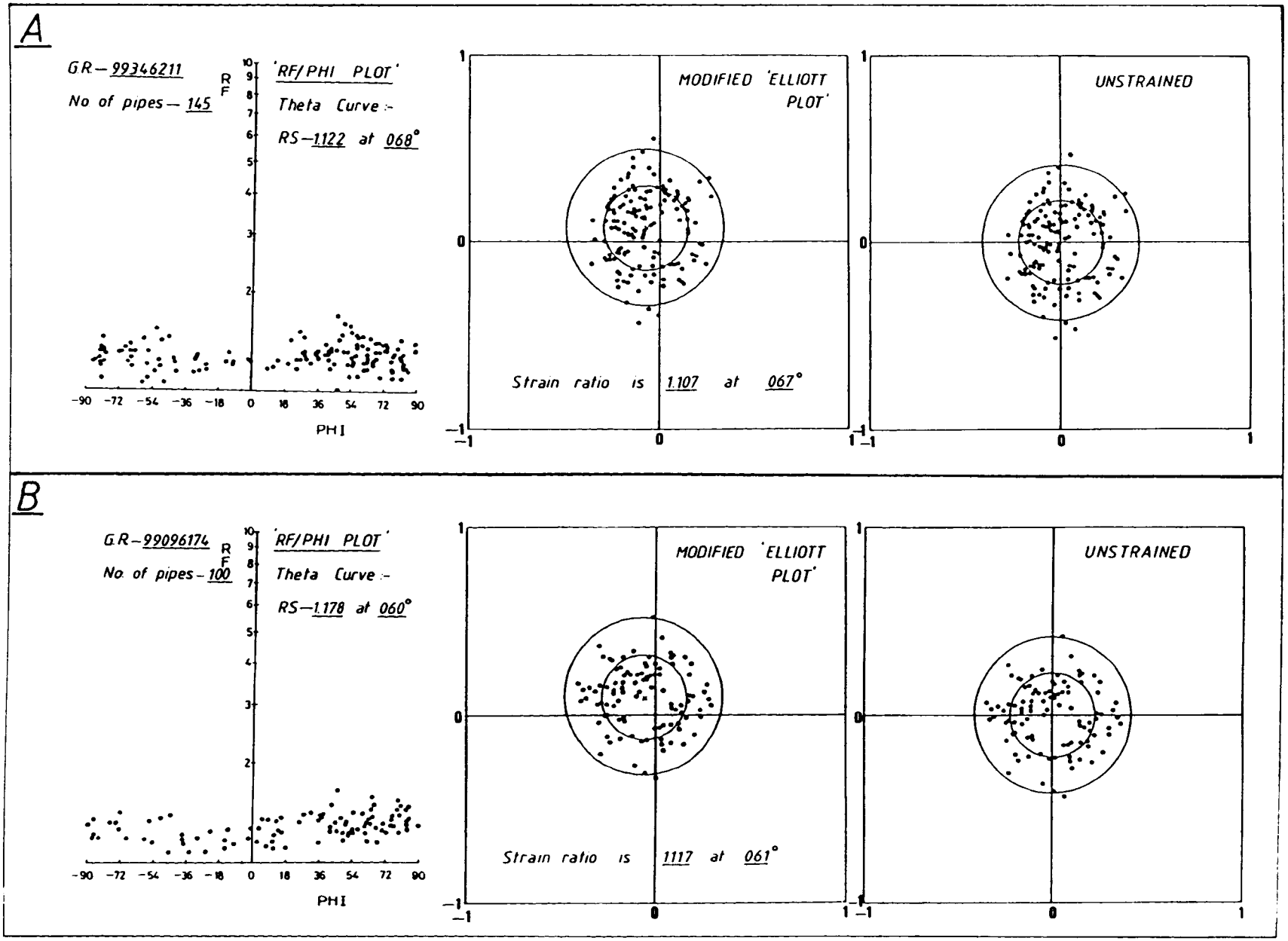

FIG. 3.29 'Rf/Phi' and 'Wheeler' plots for localities (99346211) and (99096174).

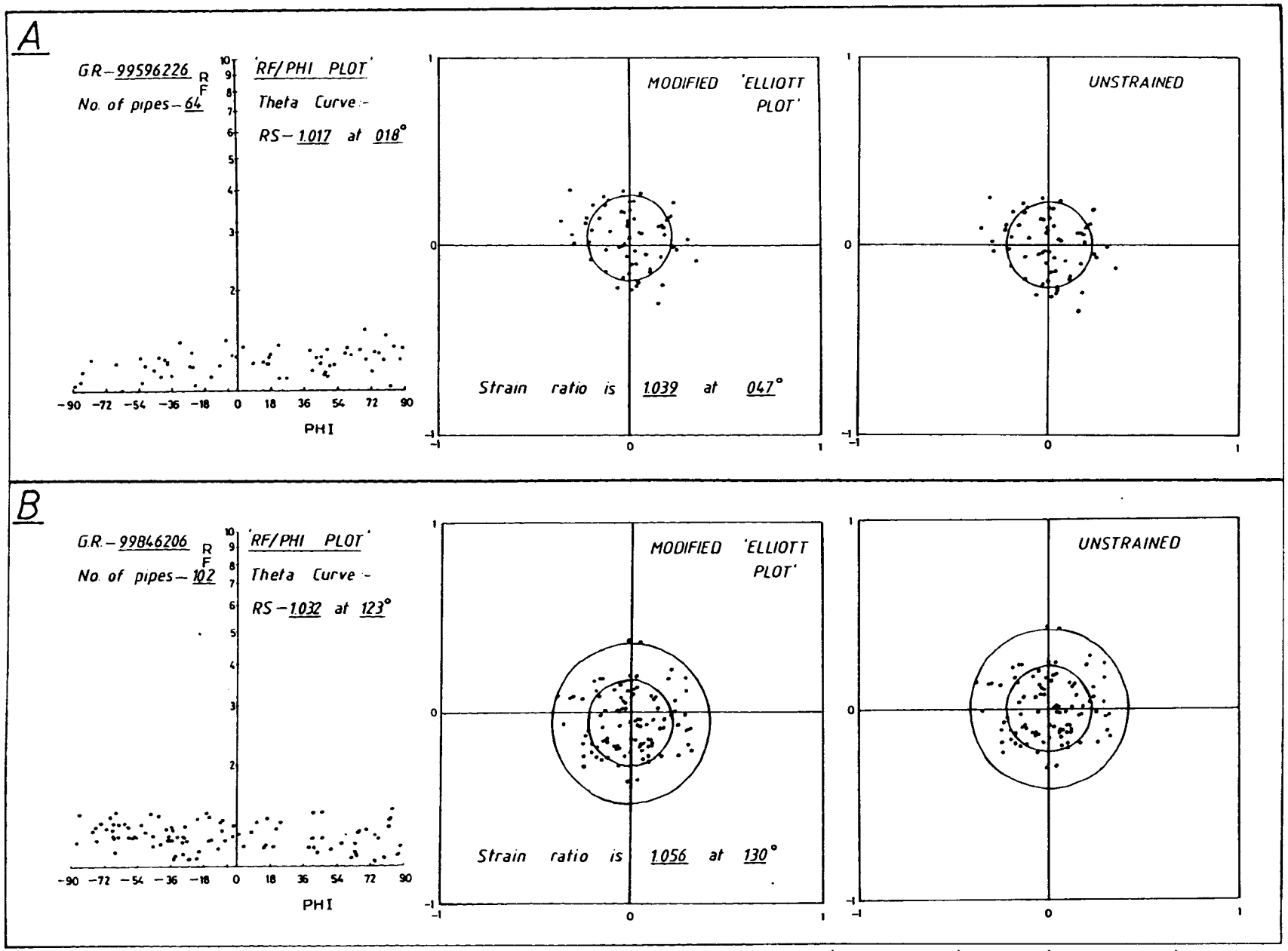

FIG. 3.30 'Rf/Phi' and 'Wheeler' plots for localities (99596226) and (99846206).

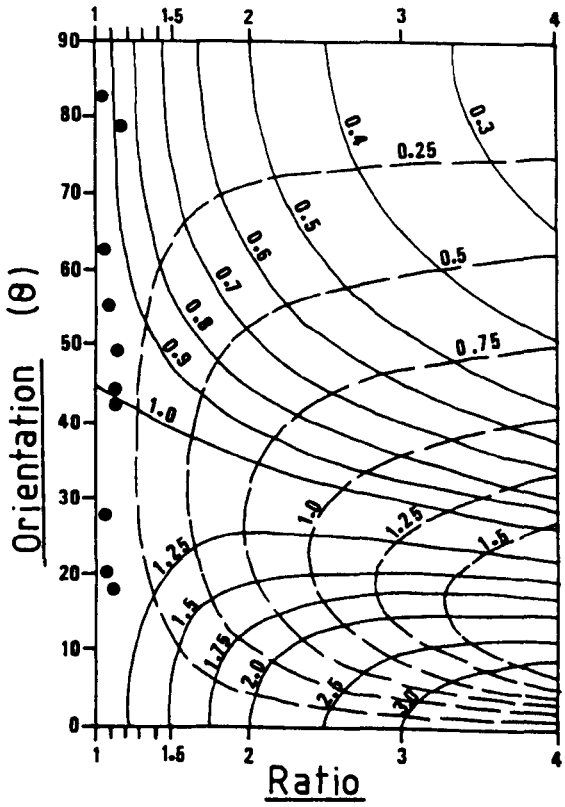

FIG. 3.31 Strain ratio plotted against the orientation of the long axis of the strain ellipse relative to the movement direction for the localities of Fig. 3.25.

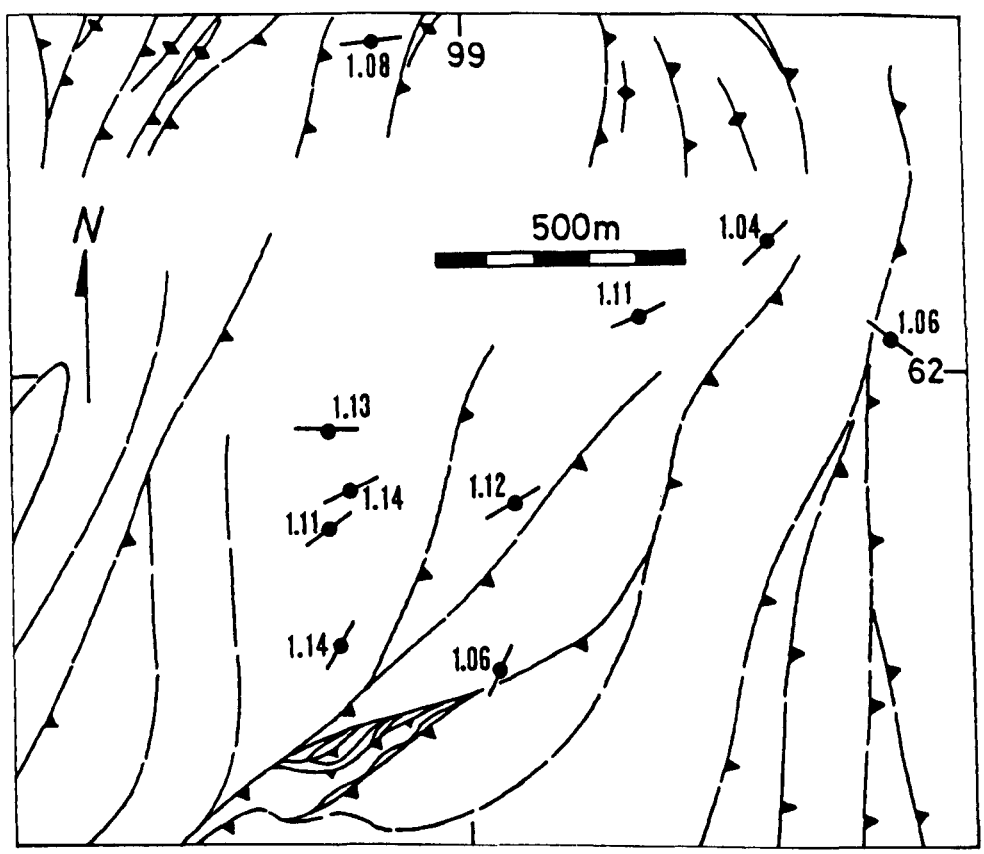

FIG. 3.32 Strain map of the localities shown in Fig. 3.25.

Further finite strain studies within the Pipe Rock have been carried out in the south of the study area between the Beinn Eighe ridge and Sgurr Dubh (NG97905570), and also within the half-window to the north of Kinlochewe. The results from these 2 areas will now be presented. It is clear from the preceding description of the finite strains within the Pipe Rock to the north of the Beinn Eighe ridge that the strain within individual horses is heterogeneous and before strain contouring can be contemplated it is essential to gauge the degree of heterogeneity. In order for this aspect of the study to be meaningful it is necessary to assume that the strain is homogeneous on the scale of the portion of the outcrop that has been photographed. It was decided to investigate the finite strain variation within individual localities by taking 2 photographs at a 1 m - 10 m separation, at 2 localities within the southern part of the study area and at 3 localities in the half-window to the N of Kinlochewe.

The results from the region between the Beinn Eighe ridge and Sgurr Dubh are now presented; the location map, Fig. 3.33, indicates the position of the strain localities. The 'Rf/Phi' and 'Hoeeler' plots for the 10 localities within this region are illustrated in Figs. 3.34 to 3.39.

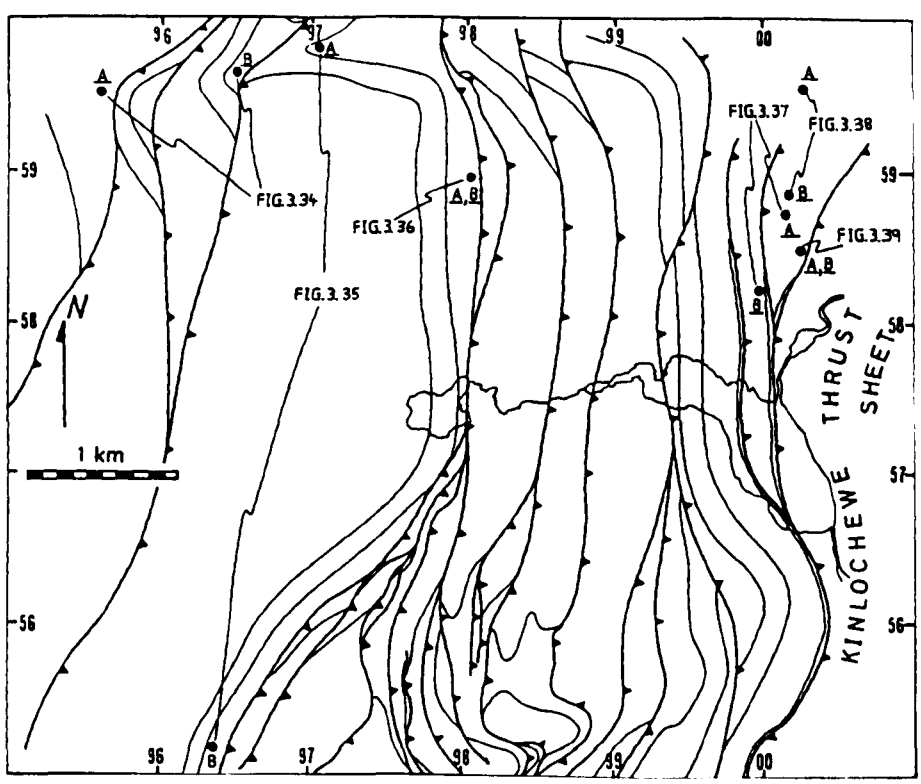

FIG. 3.33 Location map of strain localities in the region between the Beinn Eighe ridge and Sgurr Dubh.

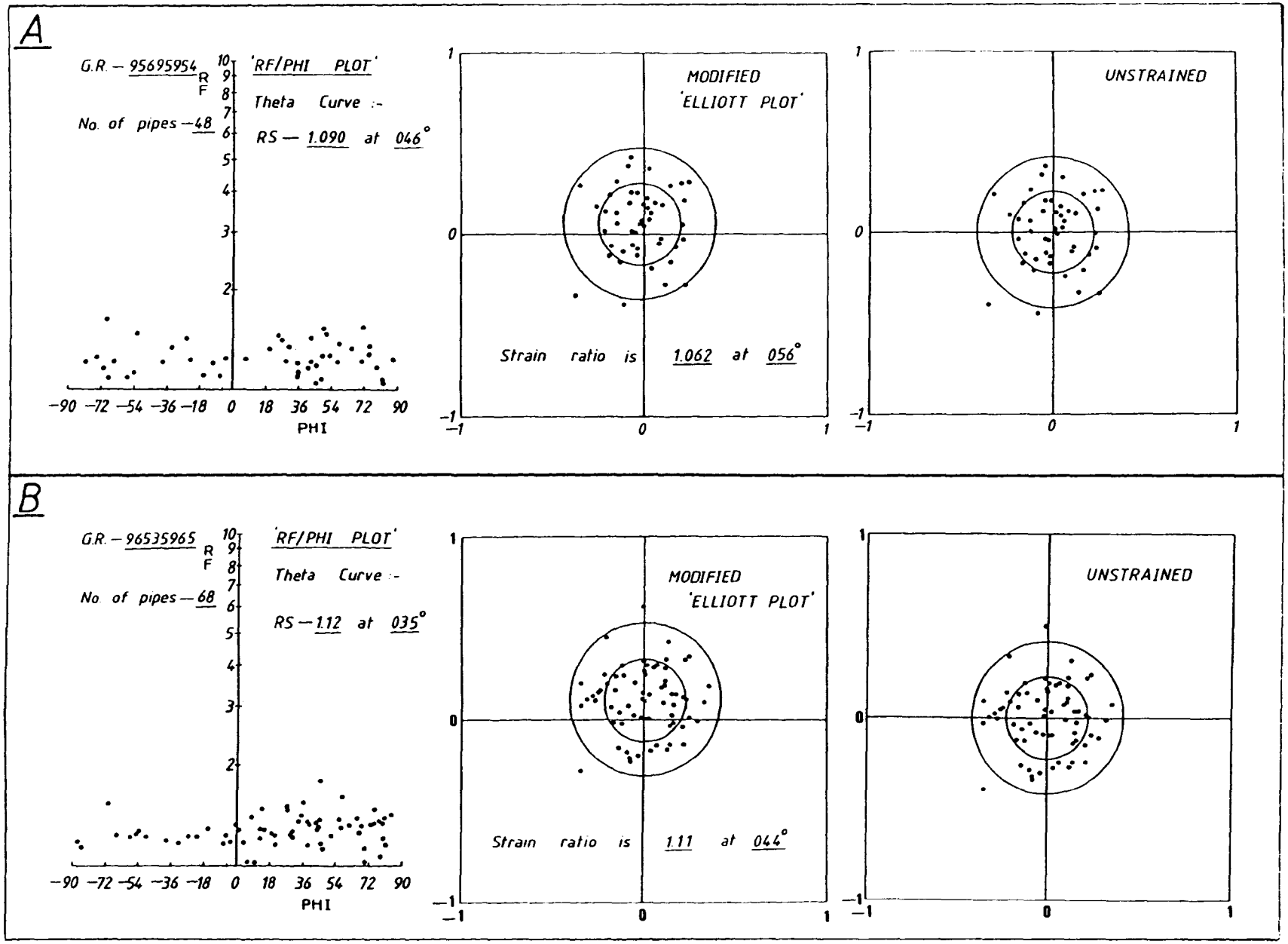

FIG. 3.34 'Rf/Phi' and 'Wheeler' plots for localities (95695954) and (96535965).

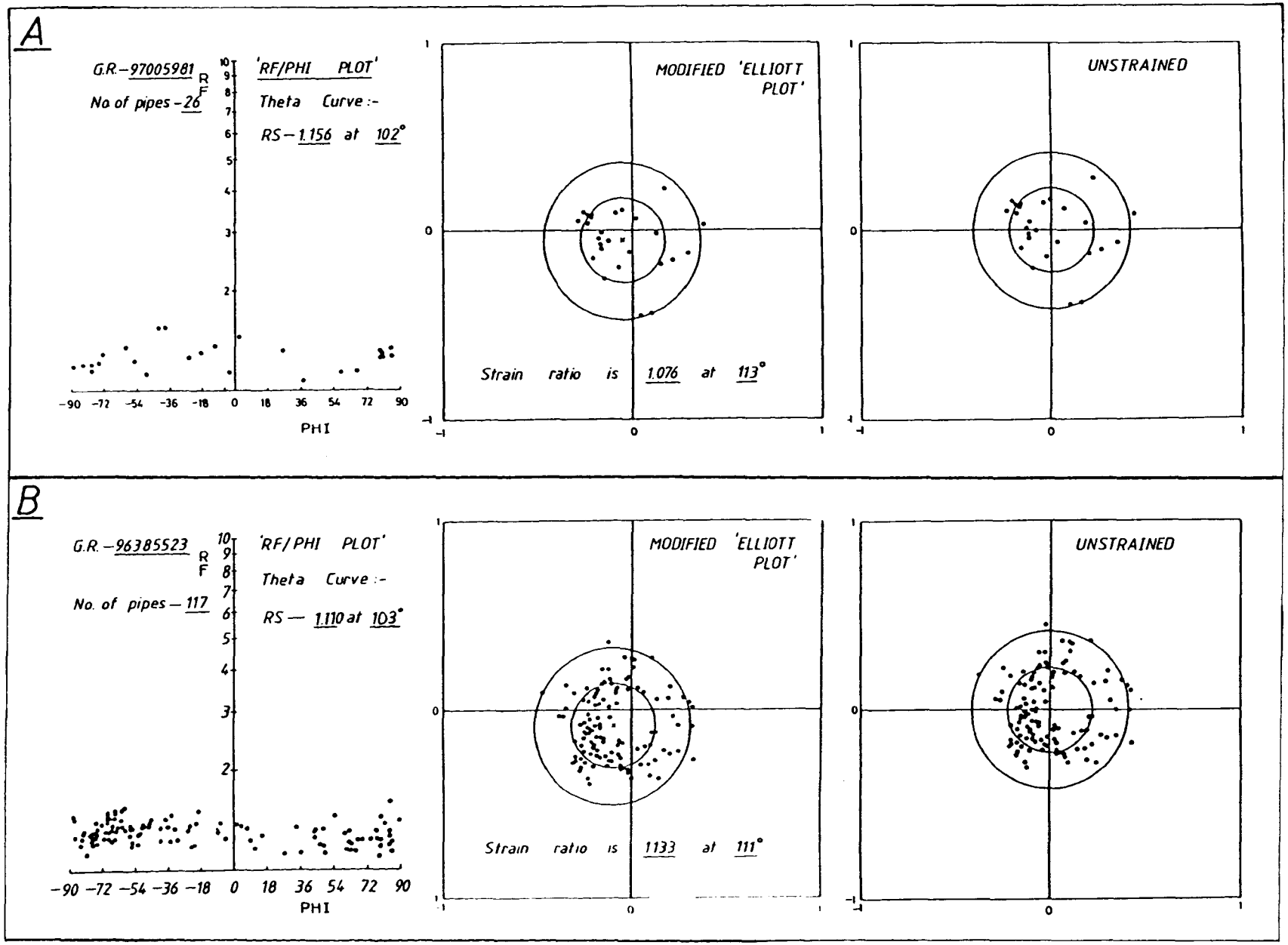

FIG. 3.35 'Rf/Phi' and 'Wheeler' plots for localities (97005981) and (96385523).

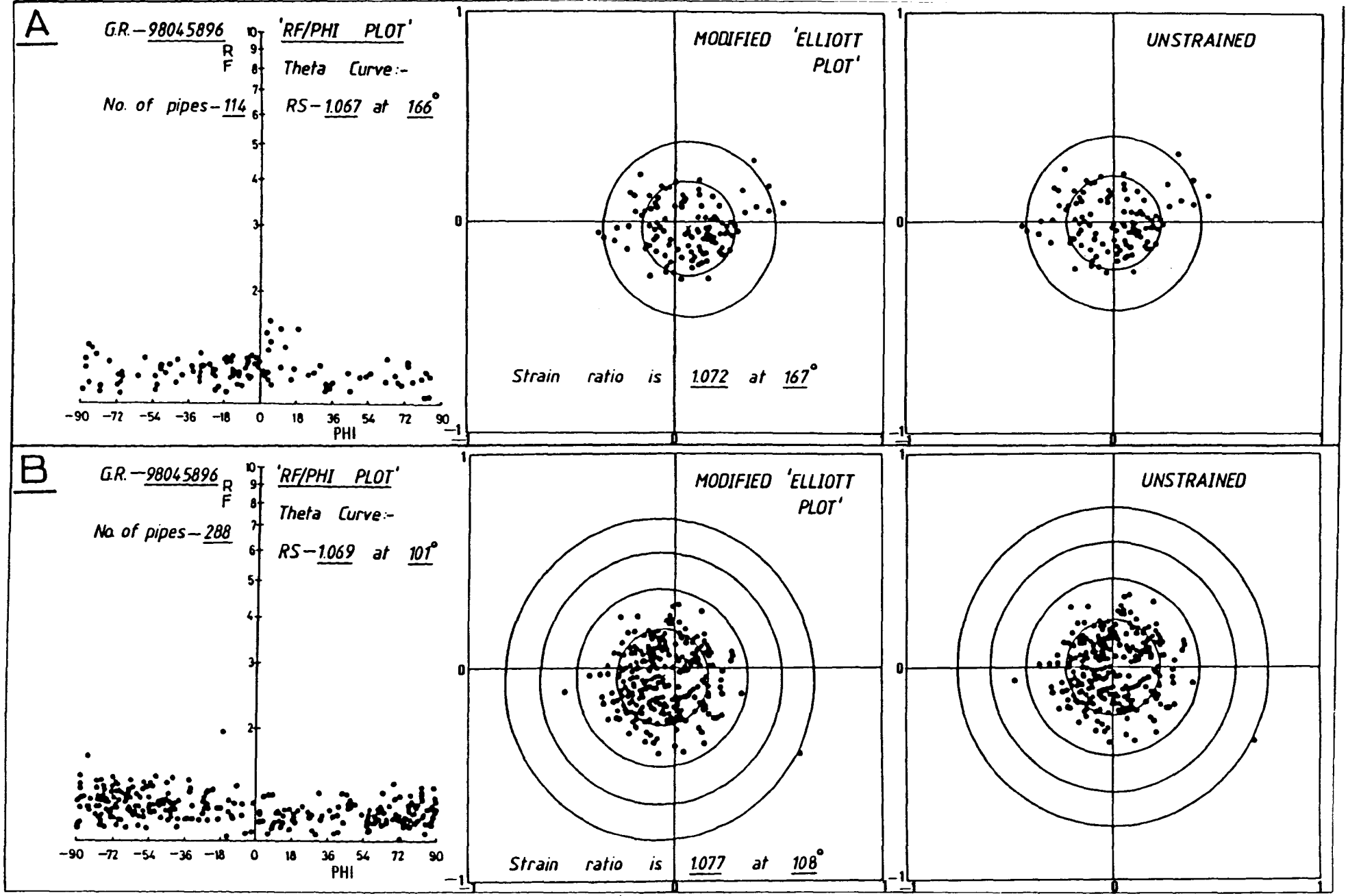

FIG. 3.36 'Rf/Phi' and 'Wheeler' plots for locality (98045896).

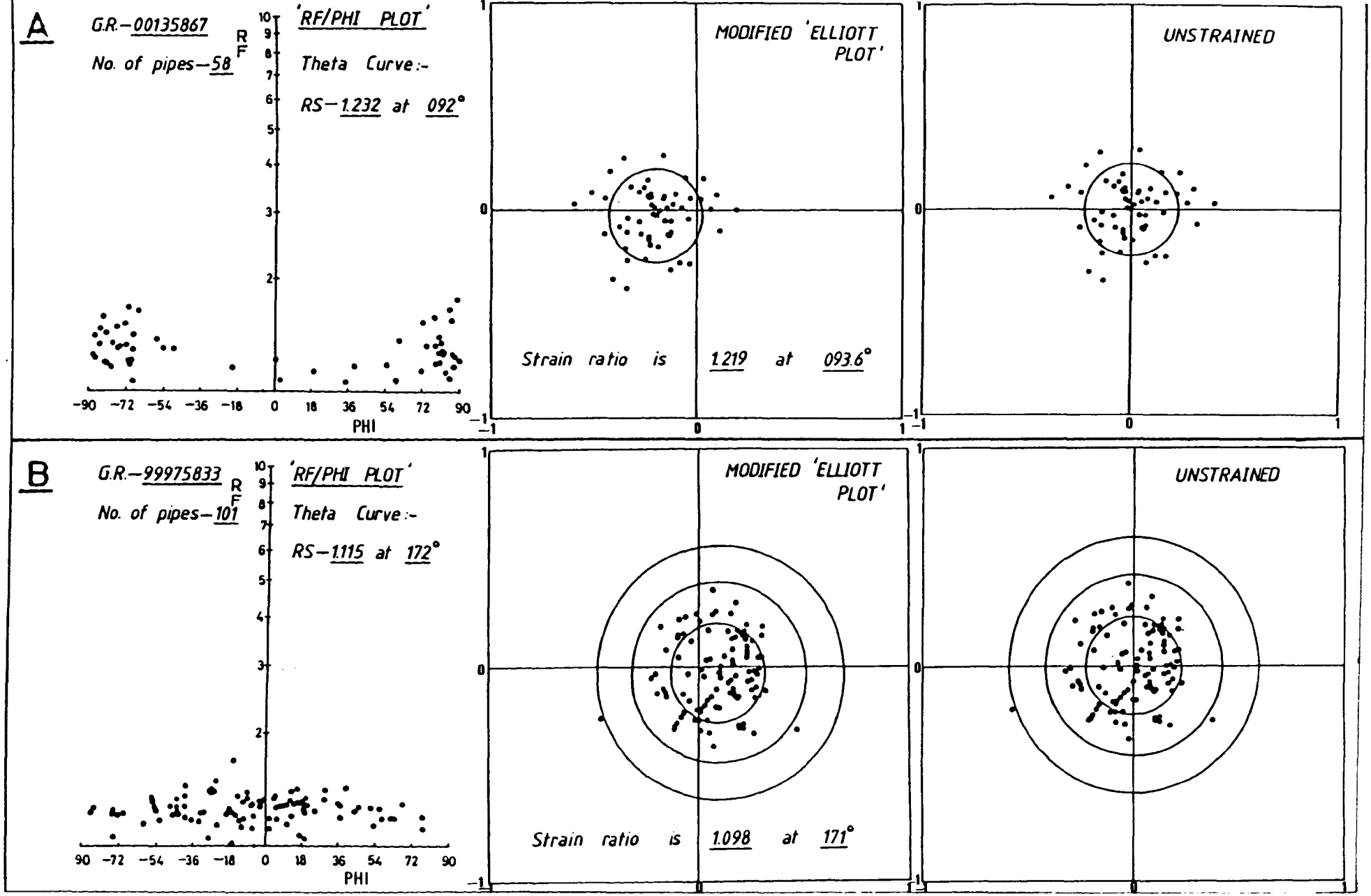

FIG. 3.37 'Rf/Phi' and 'Wheeler' plots for localities (00135867) and (99975833).

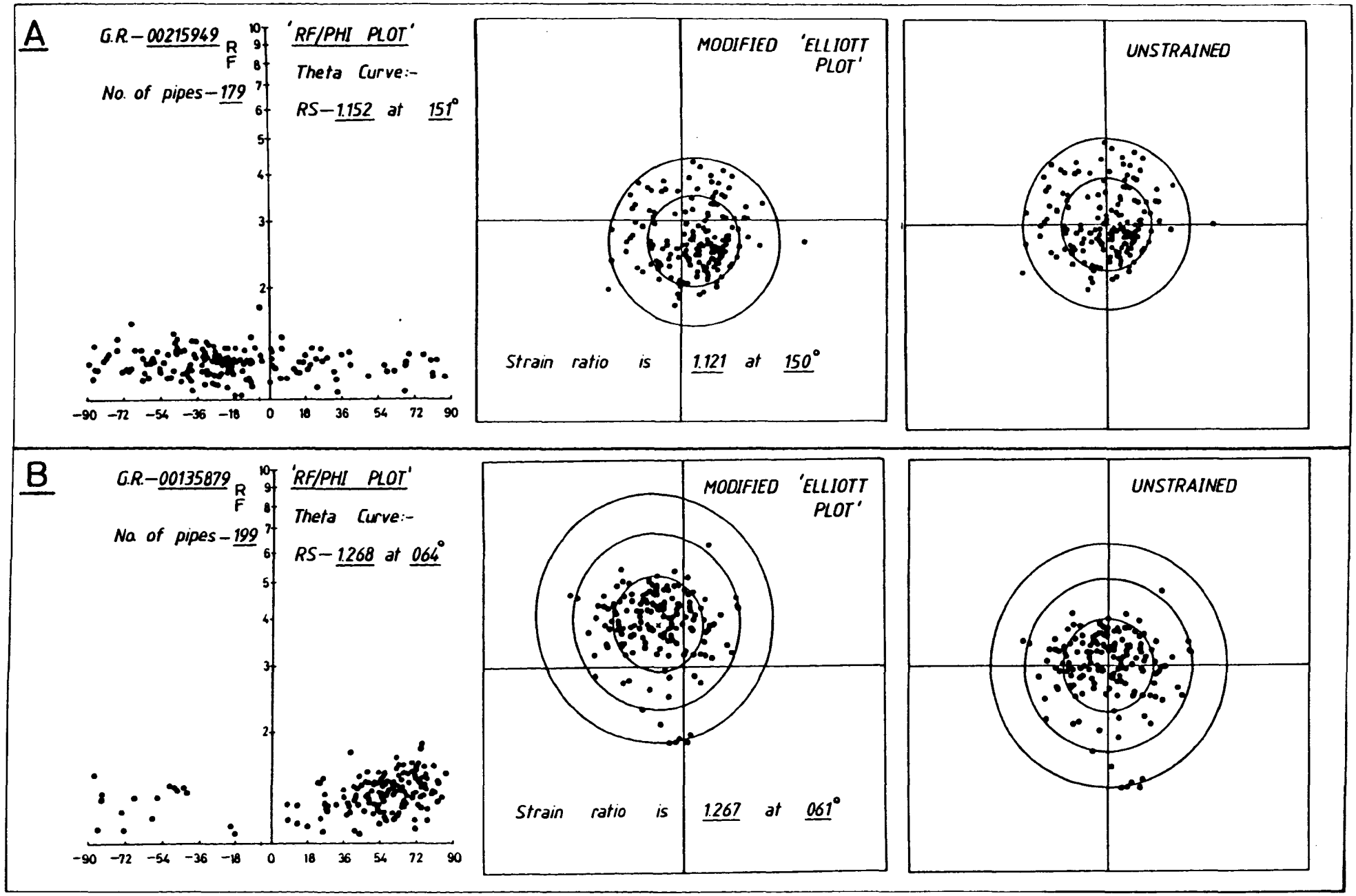

FIG. 3.38 'Rf/Phi' and 'Wheeler' plots for localities (00215949) and (00135879).

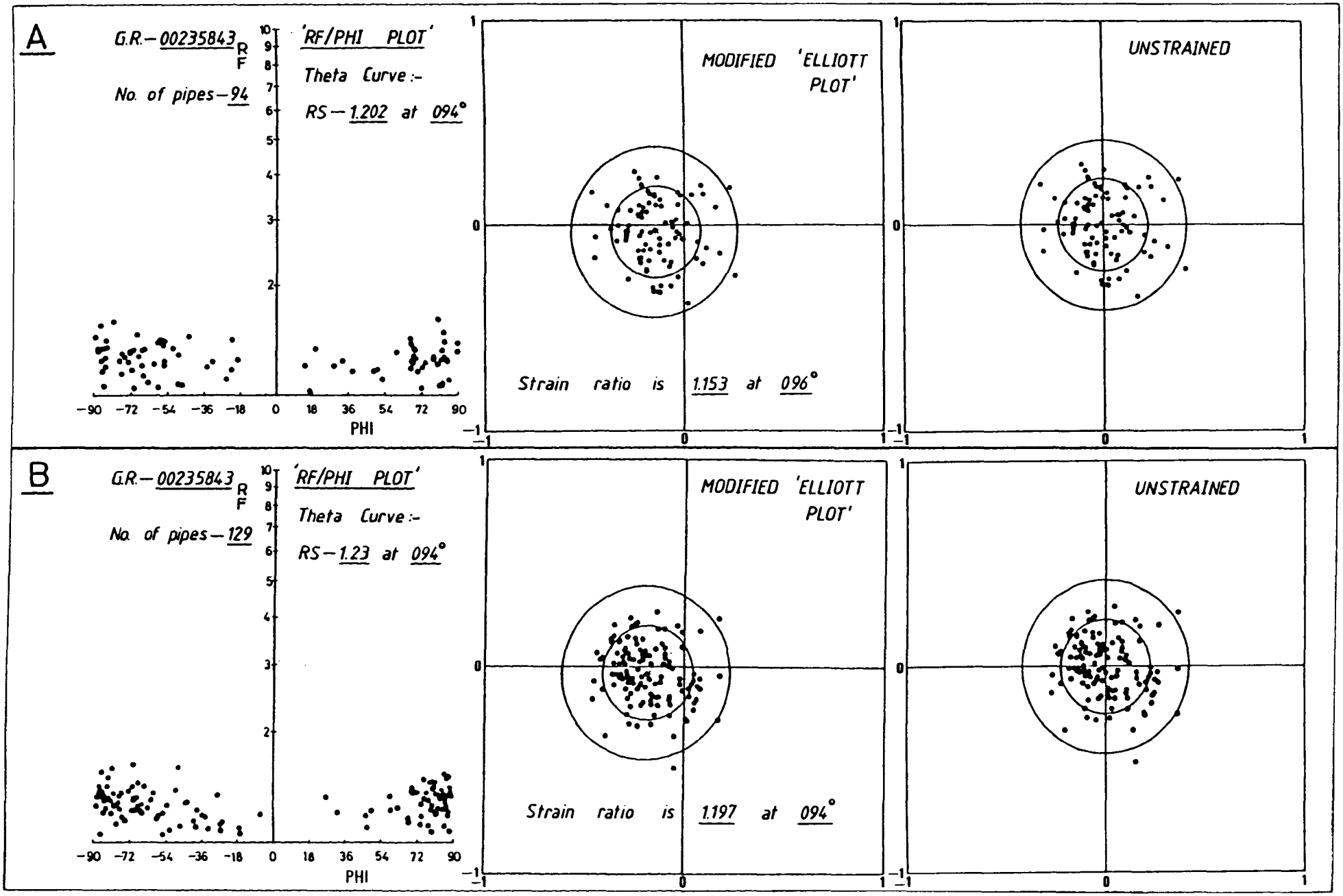

FIG. 3.39 'Rf/Phi' and 'Wheeler' plots for locality (00235843).

The results of application of the 'Theta-Curve' and 'Shimamoto & Ikeda' methods are illustrated in Table 3.6 and the strain map is presented in Fig. 3.40.

Locality	Fig.	No. of Pipes	'Theta-Curve' Rs	'Theta-Curve' Direction	'Shimamoto & Ikeda/Wheeler' Rs	'Shimamoto & Ikeda/Wheeler' Direction	J
95695954	3.34	48	1.09	046	1.06	056	1.03
96535965	3.34	68	1.12	035	1.11	044	1.03
97005981	3.35	26	1.16	102	1.08	113	1.03
96385523	3.35	117	1.11	103	1.13	111	1.03
98045896	3.36	114	1.07	166	1.07	167	1.02
98045896	3.36	288	1.07	101	1.08	108	1.02
00135867	3.37	58	1.23	092	1.22	094	1.02
99975833	3.37	101	1.12	172	1.10	171	1.03
00215949	3.38	179	1.15	151	1.12	150	1.02
00135879	3.38	199	1.27	064	1.27	061	1.03
00235843	3.39	129	1.23	094	1.20	094	1.02
00235843	3.39	94	1.20	094	1.15	096	1.02

TABLE 3.6 Rs values and principal strain directions of the localities illustrated in Fig. 3.33.

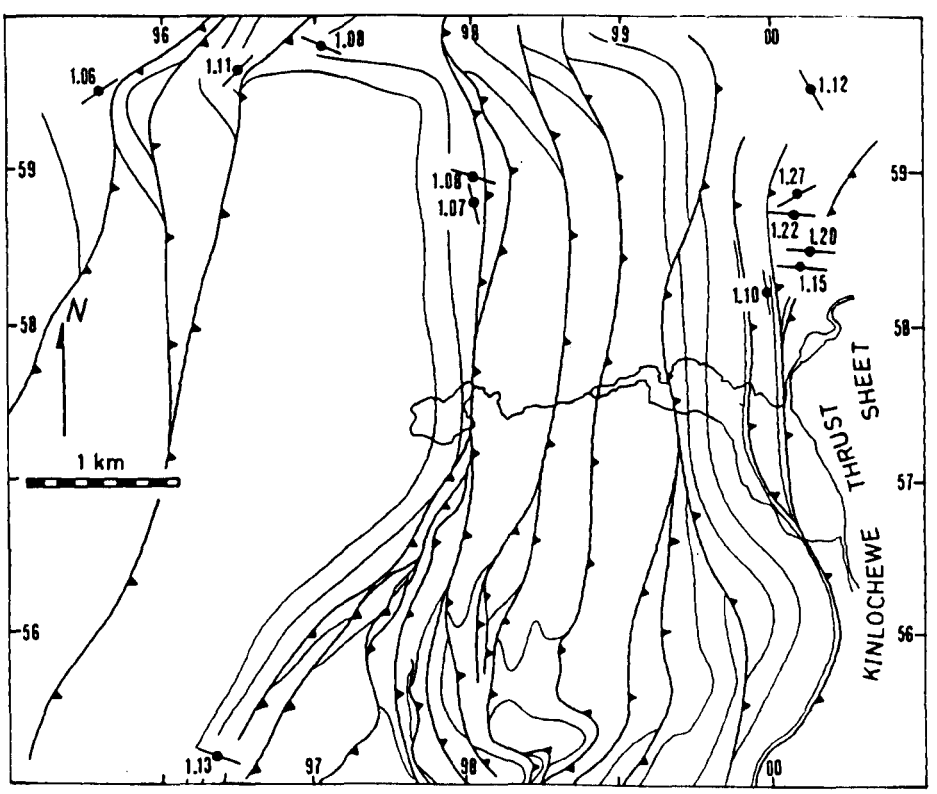

FIG. 3.40 Strain map of the region between the Beinn Eighe ridge and Sgurr Dubh.

The most important results from this area occur in the most easterly exposed horse at the following 4 strain localities: (00215949), (00135879), (00135867) and (00235843). Localities (00235843), (00135867) and (00215949) show evidence for between 1% and 20% layer parallel extension, $\sqrt{\lambda}$ values of between 1.01 and 1.20 are inferred from Fig. 3.41, followed by a small component of layer parallel shear. Locality (00135879) shows evidence for approximately 6% layer parallel shortening, $\sqrt{\lambda}$ = 0.94, followed by a layer normal shear component of γ_2 = 0.24.

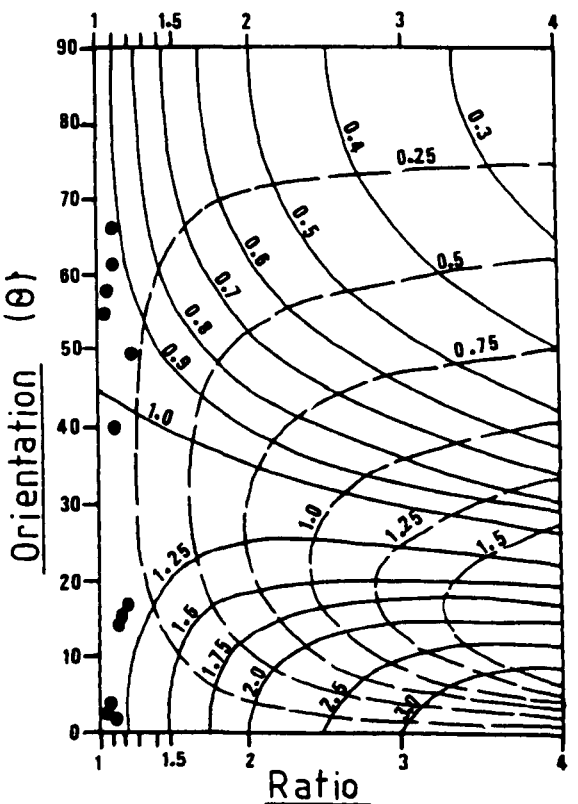

FIG. 3.41 Strain ratio plotted against the orientation of the long axis of the strain ellipse relative to the movement direction for the localities illustrated in Fig. 3.33.

These results illustrate further the heterogeneity of strain within individual horses, all 4 localities are situated above the underlying footwall flat, this segment of the hangingwall having slipped along the ramp segment of the underlying thrust surface. The amount of longitudinal strain and layer normal shear observed within the horse is assessed in terms of the geometry in Section 3.2. Two photographs were taken at locality (00235843) at a 1 m separation to assess the strain heterogeneity. The results obtained from these 2 photographs show similar Rs values (1.15 and 1.20) and principal direction of strain (096° and 094°), suggesting a $\sqrt{\lambda}$ variation of approximately 2% - 3% and an insignificant γ_2 variation.

Immediately below this horse, locality (99975833) shows evidence for approximately 5% layer parallel shortening followed by a very small layer parallel shear component. The remaining 5 localities within this region suggest a variation of between 1% and 3% longitudinal strain within individual horses, all with small components of layer normal shear, see Fig. 3.41. Two photographs were taken at locality (98045896) at a 10 m separation to test for strain heterogeneity, the results (Table 3.6) suggest that the strain is significantly heterogeneous over this distance and this precludes strain contouring based on the existing density of strain localities.

The 4 strain localities within the half-window to the north of Kinlochewe are shown in Fig. 3.42, and the results of application of the 'Theta-Curve' and 'Shimamoto & Ikeda' methods are presented in Table 3.7. 'Rf/Phi' and 'Wheeler' plots are illustrated in Figs. 3.43, 3.44, 3.45 and 3.46.

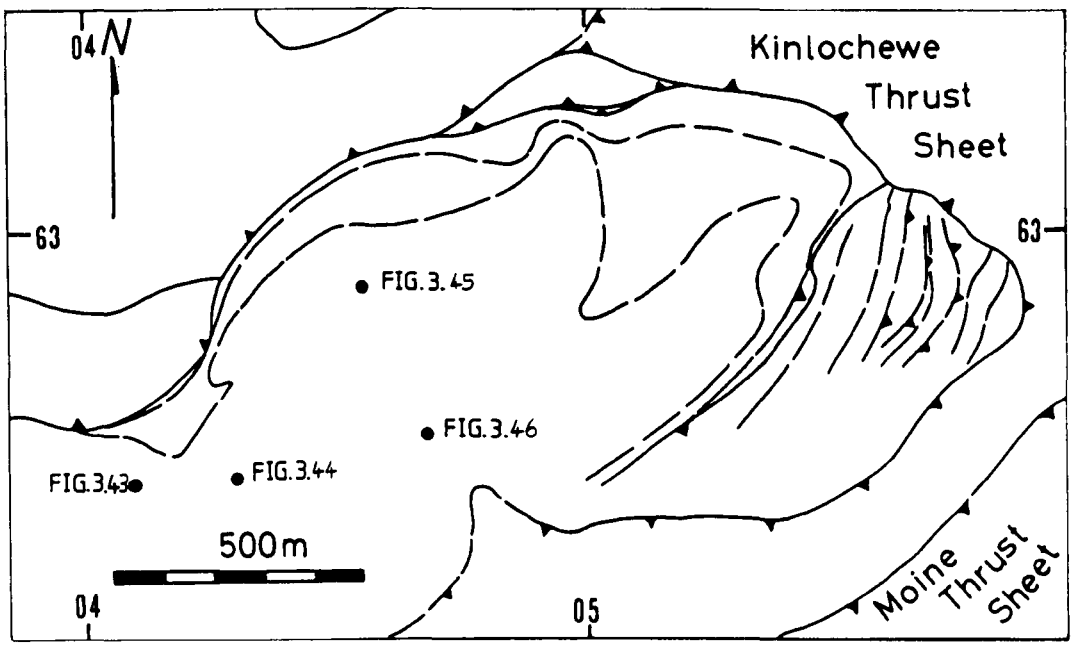

FIG. 3.42 Location map of strain localities within the half-window to the north of Kinlochewe.

Locality	Fig.	No. of Pipes	'Theta-Curve' Rs	'Theta-Curve' Direction	'Shimamoto & Ikeda/Wheeler' Rs	'Shimamoto & Ikeda/Wheeler' Direction	J	R
04126250	3.43	113	1.02	000	1.00	-	1.04	1.31
04126250	3.43	101	1.05	047	1.05	049	1.03	1.28
04306252	3.44	69	1.13	081	1.12	084	1.02	1.23
04306252	3.44	58	1.02	045	1.05	072	1.02	1.24
04556290	3.45	140	1.08	072	1.03	081	1.03	1.25
04556290	3.45	163	1.03	001	1.02	027	1.03	1.26
04696260	3.46	107	1.03	001	1.03	064	1.03	1.30

TABLE 3.7 Rs values and principal strain directions for the localities illustrated in Fig. 3.42.

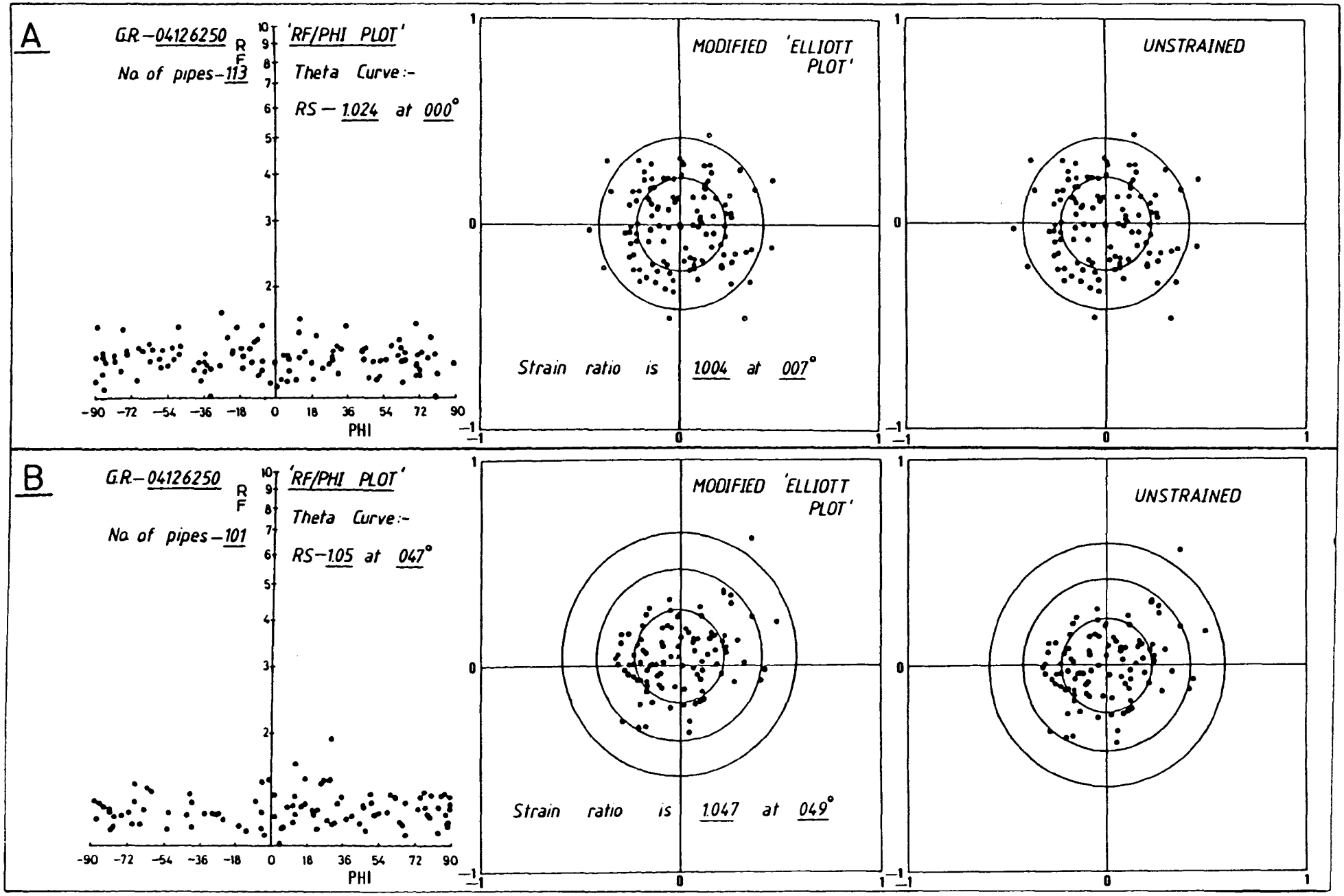

FIG. 3.43 'Rf/Phi' and 'Wheeler' plots for locality (04126250).

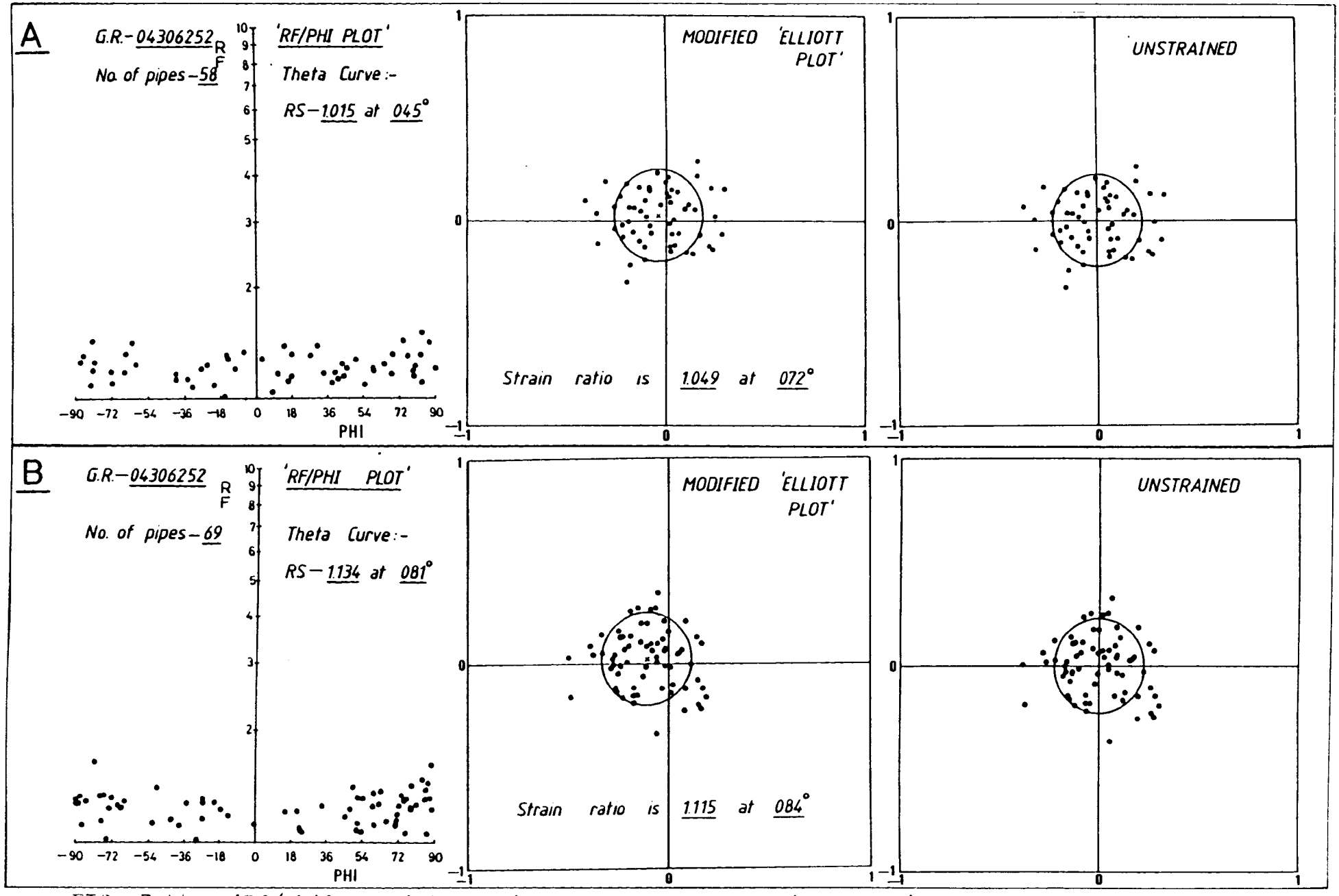

FIG. 3.44 'Rf/Phi' and 'Wheeler' plots for locality (04306252).

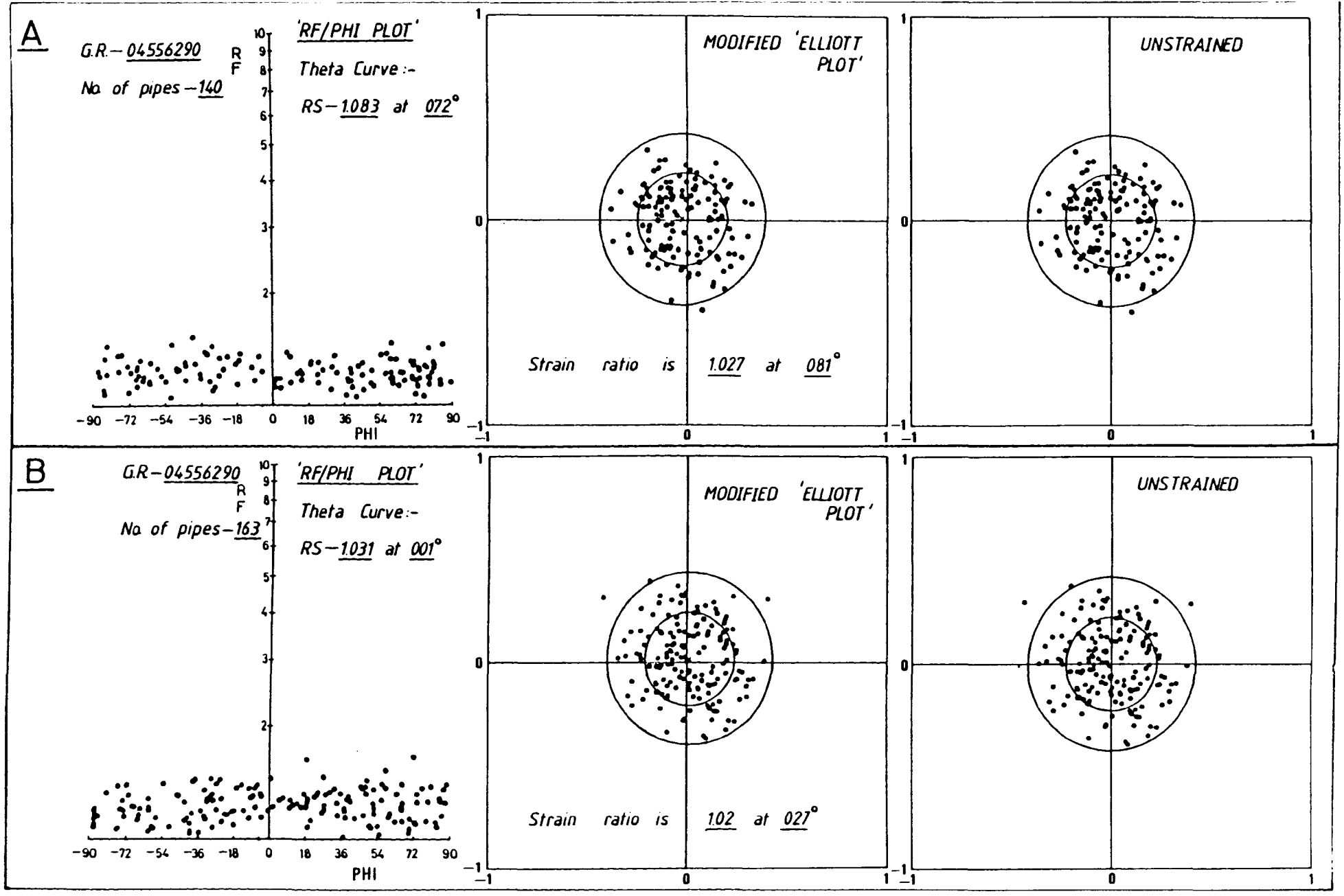

FIG. 3.45 'Rf/Phi' and 'Wheeler' plots for locality (04556290).

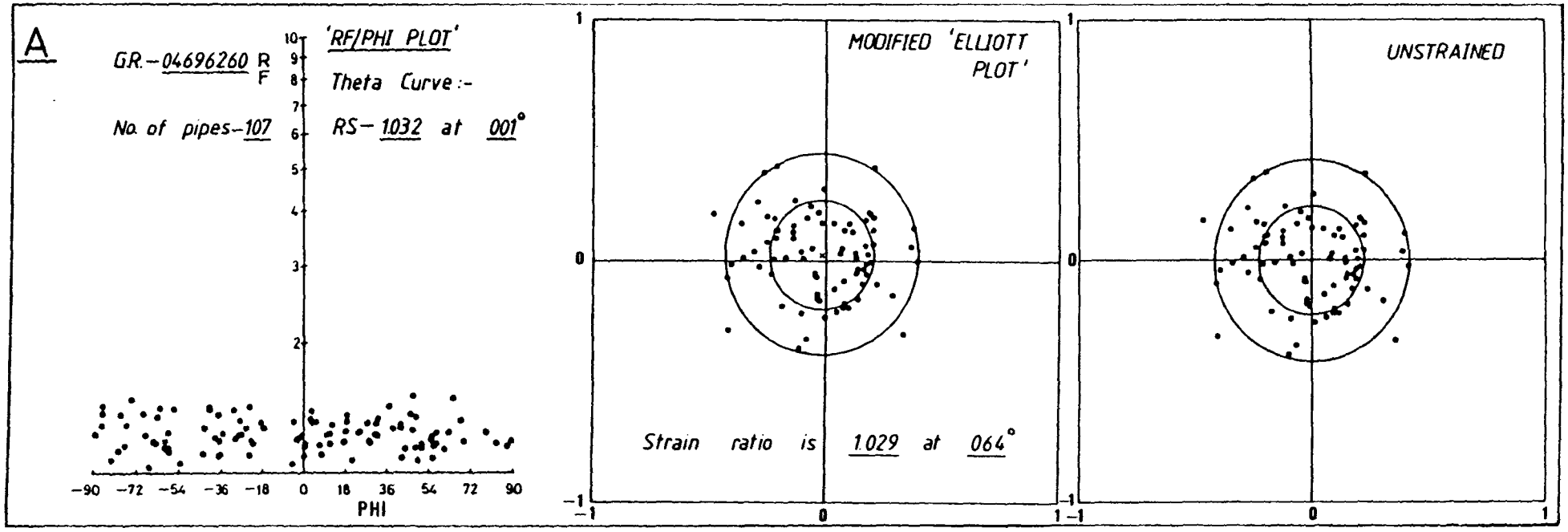

FIG. 3.46 'Rf/Phi' and 'Wheeler' plots for locality (04696260).

At 3 of these localities, (04126250), (04306252) and (04556290), 2 photographs were taken at 5 m, 1 m and 1 m separation respectively. The variation in $\sqrt{\lambda}$ at these localities is greatest in the case of (04306252) where a small amount of early layer parallel extension (1% - 8%) is inferred from Fig. 3.47. A small variation in longitudinal strain is therefore present over a 1 m separation. The longitudinal strain is below 5% for each of the localities examined within the half-window except for locality (04306252 - Rs = 1.12); the strain map is illustrated in Fig. 3.48.

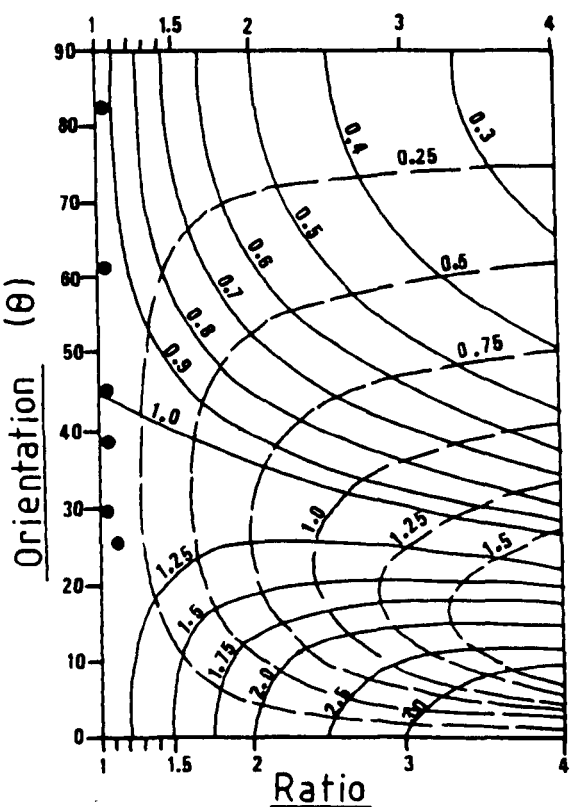

FIG. 3.47 Strain ratio plotted against the orientation of the long axis of the strain ellipse relative to the movement direction for the localities illustrated in Fig. 3.42.

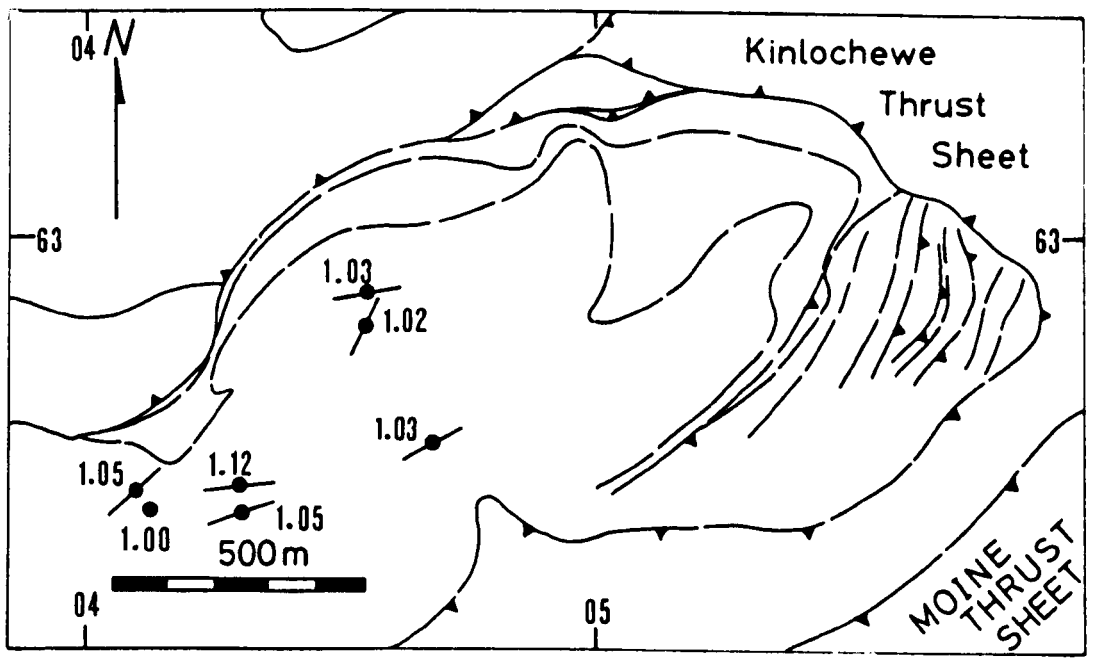

FIG. 3.48 Strain map of the half-window to the north of Kinlochewe.

3.2 EVOLUTION OF STRAIN WITHIN THRUST SHEETS

Measurement of bed lengths and changes in angular relationships at incremental stages as a thrust sheet slips along a flat - ramp - flat thrust surface demonstrates that deformation within the hangingwall is a consequence of slip along the thrust surface. Elliott (1976b, Fig. 2), demonstrates that a substantial component of simple shear parallel to bedding is a direct consequence of a thrust sheet moving along a thrust surface up section in the direction of motion. Each time the thrust sheet moves over a bump or obstacle in the base, the entire sheet has to deform into conformity with the bump so that no voids open up. Elliott envisaged that at low metamorphic grades this deformation would be essentially flexural slip folding with sliding on a large number of discrete surfaces throughout the sheet. Fischer & Coward (1982, Fig.6) suggested that bedding parallel shear strain may be distributed within the hangingwall above the upper footwall flat and also behind the ramp, above the lower footwall flat.

(i) Evolution of strain within the Beinn Eighe Imbricate Fan

Study of the development of internal deformation within a thrust sheet, with a view to establishing the strain history, requires careful microstructural work to be integrated with as much field outcrop strain data as possible. An essentially 2 dimensional study, attempting to develop the Fischer & Coward model, would require extensive strain sampling along the cross sectional length of a thrust sheet at numerous closely spaced stratigraphic levels. Such a detailed study is outside the scope of this project, however information on the development of longitudinal strain at 51 widely spaced localities within the Beinn Eighe Imbricate Fan has been presented in Section 3.1. To analyse these results a simplified, 2 dimensional view of a thrust sheet and its footwall have been subdivided into 3 sectors, Fig. 3.49. The variation in observed longitudinal strain between these 3 sectors is now examined.

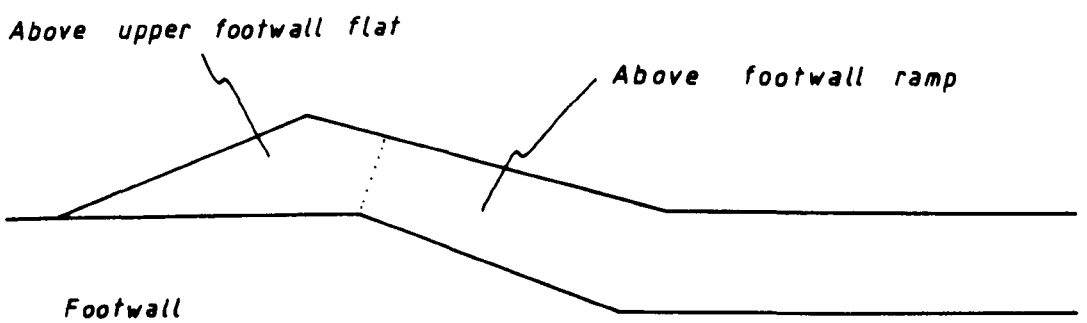

FIG. 3.49 Simplified 2 dimensional geometry of a thrust sheet and its footwall, subdivided into 3 sectors.

The components of layer parallel shortening or layer parallel extension, expressed as percentages, are listed in Fig. 3.50 for each of the strain localities. The values of

layer parallel shortening or extension illustrate further the heterogeneity of the longitudinal strain. The simplified 2 dimensional model illustrated in Fig. 3.49 is not applicable to all of the horses within the imbricate fan; numerous examples of folds which formed prior to the development of thrust surfaces have been described in Chapter 2.

Fischer & Coward (1982, Fig. 6) present a model which examines flexural shear strains near a thrust ramp; their model assumes that all deformation is by bedding parallel slip with no layer parallel shortening or extension. There is good evidence from localities (NH 00135867) and (NH 00235843) that layer parallel extensional strains may develop above the hangingwall ramp as it slips across the upper footwall flat. A simplified 2 dimensional diagram is presented in Fig. 3.51 which predicts the extension within the thrust sheet as it slips from the footwall ramp to the upper footwall flat. Assuming consistent slip along the thrust surface, position A in the hangingwall slips to position A', position B slips to position B', etc. To conserve cross sectional area, prism A'B'C' must equal area ABC; this involves layer thinning in the prism A'B'C' and consequent extension of the line A'C'. This line length extension is equal to $\underline{e}$ in Fig. 3.51, $\underline{e}$ is related to the ramp angle and the displacement by $\underline{e} = D \sin^2\theta$.

Detailed microstructural studies in the Kishorn region of the Moine Thrust Zone, approximately 16 km SSW of the Beinn Eighe ridge, reveal that there is a negligible component of plastic deformation within thrust sheets in this area (R.K. Morgan, pers. comm.). It appears that the geometrically necessary modification within the hangingwall is achieved by a complex system of microfaults and microfractures. This is in contrast to the Heilam region of the northern Moine Thrust Zone where significant layer parallel shear strains, longitudinal strains and layer normal shear strains have developed during thrust sheet evolution.

Locality	Footwall %LPS	Footwall %LPE	Above Upper Footwall Flat %LPS	Above Upper Footwall Flat %LPE	Above Footwall Ramp %LPS	Above Footwall Ramp %LPE
96816348		2				
96776371	2					
96646360	2					
96806323	-	-				
96806355	2					
97036309	2					
96866307		2				
96896310		2				
97026294	2					
96946303	2					
99456475		3				
99156450	2					
99786344						5
99646311					17	
99506317						7
99486350			4			
99356337				6		
99166339			4			
99326349			12			
99356360					1	
99396354			2			
99426362						11
99556374						4
98886298			19			
98606249					1	
98956320			4			
00816317						11
98726188						9
98756177						1
98806265				3		
98726169					4	
98746146					12	
99056141					2	
99346211						1
99096174					5	
99596226					3	
99846206				4		
95695954					4	
96535965					8	
97005981						7
96385523						12
98045896					4	
98045896						6
00135867				12		
99975833					4	
00215949				2		
00135879			8			
00235843				2		
00235843				10		
04126250					-	-
04126250					2	
04306252						8
04306252						1
04556290						2
04556290					3	
04696260					1	

FIG. 3.50 Maximum longitudinal strain values (% layer parallel shortening or extension).

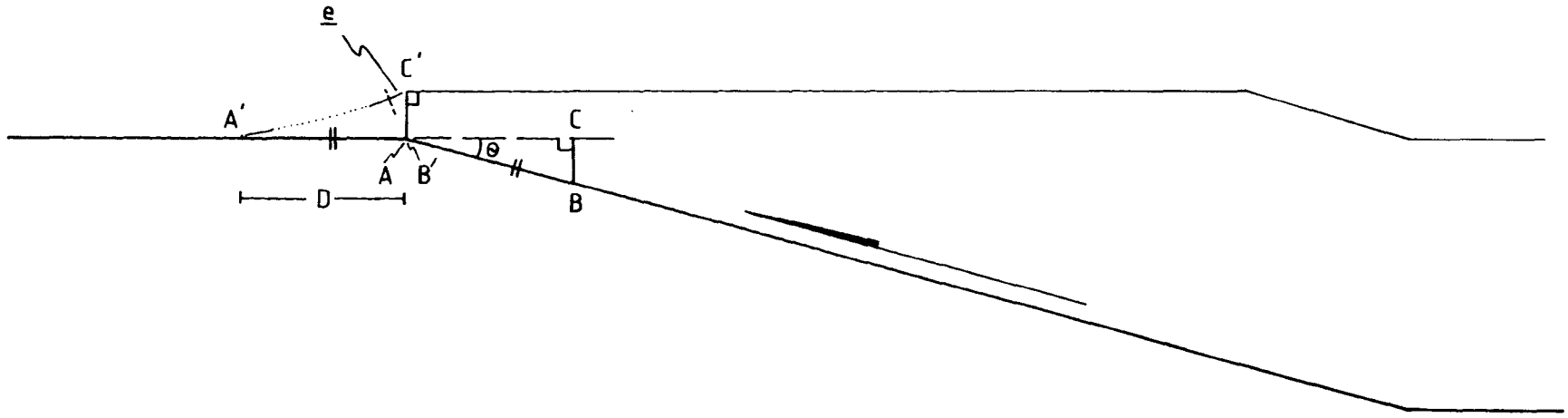

FIG. 3.51 Simplified 2 dimensional model illustrating the amount of extension within the hangingwall using thrust sheet dimensions typical of the Beinn Eighe Imbricate Fan.

(ii) Summary

The presentation of results in this chapter has followed the approach first used by Coward & Kim (1981) and later of Fischer & Coward (1982). Strains within the imbricate systems of the Moine Thrust Zone clearly have a complex history, an incremental stage of which may be elucidated by reference to simple models such as that illustrated in Fig. 3.51.

A full discussion on the evolution of strain within thrust sheets is given in Chapter 6, following Part 2 of this thesis.

P A R T T W O

THE PELVOUX - BRIANÇONNAIS REGION OF THE FRENCH ALPS

Frontispiece : E. Pelvoux-Briançonnais

CHAPTER 4

REGIONAL GEOLOGY OF THE PELVOUX - BRIANÇONNAIS

4.1 REGIONAL STRATIGRAPHY

The external regions of the Western Alps are composed of several distinct stratigraphic domains which are separated from each other by major thrusts. From W (external) to E (internal) these domains are:

1. External Zones (Dauphinois and Ultradauphinois Zones) which are laterally continuous with the Helvetic Zone of Switzerland.
2. Internal Zones (Pennine Zones) which are subdivided into the Valais, Subbriançonnais, Briançonnais and Piémontaise Zones.

These stratigraphic domains are illustrated in Fig. 4.1; the following introduction is concerned only with the stratigraphical characteristics of the Pelvoux-Briançonnais. Excellent regional summaries of Western Alpine stratigraphy and palaeogeography are provided by Trumpy (1960), Ramsay (1963) and Debelmas & Lemoine (1970).

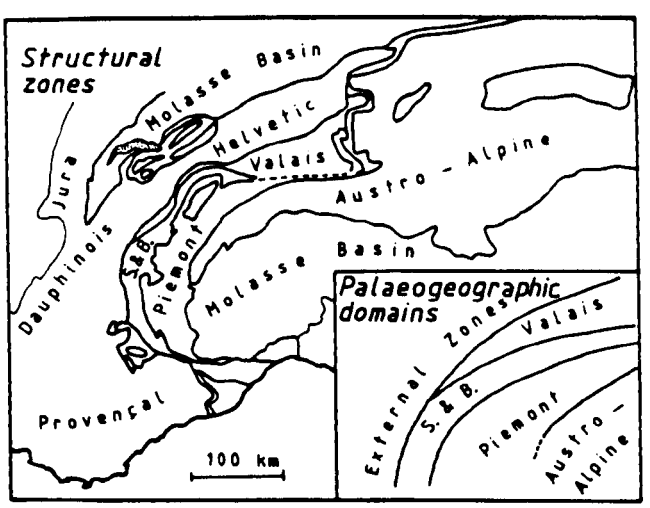

FIG. 4.1 Structural zones and palaeogeographic domains of the Western Alps. (Slightly modified from Debelmas & Lemoine (1970).
S. & B. = Subbriançonnais and Briançonnais Zones.

(i) Briançonnais Zone

The external Briançonnais Zone comprises a pre-Triassic basement of Carboniferous to early Permian sediments and volcanics which are unconformably overlain by a late Permian to Tertiary succession (Fig. 4.2).

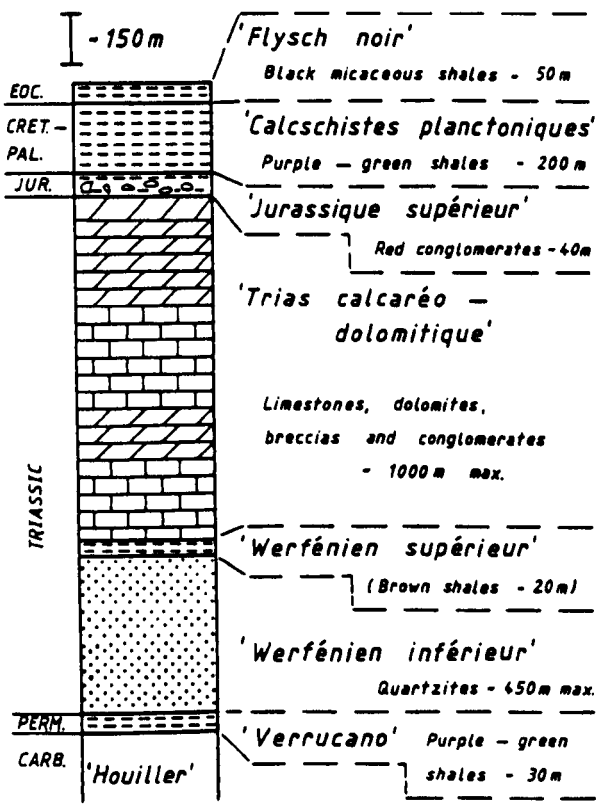

FIG. 4.2 Briançonnais Zone stratigraphy within the study area.

Numerous detailed descriptions of Briançonnais stratigraphy are scattered throughout the French literature, principally resulting from the detailed work of the Grenoble research group, e.g. Debelmas (1955, 1963, 1966). An extremely detailed and precise account of stratigraphical variations within the Briançonnais Zone immediately to the

S.W. of the study area is presented by Debelmas (1955). This work emphasises the laterally variable nature of post-Triassic lithological units and the important thickness variations between different nappe units within the Briançonnais and hence suggests the importance of an evolving normal fault/tear fault system (extensional basin) throughout the Mesozoic.

(a) Pre-Triassic Basement

The pre-Triassic basement of the external Briançonnais Zone consists of a thick (2000-3000 m) development of conglomerates, sandstones, shales, coals and volcanics. This basement succession is Carboniferous to early Permian in age and is termed 'la zone houillère briançonnaise'. Fabre et al. (1952) noted that the Carboniferous shows more complex folding than the overlying Permian, suggesting that the Houiller was deformed during the late Hercynian. In the internal Briançonnais the basement suite shows evidence of Alpine metamorphism (e.g. Ambin massif) - see Fig. 4.5 - and is unconformably overlain by Permo-Triassic or Triassic cover rocks.

(b) Late Permian to Tertiary Cover

In the Briançon region the Houiller is unconformably overlain by up to 50 m of unfossiliferous quartz conglomerates and purple-green shales. These are thought to be late Permian in age based on lithostratigraphical correlation with the Permian of Alpes Maritimes. The basal conglomerates and shales are known as 'Verrucano' and are overlain by up to 400 m of white quartzites, 15 m of shales, evaporites or cargneule and up to 1000 m of limestones, dolomites and carbonate breccias or conglomerates. This quartzite-shale-carbonate sequence is Triassic in age and it provides an excellent comparison with the stratigraphically similar continental shelf succession of the Moine Thrust Zone, described in Chapter 1, particularly for a study of scale, geometry and style of compressional structures developed within similar sedimentary successions.

The stratigraphic variations within the Triassic sequence are described by Debelmas (1955). Distinct lithological thickness variations are evident from W to E within the following nappe units, the 'Roche-Charnière nappe', the 'Champcella nappe' and the 'Peyre-Haute nappe'. These thrust sheets are described from a geometrical point of view in Chapter 5 and from this description it is

possible to derive a reasonably constrained estimate of the original distance between the measured sections of Debelmas (1955). This leads to a constrained picture of the geometry and displacement on pre-Alpine extensional faults.

Sedimentation between the late Triassic and late Cretaceous was extremely localised within the external Briançonnais Zone, characterised by accumulations of breccias and shales, which in many cases are located near to extensional faults which were active in the Triassic. Thin developments of Liassic, Oxfordian and early Cretaceous are described by Debelmas (1955) and Barfety (1965, 1967).

A thick sequence (up to 500 m) of late Cretaceous calcareous shales, termed 'calcschistes planctoniques', were deposited across the underlying Triassic and Jurassic substratum, a rapid thickness increase occurs from W to E within the northern part of the study area and appears to be a result of late Cretaceous movement on extensional faults. These calcareous shales are overlain by Eocene 'Flysch noir', a sequence of dark coloured shales and sandstones which represent the basal unit of a thick synorogenic turbidite dominated Eocene sequence.

Classic structural interpretations (e.g. Debelmas & Lemoine, 1970) which are based on almost one century of field mapping, stratigraphical analysis, palaeogeographic reconstructions and structural geometrical appraisal have resulted in the popular idea that the Flysch noir was originally overlain by the 'Embrunais Flysch' which slipped towards the W into its present position during Alpine compression. The original stratigraphic position of the Embrunais nappes is a crucial problem which has to be resolved to unravel the interplay between movement on thrusts which branch off compressional detachment systems and major faults which cut down through stratigraphic successions.

(ii) Subbriançonnais Zone

The stratigraphy of the Subbriançonnais Zone to the SE and E of the Pelvoux massif, Fig. 4.3, has been described in detail by Debelmas (1955, 1961) and Barfety (1965). No pre-Triassic basement rocks are exposed within the study area and it is difficult to assess whether the Subbriançonnais substratum was pre-Hercynian crystalline basement or Carboniferous sediments similar to the Houiller of the Briançonnais Zone. The oldest Subbriançonnais rocks exposed within the Briançon region are Triassic dolomites, evaporites and cargneule. Early Jurassic sedimentation was restricted within the Subbriançonnais Zone suggesting that late Triassic - early Jurassic extensional faulting may have controlled Subbriançonnais sedimentation. As a result the 'Lias' is not well developed within the study area and it is usual for middle Jurassic ('Dogger') sediments to overlie the Trias. The 'Dogger' is typically represented by up to 100 m of dolomitic limestones and breccias which have yielded Bathonian fossils.

A thin development (up to 50 m) of black shales commonly overlies the 'Dogger' and sediments of this type occur within the study area to the N of Col du Galibier and near to Col de l'Eychauda - see the maps enclosed in the back pocket of this thesis. To the N of the study area these shales overlie a thick conglomerate sequence, thought to be Callovian in age and termed the 'brèche du Télégraphe'.

The early Cretaceous is well developed within the area and up to 75 m of thin limestones and calcareous shales have been dated as Neocomian in age; these sediments are well exposed in the Pont de l'Alpe and Galibier regions (see geological map). Late Cretaceous to early Tertiary 'calcschistes planctoniques' overlie Neocomian or older sediments; these calcareous shales are very similar to the equivalent rocks of the Briançonnais Zone and may have been deposited in the same basin. World-wide sea levels were at a high peak for much of the late Cretaceous (Vail et al.

1977) and it is likely that the Subbriançonnais and Briançonnais basins were transgressed in the early Senonian, losing their distinction as individual depositional basins.

Tertiary sediments within the Subbriançonnais Zone are very similar to those of the Briançonnais Zone. Black shales and dark brown sandstones termed 'Flysch noir' typically overlie the calcschistes planctoniques. The original thickness of Eocene sediments that were deposited across the underlying Subbriançonnais and Briançonnais Zones cannot be gauged from a study of the E. Pelvoux region. The intricate evolution of compressional structures and Eocene sedimentary facies within the Subbriançonnais/ Briançonnais basin is a fascinating problem which can only be resolved by integrating existing knowledge contained in French theses and publications, e.g. Latreille (1961) and Kerckhove (1969), with new stratigraphical, sedimentological and structural fieldwork in the area to the S of the Pelvoux massif. This task forms part of the current research effort of the Alpine research team at University College, Swansea.

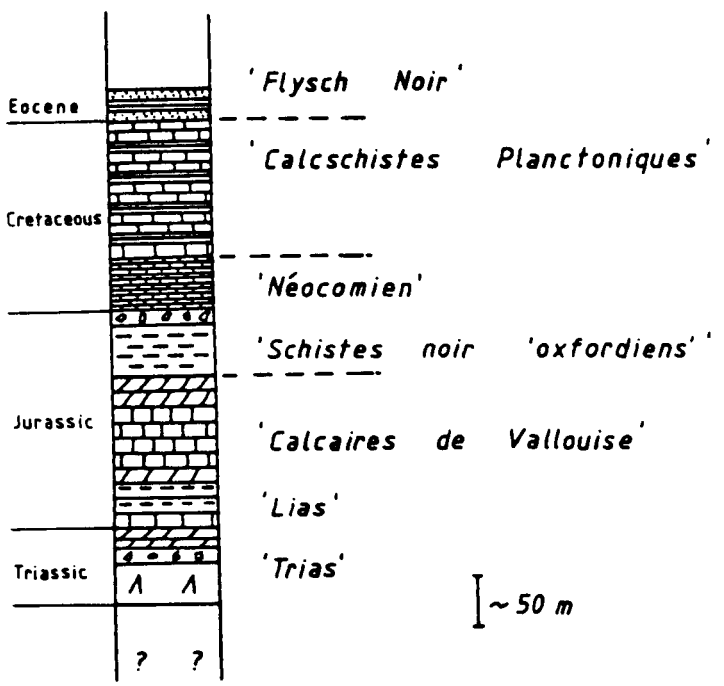

FIG. 4.3 Stratigraphy of the Subbriançonnais Zone.

(iii) External Zones

The External Zones of the French Alps are characterised by a thick (up to 7 km) Mesozoic to Tertiary succession which overlies crystalline basement or Carboniferous 'Houiller' sediments. In very broad terms the external zones are subdivided into regional palaeogeographic domains based on differences in sediment type and thickness. This is illustrated in Fig. 4.1 which shows the Dauphinois and Provençal facies.

A thin Triassic sequence (up to 50 m) of evaporites, quartzites, sandstones or dolomitic limestone overlie the external zone basement. A sustained period of subsidence and sedimentation is typical of the external zones from late Triassic to late Cretaceous and a complete Jurassic and early Cretaceous succession occurs in the Subalpine Chains. The lithologies and approximate age ranges of the external zone stratigraphy are illustrated in Fig. 4.4.

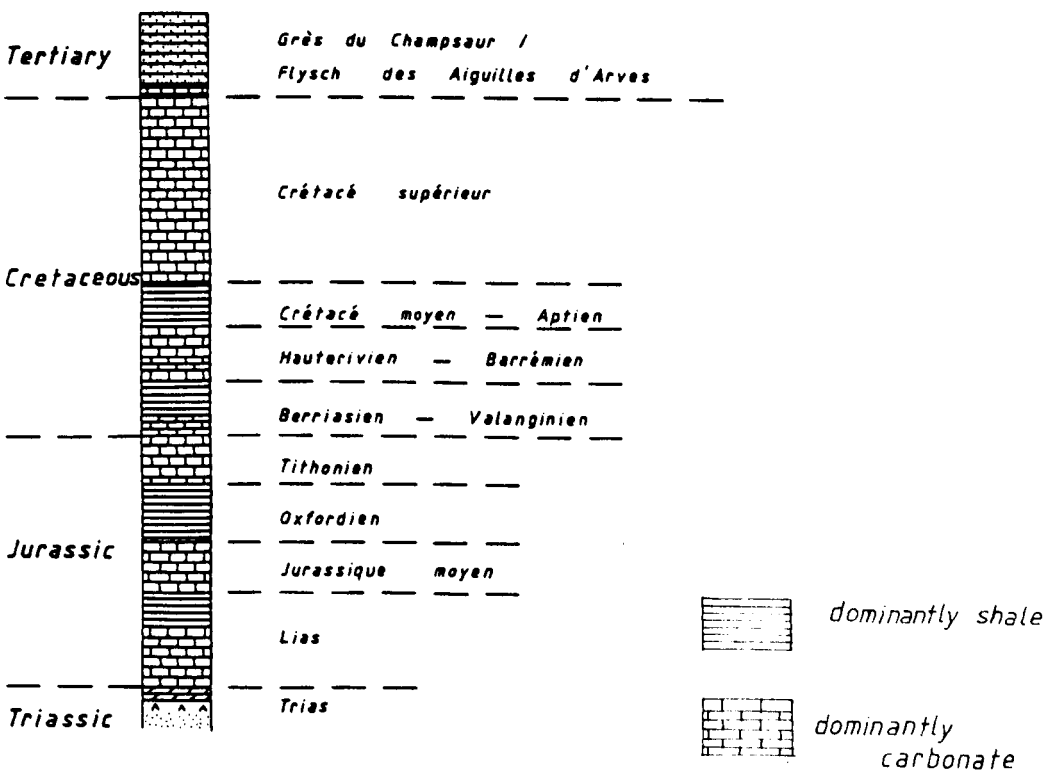

FIG. 4.4 Stratigraphy of the external zones. (No vertical scale intended)

The External Zones within the study area are termed the Ultradauphinois Zone; this term is used to distinguish the most internal portion of the External Zones, which display complex thrust structures and clearly involve a substantial amount of shortening, from the more external portions which have not slipped a great distance towards the W. This subdivision is not intended to imply a distinct sedimentological or stratigraphic contrast between the Dauphinois and Ultradauphinois. However, it is sensible to expect significant contrasts in thickness and/or lithologies between stratigraphic successions which were originally a significant distance apart.

The early Jurassic of the study area is fossiliferous and a complete 'Lias' and lower part of the middle Jurassic are represented between the La Meije and Combeynot massifs (Gidon 1954). No Cretaceous sediments occur within the external zones of the study area. This may be a result of tectonic removal of the Cretaceous during Alpine thrusting, an irregular Hercynian relief of basement massifs or Cretaceous extensional faulting being confined to the W of the external zone crystalline massifs. Eocene flysch (Aiguilles d'Arves Flysch) is unconformable on crystalline basement or Jurassic limestones and shales to the E and N of the Pelvoux massif; similar relationships occur between the 'Grès du Champsaur' and underlying rocks to the S and W of the Pelvoux massif (Harwood, pers. comm.). The stratigraphic and structural relationships within the external zones are described in more detail in Chapter 5 with a view to unravelling the timing of thrusting and Eocene sedimentation.

4.2 REGIONAL STRUCTURE

The structural evolution of the Western Alps has been a major research interest since the classic studies in the early years of this century, e.g. Argand (1916). Almost 70 years later no consensus of opinion has emerged concerning the evolutionary sequence, timing and movement direction of Alpine thrust systems. This point is perhaps best illustrated by the conflicting ideas of Ricou & Siddans (in press) and Butler et al. (in press), where two apparently irreconcilable views are presented concerning the structural evolution of part of the Western Alps.

Fortunately every Alpine geologist is in agreement on the present-day distribution of structural zones and a structural map which is based on Fig. 1 of Debelmas & Lemoine (1970), is illustrated in Fig. 4.5.

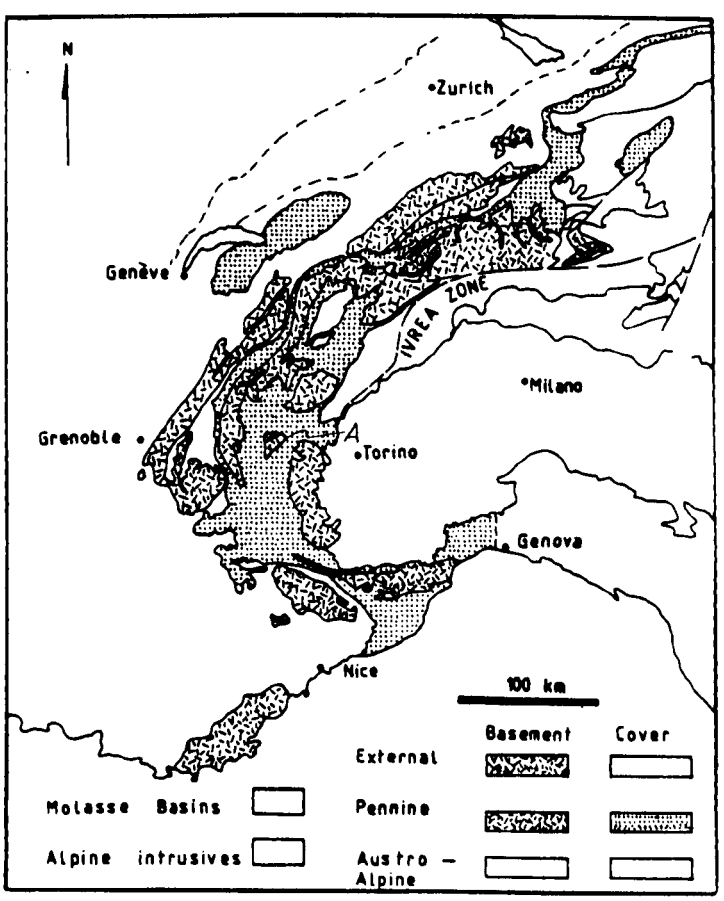

FIG. 4.5 Structural subdivisions of the Western Alps. (Slightly modified from Debelmas & Lemoine (1970), A = Ambin massif).

The intention of this short review is to outline the existing structural interpretations of the Pelvoux - Briançonnais and to summarise previous research in this area.

(i) Briançonnais and Subbriançonnais Zones

The structural geology of the Briançonnais and Subbriançonnais Zones in the classic region near to Briançon has been the subject of several research theses in recent years, e.g. Debelmas (1955), Barfety (1965) and Tricart (1980). The detailed field observations and interpretations of these workers provide an excellent structural framework around which to test the applicability of currently fashionable geometrical principles in unravelling fold and thrust structures and predicting the deep structure of thrust terrains. The study areas of the above authors are illustrated in Fig. 4.6.

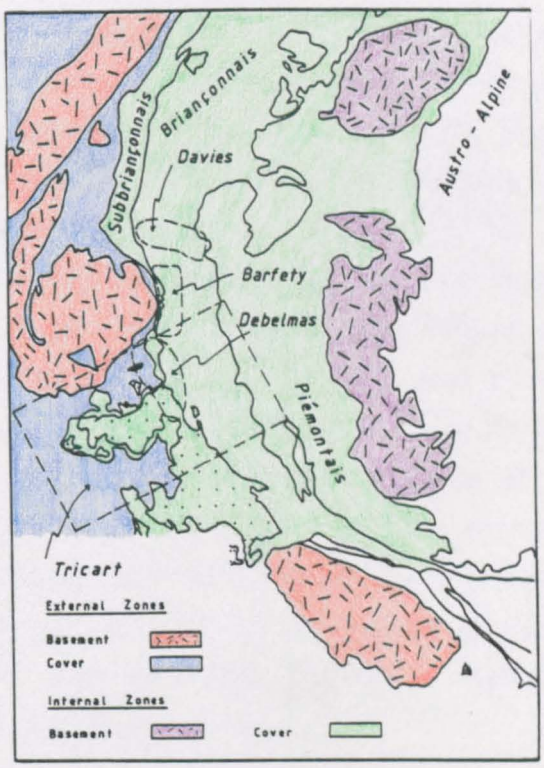

FIG. 4.6 Approximate study areas of Debelmas (1955), Barfety (1965), Tricart (1980) and Davies (1983).

The area studied by Barfety (1965) corresponds almost exactly with the study area of this thesis, the work of Debelmas (1955) and Tricart (1980) covers the region to the S and SE of the Pelvoux massif. The Ph.D. thesis of Davies (1983) is partly concerned with the structural geology of the Briançonnais Zone immediately to the NE of the study area; this work of Davies is the first attempt to apply a modern geometrical approach to deciphering the structural evolution of the Briançonnais Zone. Her study area is also illustrated in Fig. 4.6.

(a) Thrust sheets (nappes) within the Briançonnais Zone

The nappe assemblage within the Briançonnais Zone is traditionally described as comprising 5 distinguishable nappe units which are listed below. The structurally highest and most internal 'nappe' consists of the 'écailles intermédiaires', the structurally lowest and most external nappe is the 'Roche-Charnière nappe', Fig. 4.7. This diagram is compiled from Sheet 189 of the Carte Geologique Détaillée de la France (Briançon - 3rd edition).

1. Roche-Charnière nappe (structurally lowest)
2. Champcella nappe
3. Peyre-Haute nappe
4. Assan nappe or Briançonnais interne
5. Écailles intermédiaires (structurally highest)

The existing geometrical interpretations are now presented.

The eastern limit of the Briançonnais Zone is marked by the tectonic contact between the Briançonnais and Piémontaise Zones, see Fig. 4.7. This contact has previously been interpreted both as a backthrust and as a backfolded foreland directed thrust (Debelmas et al. 1980). Two cross sections which illustrate the geometrical relationships between the Piémontaise Zone and the underlying Briançonnais nappes are presented by Debelmas et al. (1980, p.110 & p.111, Figs. 5.2 & 6.1). These cross sections are combined in Fig. 4.8(A). An attempted restoration of these cross sections, Fig. 4.8(B) illustrates the amount of implied tectonic shortening and also highlights the geometrical problems within the original cross sections. The approximate position of the section lines of Debelmas et al. (1980) are illustrated in Fig. 4.7.

The exposed portion of the Briançonnais Zone in Fig. 4.8(A) consists of 2 major thrust sheets, a higher thrust sheet (écailles intermédiaires) and a lower sheet which constitutes the bulk of the Briançonnais Zone on this section line. This lower sheet is termed the 'Champcella nappe' in the region structurally below Serre Chevalier,

Fig. 4.8(A), and the 'Briançonnais interne' in the region of the Clarée valley.

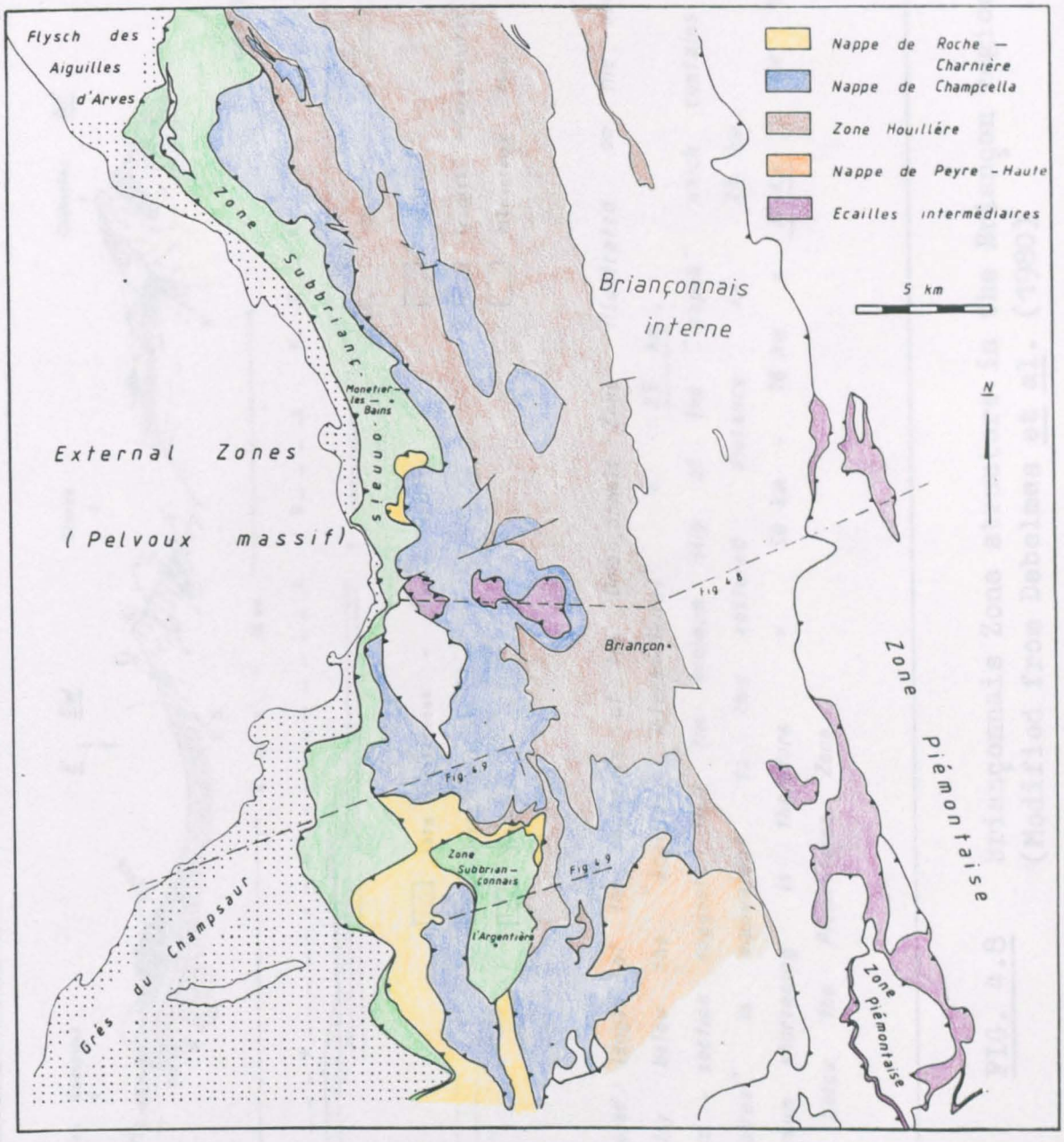

FIG. 4.7 Classical nappe nomenclature for the Briançon region.

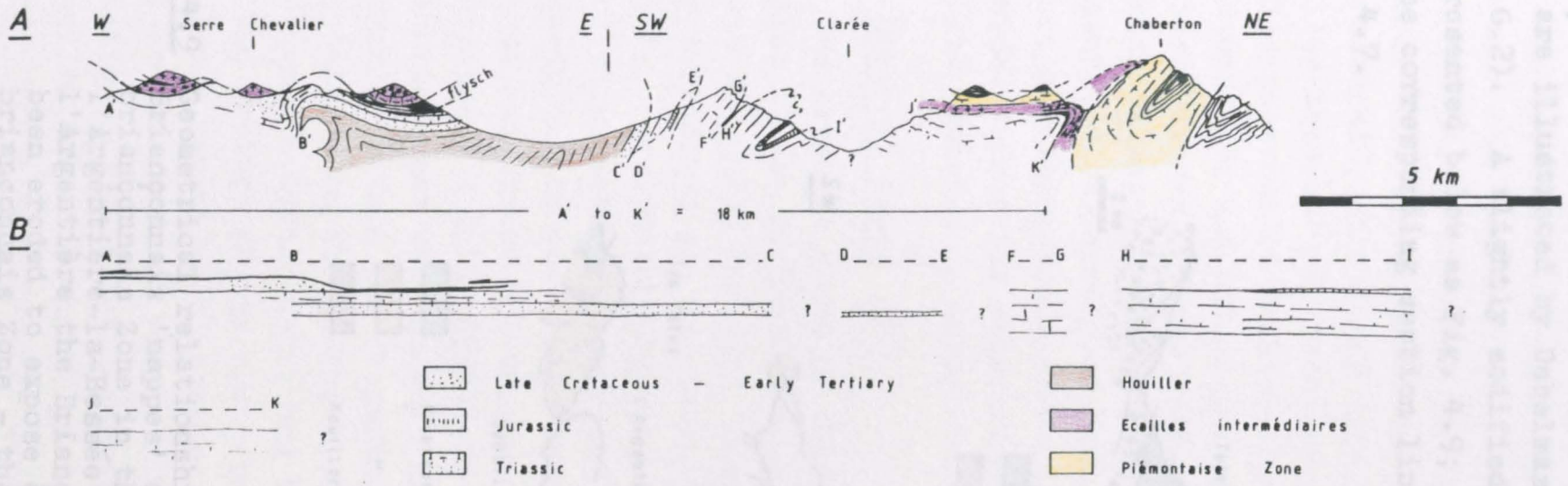

The restored length of the segments of the Briançonnais Zone illustrated on the above cross - section, structurally below the "écailles intermèdiaires" = 25 km .
The cross - section suggests that the minimum slip of the "nappe" which contains the "écailles intermédiaires" is equivalent to this restored distance i.e. 25 km .
The minimum shortening is therefore = 50 km - 18 km = 32 km , for the Briançonnais "nappes" below the Piémontaise Zone .

FIG. 4.8 Briançonnais Zone structure in the Briançon region. (Modified from Debelmas et al. (1980)

The geometrical relationships between the external Briançonnais 'nappes' and the underlying Subbriançonnais Zone are illustrated by Debelmas et al. (1980, p.111, Fig. 6.2). A slightly modified version of this diagram is presented below as Fig. 4.9; the approximate positions of the corresponding section lines are indicated in Fig. 4.7.

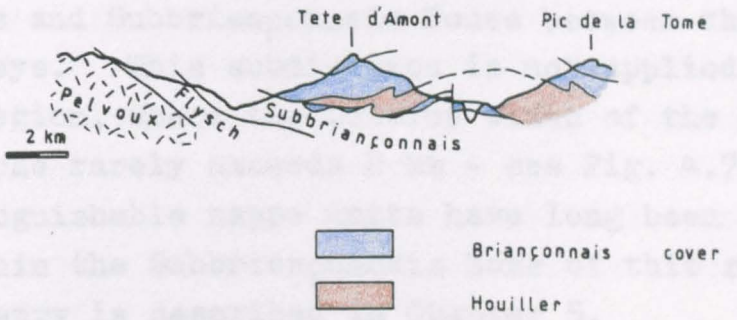

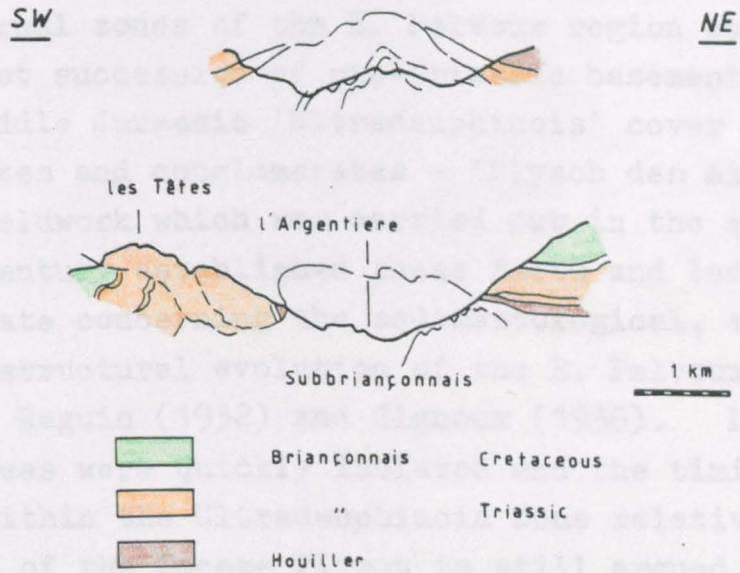

FIG. 4.9 Geometrical relationships between the external Briançonnais 'nappes' and the underlying Subbriançonnais Zone in the region near to l'Argentière-la-Bessée (Durance Valley). At l'Argentière the Briançonnais 'nappes' have been eroded to expose a window on the Subbriançonnais Zone - the 'fenêtre de l'Argentière'. Slightly modified from Debelmas et al. (1980, p.111, Fig.6.2)

(b) Thrust sheets (nappes) within the Subbriançonnais Zone

The structure of the Subbriançonnais Zone within the study area has been described by Debelmas (1955) and Barfety (1965). To the north of the study area, in the region of St. Jean de Maurienne, the Subbriançonnais Zone is structurally subdivided into 'écailles externe', 'écailles interne' and 'zone des Gypses', following the detailed research of Barbier (1948) who studied the Ultradauphinois and Subbriançonnais Zones between the Arc and Isére valleys. This subdivision is not applied to the Briançon region, where the outcrop width of the Subbriançonnais Zone rarely exceeds 2 km - see Fig. 4.7; however, distinguishable nappe units have long been recognised within the Subbriançonnais Zone of this region and their geometry is described in Chapter 5.

(ii) External Zones

The external zones of the E. Pelvoux region comprise a complex thrust succession of pre-Triassic basement, Triassic to middle Jurassic 'Ultradauphinois' cover and Eocene turbidites and conglomerates - 'Flysch des Aiguilles d'Arves'. Fieldwork which was carried out in the early part of this century established these facts and led to subsequent debate concerning the sedimentological, stratigraphical and structural evolution of the E. Pelvoux area, e.g. Gignoux & Raguin (1932) and Gignoux (1936). Local problematic areas were quickly isolated and the timing of thrusting within the Ultradauphinois Zone relative to the deposition of the Eocene Flysch is still argued, e.g. Bravard & Gidon (1979) and Beach (1981b).

The geology of the southern and eastern margins of the Pelvoux massif was described in great detail by Gidon (1954) and the work of Vernet (1965 & 1966a) resulted in recognition and detailed descriptions of imbricate zones and complex fold and thrust geometries within the E. Pelvoux region. There were further structural investigations during the 1970s, e.g. Gratier, Lejeune & Vergne (1973),

Bartoli et al. (1974) and Gratier & Vialon (1980) which contributed very detailed textural and local geometrical observations and interpretations to the pre-existing geological base, established by the work carried out in the first half of the century.

Beach (1981a, 1981b, 1981c & 1981d) presented new structural information involving strain data and thrust sheet geometry to examine the structural evolution of thrust sheets within the Ultradauphinois Zone. The complex pre-compressional geometry of this region is emphasised by Beach and described by Davies (1982). Butler et al. (in press) integrate the results of recent field mapping within the Dauphinois and Ultradauphinois Zones to provide a broad estimate of orogenic contraction and an interpretation of how individual thrust systems link along the strike of the belt.

A comprehensive account of the detailed geological relationships between the Ultradauphinois Zone and the Aiguilles d'Arves Flysch in the region to the N of the Pelvoux massif is presented by Barbier (1948). Complex fold trends within the Flysch in the region near to Mt. Charvin - see Fig. 4.10 - are described by Barbier and Barfety (1972) and Antoine et al. (1978) investigate the relationship between the Flysch and the overlying Valais Zone in Savoie.

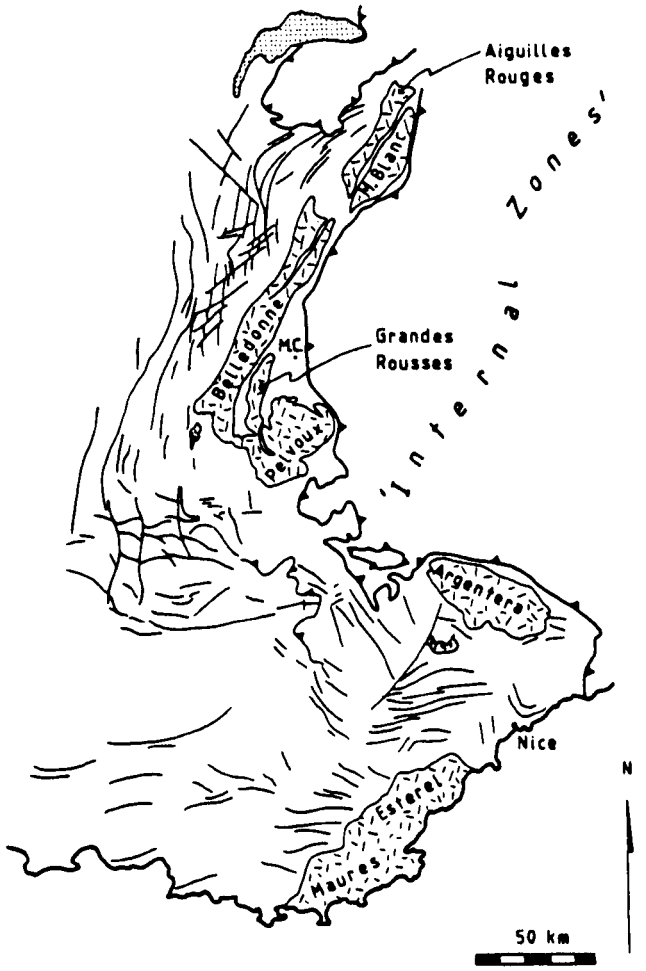

FIG. 4.10 Structural configuration of the external zones of the French Alps, illustrating crystalline basement massifs, fold trends and wrench faults (décrochements) within the Mesozoic cover. (modified from Goguel, 1963).
M.C. = Mt. Charvin.

The geology and structure of the Pelvoux-Briançonnais is long established and well known. However, no published account exists which attempts to harness the structure of the Ultradauphinois-Briançonnais Zones in the Briançon region in terms of an evolving thrust terrain, with particular emphasis on the inter-relationship and geometry of folds and thrusts to produce constrained estimates of thrust displacements and a picture of the evolutionary sequence of thrust systems. This is the subject of Chapter 5.

C H A P T E R 5

THRUST SHEET EVOLUTION IN THE PELVOUX - BRIANÇONNAIS

This chapter describes the 3 dimensional geometry of thrust sheets within the Pelvoux-Briançonnais and examines the evolutionary sequence of folding and fault development. For ease of description the Briançonnais Zone is subdivided into 3 sub-areas; from S to N these are:

1. Montbrison - Serre Chevalier
2. Tête Noire - Grand Aréa
3. Grand Galibier

These sub-areas are illustrated below in Fig. 5.1.

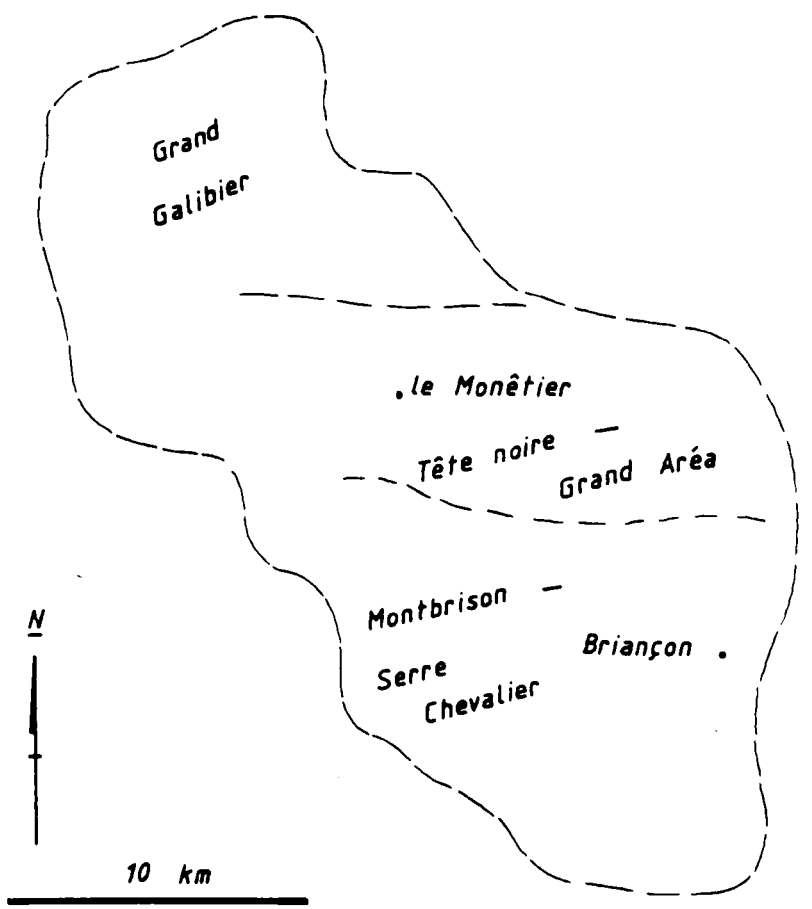

FIG. 5.1 Sub-areas within the study region.

5.1 BRIANÇONNAIS AND SUBBRIANÇONNAIS ZONES

(i) Movement direction of thrust sheets

Establishing the movement directions of thrust sheets within the Briançonnais and Subbriançonnais thrust systems requires careful assessment of the 3 dimensional geometry of thrust surfaces and fold structures in conjunction with the orientation of finite strain markers and slip direction indicators. The arcuate trace of the frontal Briançonnais and Subbriançonnais thrusts in the French Alps and the arcuate trend of folds within these thrust systems provides an excellent location to test rival ideas concerning unidirectional and divergent thrust sheet movement directions. The solution to this particular problem cannot be gained from study of a single area. The contribution of this chapter to the current debate on Alpine thrust sheet movement directions must be integrated with ideas arising from ongoing field studies around the Alpine arc and with existing structural interpretations of the Alpine system.

No localities have been encountered within the study area which provide unequivocal proof of a particular movement direction, in contrast to the fortuitous outcrop geometries (based on opposed lateral ramp complexes) of the Beaufortain region of the French Alps which allow almost exact movement directions to be quickly resolved (Butler 1983). The problem of movement directions is discussed throughout this chapter as the geometrical variations within the area are described. It has been demonstrated in Chapter 2 that an assumption of a movement direction perpendicular to the local strike may be incorrect, especially in a region which has evolved by slip across oblique-lateral ramps.

A contoured stereogram of poles to bedding within the Briançonnais Zone from the whole of the study area is illustrated in Fig. 5.2; this initially suggests a movement direction towards 265°. However, the orientation of structures within the Briançonnais Zone may have been modified by large scale, structurally lower thrusting.

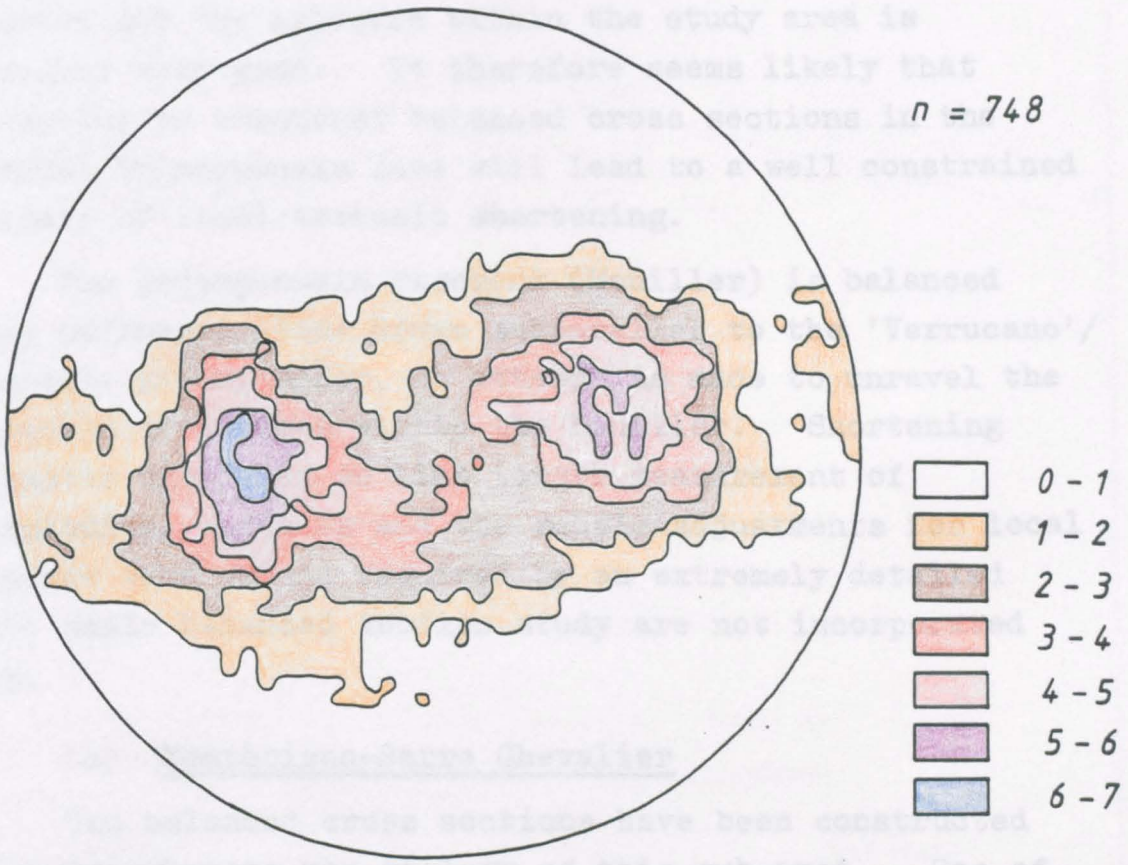

FIG. 5.2 Contoured stereogram of poles to bedding for the Briançonnais Zone within the study area. Contours drawn at 1% intervals.

(ii) Tectonic shortening, balanced and restored cross sections

The most accurate method of obtaining an estimate of tectonic shortening within a thrust belt is to compare the length of a balanced cross section with its restored version. The accuracy and applicability of this method is determined by the complexity of the pre-compressional geometry (which may result in large lithological thickness variations), the complexity of the thrust structures and the degree of exposure.

The stratigraphic variations within the Briançonnais Zone are described by Debelmas (1955); the existing structural interpretations partly explain the outcrop geometry and the exposure within the study area is generally very good. It therefore seems likely that attempting to construct balanced cross sections in the external Briançonnais Zone will lead to a well constrained estimate of local tectonic shortening.

The Briançonnais basement (Houiller) is balanced using reference lines drawn subparallel to the 'Verrucano'/ quartzite unconformity, no attempt is made to unravel the Hercynian structures within the Houiller. Shortening estimates are based on line length measurement of lithological contacts and the subtle adjustments for local cleavage development required by an extremely detailed small scale balanced section study are not incorporated here.

(a) Montbrison-Serre Chevalier

Two balanced cross sections have been constructed which incorporate the geology of this sub-area. One of these cross sections (C-C') extends outside the sub-area to illustrate the geology as far W as the frontal Briançonnais Thrust. Sections (A-A') and (B-B') are sketch sections which illustrate the outcrop geology and are used to establish the geometrical relationships which are incorporated at depth onto balanced cross section (C-C'). Section (D-D') is a balanced cross section which extends from the Montbrison-Serre Chevalier sub-area into the Tête Noire-Grand Arêa sub-area. All sections are drawn in an E-W orientation ± 20° (subperpendicular to strike) to cross important structures; the position of these section lines is shown in Fig. 5.3.

Cross section (A-A') - Fig. 5.4, illustrates the geometry of the Champcella nappe on a WNW-ESE section line drawn approximately 1 km N of Queyrieres (Fig. 5.3). In the W of the cross section the hangingwall to the Champcella

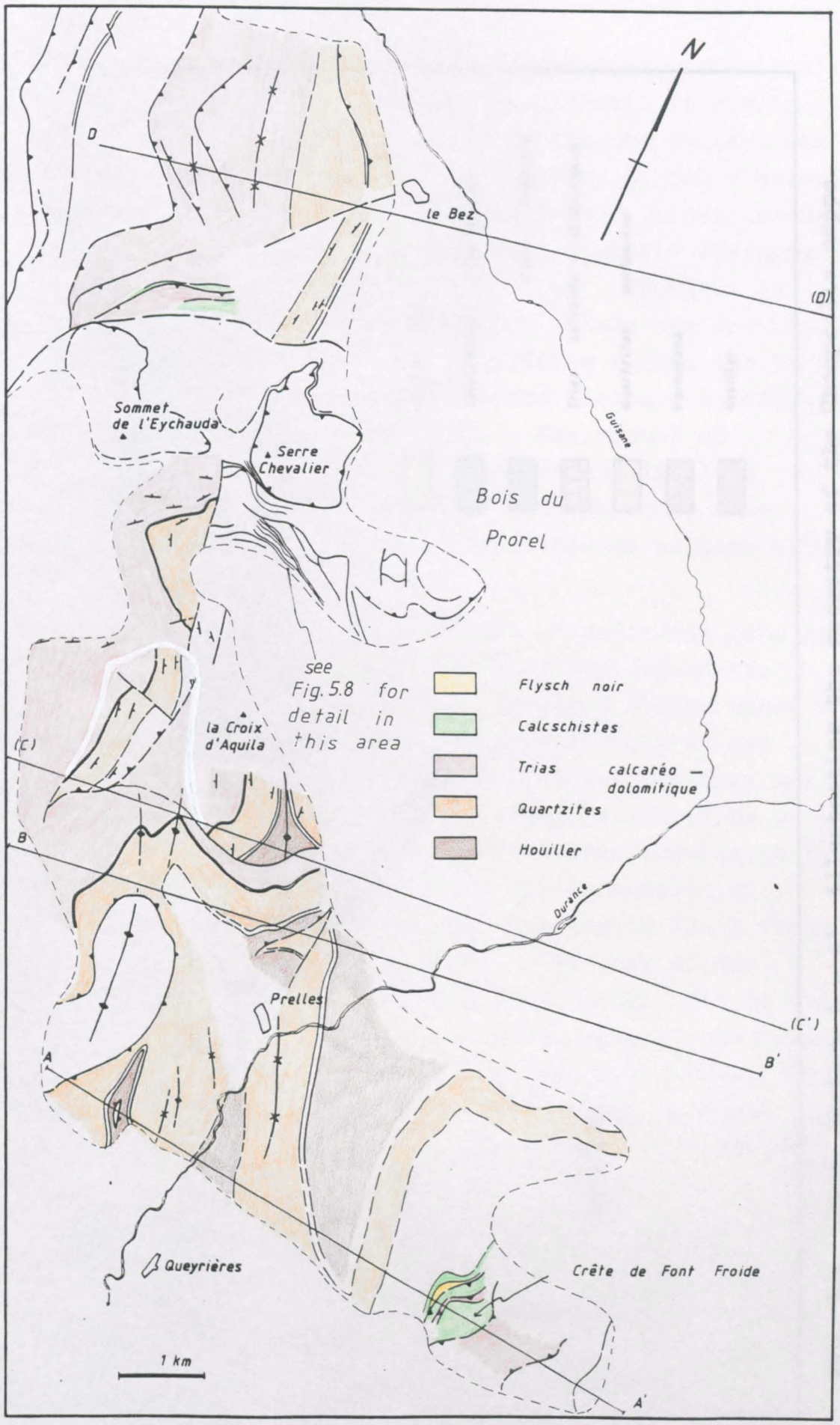

FIG. 5.3 Geological map of the Montbrison-Serre Chevalier sub-area, illustrating the position of lines of section. Consult map in back-pocket of thesis for detail.

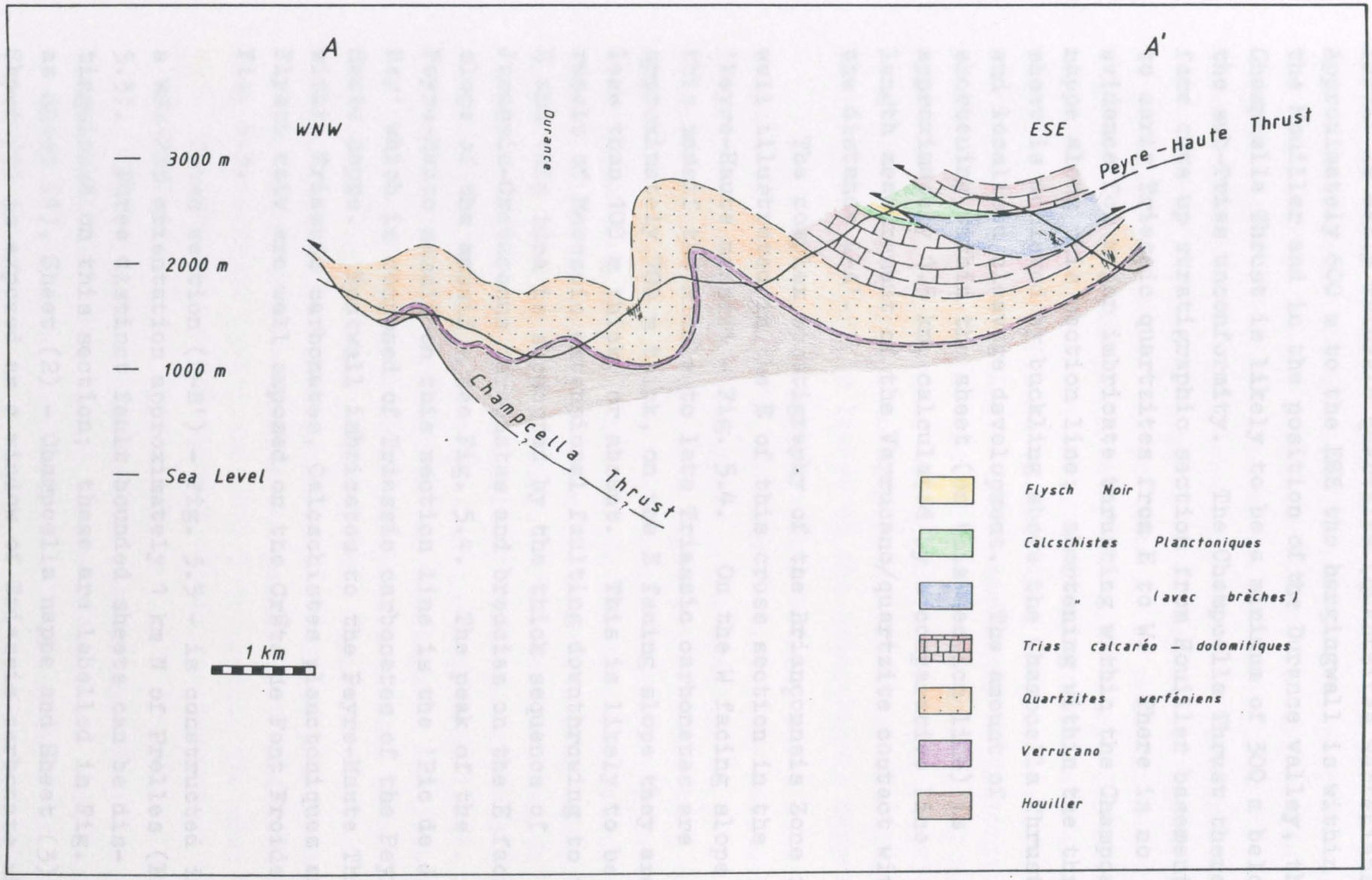

FIG. 5.4 Cross section A - A', illustrating the geometry of the Champcella nappe.

Thrust is early Triassic quartzite (quartzites werféniens). Approximately 600 m to the ESE the hangingwall is within the Houiller and in the position of the Durance valley, the Champcella Thrust is likely to be a minimum of 300 m below the sub-Trias unconformity. The Champcella Thrust therefore cuts up stratigraphic section from Houiller basement to early Triassic quartzites from E to W. There is no evidence for major imbricate thrusting within the Champcella nappe along this section line; shortening within the thrust sheet is achieved by buckling above the Champcella Thrust and localised cleavage development. The amount of shortening within the sheet (on this section line) is approximately 1.5 km, calculated by a comparative line length measurement of the Verrucano/quartzite contact with the distance A-A'.

The complex stratigraphy of the Briançonnais Zone is well illustrated in the E of this cross section in the 'Peyre-Haute massif' - Fig. 5.4. On the W facing slope of this massif the middle to late Triassic carbonates are approximately 700 m thick, on the E facing slope they are less than 100 m thick, or absent. This is likely to be a result of Mesozoic extensional faulting downthrowing to the E and this idea is supported by the thick sequence of Jurassic-Cretaceous carbonates and breccias on the E facing slope of the massif - see Fig. 5.4. The peak of the Peyre-Haute massif on this section line is the 'Pic de Jean Rey' which is composed of Triassic carbonates of the Peyre-Haute nappe. Footwall imbricates to the Peyre-Haute Thrust, within Triassic carbonates, Calcschistes planctoniques and Flysch noir are well exposed on the Crête de Font Froide, Fig. 5.3.

Cross section (B-B') - Fig. 5.5 - is constructed in a WSW-ENE orientation approximately 1 km N of Prelles (Fig. 5.3). Three distinct fault bounded sheets can be distinguished on this section; these are labelled in Fig. 5.5 as Sheet (1), Sheet (2) - Champcella nappe and Sheet (3). Sheet (3) is exposed as a window of Triassic carbonate which

underlies early Triassic quartzites of the Champcella nappe. This structurally lowest sheet is included as part of the Champcella nappe in the classical French interpretation - e.g. see Fig. 4.7. The carbonates of Sheet (3) are folded into an anticline with an interlimb angle of approximately 110°; this fold may have grown as a response to sticking at a thrust tip line. If so, then it is possible to suggest that the Champcella nappe overlay Sheet (3) prior to formation of the anticline within the carbonates, as the Champcella nappe is folded by it; this is good evidence for in-sequence thrusting. It is necessary to distinguish Sheet (3) from Sheet (2) and following the traditional nappe succession of the external Briançonnais, Debelmas (1955), Sheet (3) is considered to be part of the Roche-Charnière nappe, the structurally lowest of the Briançonnais nappes.

The structurally highest fault bounded sheet on cross section (B-B'), Sheet (1), is also traditionally included as part of the Champcella nappe. The hangingwall to Fault (1) in Fig. 5.5 has been projected into the line of section from approximately 1 km to the N. Fault (1) cuts through an anticline in Houiller to Triassic carbonates in the hangingwall and slices through the underlying Champcella nappe at a low angle to bedding. This geometry cannot develop as a result of conventional foreland directed thrusting as the cut-off angles of corresponding lithological units are different in the hangingwall and footwall. Fault (1) cuts up and down stratigraphic section in an E to W direction and has the geometry of a 'late' out-of-sequence thrust or extensional fault. These possibilities are now examined by combining the geometrical relationships of cross sections (A-A') and (B-B') to produce the most southerly balanced cross section within the study area (C-C') - Fig. 5.6.

This balanced cross section illustrates the 3 fault sheets described from Fig. 5.5, the section has been constructed in a similar direction and 700 m to the N of (B-B'). Two major thrust sheets are illustrated: the Champcella nappe and the Roche-Charnière nappe. A thrust

with a displacement in excess of 1.5 km may exist within the Champcella nappe on this section line near to the point where the section line crosses the Torrent de Sachas. Approximately 4 km to the S, a corresponding blind thrust may exist at depth within the Champcella nappe, in the core of the major fold illustrated in Fig. 5.4. The structurally highest sheet on the balanced cross section (Sheet (1) of Fig. 5.5) is shown to overlie a fault which slices through underlying thrust structures within the Champcella nappe and is flexured by folding which has resulted from movement of the Roche-Charnière nappe. This proposed geometrical configuration has important implications on the relative timing of folding and faulting in the Montbrison-Peyre-Haute region.

The broad sequence of deformation implied by this balanced cross section and by section (A-A') and (B-B') is as follows:

1. Development of a (frontal) ramp from a minimum depth of 3.5 km below the sub-Trias unconformity as a splay from a regional, more internal floor thrust (or local floor thrust).

2. Formation of a major buckle within early Triassic quartzites and overlying formations as a response to stick on this thrust, with possible continued propagation of the thrust along strike towards the N.

3. Development of the major Champcella Thrust as a splay from the floor thrust approximately 3.5 km below the sub-Trias unconformity. Growth of minor folds within the Champcella nappe resulting from a variable ratio of slip rate:fault propagation rate. Eventual slip of the Champcella nappe across its footwall to achieve a displacement of approximately 3 km.

4. Sticking of the Champcella nappe in its frontal portion and continued slip in the rear of the sheet leading to buckling and eventually inverting

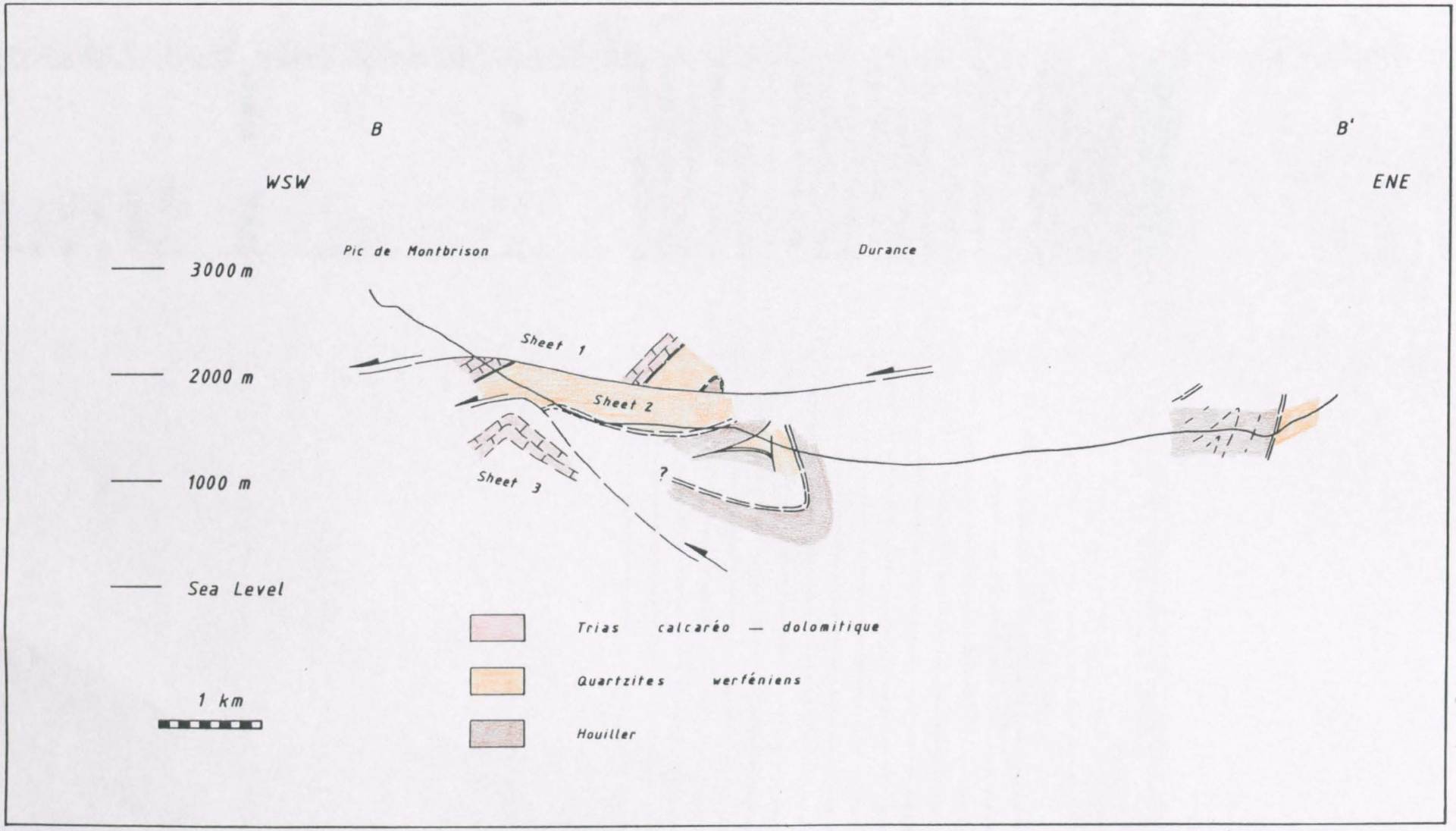

FIG. 5.5 Cross section B-B', illustrating the geometrical relationships between Sheets (1), (2) and (3).

Fig. 5.6

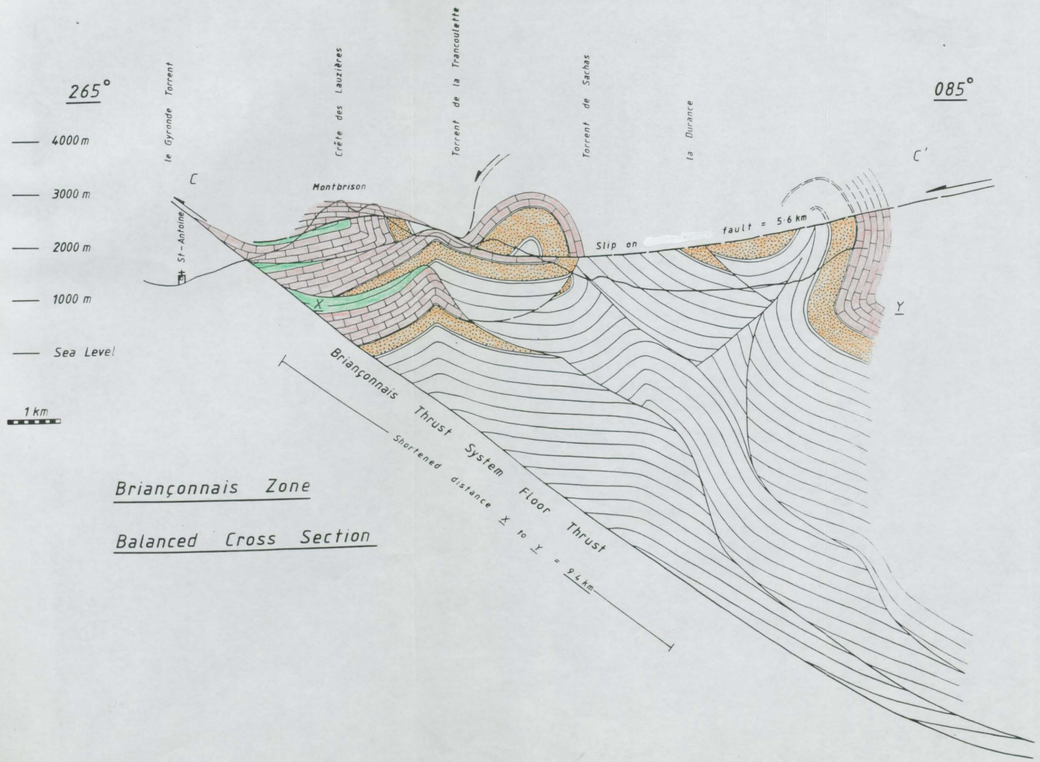

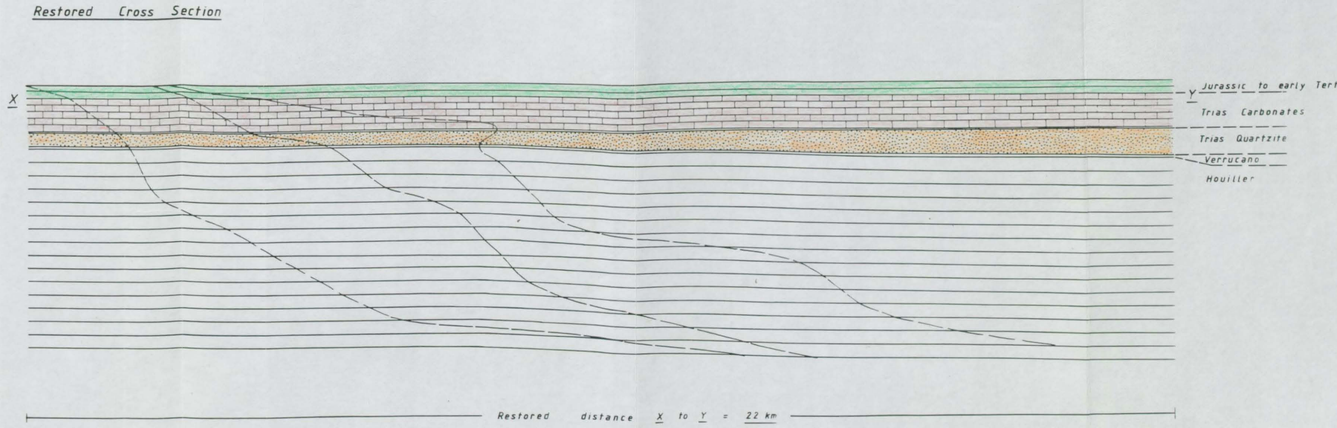

Shortening within the Briançonnais Thrust System between X and Y = 22 − 9·4 = 12·6 km

The structural interpretation presented on this cross-section is based on field observation at the present topographic level and on subsequent balanced cross-section construction techniques. The assumptions which are required to produce balanced cross-sections are outlined on pages 10, 11 and 12 and local assumptions are described in this section of the text.

the stratigraphy to produce a 'backfold' or 'retrocharriage' structure.

5. Slip of Sheet (1) possibly as an extensional fault sheet, possibly partially driven by growth of the major backfold structure. (Two distinguishable segments can be isolated within this fault sheet on the balanced cross section; segment (1) appears to restore to a position near to the backfold structure, and segment (2) appears to restore to a position on the steep limb of the fold in early Triassic quartzites near to Torrent de Sachas.

6. Development of a ramp from a minimum depth of 3 km within the Houiller as the Roche-Charnière Thrust, sticking during development of the thrust plane and folding within the sheet inducing flexuring of the overlying sheets.

7. Slip of the above fault-sheet assemblage as a 'locked-package' across a footwall of Briançonnais Zone and subsequently Subbriançonnais Zone strata.

This is the simplest deformation sequence which can be derived from the regional geometrical evidence. The broad timing is probably accurate, the detailed relationship of slip on extensional faults driven dominantly by gravitational instability and on thrusts driven dominantly by crustal compression is not likely to be systematic.

The geometrical relationships between the postulated extensional fault and its hangingwall and footwall suggest that the 'retrocharriage' structure - the major backfold which can be traced as a single fold for at least 35 km along strike (into the area studied by Davies (1983)) - is likely to have grown at an early stage in the evolution of the Briançonnais Thrust System. This is in contrast to the traditional French hypothesis, e.g. Debelmas & Lemoine (1970), which prefers most backfold/backthrust structures to be 'late' and therefore postdate the main period of foreland directed

thrusting. A slight adjustment of this approach may be required for this portion of the Briançonnais Zone; the backfold most probably postdates foreland propagation of the structurally lower thrust (Champcella Thrust); however, it most probably pre-dates thrusting within the more external Roche-Charnière nappe, Subbriançonnais and External Zones.

The major extensional fault places younger or older rocks over younger or older. It is tempting to suggest that the Peyre-Haute nappe is also part of this extensional sheet; it is in the correct tectonic position - see Fig. 5.4 - and although locally it places older rocks over younger this does not preclude an extensional origin. The strongest evidence to suggest that the Peyre-Haute nappe is part of this extensional sheet is that the Peyre-Haute Thrust does not link down-dip to the E below a more internal thrust unit, either within the study area or on Sheet 189 of the Carte Geologique Détaillée de la France (Briançon - 3rd edition).

The tectonic shortening implied for the portion of the Briançonnais Thrust System on cross section (C-C') is approximately 12.6 km, from an original across strike width of 22 km to a present day width of 9.4 km. Within the context of recent estimates of the amount of orogenic contraction in the Western Alps this value seems almost insignificant. However, only two major thrust sheets within the Briançonnais Thrust System have been encountered on this cross section. The total slip on the Briançonnais Floor Thrust must be extremely large to carry the Briançonnais Zone across its Briançonnais footwall and onto a Subbriançonnais succession of a different depositional basin.

Balanced cross section (D-D') - Fig. 5.7 - has been constructed from the N of the Montbrison-Serre Chevalier sub-area into the S of the Tête Noire-Grand Aréa sub-area, approximately 10 km N of section line (C-C'). The cross section illustrates one major thrust sheet (Champcella

nappe) with a displacement of approximately 4.5 km across its footwall. The underlying thrust sheet has similar geometry to the Roche-Charnière nappe of section (C-C') and is likely to be an along-strike equivalent. Traditionally this lower thrust sheet is included as part of the Champcella nappe. It is suggested here that this now be termed the Roche-Charnière nappe. Minor thrusts with displacements of approximately 800 m occur within the Roche-Charnière nappe in the region to the W of Le Bez - Fig. 5.3.

The major backfold within the Champcella nappe is illustrated in section (D-D'). Growth of this fold has resulted in back-steepening of the more internal, structurally higher thrust sheets, proving that thrusts evolved from E to W within this portion of the Briançonnais Thrust System.

The tectonic shortening suggested by this balanced cross section is 12.7 km, based on a comparison of the present day across strike width of the section (15.3 km) with its restored version (28 km). This value substantiates the shortening estimate of 12.6 km derived from section (C-C') for an equivalent along strike segment of the Briançonnais Thrust System.

The cross sectional geometry of the Briançonnais Zone in the region between Le Bez and Queyrières can be summarised most simply by isolating 3 major fault bounded units; the Roche-Charnière nappe, the Champcella nappe and the structurally highest extensional fault sheet. It is suggested that this major extensional fault has a displacement of approximately 5 km, based on the offset of the backfold structure, assuming an approximately E-W slip direction.

The fault at the base of the sheet which carries the metamorphic écailles intermédiaires klippen of Serre Chevalier and l'Eychauda, slices through underlying fold and thrust structures. It seems likely that these klippen are part of the same fault sheet that is illustrated in

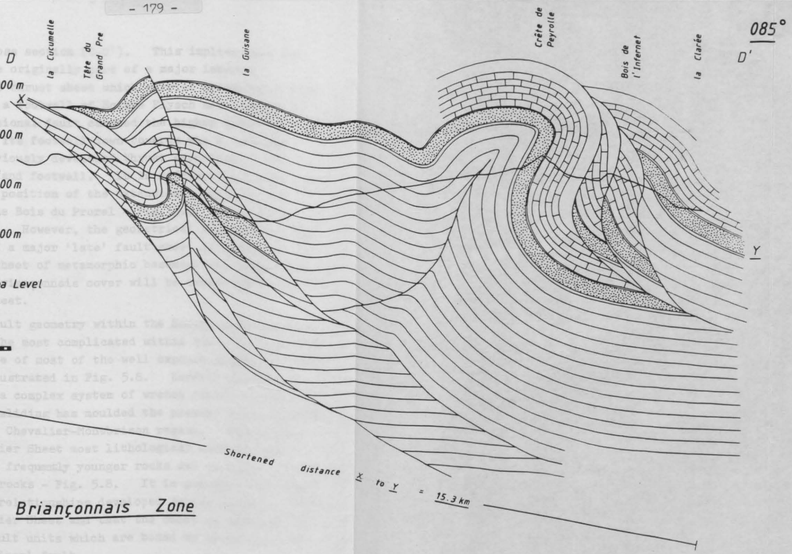

Briançonnais Zone

Balanced Cross Section

Restored Cross Section

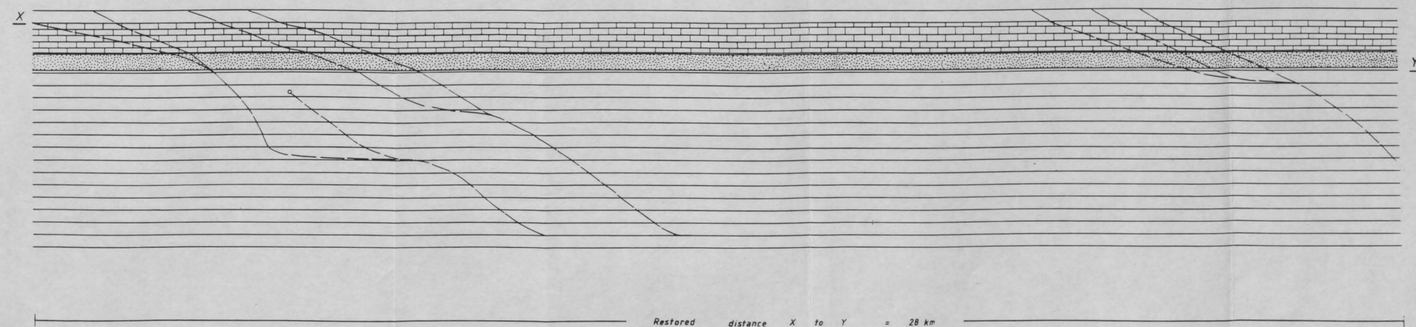

Jurassic to early Tertiary

Trias Carbonates

Trias Quartzites

Verrucano

Houiller

Shortening within Briançonnais Thrust System between X and Y = 28 — 15·3 = 12·7 km

The structural interpretation presented on this cross-section is based field observation at the present topographic level and on subsequent balanced cross-section construction techniques. The assumptions which are required to produce balanced cross-sections are outlined on pages 10, 11 and 12 and local assumptions are discussed in this section of the text.

balanced cross section (C-C'). This implies that the klippen were originally part of a major internal Briançonnais thrust sheet which carried metamorphic basement across a footwall of Eocene Flysch noir, before a later extensional fault carried the higher thrust sheet and part of its footwall down towards the W, slicing through previously developed thrust structures in the hangingwall and footwall. It is difficult to trace the approximate position of the extensional fault in the region of the Bois du Prorel - Fig. 5.3, due to a lack of exposure. However, the geometrical evidence for the existence of a major 'late' fault sheet is strong. This fault sheet of metamorphic basement and underlying imbricated Briançonnais cover will be termed the Serre Chevalier Sheet.

The fault geometry within the Serre Chevalier Sheet is perhaps the most complicated within the study area and the structure of most of the well exposed portion of this sheet is illustrated in Fig. 5.8. Barfety (1968) concluded that a complex system of wrench faults and recent superficial sliding has moulded the present fault geometry of the Serre Chevalier-Montbrison region. Within the Serre Chevalier Sheet most lithological contacts are tectonic and frequently younger rocks are in fault contact above older rocks - Fig. 5.8. It is possible that these geometrical relationships developed during movement of the Serre Chevalier Sheet and that the Sheet is composed of a series of fault units which are bound by splays from the basal extensional fault.

The cross sectional geometry of the Briançonnais Zone in the Tête Noire-Grand Aréa sub-area is now described.

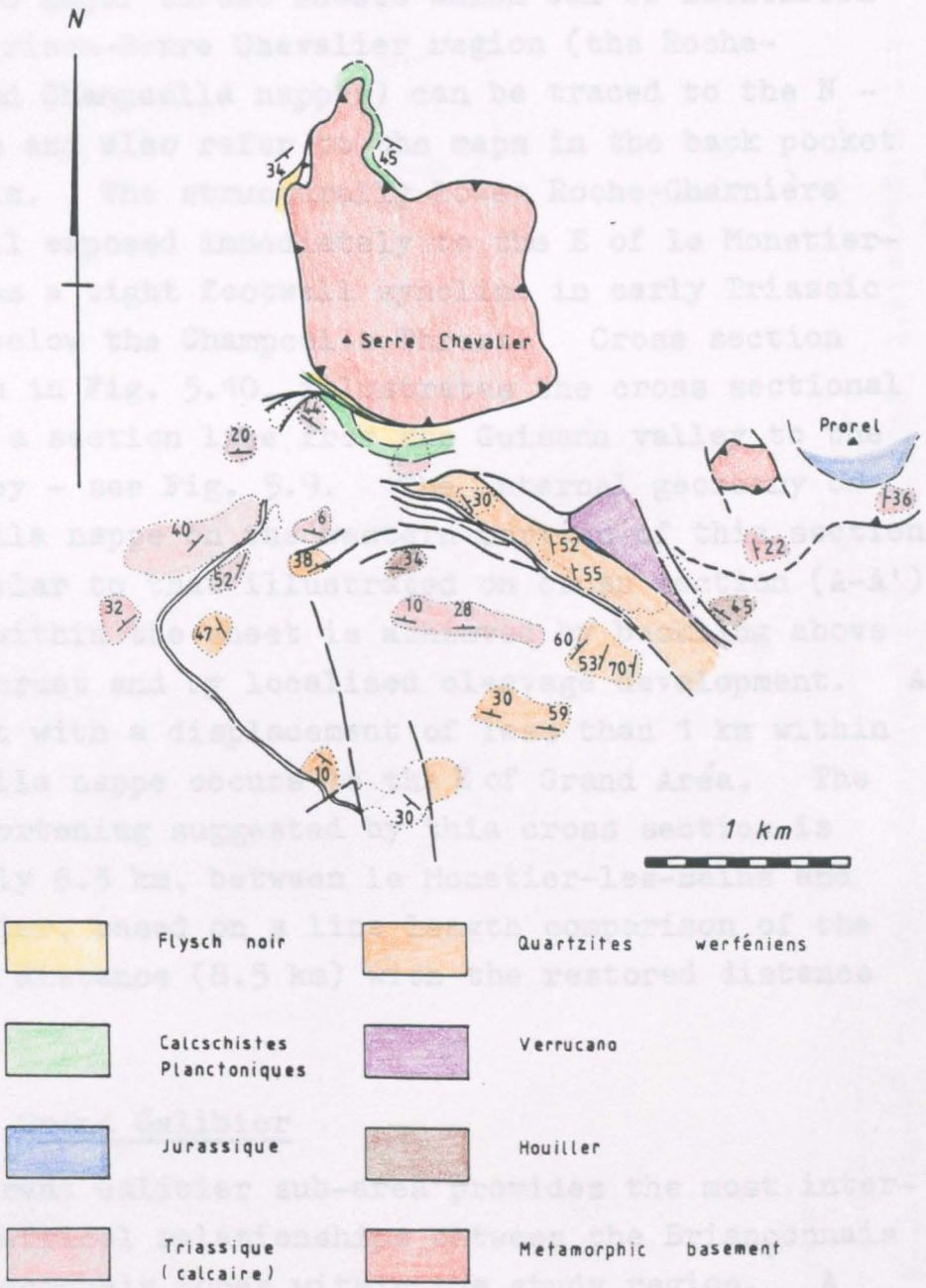

FIG. 5.8 Sketch map of part of the Serre Chevalier Sheet.

(b) Tête Noir-Grand Aréa

The two major thrust sheets which can be identified in the Montbrison-Serre Chevalier region (the Roche-Charnière and Champcella nappes) can be traced to the N - see Fig. 5.9 and also refer to the maps in the back pocket of the thesis. The structurally lower Roche-Charnière nappe is well exposed immediately to the E of le Monetier-les-Bains, as a tight footwall syncline in early Triassic quartzites below the Champcella Thrust. Cross section (E-E') shown in Fig. 5.10, illustrates the cross sectional geometry on a section line from the Guisane valley to the Clarée valley - see Fig. 5.9. The internal geometry of the Champcella nappe on the western portion of this section line is similar to that illustrated on cross section (A-A'); shortening within the sheet is achieved by buckling above the floor thrust and by localised cleavage development. A minor thrust with a displacement of less than 1 km within the Champcella nappe occurs to the E of Grand Aréa. The tectonic shortening suggested by this cross section is approximately 6.3 km, between le Monetier-les-Bains and Roche Gauthier, based on a line length comparison of the present day distance (8.5 km) with the restored distance (14.8 km).

(c) Grand Galibier

The Grand Galibier sub-area provides the most interesting geometrical relationships between the Briançonnais and Subbriançonnais Zones within the study region. A geological sketch map of this area is shown in Fig. 5.11. The Roche-Charnière and Champcella nappes are continuous from the S into this sub-area; traditionally these nappe names are reserved for the thrust sheets in the vicinity of Montbrison and Serre Chevalier, however, it is useful to extend this nomenclature to the N to emphasise the continuity of individual thrust sheets. Localised imbricate systems can be mapped out in the footwall to the Champcella Thrust which cut through the inverted limb of the

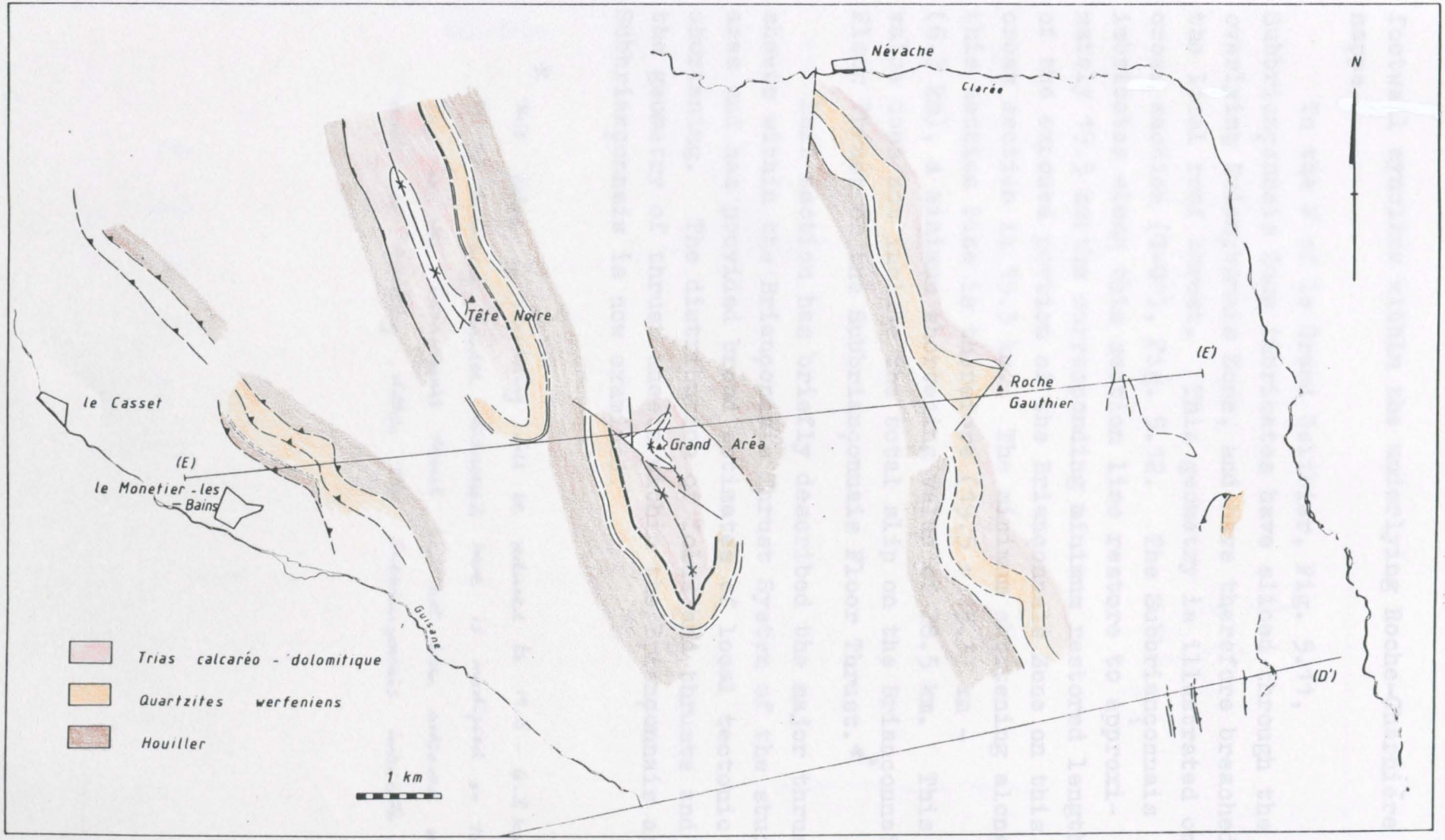

FIG. 5.9 Geological sketch map of the Tête Noire-Grand Aréa sub-area, illustrating lines of section.

footwall syncline within the underlying Roche-Charnière nappe.

To the W of le Grand Galibier, Fig. 5.11, Subbriançonnais Zone imbricates have sliced through the overlying Briançonnais Zone, and have therefore breached the local roof thrust. This geometry is illustrated on cross section (G-G'), Fig. 5.12. The Subbriançonnais imbricates along this section line restore to approximately 19.5 km; the corresponding minimum restored length of the exposed portion of the Briançonnais Zone on this cross section is 15.3 km. The minimum shortening along this section line is therefore (19.5 + 15.3) km - (6.3 km), a minimum shortening value of 28.5 km. This value does not include the total slip on the Briançonnais Floor Thrust or the Subbriançonnais Floor Thrust.*

This section has briefly described the major thrust sheets within the Briançonnais Thrust System of the study area and has provided broad estimates of local tectonic shortening. The distribution of folds and thrusts and the geometry of thrust sheets within the Briançonnais and Subbriançonnais is now examined.

* This value of shortening will be reduced to 19.5 - 6.3 km = 13.2 km if the breaching-model discussed here is modified so that total slip on the Briançonnais thrust had not been achieved at the onset of thrusting within the Subbriançonnais imbricate system.

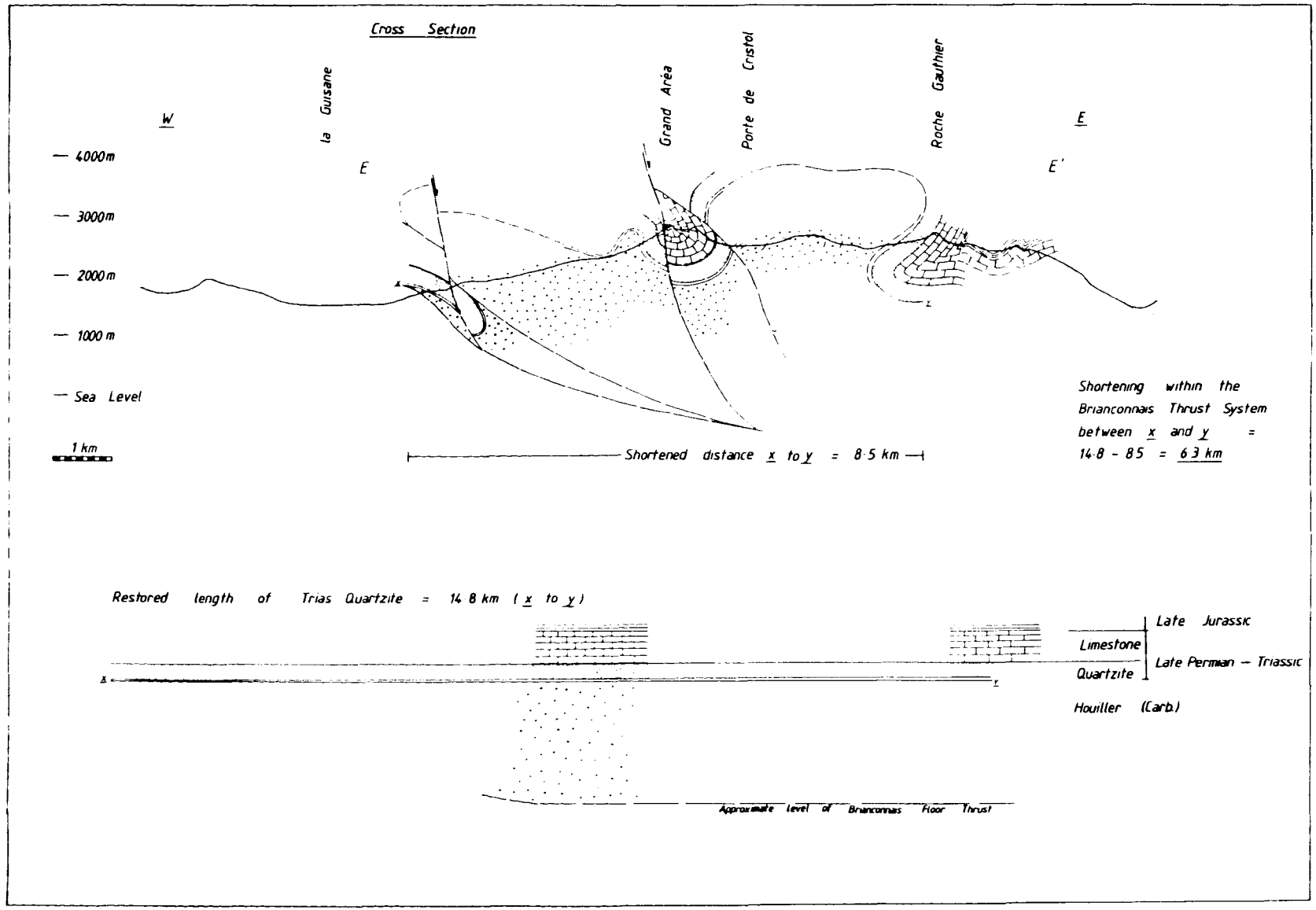

FIG. 5.10 Cross section (E-E') between the Guisane valley and Clarée valley.

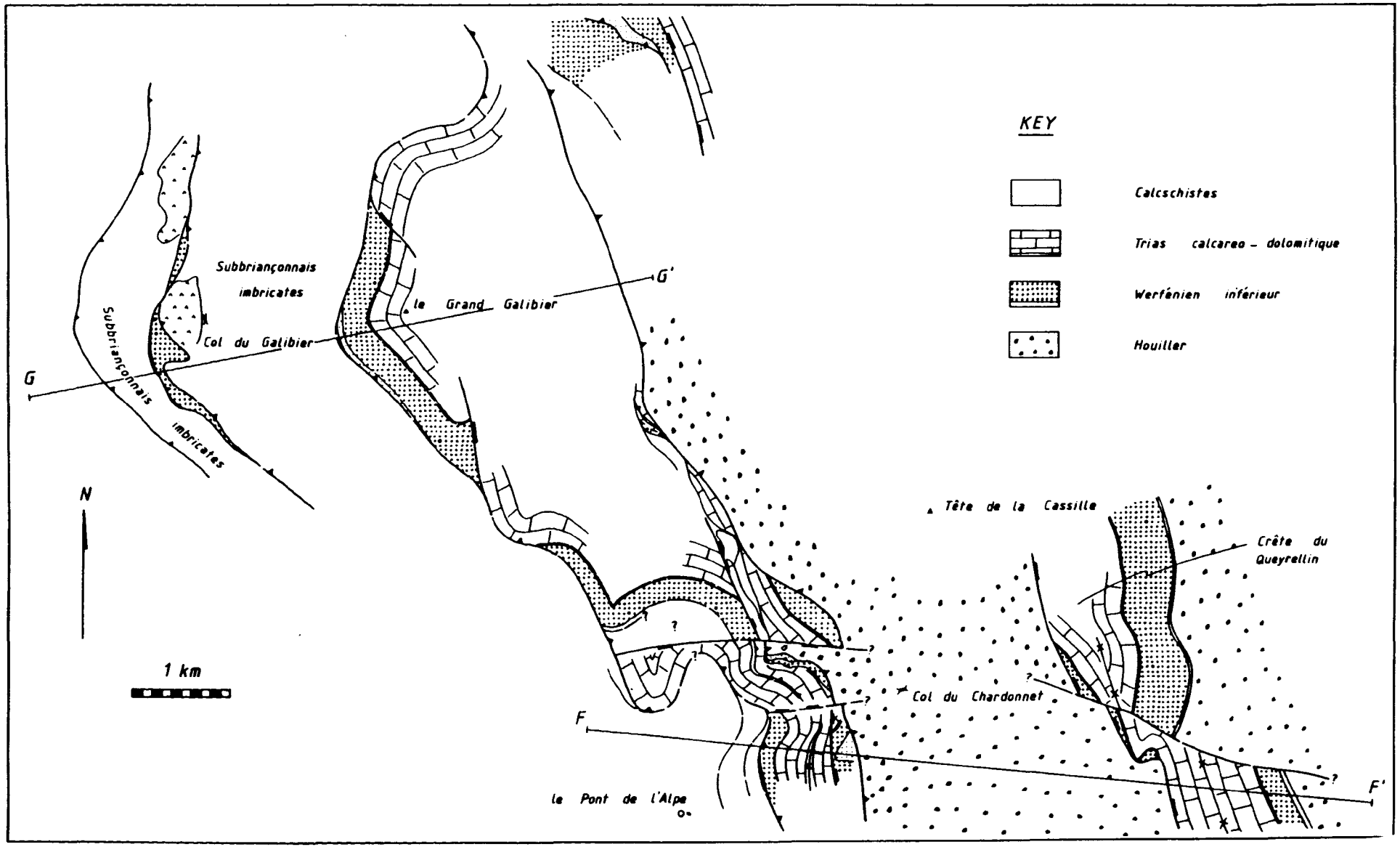

FIG. 5.11 Geological sketch map of the Grand Galibier sub-area, illustrating lines of section.

BALANCED CROSS SECTION

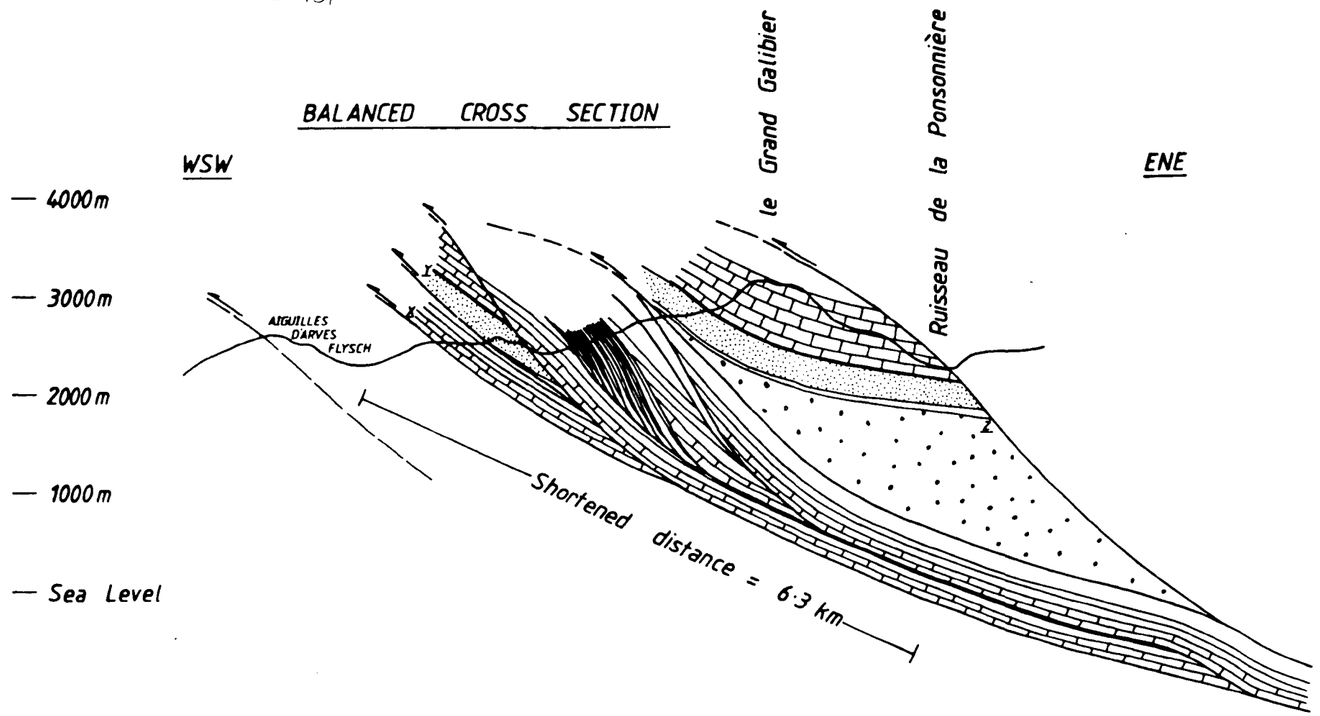

Subbrianconnais stratigraphy

Brianconnais stratigraphy

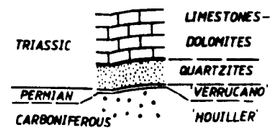

The structural interpretation presented on this cross-section is based on field observation at the present topographic level and on subsequent balanced cross-section construction techniques. The assumptions which are required to produce balanced cross-sections are outlined on pages 10, 11 and 12, and local assumptions are described in this section of the text.

Shortening between x and z =

(19·5 + 15·3) minimum − 6·3 = 28·5 km (min.)

This value does not include the total slip on the Brianconnais floor thrust

Subbrianconnais Thrust System : Restored section

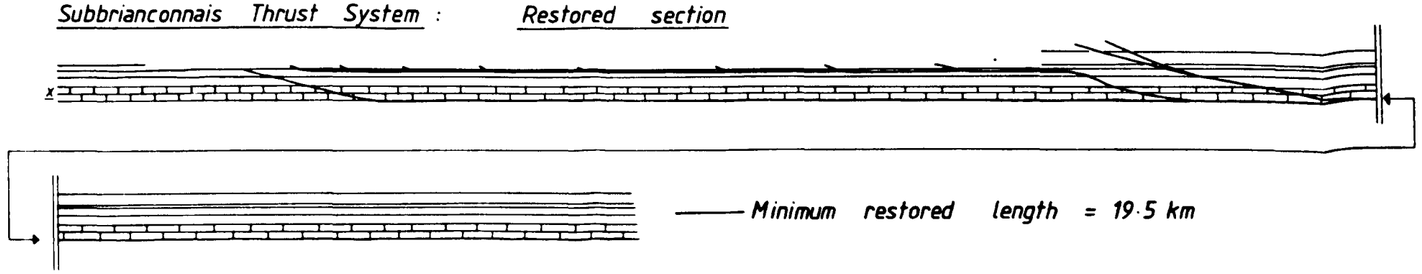

Brianconnais Thrust System : Restored section

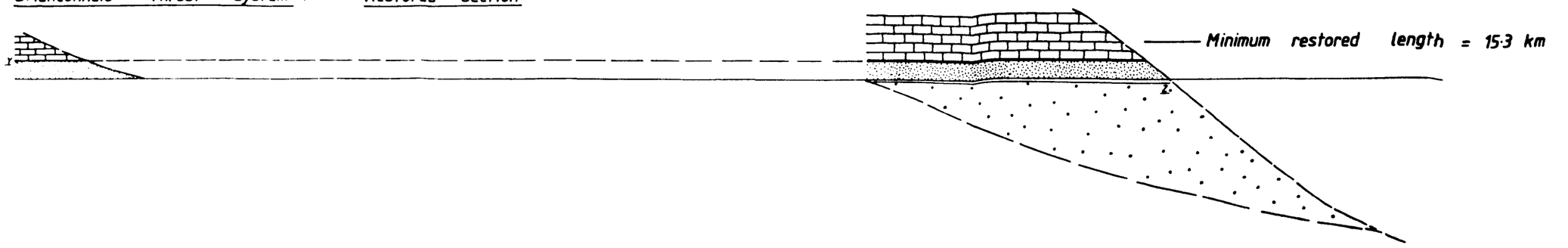

(iii) Thrust sheet geometry and the distribution of folds and thrusts

The contrast in scale and geometry of the Briançonnais Thrust System with the Beinn Eighe Imbricate Fan (described in Chapter 2) is clear; constrained measurement of ramp angles and the 3 dimensional geometry of individual thrust sheets is not possible within this region of the Briançonnais. The bulk of the area comprises one thrust sheet (the Champcella nappe) within the Briançonnais Thrust System, a study of thrust geometry must therefore be limited to a description of the relatively small scale footwall imbricates to the Champcella Thrust and to the stratigraphic level of the hangingwall and footwall to the Roche-Charnière and Champcella Thrusts. The geometry of folds within the Champcella nappe and in the footwall to the Champcella Thrust, and the geometry of normal faults and wrench faults within the thrust sheets are now examined.

(a) Montbrison-Serre Chevalier

The proposed evolutionary sequence of folding and faulting for this sub-area has been discussed in section 5.1 (ii). The geometry of folds immediately above and below the Champcella Thrust in the region of St. Martin-de-Queyrières is now examined in more detail and a geological map is shown in Fig. 5.13.

The Champcella Thrust can be traced from near to Croix de la Salcette towards the N for approximately 1 km into the Torrent de Combe Brune, the trace of the thrust then curves around to the SE towards la Blétonnée, before trending N-S into the Bois de Bouchier. This outcrop pattern results from folding of the Champcella nappe after slip on the Champcella Thrust. The geometry of this fold suggests that it has developed from sticking on the Roche-Charnière Thrust rather than late folding of the complete nappe assemblage. The fold plunges to the NNW at approximately 30°, and cannot be traced for more than 2.5 km towards the NNW within the Champcella nappe. This may be partly due

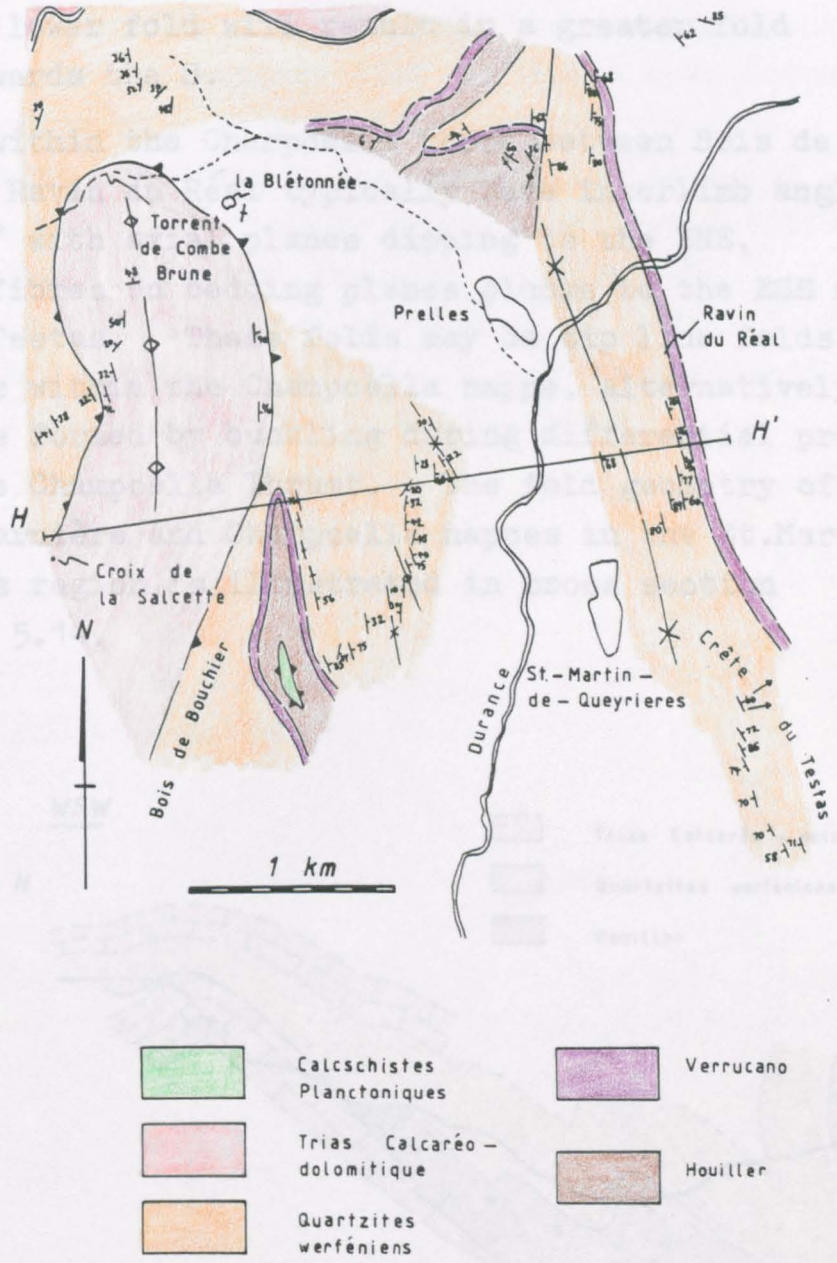

FIG. 5.13 Geological map of the St. Martin-de-Queyrières region.

to the Champcella Thrust cutting up stratigraphic section in its footwall from NNE to SSW and hence growth of a structurally lower fold will result in a greater fold amplitude towards the S.

Folds within the Champcella nappe between Bois de Bouchier and Ravin du Réal typically have interlimb angles of 45° to 70° with axial planes dipping to the ENE, slickenside fibres on bedding planes plunge to the ESE near to Crête du Testas. These folds may be tip line folds to blind thrusts within the Champcella nappe, alternatively they may have formed by buckling during differential propagation of the Champcella Thrust. The fold geometry of the Roche-Charnière and Champcella nappes in the St.Martin-de-Queyrières region is illustrated in cross section (H-H'), Fig. 5.14.

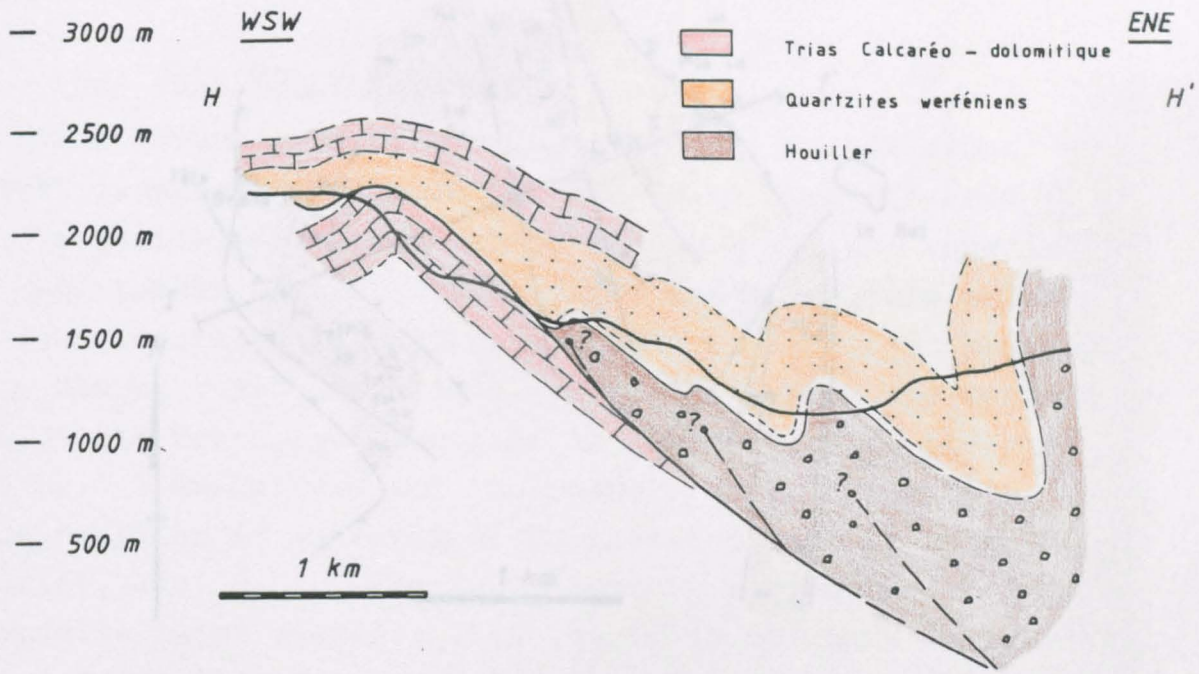

FIG. 5.14 Cross section (H-H'), illustrating fold geometry within the Roche-Charnière and Champcella nappes in the region of St.Martin-de-Queyrières.

To the N of Serre Chevalier, in the region between Tête du Grand Pré and le Bez (see the geological map of Fig. 5.15), the geometry of folds and thrusts within the Roche-Charnière nappe suggests that the folds have formed following sticking at a ramp or floor thrust tip line. Subsequent thrust propagation has resulted in slip and formation of a footwall syncline and a hangingwall anticline. The cross sectional geometry on a WSW-ENE section line is shown in cross section (I-I'), Fig. 5.16. An axial planar, NNW-SSE trending cleavage is developed within the middle to late Triassic carbonates.

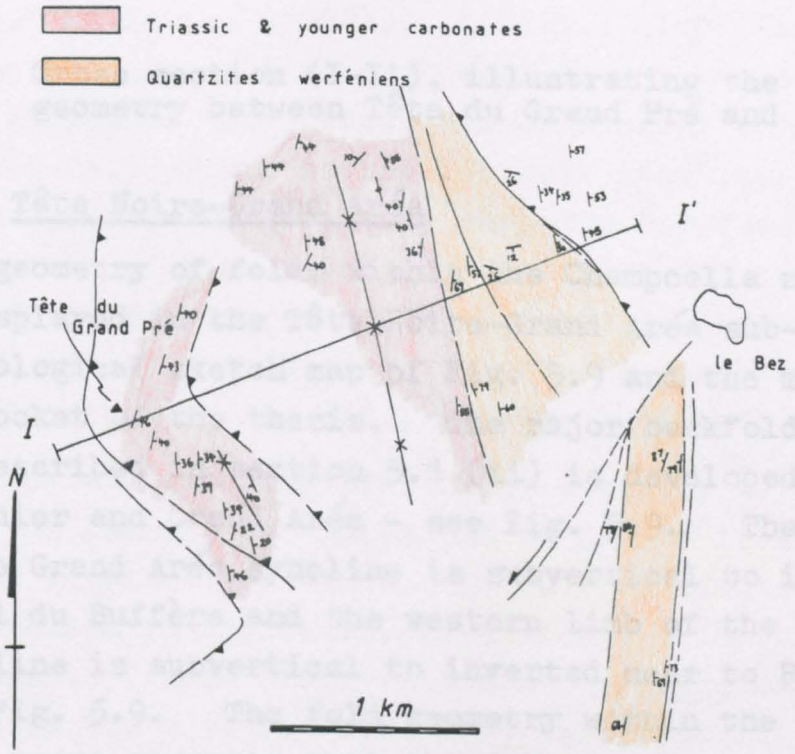

FIG. 5.15 Geological map of the Tête du Grand Pré - le Bez region.

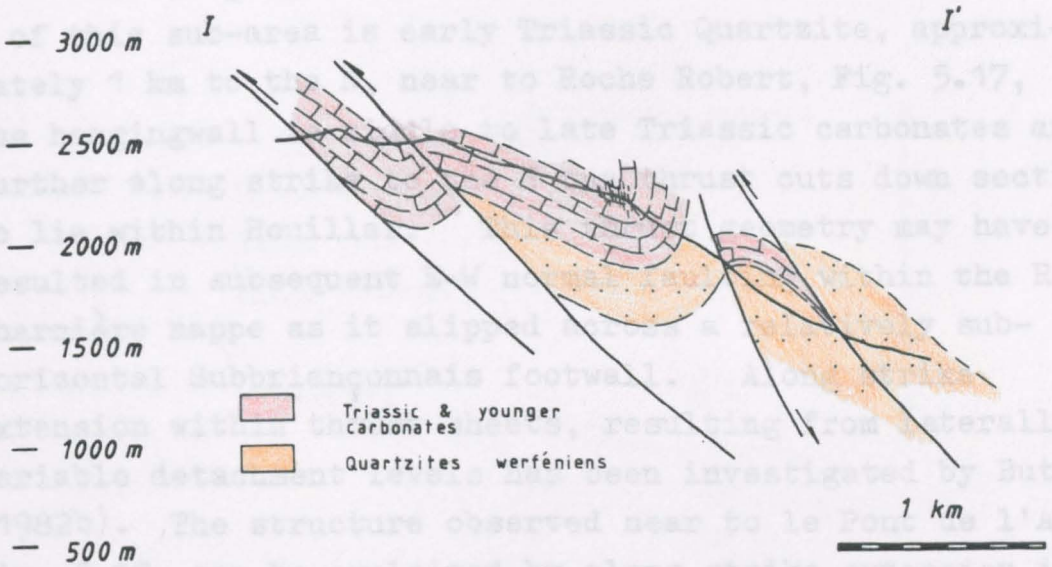

FIG. 5.16 Cross section (I-I'), illustrating the fold geometry between Tête du Grand Pré and le Bez.

(b) Tête Noire-Grand Aréa

The geometry of folds within the Champcella nappe is best displayed in the Tête Noire-Grand Aréa sub-area - see the geological sketch map of Fig. 5.9 and the maps in the back pocket of the thesis. The major backfold which has been described in section 5.1 (ii) is developed between Roche Gauthier and Grand Aréa - see Fig. 5.9. The western limb of the Grand Aréa syncline is subvertical to inverted near to Col du Buffère and the western limb of the Tête Noire syncline is subvertical to inverted near to Roche du Monêtier, Fig. 5.9. The fold geometry within the Champcella nappe suggests that the folds may have evolved by a systematic sequence of tip line fold development to foreland directed thrusts and backthrusts.

To the E of le Monêtier-les-Bains, a footwall syncline to the Champcella Thrust exists within early Triassic quartzites of the Roche-Charnière nappe; this is continuous along strike to the N into the Grand Galibier sub-area.

(c) Grand Galibier

The hangingwall to the Roche-Charnière Thrust in the S of this sub-area is early Triassic Quartzite, approximately 1 km to the N, near to Roche Robert, Fig. 5.17, the hangingwall is middle to late Triassic carbonates and further along strike to the N the thrust cuts down section to lie within Houiller. This thrust geometry may have resulted in subsequent E-W normal faulting within the Roche-Charnière nappe as it slipped across a relatively sub-horizontal Subbriançonnais footwall. Along strike extension within thrust sheets, resulting from laterally variable detachment levels has been investigated by Butler (1982b). The structure observed near to le Pont de l'Alpe, Fig. 5.17, can be explained by along strike extension in the form of normal faulting - similar to the 'hangingwall drop faults' of Butler (1982b). A highly simplified sketch of the proposed sequence of faulting in this region is presented in Fig. 5.18. These normal faults, or drop faults, post-date growth of the footwall syncline to the Champcella Thrust; this further supports the view that they developed after slip on the Roche-Charnière Thrust. Minor footwall imbricate thrusts to the Champcella Thrust slice through the inverted limb of this footwall syncline between Col de la Ponsonnière and l'Aiguillette du Lauzet, Fig. 5.17.

An indication of the pre-thrust geometry of the Roche-Charnière and Champcella nappes can be gained from an estimate of displacement on Mesozoic normal faults which have been folded during development of the Briançonnais Thrust System. These early extensional faults can be mapped out to the W of le Grand Lac, on l'Aiguillette du Lauzet, Fig. 5.17, and on the western flank of Crête du Queyrellin, Fig. 5.11. The displacements suggested by a restoration of cross section (F-F'), Fig. 5.19, are between 200 m and 1 km on the major extensional faults of l'Aiguillette du Lauzet and Crête du Queyrellin, down-throwing to the E.

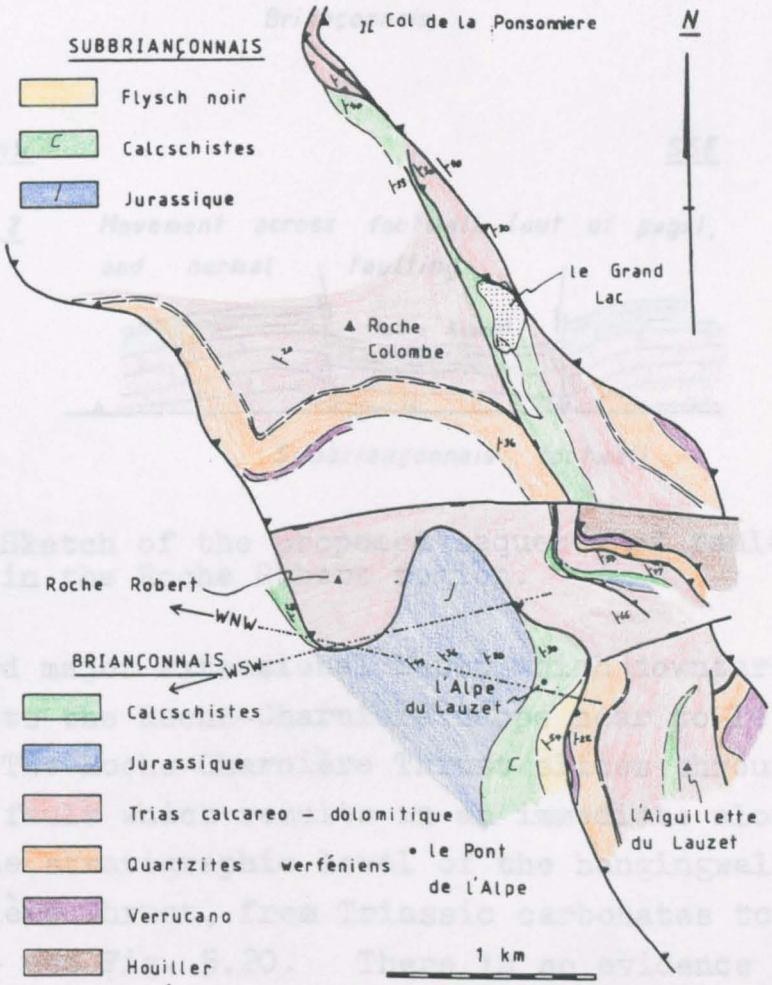

FIG. 5.17 Geological map of le Pont de l'Alpe region.

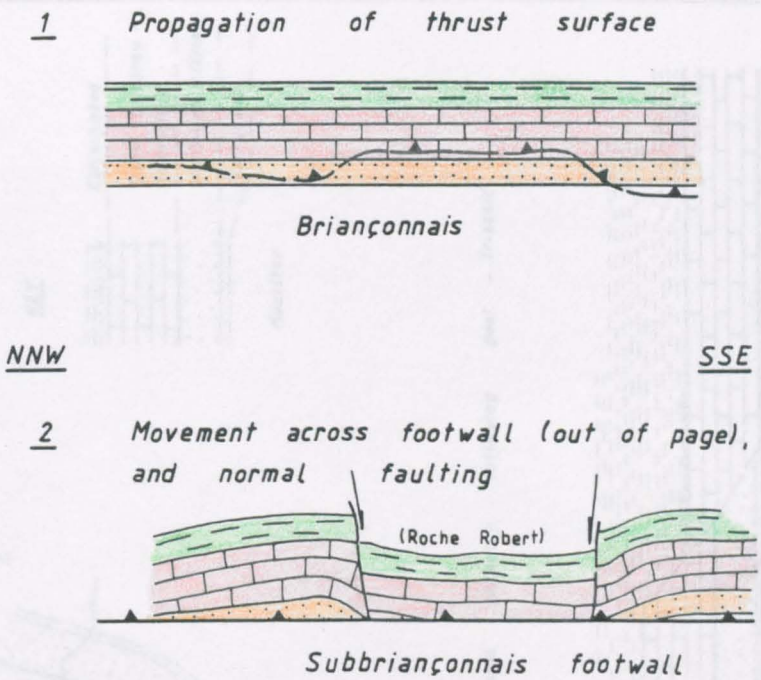

FIG. 5.18 Sketch of the proposed sequence of faulting in the Roche Robert region.

A third major extensional fault which downthrows to the E, affects the Roche-Charnière nappe near to le Grand Galibier. The Roche-Charnière Thrust slices through this extensional fault which results in an immediate along strike change in the stratigraphic level of the hangingwall to the Roche-Charnière Thrust, from Triassic carbonates to quartzites - see Fig. 5.20. There is no evidence that pre-thrust extensional faults within the Briançonnais Zone have been utilised as thrusts during the evolution of the Briançonnais Thrust System.

Approximately 3 km to the NE of le Grand Galibier, an imbricate system within early Triassic quartzites occurs within the Champcella nappe, this imbricate system is overlain by a major imbricate thrust which carries Verrucano rocks over quartzites to the W of Col des Rochilles, Fig. 5.20. Slickenside fibres on bedding surfaces within the quartzite imbricates plunge to the ESE, the implications of observed fold trends; slip direction indicators and thrust surface geometry are discussed in terms of movement directions in Chapter 6.

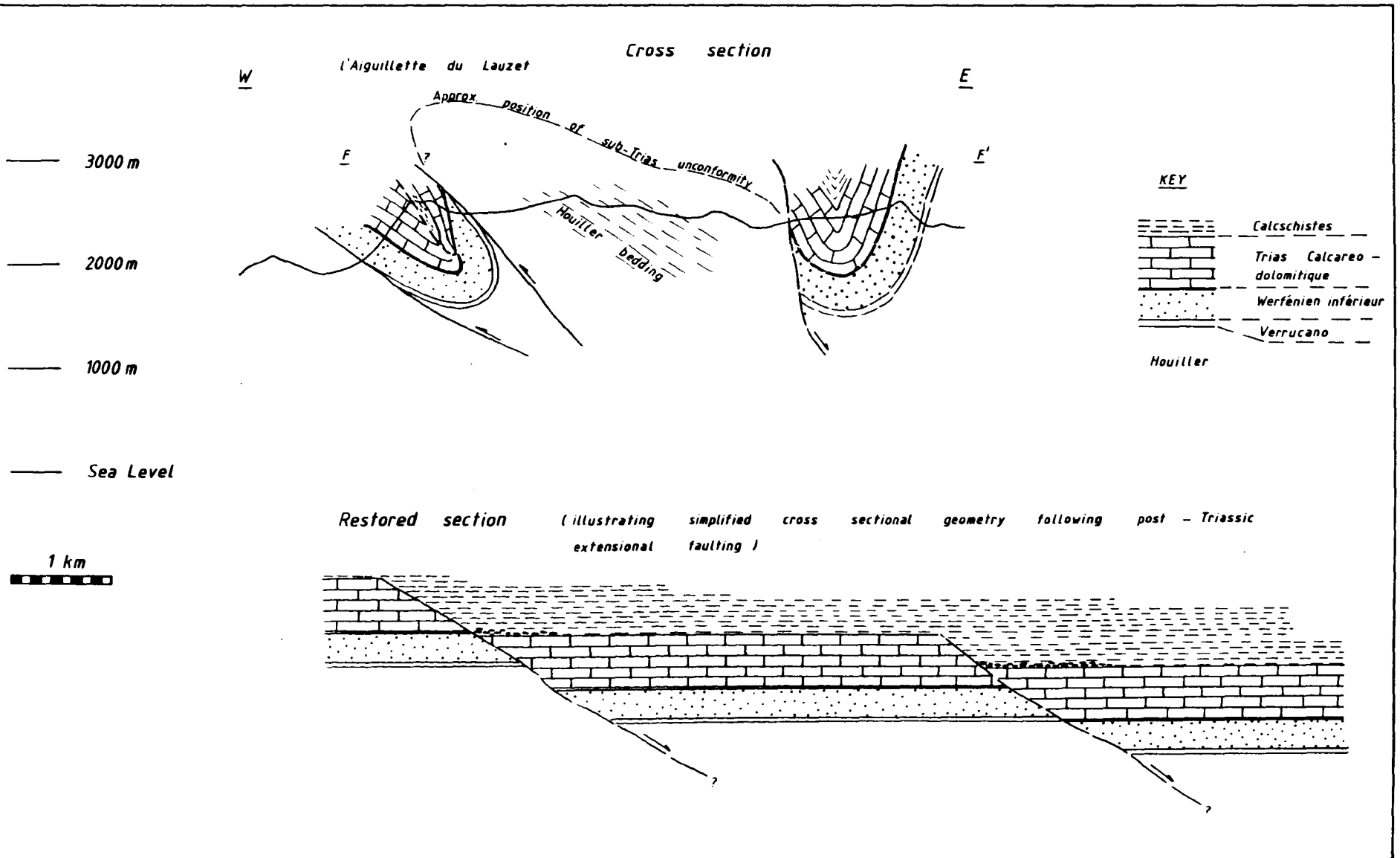

FIG. 5.19 Cross section (F-F'), restored section illustrating simplified pre-thrust geometry.

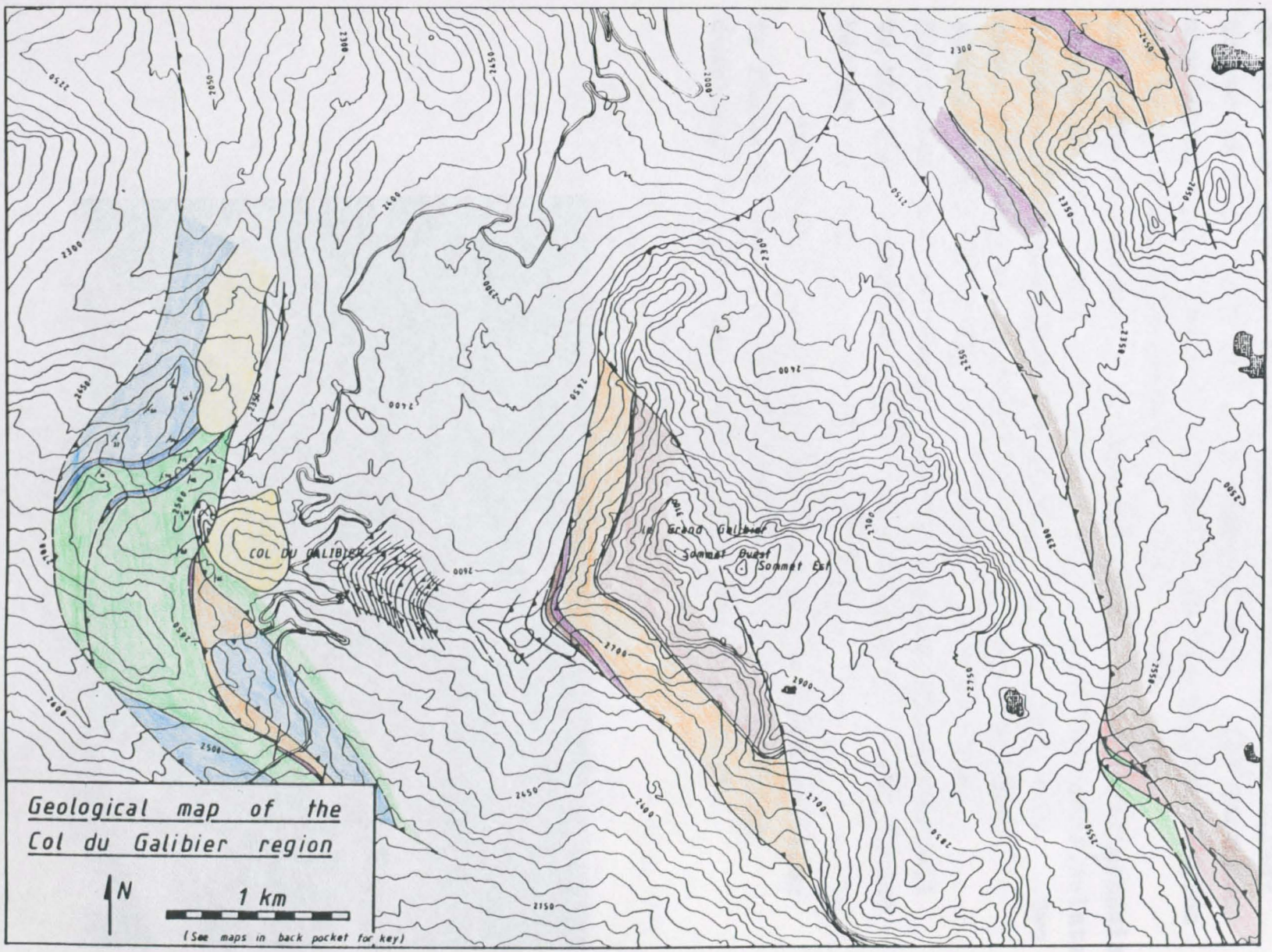

FIG. 5.20 Geological map of the Col du Galibier region.

(d) Thrust sheets and folds within the Subbriançonnais Zone

The structure of the Subbriançonnais Zone in the Col du Galibier area and the le Pont de l'Alpe area is illustrated in Figs. 5.20 and 5.17 respectively. The tectonic shortening and sequence of thrusting in the Galibier region has been outlined in section 5.1 (ii). Two major imbricate slices can be mapped out within the Subbriançonnais Thrust System to the W of Col du Galibier, within middle-late Jurassic and Cretaceous-Tertiary sediments, Fig. 5.20. Two minor imbricate slices occur structurally above this, approximately 500 m WNW of the Col. A third major Subbriançonnais imbricate slice occurs in the hangingwall to the thrust which breaches the Briançonnais Floor Thrust between la Mandette and Col du Galibier.

The thrust assemblage to the W of le Grand Galibier is flexured and pierced as a result of post-thrusting diapirism by Subbriançonnais evaporites, Fig. 5.21.

FIG. 5.21 Flexuring of the thrust assemblage in the Col du Galibier region by diapirism of Subbriançonnais evaporites.

The large amount of shortening (approximately 16 km) represented by the Subbriançonnais imbricates in the Galibier region must be transferred along strike to the S onto the Subbriançonnais Floor Thrust rather than up onto the Briançonnais Floor Thrust, as there is no evidence for large scale differential movement within the Briançonnais Thrust System.

In the le Pont de l'Alpe area, Fig. 5.17, the exposed portion of the Subbriançonnais Zone consists of one imbricate slice which is folded into an anticline to the W of Roche Robert. This may be a hangingwall anticline to a structurally lower thrust, *but* , no thrust surface is exposed due to drift cover. The outcrop pattern of the Briançonnais Floor Thrust (Roche-Charnière Thrust) relative to the Subbriançonnais lithologies provides strong evidence for a movement direction towards the WSW - (265°), any movement direction further around towards the N would involve the Roche-Charnière thrust cutting down stratigraphic section in the footwall. This WSW direction is illustrated in Fig. 5.17 as a line which joins the cut-offs of the calcschistes planctoniques against the Roche-Charnière Thrust in the Roche Robert and l'Alpe du Lauzet areas. A WNW movement direction would involve cutting down section in the footwall from Eocene flysch to Jurassic limestones over a distance of 1 km, this alternative is also illustrated in Fig. 5.17.

Three laterally persistent thrust sheets can be mapped out within the Subbriançonnais Zone between Le Casset and Roche Gauthier, Fig. 5.22. Occasional outcrops of Triassic evaporites in the hangingwall suggest the floor thrust to the Subbriançonnais Thrust System lies at the basement/evaporite interface. No lithological cut-offs can be mapped out between these three thrust sheets and the implied shortening is therefore large, as the thrust surfaces must be at a low angle to bedding. No large scale folds are exposed in the footwall or hangingwall to these 3 Subbriançonnais thrusts within this area.

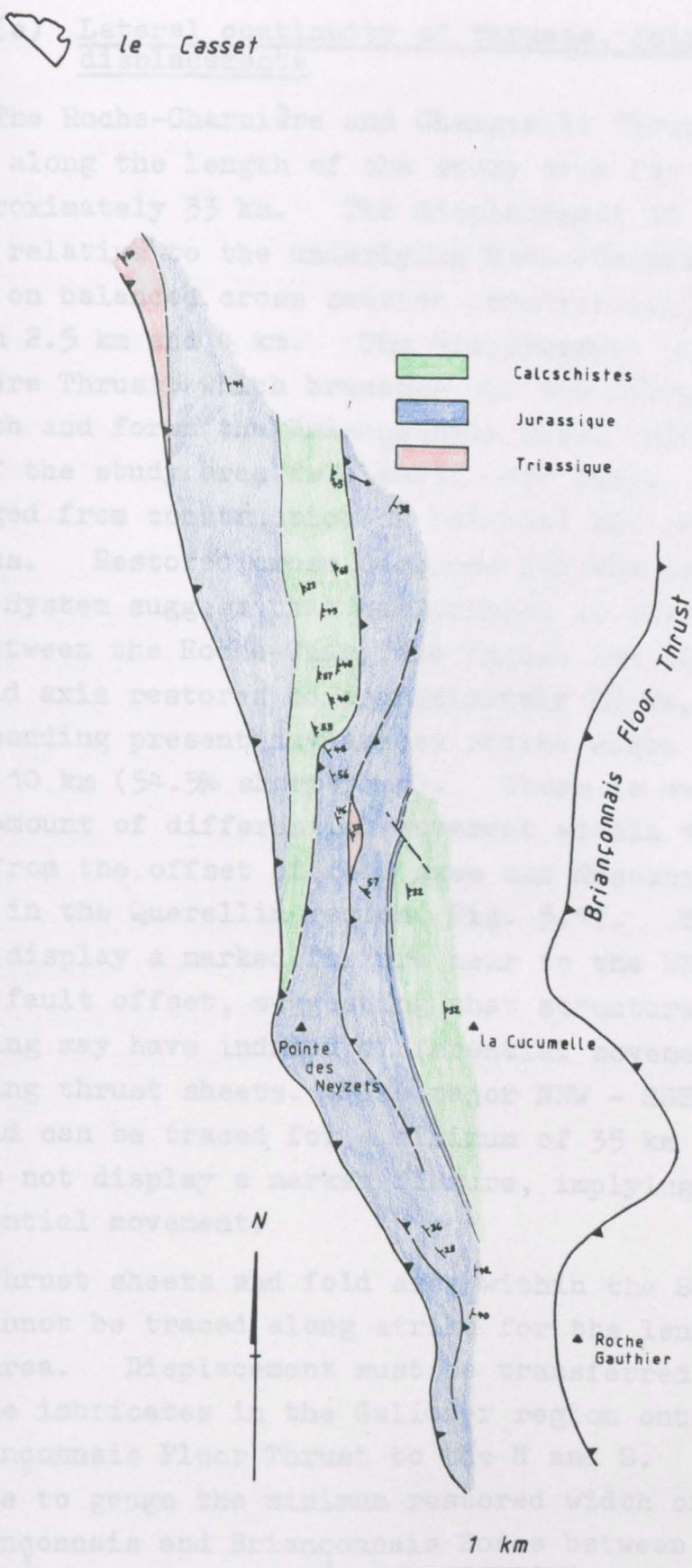

FIG. 5.22 Geological map of the Subbriançonnais Zone between Le Casset and Roche Gauthier.

(e) Lateral continuity of thrusts, folds and displacements

The Roche-Charnière and Champcella Thrusts can be traced along the length of the study area for a distance of approximately 33 km. The displacement of the Champcella Thrust relative to the underlying Roche-Charnière nappe (based on balanced cross section construction) varies between 2.5 km and 4 km. The displacement on the Roche-Charnière Thrust, which branches off the Champcella Thrust at depth and forms the Briançonnais Floor Thrust for the bulk of the study area is clearly very large, and cannot be gauged from construction of balanced and restored cross sections. Restored cross sections for the Briançonnais Thrust System suggest that the portion of the Briançonnais Zone between the Roche-Charnière Thrust and the major backfold axis restores to approximately 22 km, from a corresponding present day across strike width of approximately 10 km (54.5% shortening). There is evidence for a small amount of differential movement within the Champcella nappe from the offset of fold axes and Mesozoic normal faults in the Querellin region, Fig. 5.11. The fold axes do not display a marked flexure near to the WNW - ESE wrench fault offset, suggesting that structurally lower thrusting may have induced differential movement within overlying thrust sheets. The major NNW - SSE trending backfold can be traced for a minimum of 35 km along strike; it does not display a marked flexure, implying little differential movement.

Thrust sheets and fold axes within the Subbriançonnais Zone cannot be traced along strike for the length of the study area. Displacement must be transferred along strike from the imbricates in the Galibier region onto the Subbriançonnais Floor Thrust to the N and S. It is now possible to gauge the minimum restored width of the Subbriançonnais and Briançonnais Zones between Col du Galibier and the backfold axis by sequentially removing the shortening:

1. The Briançonnais Zone between Y and Z, Fig. 5.23, restores to approximately 22 km from Y.

2. The Subbriançonnais imbricates between X and Y, Fig. 5.23, restore to approximately 16 km from X, thereby restoring the overlying Briançonnais a further 16 km to the ENE.

3. The Briançonnais at position W, Fig. 5.23, has to restore back across the entire Subbriançonnais succession for a minimum distance of 16 km from W, thereby restoring the entire Briançonnais a further 16 km to the ENE.

This implies that the minimum restored across strike width of the Subbriançonnais and Briançonnais Zones in the Galibier region is (22 + 16 + 16) km = 54 km, the present across strike width is approximately 15 km, the minimum shortening is therefore (54 - 15) km = 39 km. No account has been made of the displacement on the Subbriançonnais and Briançonnais Floor Thrusts. It has been assumed for the purposes of balanced cross section construction and restoration that the movement direction was towards 265° (subperpendicular to fold axes and thrust trends within the Subbriançonnais and Briançonnais Thrust Systems), and suggested by the cut-off relationships in the le Pont de l'Alpe area.

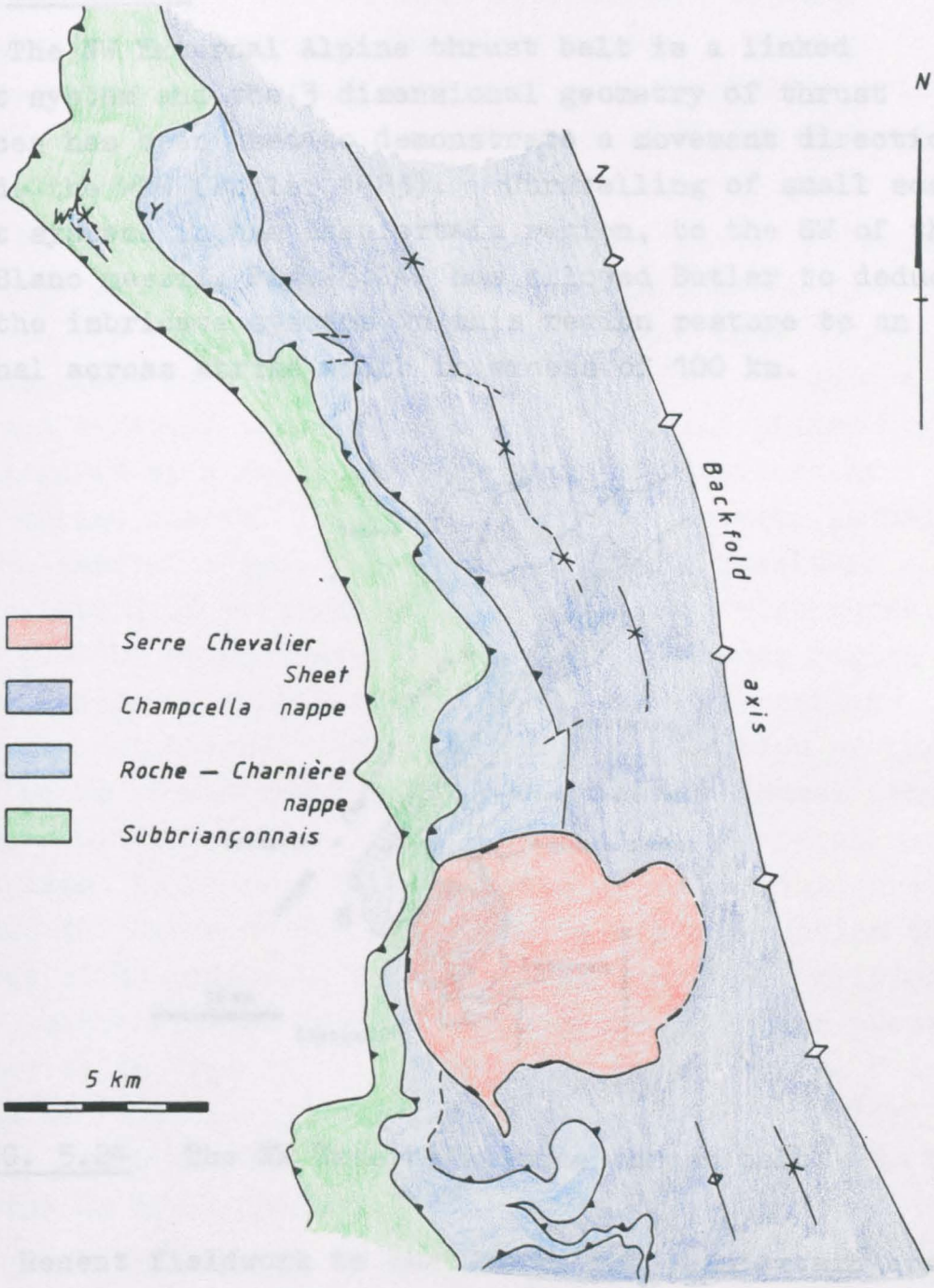

FIG. 5.23 Thrust continuity for the Subbriançonnais and Briançonnais Thrust Systems.

5.2 EXTERNAL ZONES

(i) Movement direction, thrust geometry and tectonic shortening

The NW External Alpine thrust belt is a linked thrust system and the 3 dimensional geometry of thrust surfaces has been used to demonstrate a movement direction towards the WNW (Butler 1983). Unravelling of small scale thrust systems in the Beaufortain region, to the SW of the Mont Blanc massif, Fig. 5.24, has allowed Butler to deduce that the imbricate systems in this region restore to an original across strike width in excess of 100 km.

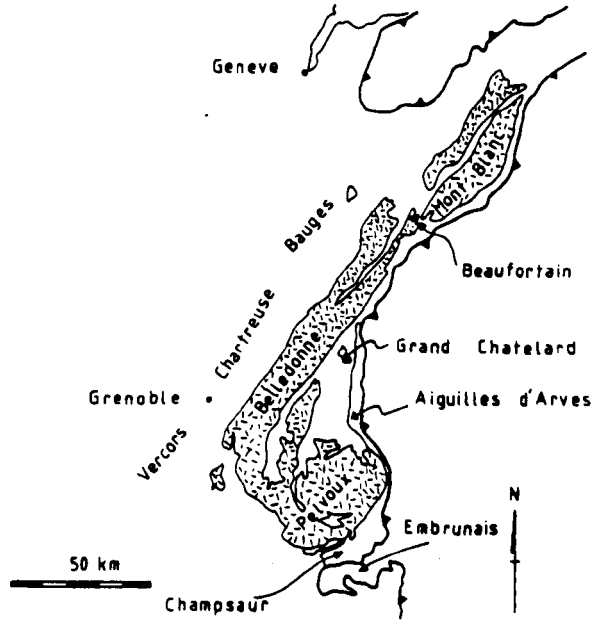

FIG. 5.24 The NW External Alpine thrust belt.

Recent fieldwork to the SSW of the Beaufortain area (Parish, pers. comm.) has demonstrated that the major detachment surfaces which have been identified by Butler can be traced along strike towards the SSW where they form the bounding surfaces to more localised smaller scale imbricate systems within the crystalline basement and Mesozoic cover. Although Parish is not able to demonstrate an independently calculated shortening value in excess of 100 km for the

External Zones in the Grand Chatelard region, Fig. 5.24, the total displacement must be broadly conserved along strike from Beaufortain towards the SSW, as there is no evidence for major differential displacement between Beaufortain and the Grand Chatelard region. Thrust surfaces within the Grand Chatelard area generally strike SSW-NNE and the 3 dimensional geometry of thrust systems suggests movement towards the WNW.

To the S of the region being investigated by Parish, the trend of thrust surfaces changes from SSW-ENE to NW-SE in the region of NE Pelvoux, and then back to a SSW-ENE trend in SE Pelvoux - see Fig. 5.24. Within a foreland directed thrust system, structurally higher horses are flexured as a result of accretion of structurally lower thrust sheets. If thrust surfaces develop as major oblique-lateral ramps, subsequent slip will result in reorientation of overlying thrust sheets and structures. Beach (1981b) demonstrated that in the N Pelvoux region thrusts climb laterally towards the N from crystalline basement into Mesozoic cover rocks. Restoration of the cover rocks within the E part of the External Zones (the Ultradauphinois Zone) reveals a shortening of approximately 70 km based on an area balance assuming an initial stratigraphic thickness of 500 m. Despite his observation that thrusts climb laterally from basement into the overlying cover, Beach (1981d) deduced a transport direction perpendicular to the strike of the thrusts, which for the bulk of the NE Pelvoux region suggests a movement direction towards the SW. The geometry of the thrust sheets to the E of the La Meije Thrust, Fig. 5.25, is now discussed.

The structurally highest thrust which carries crystalline basement over early Jurassic cover rocks is the Combeynot Thrust, Fig. 5.25. To the NW and SE of the Combeynot Massif this thrust cuts up section from crystalline basement into the overlying unconformable cover succession of Eocene shales and turbidites. The complete outcrop trace of the Combeynot Thrust is illustrated more

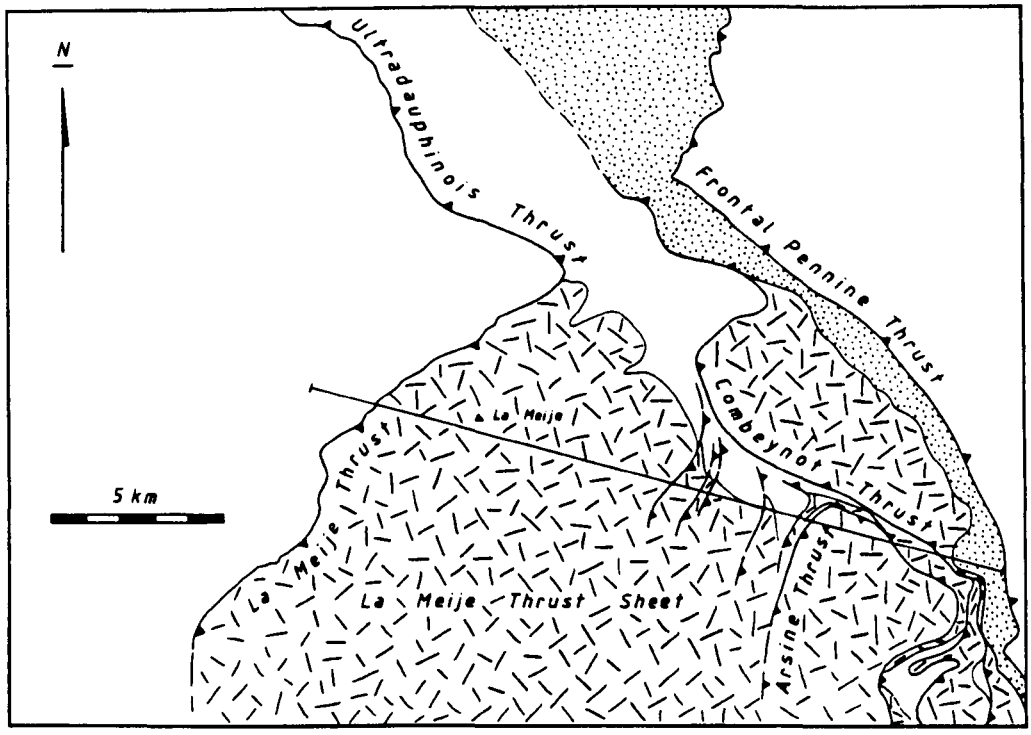

FIG. 5.25 Sketch map of thrust sheets in the NE Pelvoux region.

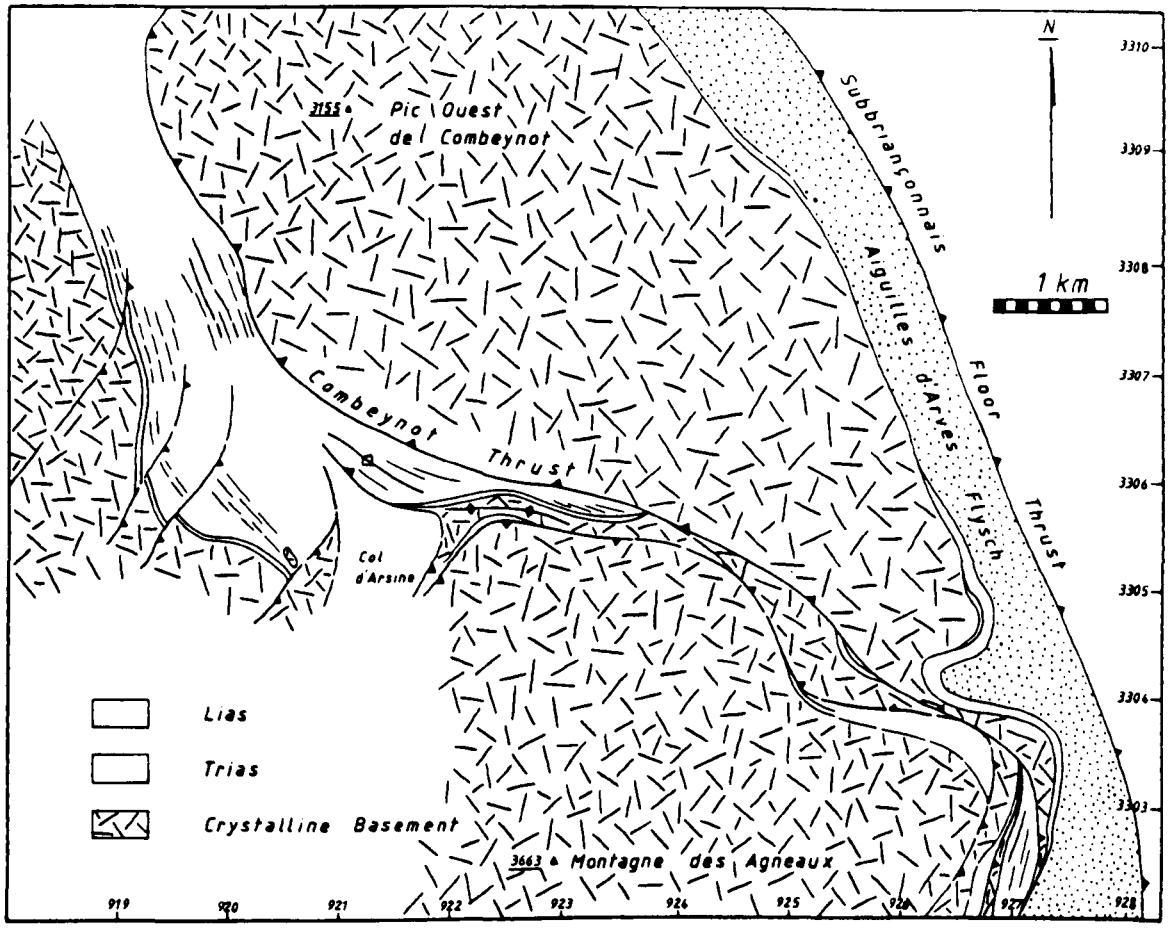

FIG. 5.26 Sketch map of the Combeynot Thrust in the N of the study area.

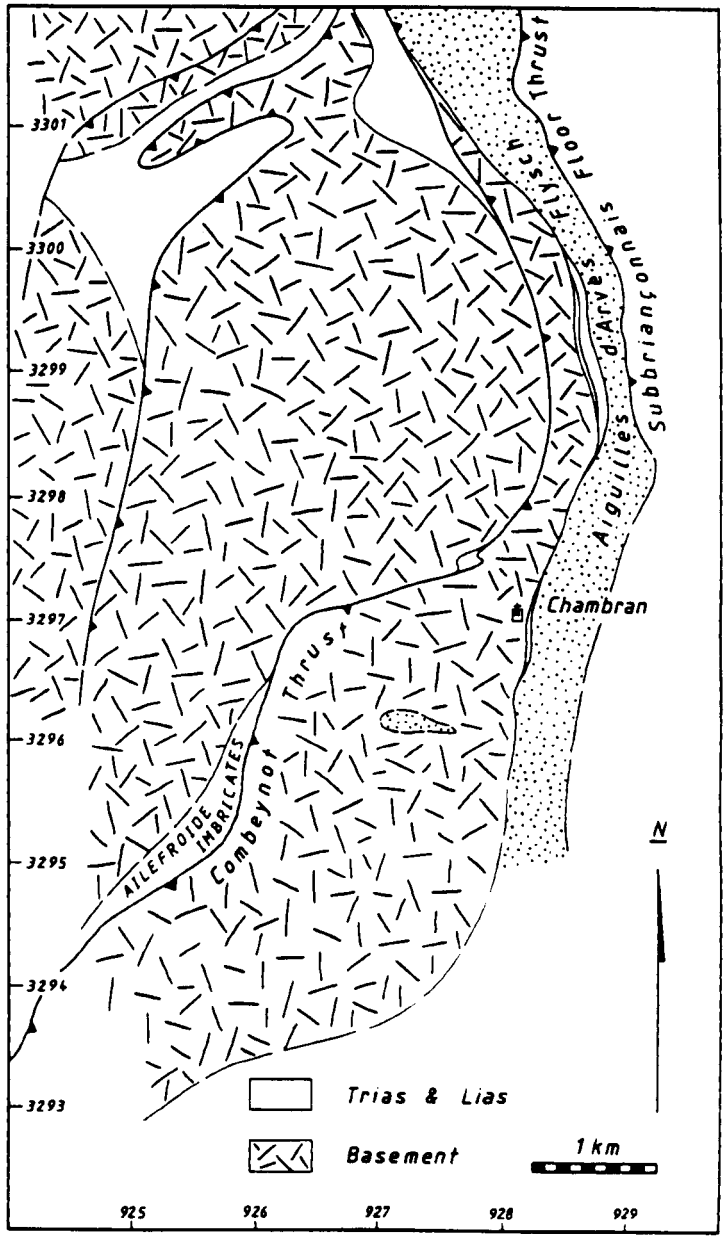

FIG. 5.27 Sketch map of the Combeynot Thrust in the S of the study area.

clearly in Figs. 5.26 and 5.27. To the S of the area illustrated in Fig. 5.25, the Combeynot Thrust cuts back down into basement and trends SSW-NNE. The present outcrop trace of this thrust has developed as a result of accretion of structurally lower imbricate slices and the evolution of this geometry is best illustrated by construction of a schematic longitudinal section viewed from a position looking directly back down the movement direction, Fig. 5.28.

The displacement on the Combeynot Thrust cannot be calculated from construction of balanced and restored cross sections as the cover stratigraphy in the hangingwall is different from that in the footwall. The footwall stratigraphy is typical of the External Zones with a thin (25 m) Triassic succession overlain by up to 700 m of Lias and early-middle Jurassic limestones and shales. In the hangingwall, local Nummulitic limestone, conglomerates, shales and turbidites of Eocene age overlie the basement, suggesting removal of the Mesozoic cover prior to Flysch deposition.

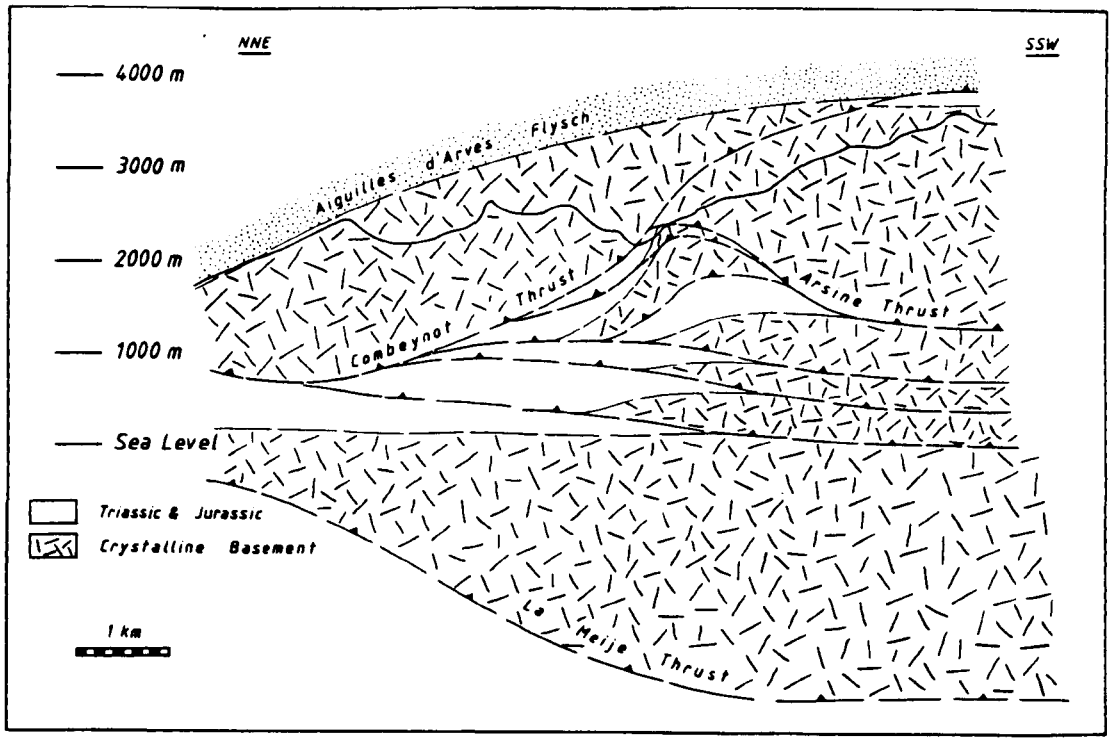

FIG. 5.28 Schematic longitudinal section illustrating the flexuring of the Combeynot Thrust Sheet by structurally lower thrusts.

The minimum shortening value derived from construction of balanced and restored cross sections for the imbricated basement and cover (Arsine imbricates) above the La Meije Thrust Sheet and below the Combeynot Thrust is 5.5 km, Fig. 5.29. The hangingwall cut-off to the Le Meije Thrust is not seen and simple projection of the basement-cover unconformity within the La Meije Thrust Sheet, using an assumed basement ramp angle of 25°, suggests a displacement on the La Meije Thrust of approximately 11.5 km, and hence leads to a rough value for the total shortening of 17 km between the La Meije and Combeynot Thrusts.

This value is considerably less than the 70 km shortening estimated by Beach (1981b) for the same thrust system to the N of La Meije, although Beach does concede that if the original stratigraphic thickness of the Triassic and Jurassic cover rocks was as high as 1 km then the estimated shortening reduces from 70 km to nearer 30 km. It is likely that the original stratigraphic thickness of the Mesozoic cover succession exceeded 500 m. In the upper Romanche Valley (Col d'Arsine area) recent mapping by this author clearly illustrates a present stratigraphic thickness of approximately 650 m for the late Triassic to late Toarcian/Aalenian sediments.

The amount of shortening in the footwall to the La Meije Thrust (Ultradauphinois Thrust) has been calculated to be 24.5 km within the Montaimont duplex approximately 40 km to the N of the upper Romanche Valley, this shortening is transferred towards the S onto the Ultradauphinois Thrust (Parish, pers. comm.) and is broadly compatible with the shortening value derived from the Combeynot region.

The pre-thrusting geometry of the External Zones in the region of the external crystalline basement massifs is not known. For the purpose of constructing cross section (J-J'), Fig. 5.29, it has been assumed that no major extensional faults occur between the La Meije and Combeynot Thrusts. Davies (1982) demonstrates the importance of

PAGE

NUMBERING

AS ORIGINAL

Fig 5.29

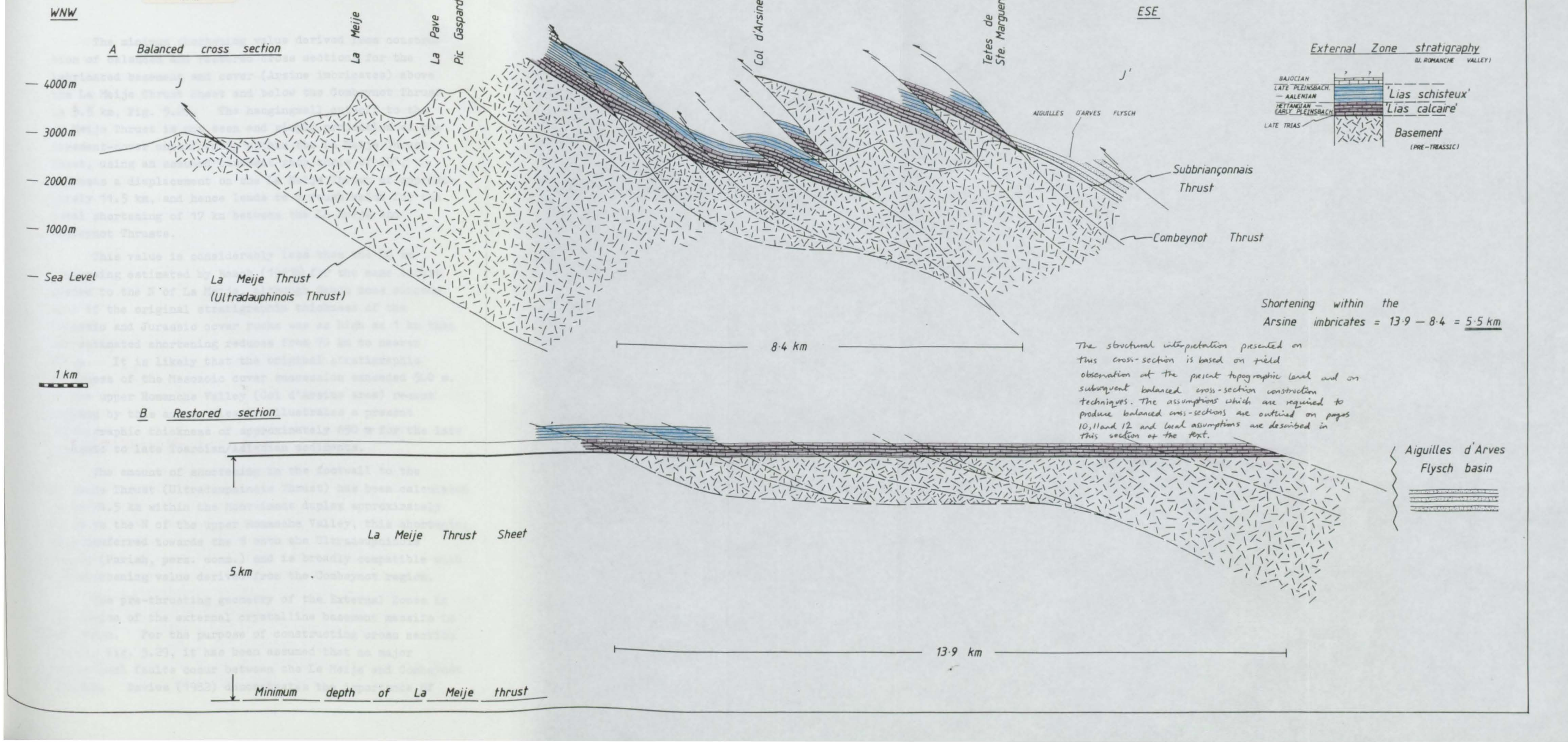
WNW
ESE
A Balanced cross section
4000 m
3000 m
2000 m
1000 m
Sea Level
J
J'
La Meije
La Pave
Pic Gaspard
Col d'Arsine
Tetes de Ste. Marguerite
AIGUILLES D'ARVES FLYSCH
La Meije Thrust
(Ultradauphinois Thrust)
Subbriançonnais Thrust
Combeynot Thrust
1 km
8·4 km
External Zone stratigraphy
(U. ROMANCHE VALLEY)
BAJOCIAN
LATE PLEINSBACH.
AALENIAN
HETTANGIAN
EARLY PLEINSBACH.
LATE TRIAS
'Lias schisteux'
'Lias calcaire'
Basement
(PRE-TRIASSIC)
Shortening within the Arsine imbricates = 13·9 − 8·4 = 5·5 km
The structural interpretation presented on this cross-section is based on field observation at the present topographic level and on subsequent balanced cross-section construction techniques. The assumptions which are required to produce balanced cross-sections are outlined on pages 10, 11 and 12 and local assumptions are described in this section of the text.
B Restored section
La Meije Thrust Sheet
5 km
Aiguilles d'Arves Flysch basin
13·9 km
Minimum depth of La Meije thrust

Mesozoic extensional faults in the N of the Grandes Rousses massif, Fig. 5.24, and it is clear that the stratigraphy of the NW External Zones was not layer-cake prior to thrusting. The degree of Mesozoic extension within this portion of the NW External Alpine thrust belt can only be properly established by sequentially removing the Alpine deformation within the basement/cover sequence to reveal the pre-compressional geometry. The complex internal deformation within the Mesozoic cover rocks of the NW External Alpine thrust belt has been described by Gratier et al. (1973), Gratier & Vialon (1980), Beach (1981d) and Beach (1982). No attempt has been made to incorporate finite strain into the balanced cross section (J-J'), Fig. 5.29; the deformation within the cover rocks of NE Pelvoux and the Aiguilles d'Arves Flysch is now discussed.

(ii) Folding and strain

(a) Deformation in the footwall to the Combeynot Thrust

No quantitative appraisal of the finite strain within thrust sheets has been carried out during the course of this study. The field observation of cleavage development and extension lineations is now documented.

In the region between the upper Romanche valley and Tête de Pradieu, Fig. 5.30, a reasonably well exposed cover succession of Triassic to middle Jurassic limestones and shales occurs between the La Meije Thrust Sheet and the Combeynot Thrust. A thrust of minor displacement (perhaps 50 m) can be mapped out near to the Chalets de l'Alpe du Villar d'Arene, Fig. 5.30. The cover succession in the hangingwall to this thrust at position (V) in Fig. 5.30 consists of approximately 2 m of conglomerates and sandstone, which directly overlies the basement. This is overlain by 15-20 m of dolomitic limestone breccia (a sedimentary breccia) which does not show any penetrative tectonic deformation. This thin sequence of sandstones,

conglomerates and breccias is interpreted as Triassic in age, based on lithological correlation with previously described Triassic rocks of this area. Approximately 40 m above the breccias the early Jurassic sediments consist of well bedded limestones and shales and contain belemnites, which at this locality (W in Fig. 5.30), are undeformed. At point X, approximately 90 m above the basement/cover interface, a well developed NNW-SSE trending cleavage exists within the limestone-shale sequence, Fig. 5.31, and ammonites within the limestones are slightly extended along strike, Fig. 5.32.

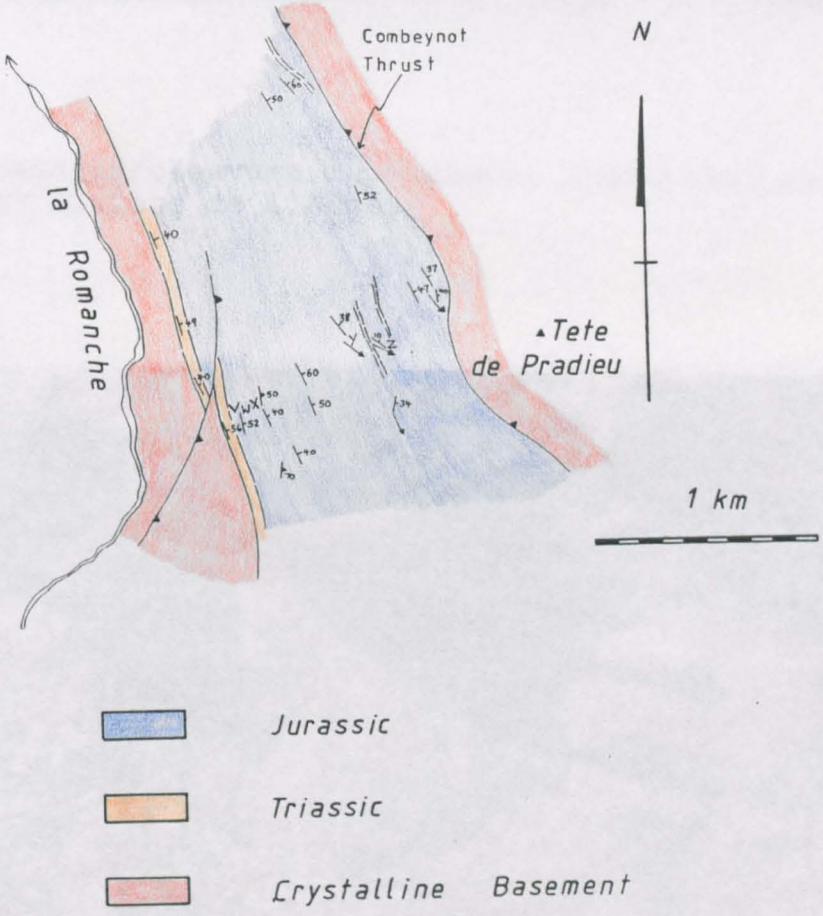

FIG. 5.30 Map of the footwall to the Combeynot Thrust in the region of the Chalets de l'Alpe du Villar d'Arene.

FIG. 5.31 Bedding/cleavage in Jurassic limestones near to Chalets de l'Alpe.

FIG. 5.32 Deformed ammonite within limestones near to above locality.

Exposure is patchy on the hillside structurally above this locality as the succession grades up-sequence into the shale dominated 'Lias schisteux'. At position (Y), Fig. 5.30, limestones which dip to the NE at 40° contain an extension lineation on the bedding planes which plunges at 9° towards 125° and is parallel to calcite fibres in pyrite pressure shadows. Two thin (approximately 10 m) lenses of cargneule of unknown age crop out immediately above this locality (Y); it is common to assign a Triassic age to any rock type which resembles a crumbly, poorly consolidated carbonate in this part of the Alps.

At locality (Z), well bedded limestones which possess a strong cleavage subparallel to bedding, dip at 10° towards the NE and contain an extension lineation in the plane of bedding which plunges at 5° towards 118°; this is parallel to fibres in pyrite pressure shadows. Immediately below the Combeynot Thrust, well bedded limestones dip to the ENE at 40° and an extension lineation on bedding planes plunges at 20° towards 141°, parallel to extended belemnites, which indicate a local extension in excess of 100%, based on measurement from photographs, e.g. Fig. 5.33.

FIG. 5.33 Extended belemnite in the footwall to the Combeynot Thrust.

These simple observations immediately question the validity of deriving shortening estimates using diagrams such as cross section (J-J'), Fig. 5.29. The finite strain within the cover rocks between the basement of the La Meije Thrust Sheet and the Combeynot Thrust shows a gradation from an undeformed zone of 30 m width immediately above the basement through a well cleaved zone with cleavage at a low angle to bedding which displays a small amount of NW-SE extension, into a high deformation zone where the dominant planar fabric is a cleavage subparallel to bedding. This structurally highest zone shows evidence for a substantial amount of NW-SE extension, from extension lineations and extended belemnites. Finite strain observations are now documented from the cover succession above the basement of the La Meije Thrust Sheet and below the Combeynot Thrust, in the region between le Pied du Col and Pyramide de Laurichard, Fig. 5.34.

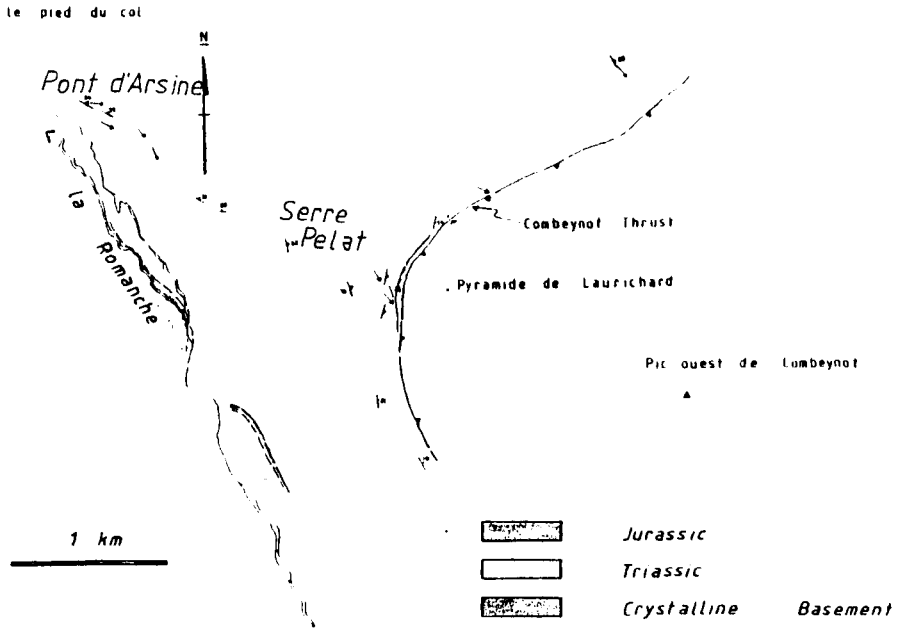

FIG. 5.34 Map of the region between le Pied du Col and Pyramide de Laurichard.

A systematic description of the deformation observed at each locality within the small area illustrated in Fig. 5.34 is not required here. Near to Pont d'Arsine the dominant cleavage is parallel to bedding in black shales and an extension lineation on the bedding/cleavage plane plunges at 15° towards 097°; quartz-carbonate veins are common in this vicinity and are subparallel to the cleavage. Locally this cleavage is tightly folded into small scale folds which plunge gently towards 120°. On Serre Pelat, Fig. 5.34, the cleavage is parallel to bedding and dips to the NE at 50°, the extension lineation on the cleavage plane plunges towards 157°. The orientation of the cleavage and extension lineations are indicated in Fig. 5.34. Structurally below the Combeynot Thrust at Pyramide de Laurichard the immediate footwall consists of Triassic sandstones. It is not possible to determine the way-up of these rocks from sedimentary structures; however the lithology immediately below the thrusts is quartzite which structurally overlies a limestone breccia, suggesting that it may be inverted Trias. These beds dip at 80° to the SE at locality (A) on Fig. 5.34, and a lineation on the bedding plane plunges at 64° towards 114°.

In the region between Pics de Chamoissiere and Pradieu, Fig. 5.35, thrusts can be mapped out which cut up stratigraphic section from basement into cover from SW to NE. Ammonites approximately 150 m above the basement/cover interface are deformed and extended in a NW-SE direction; some of the localities which display this deformation are indicated in Fig. 5.35 and one example is shown in Fig. 5.36. Exposure is very poor in the region of Col d'Arsine; however, between Col d'Arsine and Chalet d'Arsine there is good evidence for imbrication of the cover from the outcrop geometry of the Jurassic limestones, Fig. 5.37. The internal deformation within this imbricate slice is intense, and similar to the deformation described for the limestones immediately below the Combeynot Thrust in the region of Tête de Pradieu, with a very strong NW-SE stretching. The hangingwall anticline illustrated in Fig. 5.37 folds this extensional fabric within the limestones.

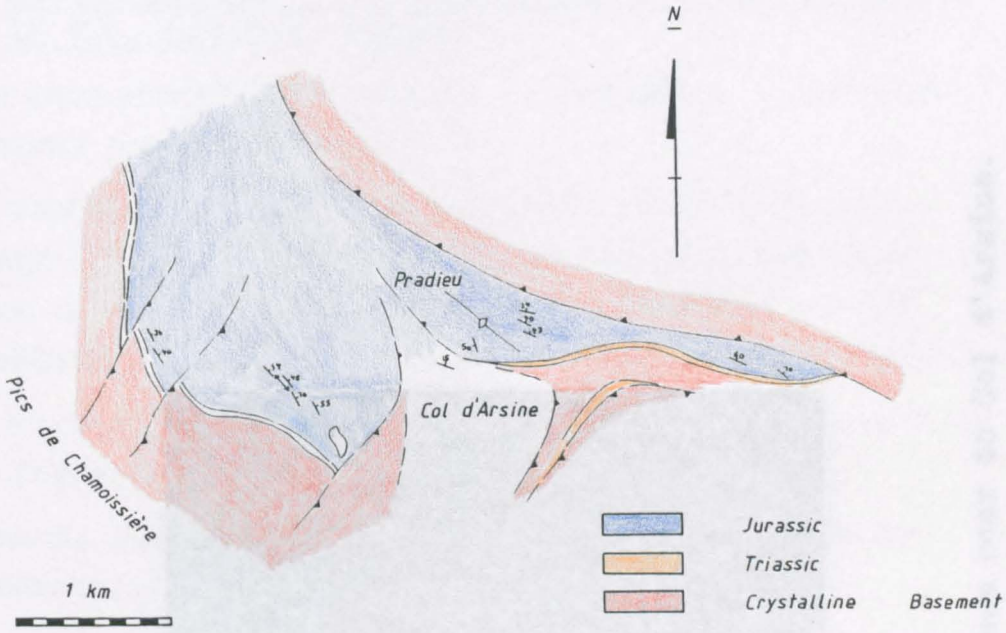

FIG. 5.35 Map of the region between Pics de Chamoissiere and Pradieu.

FIG. 5.36 Deformed ammonite from the Col d'Arsine area.

FIG. 5.37 Hangingwall anticline in Jurassic limestones near to Col d'Arsine.

(b) Interpretation of the deformation in the footwall to the Combeynot Thrust

This interpretation attempts to reconcile the following structural observations:

1. The Combeynot Thrust has carried a thick (approximately 2 km) slab of crystalline basement and overlying cover for a considerable distance across its immediate footwall of Jurassic limestones and shales.

2. The intensity of deformation within the cover rocks of the footwall decreases down structural section.

3. There is strong evidence for inverted stratigraphy immediately below the Combeynot Thrust.

4. The dominant extension direction is NW-SE, Fig. 5.38.

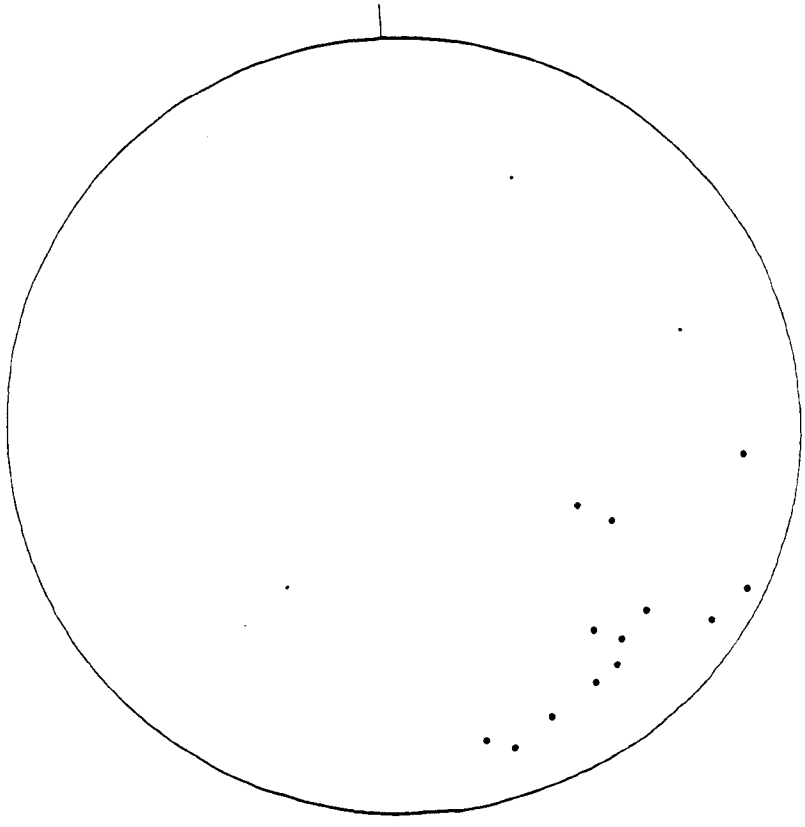

FIG. 5.38 Stereogram of extension lineations in the footwall to the Combeynot Thrust.

The inverted footwall to the Combeynot Thrust in the Pyramide de Laurichard area suggests that the thrust was developed through a fold within the cover. This implies that the Combeynot basement was overlain by Triassic and Jurassic sediments prior to thrusting. Isolated lenses of Mesozoic strata crop out in the hangingwall to the Combeynot Thrust between the Combeynot basement and the overlying Eocene Flysch. Slip across the footwall must have followed propagation of the thrust through the fold. Following stick on the Combeynot Thrust, deformation must have proceeded in its footwall during propagation of the structurally lower floor thrust within basement, and subsequent development of a ramp to form the La Meije Thrust. The evidence from the deformation within the footwall, suggests that the zone between the La Meije basement and the (abandoned) Combeynot Thrust, acted as a shear zone of approximately 1.5 km width. The intense NW-SE stretching in the upper portion of this shear zone reflects movement towards the NW during propagation of the La Meije Thrust. The present day NW-SE strike of the cover in this area results from the La Meije Thrust cutting up stratigraphic section towards the NE and subsequently moving in a NW direction across a subhorizontal footwall. This has produced a significant flexure in the hangingwall and has reorientated the cleavage in the region of le Pied du Col. This interpretation is summarised in Fig. 5.39.

Small scale imbricate slices of crystalline basement and Mesozoic cover near to le Grand Tabuc, Fig. 5.40, display a well developed cleavage at a low angle to bedding and an extension lineation which plunges at 25° towards 130°, parallel to calcite fibres in pyrite pressure shadows, Fig. 5.41, providing further evidence for NW movement.

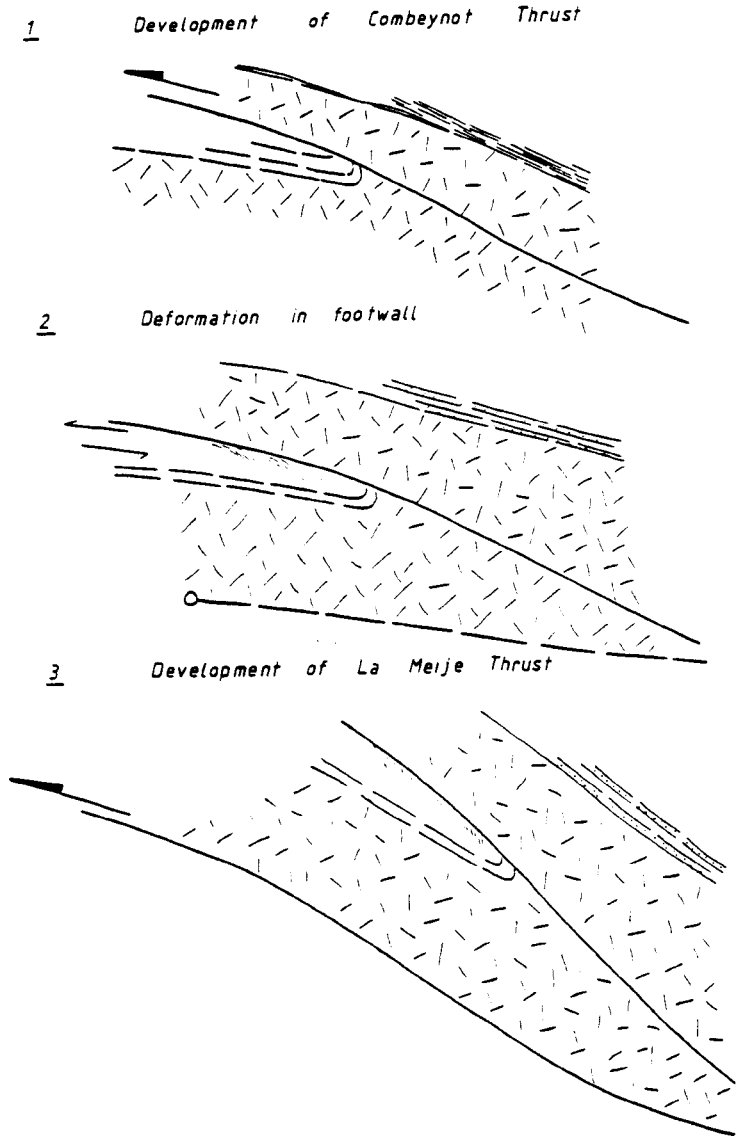

FIG. 5.39 Model for the deformation sequence in the footwall to the Combeynot Thrust.

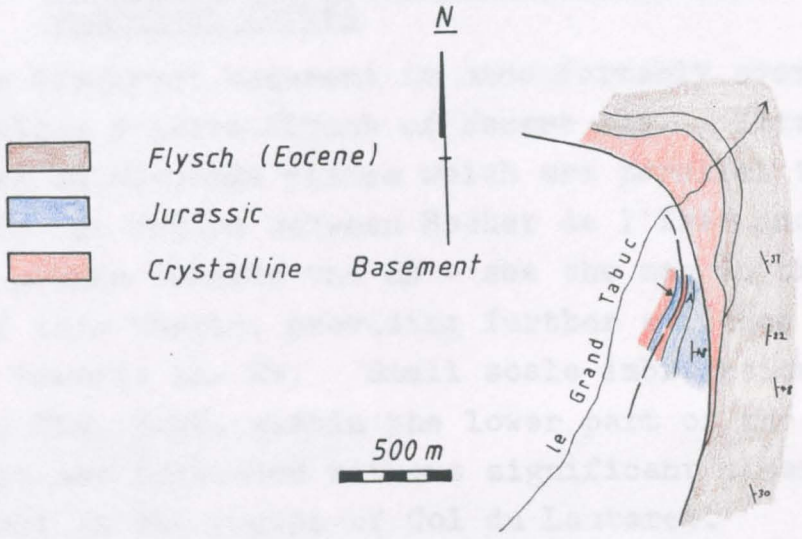

FIG. 5.40 Map of the region near to le Grand Tabuc.

FIG. 5.41 Bedding/cleavage at locality (A), see Fig. 5.40.

(c) Deformation in the hangingwall to the Combeynot Thrust

The Combeynot basement is unconformably overlain by the Aiguilles d'Arves Flysch of Eocene age. Extension lineations on cleavage planes which are parallel to bedding in the region between Rocher de l'Yret and Chambran plunge towards the SE - see the map in the back pocket of this thesis, providing further evidence for movement towards the NW. Small scale imbrication and buckling, Fig. 5.42, within the lower part of the flysch succession has developed without significant cleavage development in the region of Col du Lautaret.

FIG. 5.42 Small scale imbrication within the Aiguilles d'Arves flysch.

Structurally up-sequence, in the immediate footwall to the Subbriançonnais Thrust, the deformation within the flysch is characterised by a well developed bedding parallel cleavage within the shaley zones and boudinaged sandstone lenses, Fig. 5.43.

FIG. 5.43 Boudinaged sandstones within the Aiguilles d'Arves flysch.

The structurally highest major thrust in the External Zones within the study area is the Combeynot Thrust. This can be traced from Combeynot towards the N where it cuts up section in the hangingwall from basement into Eocene cover. Towards the S it cuts up-section into Eocene cover and then back down into basement in the region of Chambran, Fig. 5.27. Deposition of Eocene flysch therefore pre-dates movement on this thrust; this is contrary to the conclusions of Bravard & Gidon (1979) who invoke a sedimentary origin for many of the imbricate slices observed within the study area.

DISCUSSION AND CONCLUSIONS

CHAPTER 6

DISCUSSION AND CONCLUSIONS

(i) Thrust sheet geometry

The 3 dimensional shape of a thrust sheet which is enclosed by leading, trailing, oblique and lateral branch lines is determined by 4 major factors:

1. The geometry of the upper thrust surface prior to slip.
2. The geometry of the lower thrust surface prior to slip.
3. The geometry of the footwall following slip on the lower thrust.
4. The geometry of structurally lower thrusts.

The geometry of thrust surfaces is defined by measurement of ramp angles (cut-off angles), which is the angle between a pre-existing tectonic or sedimentary fabric, e.g. bedding, and the thrust surface. Measurement of ramp angles in the Moine Thrust Zone, in a vertical plane subparallel to the movement direction, reveals that the thrust surfaces are listric shaped, i.e. the ramp angle decreases with depth. This is frequently assumed to be the case within thrust belts but it is possible to prove this from the Kinlochewe region. Construction of balanced cross sections suggests that the thrusts within the Beinn Eighe Imbricate Fan branch from a basal detachment zone or floor thrust within the Torridonian sandstone. The stratigraphic level of this floor thrust becomes shallower in the WNW movement direction and cuts up and down section perpendicular to this movement direction. Imbricate thrusts which branch off this floor thrust mirror these geometrical characteristics and always cut up stratigraphic section at between 18° and 30° in the direction of movement. The balanced cross sections and geological map patterns of individual imbricate slices within the Beinn Eighe Imbricate Fan demonstrate that the imbricates evolved as an in-sequence

thrust system, structurally lower thrusts are youngest and higher imbricate slices are flexured and reorientated as a result of movement on these lower thrusts. The 3 dimensional geometry of horses within the Beinn Eighe Imbricate Fan can be assessed by examining the lateral continuity and cross sectional geometry of imbricate slices. It has been found that for the major frontal horses, the along strike length is approximately 5-6 times as great as the across strike width which is approximately 5-6 times as great as the thickness of the horse.

The geometry of thrust sheets in the Pelvoux - Briançonnais shows similar characteristics to the Kinlochewe region. Balanced cross sections and geological maps indicate that the Champcella nappe has a restored across strike width of approximately 15 km, the thickness of the sheet on the restored section is approximately 4.5 km and the sheet continues to the N and S of the study region, implying a length in excess of 35 km. Similar ratios of length : width : thickness occur in the External Zones, although the lateral ramps in the N Pelvoux region are relatively steep (approximately 45°), and no simple along strike length prediction is possible.

(ii) Sequence of emplacement of thrust sheets

Balanced cross sections and geological maps illustrate the geometrical relationships between the hangingwall and footwall of thrust surfaces. These relationships define the sequence of propagation of thrust surfaces. In the Moine Thrust Zone the Kinlochewe Thrust cuts through a relatively small scale duplex indicating that the propagation rate of the major regional thrust may fluctuate and smaller scale imbricate thrusts may develop in a structurally lower position, forming small scale duplex systems. A subsequent increase in the propagation rate of the major thrust may result in slicing through of this lower imbricate system, as an out-of-sequence thrust. The geometrical evidence from the Kinlochewe region suggests that the movement on major thrusts is broadly in-sequence; however, the

detailed evolution of major and minor thrust surfaces is likely to be extremely complex.

In the Briançonnais, the Champcella nappe is folded by the Roche-Charnière nappe, indicating that the structurally higher Champcella nappe overlay the Roche-Charnière nappe prior to movement on the Roche-Charnière Thrust. Further evidence of in-sequence movement on thrust surfaces is displayed in the Galibier region where thrusts within the Subbriançonnais Zone have sliced up through the frontal Briançonnais Thrust, thereby forming a 'breached roof' structure and proving the in-sequence nature of thrusting. In the External Zones, movement on the La Meije Thrust has reorientated fabrics and thrust sheets in its hangingwall, suggesting that thrusts developed sequentially towards the foreland.

(iii) Tectonic shortening and thrust displacements

The most accurate method of obtaining an estimate of tectonic shortening is to construct a balanced cross section. Shortening estimates for the Moine Thrust Zone in the Kinlochewe region suggest a minimum shortening value of approximately 16 km. The amount of shortening within the Beinn Eighe Imbricate Fan decreases towards the N from its central portion, and the displacement on individual thrusts may increase or decrease along strike. This can be proved from the Kinlochewe region where displacements on individual thrusts can be compared along the strike of the thrust zone. Displacements are not conserved along strike within thrust belts, the total displacement observed on a major thrust may be partially transferred along strike onto two or more thrusts which branch off the major thrust. The maximum shortening estimate derived from the Beinn Eighe Imbricate Fan is 7.3 km on a section line through Sgurr Dubh.

Deriving an accurate estimate of tectonic shortening for the Pelvoux-Briançonnais is made difficult by the contrasting stratigraphic successions of the Ultradauphinois, Subbriançonnais and Briançonnais Zones. However

construction of balanced cross sections across each of these zones demonstrates a minimum restored width of 17 km between the La Meije Thrust and the Combeynot Thrust, and 54 km between the frontal Subbriançonnais Thrust and the Briançonnais backfold axis. This restored width does not take into account the following factors:

1. Displacement on the Combeynot Thrust.
2. Shortening within the Aiguilles d'Arves flysch.
3. Displacement on the Subbriançonnais Floor Thrust.
4. Displacement on the Briançonnais Floor Thrust.

To obtain an estimate of orogenic contraction across the External, Subbriançonnais and Briançonnais Zones, the External Zones must be 'pinned' near to the Rhone Valley and restored in an ESE direction, the Subbriançonnais and Briançonnais would then have to be restored in an ENE direction, implying a change in thrust sheet movement directions during evolution of the French Alps.

(iv) Strain within thrust sheets

Strains within thrust sheets can be assessed in terms of strains which develop in the footwall to an abandoned thrust, strains which develop during slip and strains which develop after stick on the lower thrust. The plastic deformation within the Beinn Eighe Imbricate Fan suggests that a small percentage of layer parallel shortening may develop in the footwall to an abandoned thrust as a tip strain to a newly developing structurally lower thrust. A variable along strike propagation rate will result in frontal, oblique and lateral tip strains. The extent of layer parallel shortening within the imbricate slices of the Beinn Eighe Imbricate Fan varies between 0% and 20% and is thought to reflect zones of relatively rapid thrust propagation and relatively slow thrust propagation respectively. The highest layer parallel shortening values are found in the portion of the imbricate fan which contains the thinnest imbricate slices, i.e. in regions overlying a relatively shallow floor thrust. Differential displacement can be documented on individual thrusts and this results in

differential movement within imbricate slices. There is evidence for a small amount of layer normal shear throughout the Beinn Eighe Imbricate Fan, especially in the northern part, which displays less shortening and corresponding small dextral layer normal shear strains. There is also evidence for flexural slip within imbricate slices which may be a response to movement across the underlying thrust surface; extensional strains have been recorded within the hangingwall to imbricate thrusts, suggesting that components of flexural slip within the sheet and ductile extension allow the sheet to modify its geometry to conform to the underlying thrust surface.

In the External Zones of the NE Pelvoux region the strains within the Mesozoic cover rocks can be interpreted in terms of layer parallel shortening and shearing within the footwall to an abandoned structurally higher thrust, which evolve during propagation of the new, structurally lower thrust. The ease of propagation of new thrusts will determine the intensity of deformation within the overlying thrust sheet. In the Mesozoic cover below the Combeynot Thrust, a low deformation zone grades up into a well cleaved zone which grades into a high deformation zone which displays a large percentage extension in the WNW movement direction. In the Briançonnais and Subbriançonnais Zones there is evidence for early layer parallel shortening prior to buckling and propagation of the thrust surface. Extension within the footwall to the Briançonnais Floor Thrust suggests that shearing within the Subbriançonnais may have developed in a similar fashion to that observed below the Combeynot Thrust. The laterally variable profile of a thrust surface prior to slip will determine the amount of geometrically necessary strain following subsequent slip across a subhorizontal footwall. The only convincing example of this mode of deformation in the Briançonnais Zone suggests that the 'hangingwall strain' is displayed within the thrust sheet as normal faults which trend parallel to the movement direction.

(v) Folds within thrust sheets

Folds within thrust sheets fall into two main categories: folds which form as a result of slip of the thrust sheet across an irregular thrust surface (fault bend folds or structurally necessary folds), and buckle folds which develop during shortening within the thrust sheet. Both styles of folding are well developed in the Kinlochewe region; within the Beinn Eighe Imbricate Fan there is evidence for buckle folds forming at thrust tip lines as a response to the slip rate on the thrust exceeding the rate of propagation of the thrust surface. Frequently the thrust has then cut across the fold to display an anticline in the hangingwall and a syncline in the footwall. Folds of this type are common within the Champcella nappe of the Briançonnais Zone where there is evidence for several generations of tip line folds directed both towards the foreland and hinterland (backfolds).

Fault-bend folds or flexures are the most common type of fold within the Beinn Eighe Imbricate Fan and result from the thrust sheet slipping from the footwall ramp across the footwall flat; typically these folds have interlimb angles in excess of 150° as a response to ramp angles of less than 30°. In regions where the ramp geometry is complex, such as the Dundonnell region of the Moine Thrust Zone, the folds may develop with axes oblique to the movement direction, a result of slip across oblique ramps rather than differential movement within the thrust sheet.

(vi) Surge Zones

Fault sheets which cut down stratigraphic section or across previously developed thrust structures, or which have extensional geometry in the hangingwall and footwall, and show extensional strains in the rear of the sheet are termed surge zones (Coward 1982). These structures can be mapped out in the Assynt region of the Moine Thrust Zone and may exist in the northern Moine Thrust Zone near to Heilam. The Kinlochewe Thrust Sheet is a candidate for a large scale surge zone; however, the evidence for this

is based on the Kinlochewe Thrust cutting down section in its footwall at an average angle of approximately 1°. The same geometrical relationships may result from a subhorizontal thrust cutting through a gently tilting sedimentary succession.

In the Briançonnais Zone, the Serre Chevalier Sheet is truncated in its footwall and hangingwall by a fault which is possibly extensional and therefore has the geometry of a surge zone.

ACKNOWLEDGEMENTS

The work described in this thesis was carried out during receipt of a Natural Environment Research Council studentship which is gratefully acknowledged.

I would like to thank Dr. Mike Coward for supervision and much encouragement throughout the duration of the project. My thanks also go to all members of the structural geology research team who worked at Leeds University between 1980 and 1983, in particular Dr. Rob Knipe, Rob Butler, Colin Davies, Bob Holdsworth, Rick Law, Richard Morgan, Tim Needham, Phil Nell, Graham Potts and John Wheeler. I have spent many pleasurable days in the Alps with students and staff of University College, Swansea and Oxford University; I would like to thank Dr. Norman Fry, Dr. Rod Graham, Vivienne Davies, Neil Harwood, Kevin Lawson, Marcus Parish, Frank Peel and John Warburton for hours of stimulating discussion on Alpine Geology.

This work could not have been completed without the considerable assistance and understanding of my family who have given much encouragement and support during my undergraduate studies at Swansea (1977-1980) and later postgraduate studies at Leeds (1980-1983). My thanks also go to my fiancee, Susan, for understanding and friendship throughout.

Finally, my thanks go to Robertson Research PLC for financial assistance during production of this thesis, and to Vera Stirling who has expertly typed the script.

REFERENCES

Antoine, P., Barbier, R., Bravard, C. & Gidon, M. 1978. Les rapports entre le Flysch des Aiguilles d'Arves et le domaine Valaisan au cirque de Valbuche (Savoie). C.R. Acad. Sc. Paris 286, 1751-1753.

Argand, E. 1916. Sur l'arc des Alpes occidentales. Eclog. geol. Helv. 14, 145-191.

Argand, E. 1922. La tectonique de l'Asie. 13th Int. Geol. Congr. Belgium 1, 171-372.

Armstrong, F.C. & Oriel, S.S. 1965. Tectonic development of Idaho-Wyoming thrust belt. Bull. Am. Assoc Pet. Geol. 49, 1847-1866.

Aubouin, J., Debelmas, J. & Latreille, M. 1980. Géologie des chaînes alpines issues de la Téthys. Mémoire du B.R.G.M. 115.

Ayrton, S. 1980. La géologie de la zone Martigny-Chamonix (versant Suisse) et l'origine de la nappe de Morcles (un exemple de subduction continentale). Eclog. geol. Helv. 73, 137-172.

Aryton, S. & Ramsay, J. 1974. Tectonic and metamorphic events in the Alps. Schweiz. Mineral. Petrogr. Mitt. 54, 609-639.

Bailey, E.B. 1935. The Glencoul nappe and the Assynt Culmination. Geol. Mag. 72, 151-165.

Bally, A.W., Gordy, P.L. & Stewart, G.A. 1966. Structure, seismic data and orogenic evolution of southern Canadian Rocky Mountains. Bull. Can. Petrol. Geol. 14, 337-381.

Barber, A.J. 1965. The history of the Moine Thrust Zone, Lochcarron and Lochalsh, Scotland. Proc. Geol. Assoc. 76, 215-242.

Barber, A.J. 1969. Geology of the country around Dornie, Wester Ross. Unpublished Ph.D. Thesis, Univ. London.

Barbier, R. 1948. Les zones ultradauphinoise et subbriançonnaise entre l'Arc et l'Isère. Mém. Carte Géol. Fr.

Barbier, R. 1956a. Découverte du Tithonique dans la zone ultradauphinoise au Nord du Pelvoux. C.R. Acad. Sc. 242, 395.

Barbier, R. 1956b. L'importance de la tectonique "anténummulitique" dans la zone ultradauphinoise au N du Pelvoux : la chaine arvinche. Bull. Soc. Géol. Fr. 6, 355-370.

Barbier, R. 1963a. La tectonique de la zone ultradauphinoise au Nord-Est du Pelvoux. Trav. Lab. Grenoble 39, 239-246.

Barbier, R. 1963b. Réflexions sur la zone dauphinoise orientale et la zone ultradauphinoise. Mém. S. Géol. Fr., livre à la mémoire du Professeur P. Fallot, t.II. 321-330.

Barbier, R. 1963c. La zone subbriançonnaise dans la région du col du Galibier. Trav. Lab. Geol. Grenoble 39, 247-257.

Barbier, R. & Barféty, J.-C. 1972. Les structures E-W de la zone ultradauphinois du pays des Arves (Savoie) et leur signification. Géol. Alpine 48, 151-158.

Barbier, R. & Debelmas, J. 1966. Réflexions et vues nouvelles sur la zone subbriançonnaise au Nord du Pelvoux (Alpes occidentales). Géol. Alpine 42, 97-107.

Barféty, J.-C. 1965. Etude géologique des environs du Monétier-les-Bains; Hautes-Alpes (zones subbriançonnaise et briançonnaise). Thèse 3e Cycle, Grenoble.

Barféty, J.-C. 1967. Au sujet d'une série post-triasique inhabituelle dans la zone briançonnaise, près de Névache (Htes-Alpes). Trav. Lab. Géol. Grenoble 43, 41-45.

Barféty, J.-C. 1968. Importance des failles et des glissements superficiels dans le Massif de Montbrison et ses environs Briançon (Htes-Alpes). Géol. Alpine 44, 49-54.

Barféty, J.-C., Gidon, M., Lemoine, M. & Mouterde, R. 1979. Tectonique synsédimentaire liasique dans les massifs crystallins de la zone externe des Alpes occidentales francaises: la faille du col d'Ornon. C.R. Acad. Sci. Ser. D 289, 1207-1210.

Bartoli, F. 1973. Etude pétrologique et structurale du haut Vénéon (Massif du Pelvoux). Thèse 3e Cycle, Grenoble. 121 p.

Bartoli, F., Pêcher, A. & Vialon, P. 1974. Le chevauchement Meije-Muzelle et la répartition des domaines structuraux alpins du massif de l'Oisans (partie Nord du Haut-Dauphiné cristallin). Géol. Alpine 50, 17-26.

Barton, C.M. 1978. An Appalacian view of the Moine thrust. Scott. J. Geol. 14, 247-257.

Beach, A. 1979. The analysis of deformed belemnites. J. Struct. Geol. 1, 127-135.

Beach, A. 1981a. Thrust tectonics and cover-basement relations on the northern margin of the Pelvoux massif, French Alps. Eclog. geol. Helv. 74, 471-479.

Beach, A. 1981b. Thrust structures in the eastern Dauphinois zone (French Alps) north of the Pelvoux massif. J. Struct. Geol. 3, 299-308.

Beach, A. 1981c. Thrust tectonics and crustal shortening in the external French Alps based on a seismic cross-section. Tectonophysics 79, T1-T6.

Beach, A. 1981d. Some observations on the development of thrust faults in the Ultradauphinois zone, French Alps. In: Thrust and Nappe Tectonics (edited by McClay, K.R. & Price, N.J.). Spec. Publs. geol. Soc. Lond. 9, 329-334.

Beach, A. 1982. Strain analysis in a cover thrust zone, external French Alps. Tectonophysics 88, 333-346.

Berger, P. & Johnson, A.M. 1980. First order analysis of deformation on a thrust sheet moving over a ramp. Tectonophysics 70, 9-24.

Bourbon, M. 1977. Reconstitution palaéomorphologique de fonds marins sur la marge nord-téthysienne: Le Jurassique supérieur et le Crétacé briançonnais dans les unités de Roche-Charnière et de Champcella et dans le massif Galibier-Cerces. Bull. Soc. géol. France 7. XIX, 4, 729-733.

Bourbon, M., Caron, J.-M., Graciansky, P.-C. de, Lemoine, M., Megard-Galli, J. & Mercier, D. 1976. Mesozoic evolution of the Western Alps: Birth and development of part of the spreading Tethys and of its European Continental Margin. Symposium: Histoire Structurale des Bassins Méditerranéens, Split, Oct. 1976, Technip Ed., 19-34.

Bourbon, M., Graciansky, P.-C. de, Lemoine, M., Megard-Galli, J. & Mercier, D. 1975. Carbonates de plate-forme et séries pélagiques condensées dans le Mésozoique de la zone briançonnaise (Alpes françaises). Livret-guide Excursion Z5, IX^{e} Congr. internation. sédim. Nice.

Bourbon, M., Graciansky, P.-C. de, Megard-Galli, J. & Lemoine, M. 1973. L'evolution palaéogéographique du domaine briançonnais du Mésozoique: carbonates de

plate-forme subsidente, révolution du Lias supérieur, instauration progressive d'un régime pélagique profond. C.R. Ac. Sci. Paris 277, 769-772.

Bourbon, M. et Hoffert, M. 1977. Nature et répartition des minéralisations liées aux lacunes dans le Mésozoique et le Palaéocène pélagiques briançonnais (Region de Briançon). Essai de comparison avec certaines minéralisations des océans actuels. Bull. Soc. géol. France 7, XIX, 4, 725-728.

Boyer, S.E. & Elliott, D. 1982. Thrust Systems. Am. Assoc. Petrol. Geol. Bull. 66, 1196-1230.

Bravard, C. & Gidon, M. 1979. La structure du revers oriental du Massif du Pelvoux: Observations et interpretations nouvelles. Géol. Alpine 55, 23-33.

B. R. G. M. Carte géologique detaillée de la France. Sheet 189 - Briançon. 1:80,000.

B. R. G. M. Carte géologique des Alpes occidentales du Léman à Digne. (1/250,000).

Bucher, W.H. 1956. The role of gravity in orogenesis. Geol. Soc. Am. Bull. 67, 1295-1318.

Butler, R.W.H. 1982a. A structural analysis of the Moine Thrust Zone between Loch Eriboll and Foinaven, N.W. Scotland. J. Struct. Geol. 4, 19-29.

Butler, R.W.H. 1982b. Hangingwall strain: a function of duplex shape and footwall topography. Tectonophysics 88, 235-246.

Butler, R.W.H. 1982c. The terminology of structures in thrust belts. J. Struct. Geol. 4, 239-245.

Butler, R.W.H. 1983. Balanced cross sections and their implications for the deep structure of the NW Alps. J. Struct. Geol. 5, 125-138.

Butler, R.W.H. in press. Balanced cross-sections and their implications for the deep structure of the NW Alps: Reply. J. Struct. Geol.

Butler, R.W.H. in press. The restoration of thrust systems and displacement continuity around the Mont Blanc massif, N.W. External Alpine thrust belt. J. Struct. Geol.

Butler, R.W.H. in press. Structural evolution of the Moine Thrust Belt between Loch More and Glendhu, Sutherland. Scott. J. Geol.

Butler, R.W.H. & Coward, M.P. in press. Geological constraints, deep geology and structural evolution of the N.W. Scottish Caledonides. Tectonics.

Butler, R.W.H., Matthews, S.J. & Parish, M. in press. The NW external Alpine thrust belt and its implications for the geometry of the western Alpine orogen. Collision Tectonics. Spec. publs. geol. Soc. Lond.

Caby, R. 1975. Geodynamic implications of transverse folding in the western Alps for the Alpine fold belt. Nature 256, 114-117.

Caby, R., Kiensat, J.-R., & Saliot, P. 1978. Structure, métamorphisme et modèle d'évolution tectonique des Alpes occidentales. Rev. Géogr. Phys. Géol. Dyn. 20, 307-322.

Caron, J.-M. 1974. Les glissements synschisteux, reflets dans les schistes lustrés de mouvements de socle ? (Exemple dans les Alpes cottiennes septentrionales, France et Italie). Géol. Alpine 50, 45-55.

Caron, J.-M. 1976. Evolution palaéogéographique et tectonique de la zone piémontaise dans les Alpes occidentales. Coll. final Géodynam. Méditerranée occidentale, Montpellier, P.58.

Chapple, W.M. 1978. Mechanics of thin-skinned fold-and thrust belts. Bull. geol. Soc. Am. 89, 1189-1198.

Christie, J.M. 1963. The Moine Thrust zone in the Assynt region, northwest Scotland. Univ. Calif. Publ. Geol. Sci. 40, 345-440.

Collet, L.W. 1927. The structure of the Alps. London. Arnold. 289 p.

Collet, L.W. 1943. La nappe de Morcles entre Arve et Rhone. Mat. Carte. Geol. Switzerland 79, 146 pp.

Cooper, M.A. 1981. The internal geometry of nappes: criteria for models of emplacement. In: Thrust and Nappe Tectonics (edited by McClay, K.R. & Price, N.J.). Spec. Publs. geol. Soc. Lond. 9, 225-234.

Cooper, M.A., Garton, M.R. & Hossack, J.R. 1982. Strain variation in the Hénaux Basse Normandie duplex, Northern France. Tectonophysics 88, 321-323.

Cooper, M.A., Garton, M.R., & Hossack, J.R. 1983. The origin of the Basse Normandie duplex, Boulonnais, France. J. Struct. Geol. 5, 139-152.

Coward, M.P. 1980. The Caledonian thrust and shear zones of N.W. Scotland. J. Struct. Geol. 2, 11-17.

Coward, M.P. 1982. Surge zones in the Moine thrust zone of N.W. Scotland. J. Struct. Geol. 4, 247-256.

Coward, M.P. 1983. Thrust tectonics, thin skinned or thick skinned, and the continuation of thrusts to deep in the crust. J. Struct. Geol. 5, 113-123.

Coward, M.P. & Kim, J.H. 1981. Strain within thrust sheets. In: Thrust and Nappe Tectonics (edited by McClay, K.R. & Price, N.J.). Spec. Publs. geol. Soc. Lond. 9, 275-292.

Coward, M.P. & Potts, G.J. 1983. Complex strain patterns developed at the frontal and lateral tips to shear zones and thrust zones. J. Struct. Geol. 5, 383-399.

Dahlstrom, C.D.A. 1969. Balanced cross sections. Can. J. Earth Sci. 6, 743-757.

Dahlstrom, C.D.A. 1970. Structural geology in the eastern margin of the Canadian Rocky Mountains. Bull. Can. Petrol. Geol. 18, 332-406.

Davies, V.M. 1982. Interaction of thrusts and basement faults in the French external Alps. Tectonophysics 88, 325-331.

Davies, V.M. 1983. Alpine structure and metamorphism in a traverse from the Grandes Rousses massif to the internal Briançonnais. Unpublished Ph.D. Thesis. Univ. Liverpool.

Debelmas, J. 1953. Schéma structural du bassin de la Durance entre Queyrières et Guillestre (Hautes-Alpes). Bull. Soc. géol. Fr. (6) 3, 123.

Debelmas, J. 1955. Les zones subbriançonnaise et briançonnaise occidentale entre Vallouise et Guillestre (Hautes-Alpes). Mém. Expl. Carte Géol. Fr. 171 p.

Debelmas, J. 1961. La zone subbriançonnaise entre Vallouise et Le Monêtier (Htes-Alpes). Bull. Carte géol. Fr. 264, 131-146.

Debelmas, J. 1963. Plissement paroxysmal et surrection des Alpes franco-italiennes. Trav. Lab. Grenoble 39, 125-171.

Debelmas, J. 1966. Progrès récents et perspectives nouvelles de la géologie des Alpes occidentales franco-italiennes. Ann. Soc. Géol. Belg., Mém. 89, 423-446.

Debelmas, J. & Lemoine, M. 1962. Remarques sur la structure de la zone briançonnaise dans le massif de Peyre-Haute entre Briançon et la vallée du Guil (Hautes-Alpes). Trav. Lab. Géol. Grenoble 38, 205.

Debelmas, J. & Lemoine, M. 1964. La structure tectonique et l'évolution palaéogéographique de la chaîne alpine d'après les travaux récents. Inform. Sci. 1, 1-33.

Debelmas, J. & Lemoine, M. 1970. The western Alps: palaeogeography and structure. Earth Sci. Rev. 6, 221-256.

Debelmas, J. & Kerckhove, C. 1973. Large gravity nappes in the French-Italian and French-Swiss Alps. In: Gravity and Tectonics (edited by De Jong, K.A. & Scholten, R.) John Wiley, New York. 189-200.

Debelmas, J., Bonin, B., Caron, J.-M., Demarcq, G., Desmons, J., Giraud, P., Gnieu, G., Irr, F., Kerkhove, C., Lemoine, M., Montjuvert, G., Philip, J. & Rousset, C. 1980. Introduction à la géologie du sud-est de la France. Géol. Alpine 56.

Dewey, J.F., Pitman III, W.C., Ryan, W.B.F. & Bonnin, J. 1973. Plate tectonics and the evolution of the Alpine system. Geol. Soc. Am. Bull. 84, 3137-3180.

Dunnet, D. 1969. A technique of finite strain analysis using elliptical particles. Tectonophysics 7, 117-136.

Dunnet, D. & Siddans, A.W.B. 1971. Non random sedimentary fabrics and their modification by strain. Tectonophysics 12, 307-325.

Durney, D.W. & Ramsay, J.G. 1973. Incremental Strains Measured by Syntectonic Crystal Growths. In: Gravity and Tectonics (edited by De Jong, K.A. & Scholten, R.) John Wiley, New York.

Elliott, D. 1970. Determination of finite strain and initial shape from deformed elliptical objects. Bull. geol. Soc. Am. 81, 2221-2236.

Elliott, D. 1976a. The Motion of Thrust Sheets. J. geophys. Res. 81, 949-963.

Elliott, D. 1976b. The energy balance and deformation mechanisms of thrust sheets. Phil. Trans. R. Soc. Lond. A. 283, 289-312.

Elliott, D. 1980. Mechanics of thin-skinned fold-and-thrust belts: Discussion. Bull. geol. Soc. Am. 91, 185-187.

Elliott, D. & Johnson, M.R.W. 1980. Structural evolution in the northern part of the Moine Thrust belt, N.W. Scotland. Trans. R. Soc. Edinb. Earth Sci. 71, 69-96.

Fabre, J., Feys, R. & Greber, Ch. 1952. Observations sur une note récente de P. Corsin et J. Debelmas "Sur la présence de stéphanien fossilifère au col de Tramouillon"(Hautes-Alpes). C.R.S.G.F. p. 123.

Fallot, P. 1949. Les chevauchments intercutanés de Roya (Alpes Maritimes). Ann. Hebert Haug Lab. Geol. Fac. Sci. Univ. Paris 7, 161-170.

Fischer, M.W. & Coward, M.P. 1982. Strains and folds within thrust sheets: an analysis of the Heilam Sheet, northwest Scotland. Tectonophysics 88, 291-312.

Flinn, D. 1962. On folding during three-dimensional progressive deformation. Q. Jl. Geol. Soc. Lond. 118, 385-428.

Frisch, W. 1979. Tectonic progradation and plate tectonic evolution of the Alps. Tectonophysics 60, 121-139.

Gidon, M. 1965. Sur l'interprétation des accidents de la bordure méridionale du massif du Pelvoux. Trav. Lab. Géol. Univ. Grenoble 41, 177-185.

Gidon, P. 1954. Les rapports des terrains cristallins et de leur couverture sédimentaire, dans les régions orientales et méridionales du massif du Pelvoux. Trav. Lab. Géol. Univ. Grenoble 31, 1-202.

Gignoux, M. 1936. Le prolongement de la zone du flysch des Aiguilles d'Arves à l'est du Pelvoux. C.R.S. Soc. Géol. Fr. 15, 247-249.

Gignoux, M. & Raguin, E. 1932. Découverte d'écailles de roches granitique au Nord-Ouest du Col du Lautaret à la base de la nappe du flysch des Aiguilles d'Arves. Bull. Soc. Géol. Fr. 5, II, 513-526.

Goguel, J. 1940. Tectonique de la chaîne de Montbrison (feuille de Briançon au 1/50,000e). Bull. Carte Géol. Fr. 42, No.203, p. 187.

Goguel, J. 1942. La chaîne de Montbrison, essai de coordination tectonique (feuille de Briançon au 1/50,000e). Bull. Carte Géol. Fr. 43, 211, p. 109.

Goguel, J. 1948. Introduction à l'étude mécanique des déformations de l'écorce terrestre. Mém. Carte Géol. Fr.

Goguel, J. 1962. L'interpretation de l'Arc des Alpes occidentales. Bull. Soc. géol. Fr. 7, 20-33.

Goguel, J. 1963. Les problèmes des chaînes subalpines. In: Livre Fallot, 2. Soc. Géol. France, Paris, 301-308.

Goguel, J. 1965. Traité de tectonique. Masson, Paris, 2nd ed. 457 pp.

Graciansky, P.-C. de, Bourbon, M., Charpal, O de, Chenet, P-Y., & Lemoine, M. 1979. Genèse et évolution comparées de deux marges continentales passives: marge ibérique de l'Océan Atlantique et marge européene de la Téthys dans les Alpes occidentales. Bull. Soc. géol. Fr. (7) 21, 663-674.

Graham, R.H. 1978a. Quantitative deformation studies in the Permian Rocks of the Alpes Maritimes. Goguel Symposium, B.R.G.M. 220-230.

Graham, R.H. 1978b. Wrench faults, arcuate fold patterns and deformation in the southern French Alps. Proc. Geol. Ass. 89 (2), 125-142.

Graham, R.H. 1981. Gravity sliding in the Maritime Alps. In: Thrust and Nappe Tectonics (edited by McClay, K.R. & Price, N.J.). Spec. Publs. geol. Soc. Lond. 9, 335-352.

Gratier, J.-P., Lejeune, B. & Vergne, J.-L. 1973. Etude des déformations de la couverture et des bordures sédimentaires des massifs critallins externes de Belledonne, des Grandes-Rousses et du Pelvoux (depuis les Aravis jusqu'à la région de Rémollon). Thèse 3e Cycle, Grenoble, 227 p. et 1 vol. de pl.

Gratier, J.-P. & Vialon, P. 1980. Deformation pattern in a heterogeneous material: folded and cleaved sedimentary cover immediately overlying a crystalline basement (Oisans, French Alps). Tectonophysics 65, 151-180.

Hallam, A. & Swett, K. 1966. Trace fossils from the lower Cambrian Pipe Rock of the N.W. Highlands. Scott. J. Geol. 2, 101-106.

Hanna, S.S. & Fry, N. 1979. A comparison of methods of strain determination in rocks from southwest Dyfed (Pembrokeshire) and adjacent areas. J. Struct. Geol. 1, 155-162.

Heim, A. 1878. Untersuchungen über den Mechanismus der Gebirgsbildung, 2. B. Schwabe, Basel. 85 pp.

Heim, A. 1921. Geologie der Schweiz. Tauchnitz, Leipzig, 1018 pp.

Homewood, P. & Caron, C. 1982. Flysch of the Western Alps. In: Mountain building processes (edited by Hsu, K.) Academic Press, London. 157-168.

Hossack, J.R. 1978. The correction of stratigraphic

sections for tectonic finite strain in the Bygdin area, Norway. J. geol. Soc. Lond. 135, 229-241.

Hossack, J.R. 1979. The use of balanced cross-sections in the calculation of orogenic contraction - a review. J. geol. Soc. Lond. 136, 705-711.

Hossack, J.R. 1983. A cross-section through the Scandinavian Caledonides constructed with the aid of branch-line maps. J. Struct. Geol. 5, 103-111.

Hsu, K.J. 1969. Role of cohesive strength in the mechanics of overthrust faulting and landsliding. Geol. Soc. Am. Bull. 80, 927-952.

Hsu, K.J. 1979. Thin-skinned plate tectonics during neo-alpine orogenesis. Am. J. Science 279, 353-366.

Hubbert, M.K. & Rubey, W.W. 1959. Role of fluid pressure in mechanics of overthrust faulting. Bull. geol. Soc. Am. 70, 115-166.

Johnson, M.R.W. 1955. The tectonics and metamorphism of the Precambrian rocks in the Lochcarron and Coulin Forest areas of Wester Ross. Unpublished Ph.D. Thesis. Univ. London.

Johnson, M.R.W. 1957. The structural history of the Moine Thrust Zone in the Coulin Forest, Wester Ross. Q. Jl. Geol. Soc. Lond. 113, 241-270.

Johnson, M.R.W. 1960. The structural history of the Moine Thrust Zone at Loch Carron, Wester Ross. Trans. R. Soc. Edinb. 64, 139-168.

Kanungo, D.N. 1956. The structural geology of Torridonian, Lewisian and Moinian rocks of Plockton, Kyle of Lochalsh, Wester Ross. Unpublished Ph.D. Thesis, Univ. London.

Kehle, R.O. 1970. Analysis of gravity sliding and orogenic translation. Bull. geol. Soc. Am. 81, 1641-1664.

Kerckhove, C. 1963. Schéma structural de la nappe du Flysch à Helminthoides de l'Embrunais-Ubaye. Trav. Lab. Grenoble 39, 7-24.

Kerckhove, C. 1969. La zone du Flysch dans les nappes de l'Embrunais-Ubaye (Alpes occidentales). Géol. Alpine 45, 205 pp.

Kligfield, R., Carmignani, L. & Owens, W.H. 1981. Strain analysis of a Northern Appenine shear zone using deformed marble breccias. J. Struct. Geol. 3, 421-436.

Knipe, R.J. 1981. The interaction of deformation and metamorphism in slates. Tectonophysics 78, 249-272.

Knipe, R.J. & White, S.H. 1979. Deformation in low grade shear zones in the Old Red Sandstone, S.W. Wales. J. Struct. Geol. 1, 53-66.

Latreille, M. 1961. Les nappes de l'Embrunais entre Durance et Haut-Drac. Thèse. Univ. Grenoble. Mém. Expl. Carte Géol. France 205 pp.

Laubscher, H.P. 1971. The large scale kinematics of the Western Alps and the Northern Appennines and its palinspastic implications. Am. J. Sci. 271, 193-226.

Laubscher, H.P. 1975. Plate boundaries and microplates in Alpine history. Am. J. Sci. 275, 865-876.

Laubscher, H.P. 1977. Fold development in the Jura. Tectonophysics 37, 347-365.

Laubscher, H.P. 1978. Foreland folding. Tectonophysics 47, 325-337.

Lefevre, R. 1982. Les nappes briançonnaises internes et ultra-briançonnaises dans Alpes Cottiennes méridionales. Thesis, Univ. d'Orsay.

Le Fort, P. 1971. Géologie du haut Dauphiné cristallin (Alpes francaises). Etude pétrologique et structurale de la partie occidentale. Thèse, Nancy, 1971: Sciences de la Terre, mém. No. 25. 375 pp.

Le Fort, P. & Pêcher, A. 1971. Présentation d'un schéma structural du haut Dauphiné cristallin. C.R. Acad. Sc. Paris 273 D, 3-5.

Le Fort, P. & Vernet, J. 1968. Sur une nouvelle structure synclinale du Massif du Pelvoux: Le synclinal du col de Colombes. Géol. Alpine 44, 153-155.

Lemoine, M. 1961. La marge externe de la fosse piémontaise dans les Alpes occidentales. Rev. Géogr. Phys. Géol. Dyn. 4, 163-180.

Lemoine, M. 1964. Sur un faisceau d'accidents transversaux aux zones briançonnaise et piémontaise à la latitude de Briançon. C.R. Acad. Sc. 259, 845-847.

Lemoine, M. 1973. About gravity gliding tectonics in the Western Alps. In: Gravity and Tectonics (edited by De Jong, K.A. & Scholten, R.) John Wiley, New York. 201-216.

Lemoine, M. 1975. Mesozoic sedimentation and tectonic evolution of the Briançonnais zone in the Western Alps - possible evidence for an Atlantic type margin between the European craton and the Tethys. Int. Congr. Sedimentology, 9th, Nice, 1975, 4, 211-219.

Lemoine, M. 1979. Serpentinites, gabbros and ophicalcites in the Piemont-Ligurian domain of the Western-Alps: Possible indicators of oceanic fracture zones and of associated serpentinites protrusions in the Jurassic-Cretaceous Tethys, symposium sur les inclusions tectoniques dans les Serpentinites, Genève, 1979, à paraîte dans Archives des Sciences (1980).

Lemoine, M., Bourbon, M. & Tricart, P. 1978. Le Jurassique et le Crétacé prépiémontais à l'Est de Briançon (Alpes occidentales) et l'évolution de la marge européenne de la Téthys: données nouvelles et conséquences. C.R. Ac. Sc. Paris 286 D, 1237-1240.

Lisle, R.J. 1977. Clastic grain shape and orientation in relation to cleavage from the Aberystwyth Grits, Wales. Tectonophysics 39, 381-395.

Maury, P. & Ricou, L.E. 1983. Le décrochement subbriançonnaise: une nouvelle interprétation de la limite interne-externe des Alpes franco-italiennes. Rév. géol. dynam. et de géogr. phys. 24, 3-22.

Ménard, G. 1979. Relations entre structures profondes et structures superficielles dans le sud-est de la France: essai d'utilisation de données géophysiques. Thèse, 3e Cycle, Univ. Grenoble.

Merle, O. 1982. Cinématique et déformation de la nappe du Parpaillon (Flysch à Helminthoides de l'Embrunais-Ubaye, Alpes occidentales). Thesis, 3e Cycle, Univ. Rennes.

Moorbath, S. 1969. Evidence for the age of deposition of the Torridonian sediments of northwest Scotland. Scott. J. Geol. 5, 154-170.

Mugnier, J.-L. & Vialon, P. 1984. The mechanisms of overlapping of the Bresse graben by the Jura formations in the Vignoble area (France). Tectonophysics 106, 155-163.

McClay, K.R. & Coward, M.P. 1981. The Moine Thrust Zone: an overview. In: Thrust and Nappe Tectonics (edited by McClay, K.R. & Price, N.J.). Spec. Publs. geol. Soc. Lond. 9, 241-260.

McLeish, A.J. 1971. Strain analysis of deformed Pipe Rock in the Moine Thrust Zone, northwest Scotland. Tectonophysics 12, 469-503.

Peach, B.N. & Horne, J. 1914. Guide to the geological model of the Assynt mountains, 1-32. Edinburgh: Geological Survey and Museum.

Peach, B.N., Horne, J., Gunn, W., Clough, C.T., Hinxman, L.W. & Cadell, H.M. 1888. Report on the recent work of the Geological Survey in the Northwest Highlands of Scotland, based on the Field Notes and Maps. Q. Jl. geol. Soc. Lond. 44, 378-441.

Peach, B.N., Horne, J., Gunn, W., Clough, C.T. & Hinxman, L.W. 1907. The geological structure of the north-west Highlands of Scotland. Mem. Geol. Surv. G.B.

Peach, C.J. & Lisle, R.T. 1979. A Fortran IV program for the analysis of tectonic strain using deformed elliptical markers. Computers & Geosciences 5, 325-334.

Perrier, G. & Vialon, P. 1980. Les connaissances géophysiques sur le SE de la France: implications géodynamiques. Géol. Alpine 56, 13-20.

Platt, J.P. in press. Balanced cross-sections and their implications for the deep structure of the northwest Alps: Discussion. J. Struct. Geol.

Plotto, P. 1977. Structures et Déformation des Grès du Champsaur au SE du Massif du Pelvoux. Thèse, 3e Cycle. Univ. Grenoble.

Potts, G.J. 1982. Finite strains within recumbent folds of the Kishorn Nappe, northwest Scotland. Tectonophysics 88, 313-319.

Potts, G.J. 1983. Origin of recumbent fold nappes. Unpublished Ph.D. Thesis, Univ. Leeds.

Price, R.A. 1973. Large-scale gravitational flow of supracrustal rocks, Southern Canadian Rockies. In: Gravity and Tectonics (edited by De Jong, K.A. & Scholten, R.) John Wiley, New York. 491-502.

Price, R.A. & Mountjoy, E.W. 1970. Geologic structure of the Canadian Rocky Mountains between Bow and Athabasca Rivers - Progress report. Geol. Ass. Can. Spec. Pap. 6, 7-25.

Ramsay, J.G. 1963. Stratigraphy, structure and metamorphism in the western Alps. Proc. Geol. Ass. 74, 357-391.

Ramsay, J.G. 1967. Folding and Fracturing of Rocks. McGraw-Hill, New York. 568 pp.

Ramsay, J.G. 1976. Displacement and strain. Phil. Trans. R. Soc. Lond. A. 283, 3-25.

Ramsay, J.G. 1981. Tectonics of the Helvetic Nappes. In: Thrust and Nappe Tectonics (edited by McClay, K.R. & Price, N.J.). Spec. Publs. geol. Soc. Lond. 9, 293-309.

Ramsay, J.G. & Graham, R.H. 1970. Strain variations in shear belts. Can. J. Earth Sci. 7, 786-813.

Ramsay, J.G., Casey, M. & Kligfield, R. 1983. Role of shear in development of the Helvetic fold-thrust belt of Switzerland. Geology 11, 439-442.

Rich, J.L. 1934. Mechanics of low angle overthrust faulting illustrated by Cumberland Thrust Block, Virginia, Kentucky and Tennessee. Bull. Am. Assoc. Pet. Geol. 18, 1584-1596.

Ricou, L.E. & Siddans, A.W.B. in press. Collision tectonics in the western Alps. Collision Tectonics. Spec. Publs. geol. Soc. Lond.

Roeder, D. 1977. Continental convergence in the Alps. Tectonophysics 40, 339-350.

Sanderson, D.J. 1982. Models of strain variation in nappes and thrust sheets: a review. Tectonophysics 88, 201-233.

Shimamoto, T. & Ikeda, Y. 1976. A simple algebraic method for strain estimation from deformed ellipsoidal objects - I. Basic Theory. Tectonophysics 36, 315-337.

Siddans, A.W.B. 1977. The development of slaty cleavage in a part of the French Alps. Tectonophysics 39, 533-557.

Siddans, A.W.B. 1979. Arcuate fold and thrust patterns in the sub-Alpine chains of SE France. J. Struct. Geol. 1, 117-126.

Soper, N.J. & Barber, A.J. 1979. Proterozoic folds on the northwest Caledonian foreland. Scott. J. Geol. 15, 1-11.

Soper, N.J. & Wilkinson, P. 1975. The Moine Thrust and Moine Nappe at Loch Eriboll, Scotland. Scott. J. Geol. 11, 339-359.

Stewart, A.D. 1969. Torridonian rocks of Scotland reviewed. In: North Atlantic Geology and Continental Drift (edited by Kay, M.). Mem. Am. Ass. Petrol. Geol. 12, 559-608.

Suppe, J. 1983. Geometry and kinematics of fault-bend folding. Am. J. Sci. 283, 684-721.

Swett, K. 1969. Interpretation of depositional and diagenetic history of Cambro-Ordovician succession of N.W. Scotland. In: North Atlantic Geology and Continental Drift (edited by Kay, M.). Mem. Am. Ass. Petrol. Geol. 12, 630-646.

Swett, K., Klein, G. de V. & Smit, D.E. 1971. A Cambrian tidal sand body - the Eriboll sandstone of northwest Scotland: an ancient-recent analog. J. Geol. 79, 400-415.

Tan, B.K. 1973. Determination of strain ellipses from deformed ammonoids. Tectonophysics 16, 89-101.

Tapponnier, P. 1982. Programme ECORS. Propositions de programme. Annexe 3, Bassin du Sud-Est, Jura-Alpes, IFP-INAG, 39-43.

Termier, P. 1903. Les montagnes entre Briançon et Vallouise. Mém. Serv. Carte Géol. Fr., Thèse.

Termier, P. 1904. Les nappes des Alpes orientales et la synthese des Alpes. Bull. géol. Soc. Fr. 4, 711-765.

Tissot, B. 1956. Étude géologique des massifs du Grand Galibier et des Cerces (zone briançonnaise, Haute Alpes et Savoie). Trav. Lab. Grenoble 32, 111-193.

Tricart, P. 1980. Tectonique superposées dans les Alpes occidentales, au sud du Pelvoux. Evolution structurale d'une chaine de collision. Thèse, Univ. Strasbourg.

Tricart, P., Caron, J.-M., Gay, M. & Vialon, P. 1977. Relais des schistosité, structures en éventail et discontinuités majeures sur la transversale du Pelvoux (Alpes Occidentales). Bull. Soc. géol. Fr. 19 (4), 873-881.

Trumpy, R. 1960. Palaeotectonic evolution of the central and western Alps. Bull. geol. Soc. Am. 71, 843-908.

Trumpy, R. 1973. The timing of orogenic events in the Central Alps. In: Gravity and Tectonics (edited by De Jong, K.A. & Scholten, R.) John Wiley, New York. 229-251.

Trumpy, R. 1975. Penninic-Austroalpine boundary in the Swiss Alps. A presumed former continental margin and its problems. Am. J. Sci. 275 A, 209-238.

Vail, P.R., Mitchum, R.M., Todd, R.G., Widmier, J.M., Thompson, S., Sangree, J.B., Bubb, J.N. and Hatlelid, W.G. 1977. Seismic stratigraphy and global changes of sea-level. In: Seismic stratigraphy - applications to hydrocarbon exploration. A.A.P.G. Memoir 26, 49-212.

Vernet, J. 1950. Les limites SE du massif du Pelvoux et de l'anticlinal amygdaloide des Ecrins. Bull. Soc. géol. Fr. 5 (20), 275-287.

Vernet, J. 1951. Le Synclinorium de l'Aiguille de Morges et le style des déformations alpines du Cristallin du Pelvoux. Bull. Soc. géol. Fr. 6 (1), 169-183.

Vernet, J. 1952. Les déformations d'âge alpin du Cristallin du Pelvoux, à la lumière d'observations nouvelles. Bull. Soc. géol. Fr. 6 (2), 175-189.

Vernet, J. 1965. Les écailles de Côte Plaine du Nord-Ouest du Lautaret. Trav. Lab. Grenoble 41, 253-257.

Vernet, J. 1966a. La zone "Pelvoux-Argentera". Bull. Serv. Carte Géol. France 275, 131-424.

Vernet, J. 1966b. Observations nouvelles sur le synclinal d'Ailefroide et les bordures du massif du Pelvoux en Vallouise. Trav. Lab. Grenoble 42, 275-280.

Vernet, J. 1970. Une hypothèse sur l'origine de la courbure des Alpes occidentales. Géol. Alpine 46, 201-204.

Vialon, P. 1966. Etude Géologique du massif cristallin de Dora Maira, Alpes cottiennes internes, Italie. Thèse Fac. Sci., Grenoble, 282 pp.

Vialon, P. 1974. Les déformations "synschisteuses superposées en Dauphiné. Leur place dans la collision des éléments du socle préalpin. Conséquences pétrostructurales. Schweiz. Mineral. Petrogr. Min. 54 (2/3), 663-690.

Wernicke, B. & Burchfiel, B.C. 1982. Modes of extensional tectonics. J. Struct. Geol. 4, 105-115.

Wheeler, J. in press (1984). A new plot to display the strain of elliptical markers. J. Struct. Geol. 6, 417-423.

Wilkinson, P., Soper, N.J. & Bell, A.M. 1975. Skolithus pipes as strain markers in mylonites. Tectonophysics 28, 143-157.

Wiltschko, D.V. 1979. A mechanical model for thrust sheet deformation at a ramp. J. geophys. Res. 84, 1091-1104.

Wiltschko, D.V. 1981. Thrust sheet deformation at a ramp, summary and extensions of an earlier model. In: Thrust and Nappe Tectonics (edited by McClay, K.R. & Price, N.J.). Spec. Pubs. geol. Soc. Lond. 9, 55-63.

Wood, D.S. 1973. Patterns and magnitudes of natural strain in rocks. Philos. Trans. R. Soc. Lond. A 274, 373-382.

Yochelson, E.L. 1983. Salterella (Early Cambrian; agmata) from the Scottish highlands. Palaeontology 26 (2), 253-260.

CONTAINS PULLOUTS


GEOLOGICAL MAP OF THE KINLOCHEWE REGION, N.W. SCOTLAND
Map 1 — Lochan Fada
Explanation
Key to maps:
Map 1 Lochan Fada
Map 2 Loch Maree
Map 3 Loch Clair
STRATIGRAPHIC UNITS
ISOLATED EXPOSURE (Mainly drift covered)
GOOD CONTINUOUS EXPOSURE
D — Durness Limestone
S — Serpulite Grit
F — Fucoid Beds
— Pipe Rock
— Lower Quartzite
— Torridonian Sandstone
— Lewisian Gneiss
STRATIGRAPHIC CONTACT (inferred position)
Key to symbols:
Dip & Strike of bedding
" " cleavage
Direction & Plunge of fold axis
Antiform
Synform
N
THRUST (Pecked line indicates inferred position, teeth in hangingwall)
NORMAL FAULT
1 Km
Lochan Fada
LIMIT OF MAPPED AREA
Gleann Bianasdail
CADH A' GHIBHAINN
Beinn a' Mhùinidh
Meallan Ghobhar
Kinlochewe River
Incheril
Abhainn Bruachaig
Torran nan Teud
LINE OF CROSS SECTION 4 (PAGE 37)
4'
02
03
04
05
06
07
62
63
64
65
66
67
68
69
70

Map 2 — Loch Maree

(See map 1 for key)

LIMIT OF MAPPED AREA

LINE OF CROSS SECTION 3 (PAGE 35)

Loch Maree

Kinlochewe

LOCH BHANAMHOIR

MEALL NA H-AIRIGH ARDAIN

MEALL A' GHUBHAIS

MAOL CHEANNAN

GLEN GRUDIE

RIVER GRUDIE

RUADH - STAC MOR

COIRE RUADH STACA

LOCHAN UAINE

MEALLAN NA CIRCE - FRAOICH

MEALL FEARNA

A' GHIAIBHE

A 896

95 96 97 98 99 00 01 02 03

65 64 63 62 61 60

This section line continued on northern sheet

924 925 926 927 928 929 930 931 932 933 934 935 936 937 938 939 940 941

3302 3301 3300 3299 3298 3297 3296 3295 3294 3293 3292 3291 3290 3289

Crête des Grangettes

Lac de l'Eychauda

Rochers de l'Yret

Chambran

Cime de la Condamine 2940

Serre Chevalier 2491

2205

Sommet du Prorel 2566

No exposure

BRIANÇON

Villard-St-Pancrace

(Page 175) C

(Page 174) B

Pic de Montbrison 2818

MONTBRISON

Tête d'Amont 2815

(Page 190) H

(Page 170) A

La Rouya 2750

Vallouise

Puy St-Vincent

St-Martin-de-Queyrières

Pic 2903 de Peyre Eyraute

See northern sheet for key

1 km

N

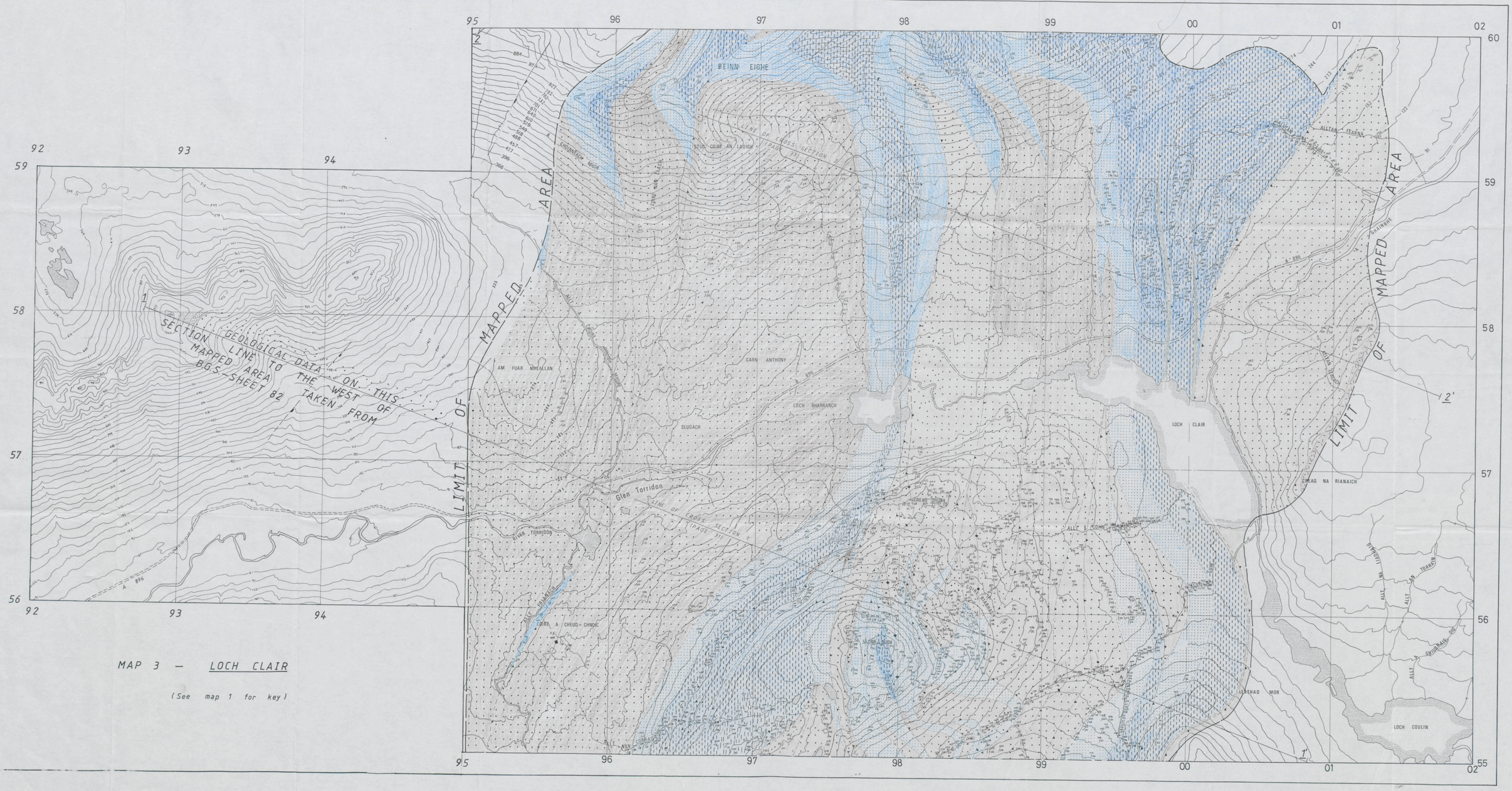

MAP 3 — LOCH CLAIR

(See map 1 for key)

GEOLOGICAL MAP OF THE PELVOUX – BRIANCONNAIS REGION, FRENCH ALPS

(based on reconnaisance mapping)

KEY TO SYMBOLS

- dip & strike of bedding
- dip & strike of cleavage
- direction & plunge of minor fold
- direction & plunge of lineation
- antiform
- synform
- thrust
- normal fault

KEY TO LITHOLOGIES

BRIANÇONNAIS		SUBBRIANÇONNAIS		ZONE EXTERNE	
Fb	Flysch Noir	Fs	Flysch Noir		Flysch des Aiguilles d'Arves
Cb	Calcschistes Planc	Cs	Calcschistes Planc	G	Schistes à Globigerines
Jb	Jurassique	O	Schistes oxfordiens	N	Calcaires à Nummulites
	Trias Calcaire		Calcaires de Vallouise	Je	Jurassique
S	Werfénien supérieur	Ts	Trias	Te	Trias
	Quartzites werféniens				Socle cristallins
V	Verrucano				
	Houiller				
	Écailles intermédiares				

N

1 km

Annecy · Chamonix · Megève · Albertville · Chambéry · St Jean-de-Maurienne · GRENOBLE · Briançon · TORINO · ITALIA · Gap · Embrun · Sisteron · Oigne · Castellane · Nice · Grasse

917 918 919 920 921 922 923 924 925 926 927 928 929 930 931 932 933 934 935 936 937 938 939 940 941 942

3311 3310 3309 3308 3307 3306 3305 3304 3303 3302

(THIS SECTION LINE CONTINUES ON SOUTHERN SHEET)

913 914 915 916

GEOLOGICAL MAP OF THE PELVOUX – BRIANCONNAIS REGION, FRENCH ALPS

(based on reconnaisance mapping)

KEY TO SYMBOLS

- dip & strike of bedding
- dip & strike of cleavage
- direction & plunge of minor fold
- direction & plunge of lineation
- antiform
- synform
- thrust
- normal fault